2020

Assessing the dynamics of soil erosion and sediment transport under increasing land use pressures in East African Rift Catchments

Wynants, Maarten

UNIVERSITY OF
PLYMOUTH

ASSESSING THE DYNAMICS OF SOIL EROSION AND SEDIMENT TRANSPORT UNDER INCREASING LAND USE PRESSURES IN EAST AFRICAN RIFT CATCHMENTS

by

MAARTEN WYNANTS

A thesis submitted to the University of Plymouth
in partial fulfilment for the degree of

DOCTOR OF PHILOSOPHY

School of Geography, Earth and Environmental Sciences

May 2020

Acknowledgements

First and foremost, I would like to thank my supervisory team, Prof. William Blake, Prof. David Gilvear, Prof. Pascal Boeckx (UGent), and Prof. Patrick Ndakidemi (NM-AIST) for their academic and mental support throughout the project. They always found the right balance between rigorous supervision and academic freedom. Furthermore, they always put my wellbeing before any of our academic goals and for that, I am very grateful.

I am also very thankful for the funding I have received from the University of Plymouth and external funding bodies, which allowed me to explore and pursue my academic goals. Furthermore, I am indebted to the incredible University of Plymouth SoGEES staff. Dr. Alex Taylor, Prof. Geoffrey Millward and Richard Hartley have been by my side from day one, training and assisting me in analytical protocols. Shaun Lewin, Tim Absalom and Jamie Quinn, were instrumental for developing my GIS skills. Donella Bone and the other administrative staff were always available to help me navigate the University bureaucracy. Dr. Claire Kelly and the entire Geography academic staff have cleared time from their busy schedules to provide valuable feedback. Moreover, I am indebted to the NM-AIST team for their support. Aloyce Patrick and Francis Mkilema have been of invaluable assistance during the sampling campaigns. Dr. Linus Munishi and Dr. Kelvin Mtei were always available for feedback and support. I would also like to thank Dr. Samuel Bodé (UGent) for his help with the Compound Specific Stable Isotope Analysis, and Carey Marks for providing great visualisations of soil erosion in the study area. Moreover, I will be forever grateful to Prof. Luc Brendonck and An Steensels for helping me to pursue my dream of working in Africa, even in the face of adversity.

Last but not least, I would like to extend a special thank you to my partner Gabriella, my mother and father, siblings, nieces and nephews for their continuous support, unconditional love and for putting up with my long absences. I also would like to thank my PhD colleagues in Plymouth: Francis, Wycliff, Tom, Christian, Hoayda, Magda, Havananda, Felipe, Simone, Giulia, Gabi, Alex, Eva, Luis, Nika, Camille, Jasper and my Tanzanian buddies: Frode and Bert, for their friendship and support. Friendships are more susceptible to erosion by exposure to forces of time and distance, and I therefore want to thank all my friends and family in Belgium for keeping me in their hearts. I am truly blessed.

AUTHOR'S DECLARATION

At no time during the registration for the degree of Doctor of Philosophy has the author been registered for any other University award without prior agreement of the Doctoral College Quality Sub-Committee.

Work submitted for this research degree at the University of Plymouth has not formed part of any other degree either at the University of Plymouth or at another establishment.

This study was financed by the University of Plymouth with additional support from European Commission (Horizon 2020 IMIXSED project ID 644320), the Research Council UK Global Challenges Research Fund (GCRF) grant NE/P015603/1, UK Natural Environment Research Council Grant NE/R009309/1 and VLIR-UOS project ZIUS2015VOA3106.

A programme of advanced study was undertaken, which included intensive training in relevant sampling methodologies, laboratory protocols, data analysis, and other research skills.

The following external institutions were visited for data collection and laboratory analysis purposes:

- Nelson Mandela African Institute of Science and Technology, Tanzania.
- Isotope Bioscience Laboratory, Ghent University, Belgium.
- Department of Geography, University of Exeter, UK.

Parts of this thesis are published in peer-reviewed scientific journals:

- Chapters 5 and 6 : Wynants, M., Solomon, H., Ndakidemi, P. & Blake, W. H. 2018. Pinpointing areas of increased soil erosion risk following land cover change in the Lake Manyara catchment, Tanzania. *International journal of Applied Earth Observation and Geoinformation* 71: 1-8. https://doi.org/10.1016/j.jag.2018.05.008
- Chapter 3: Wynants, M., Kelly, C., Mtei, K.,…, & Ndakidemi, P. 2019. Drivers of increased soil erosion in East Africa's agro-pastoral systems: changing interactions between the social, economic and natural domains. *Regional Environmental Change* 19: 1909-1921. https://doi.org/10.1007/s10113-019-01520-9
- Chapter 7: Wynants, M., Millward, G., Patrick A., …, & Blake, W.H. 2019. Determining tributary sources of increased sedimentation in East African Rift Valley Lakes. *Science of the Total Environment* 717: 137266. https://doi.org/10.1016/j.scitotenv.2020.137266

Multiple scientific conferences were attended for disseminating results:

- The response of sediment source and transfer dynamics to land use (change) in the Lake Manyara catchment. Geophysical Research Abstracts 19: EGU2017-5547. https://dx.doi.org/10.13140/RG.2.2.31581.97769
- Pinpointing areas of increased surface erosion following land cover changes using RUSLE modelling and sediment fingerprinting: a case study of the Lake Manyara catchment, Tanzania. TerraEnvision 2018. http://doi.org/10.13140/RG.2.2.27177.95846
- Identifying changing erosion processes, -sources and sediment transport dynamics in Northern Tanzania using ground surveys and sediment tracing. BHS 13th National Hydrology Symposium 2018. http://doi.org/10.13140/RG.2.2.17111.62881
- Land degradation in East Africa: erosion of social and natural domains in socio-ecological systems. British Ecological Society Annual Meeting 2018. http://doi.org/10.13140/RG.2.2.36615.14244
- Identifying sources and dynamics of eroded sediment in an East African rift lake using erosion modelling and sediment fingerprinting. Geophysical Research Abstracts 21: EGU2019-15752. https://dx.doi.org/10.13140/RG.2.2.13127.04008

Word count of main body of thesis: 43041

Signed: …… 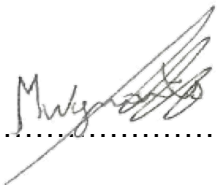 ……

Dated: ……27/05/2020……

Maarten Wynants

ASSESSING THE DYNAMICS OF SOIL EROSION AND SEDIMENT TRANSPORT UNDER INCREASING LAND USE PRESSURES IN EAST AFRICAN RIFT CATCHMENTS

Abstract

State-of-the-art environmental diagnostic tools were applied to further the understanding of the complex spatial and temporal dynamics in land use and land cover change, soil erosion and sediment transport in East African Rift Catchments. This contribution forms a blueprint for future studies using sediment tracing, radionuclide dating, Bayesian Mixing Models and soil erosion mapping, and their reciprocal integration in this challenging environment. An integrated quantitative assessment of soil erosion and sediment dynamics in the Lake Manyara catchment, northern Tanzania, revealed drastic changes in land cover, a tenfold increase in upstream sediment yield, and a fivefold increase in downstream lake sedimentation over the past 120 years. Integrated spatial analysis identified two tributaries as the main sources of accelerating sedimentation in Lake Manyara. The sediment in the most problematic tributary currently mainly originates from hillslope erosion on the open rangelands and maize croplands in the middle catchment zone. However, detailed historical analysis of upstream sediment deposits revealed distinct changes in source zones, land use types and erosion processes over recent decades. Deforestation, continued cropland expansion and increasing grazing pressures resulted into accelerating rates of sheet erosion. Progressive soil degradation and convergence of surface flows eventually led to a regime shift into a highly incised landscape, where high amounts of eroded soils from all over the catchment are rapidly transported downstream by strongly connected ephemeral drainage networks. Increasing land use pressures are the major driver for the

upstream exponential increase in sediment yield. However, on the basin scale, rainfall dynamics and sediment connectivity are important factors for explaining observed changes in downstream sediment delivery. This is illustrated by the dominant contribution of one specific sub-tributary, which has experienced similar exponential increased in sediment yield, but is mainly characterised by a higher sediment connectivity compared to other sub-tributaries, to the total downstream sediment transport. By integrating complementary spatial and temporal evidence bases, this study demonstrated links between land use change, increased soil erosion and downstream sedimentation. Such evidence can guide stakeholders and policy makers in targeted management interventions to safeguard soil health and water quality. To be successful, these management plans need to be tailored to the specific local socio-ecological context, while at the same time being integrated in regional and national governance structures.

.

List of Contents

List of Contents i
List of Figures v
List of Tables ix
List of Appendices x
List of Abbreviations xiii
Chapter 1. Introduction 1
1.1 Problem analysis 1
1.2 Aims and objectives 4
Chapter 2. The soil-sediment continuum in East African Rift Lake catchments 7
2.1 Detachment and transport processes 7
2.1.1 Surface erosion 9
2.1.2 Subsurface erosion: gully- and riverine erosion 11
2.2 Natural controlling factors of soil erosion processes 16
2.2.1 Topography and geology 17
2.2.2 Soil characteristics 19
2.2.3 Climate 20
2.2.4 Vegetation 22
2.3 Sediment connectivity 24
2.4 Sedimentation and storage 28
Chapter 3. Drivers, impacts and feedbacks of increased soil erosion in East Africa's agro-pastoral landscapes 31
3.1 Land use and land cover change 32
3.2 Increased soil erosion and land degradation 34
3.2.1 Nutrients, organic matter, biodiversity and productivity 35
3.2.2 Runoff and water availability 36
3.2.3 Regime shifts 37
3.3 Disruption pathways to degradation 39
3.3.1 Indigenous agro-pastoral systems 42
3.3.2 The colonial disruption 45
3.3.3 Post-independence disruption 47
3.4 Contemporary drivers of increased soil erosion 51
3.4.1 Poverty 51
3.4.2 Population growth 52

3.4.3 Governance and political marginalisation 54
3.4.4 Land rights and –access 55
3.5 Siltation, eutrophication and pollution 58
Chapter 4. Study site: The Lake Manyara catchment 61
4.1 Mapping the hydrological network 63
4.2 Catchment characteristics 64
Chapter 5. Quantifying and mapping land cover changes using Landsat images 69
5.1 Introduction 69
5.2 Material and methods 70
5.2.1 Land cover classification and validation 70
5.3 Results and discussion 73
5.3.1 Land cover changes 73
5.3.2 Limitations and future possibilities 76
5.4 Conclusion 78
Chapter 6. Pinpointing areas of increased soil erosion risk following land cover change 79
6.1 Introduction 79
6.2 Material and methods 81
6.2.1 Erosion risk mapping and comparison 81
6.2.2 Model sensitivity analysis 85
6.2.3 Modelling tributary sediment delivery 86
6.3 Results and discussion 87
6.3.1 Erosion risk change 87
6.3.2 Tributary sediment delivery 90
6.3.3 Limitations 91
6.4 Conclusion 93
Chapter 7. Determining tributary sources of increased sedimentation in Lake Manyara 94
7.1 Introduction 94
7.2 Material and Methods 96
7.2.1 Sampling strategy 96
7.2.2 Laboratory Analysis 98
7.2.3 Sediment dating and mass accumulation rates 99
7.2.4 Bayesian mixing model for source apportionment 101
7.3 Results and discussion 107

7.3.1 Sedimentation rates 107
7.3.2 Proportional tributary contribution 111
7.3.3 Archived changes in tributary sediment delivery 113
7.4. Conclusion 115
Chapter 8. Deconvoluting sediment fluxes within the Makuyuni tributary. 119
8.1 Introduction 119
8.2 Material and methods 119
8.2.1 Sample collection and analysis 119
8.2.2 Deconvolutional Bayesian mixing model 121
8.3 Results and discussion 123
8.3.1 Deconvoluted riverine source apportionment 123
8.3.2 Historical sediment fluxes from subtributaries 126
8.4 Conclusion 129
Chapter 9. Understanding the dynamics of increased soil erosion and sediment transport in the northern Makuyuni catchment. 130
9.1 Introduction 130
9.2.1 Sampling strategy 132
9.2.2 Laboratory analysis 133
9.2.3 Data analysis 135
9.3 Results and Discussion 138
9.3.1 Hillslope soil to riverine sediment analysis 138
9.3.2 Changing landscape dynamics 148
9.4 Conclusion 156
Chapter 10. Conclusions, challenges and future research 159
10.1 Quantifying temporal changes in land cover, soil erosion and sediment delivery 159
10.2 A multiscalar comparison of RUSLE-SDR and $^{210}Pb_{ex}$-CRS sediment yield estimations 161
10.3 Pinpointing areas of increased erosion risk and spatial sources of increased sediment delivery 164
10.4 Understanding processes of increased erosion and sediment transport 167
10.5 Multifaceted drivers of soil erosion 169
Appendices 172
A. Lake Manyara bathymetry 172
B. Rainfall fluctuations 173

C. Satellite evidence of Tarangire-Manyara connectivity 173
D. Land cover change 174
E. Erosion risk mapping 176
F. CRS-standard approach 179
G. CRS-fitted approach 179
H. Lake $^{210}Pb_{ex}$ profiles and Tributary $^{210}Pb_{ex}$ activities 180
I. Lake and tributary geochemical characteristics 181
J. Bayesian Mixing model output 186
K. Makuyuni sub-tributary range tests 186
L. Meserani core Bayesian Mixing Model output 190
M. Tracer selection for northern Makuyuni sub-tributaries 190
N. Soil-to-sediment tracer range tests and PCA plots 190
O. Northern Makuyuni Bayesian Mixing Model outputs 202
P. Geochemical profiles of northern Makuyuni sediment cores 202
Q. Soil organic matter and aggregate stability 206
R. Photographic evidence of soil degradation and erosion 207
References 211

List of Figures

Figure 1: A global overview of SY, clearly showing the higher yields in semi-arid and mountainous regions (Walling & Webb, 1983). 8
Figure 2: Simplified relation between the combined functions of cohesion (blue dashed) and friction (green dashed) effects resulting in the specific relative resistance (red full) of soil particles to detachment with the lowest resistance to detachment in intermediate grain fractions. Adapted from Kirkby (2008).....11
Figure 3: Stages in gully development on a hillslope (Leopold, Wolman & Miller, 2012).....12
Figure 4: Channel planform change and meander development over a thirty year period in the semi-arid Luangwa River, Zambia (Gilvear, Winterbottom & Sichingabula, 2000). 14
Figure 5: Comparison of soil erosion rates (in mm yr^{-1}) from agricultural fields under conventional agriculture and natural erosion rates from low gradient continental cratons, soil-mantled landscapes, and alpine terrain. Note that soil erosion rates from agricultural fields in all terrains is similar to natural rates in alpine regions. Shaded area represents range of the USDA standards (0.4-1.0 mm yr^{-1}) for tolerable soil loss (Montgomery, 2007). 18
Figure 6: A) Seasonal cycle of rainfall and response of vegetation cover and erosion in a semi-arid climate (Kirkby, 1980), and B) the simplified relationship between SY and mean annual precipitation, adapted from Langbein and Schumm (1958). 23
Figure 7: Croke, Fryirs and Thompson (2013) conceptual representation of a) hillslope connectivity where the probability of connectivity increases linearly with increasing discharge until sediment exhaustion occurs and b) reach-scale/channel-floodplain connectivity where the probability of connectivity only goes up after reaching a treshhold of flow (Q_{bf}) and after varies as a function of bankfull recurrence interval. 24
Figure 8: A) Illustration of connected and disconnected hillslope-channel systems (Michaelides & Wainwright, 2002) and B) riparian vegetation buffering the runoff and leading to sedimentation (Bracken & Croke, 2007). 26
Figure 9: Country-specific percentages of increase or decrease of the annual average soil erosion rates between 2001 and 2012 obtained by comparing the pixel-based LUCC and agricultural inventory data of every country (Borrelli *et al.*, 2017). 34
Figure 10: A schematic representation of East Africa's agro-pastoral systems structured by internal interactions between social, economic and natural domains, which are in turn influenced by external pressures, possibly altering the balance in the system. 40
Figure 11: Conceptual pathways of degradation and co-adaptation in East Africa's agro-pastoral systems. Circle sizes illustrate the benefits generated for the agro-pastoral systems by the interactions of the domains. a) Collapse of natural resources is preceded by a gradual erosion of social structures necessary for sustainable resource management. The horizontal dashed line illustrates the ecological tipping point and the vertical dashed line the

hypothetical social threshold where after communities lack the social structures to internally manage natural resources and co-adapt to external pressures. The different starting points represent natural differences in productivity. The circular arrows illustrate the adaptive capacity of systems with a well-developed social domain to higher or sustained high productivity. b) Interaction between the natural and economic domains. If economic production is increased by degrading natural resources, ecosystems will move towards a tipping point, after which both collapse. Communities with a well-developed social domain can however, sustainably intensify production without degrading the natural domain, as illustrated by the co-adaptation arrow. 50
Figure 12: Location of the Lake Manyara catchment within Africa. Detailed topographic map of the Catchment with its major tributary systems: A) Marera, B) Kirurumo, C) Simba, D) Mto Wa Mbu, E) Makuyuni, F) Tarangire, G) Dudumera, H) Magara, I) Endabash. 64
Figure 13: Spatial distribution of A) precipitation (Source: CHELSA model), B) soil types (Source: Harmonised world soil database), and C) Lithology (Source: Tanzanian Geological Survey). 66
Figure 15: Land cover maps and percentages of land cover types derived from Landsat imagery of a) 1988 and b) 2016. 75
Figure 16: The model input maps of the a) dimensionless slope length and slope steepness factor LS, b) Rainfall erosivity factor R (in MJ mm ha^{-1} h^{-1} yr^{-1}), and c) Soil erodibility factor K (in t ha h ha^{-1} MJ^{-1} mm^{-1}). 81
Figure 17: The dimensionless land cover erosivity factor input maps for a) 1988 and b) 2016. 86
Figure 18: Modelled output maps of the annual average soil loss E (in t ha-1 yr-1 or as qualitative proxy for erosion risk) for a) 1988 and b) 2016. With c) the predicted changes in erosion risk (Delta E) following land conversion between 1988 and 2016. In the green areas erosion risk has decreased, while in the red areas it has increased. 89
Figure 19: Riverine sediment sampling locations (black circles). Focus of Lake Manyara with locations of the sediment grabs (red circles) and cores (numbers correspond with core numbers). 97
Figure 20: Ordination biplot visualising the geochemical drivers of variance in the DS fingerprint from different tributary sources and lake mixture using the two largest eigenvalues (explaining 47.6% and 21.2% of variance), with grouping of different lake areas. 103
Figure 21: $^{210}Pb_{ex}$ and ^{137}Cs mass depth profiles of a) core two and b) core three. Age-depth relationship (full) and Mean Accumulation rates (dashed) using the standard CRS (black) and CRS-fitted (blue) approach for c) core two and d) core three. 110
Figure 22: MixSIAR proportional sediment contribution of the tributary rivers (Dudumera, Endabash, Makuyuni, Mto Wa Mbu, Ngorogoro, and Tarangire) to the ‘total’ lake sediment (white) and different lake areas (blue shades). The density distributions are represented as boxplots with median shown by central line, interquartile range by box, and range by whiskers. 112

Figure 23: Changing proportional sediment contributions of tributary rivers over time to a) core 2, and b) core3. 115
Figure 24: Changes in absolute sediment delivery from tributaries (DUD=Dudumera, END=Endabash, MAK=Makuyuni, MWM= Mto Wa Mbu, NGO= Ngorogoro, and TAR=Tarangire) to Lake Manyara over time as reconstructed from $^{210}Pb_{ex}$ dating and BMM of core 3. 116
Figure 25: Sampling locations in the Makuyuni system. Four nested river samples: M1, M2, M3 and M4. Eight sub-tributaries: Lesimingore A (MS1), Lesimingore B (MS2), Nanja (MS3), Lolkisale (MS4), Meserani Chini (MS5), Ardai (MS6), Meserani Juu (MS7) and Musa (MS8). One nested floodplain core: Meserani floodplain (MC2). 121
Figure 26: Ordination biplot visualising the geochemical drivers of variance in the fingerprint from upstream sub-tributaries and nested river samples using the two largest eigenvalues (explaining 35.3% and 21.3% of variance). 123
Figure 27: The location of A) Nanja lake and B) Duka Bovu Floodplain (image source: CNES/Airbus, Google Earth) that respectively disconnect the upstream Nanja reaches and the Musa sub-tributary with the main Makuyuni river. 125
Figure 28: Ordination biplot visualising the geochemical drivers of variance in the Meserani core using the two largest eigenvalues (explaining 24.5% and 16.2% of variance), with depth groups in corresponding colours. 127
Figure 29: Changing proportional sediment contributions of sub-tributaries (Ardai=red; Lolkisale=blue; Musa=green; Meserani Juu=yellow; Meserani Chini=purple) over depth 128
Figure 30: Overview map of Makuyuni catchment depicting the sampling locations of source soils (black triangles), riverine sediment (purple circles), and sediment cores (red squares) within the A) Ardai sub-catchment, B) Nanja sub-catchment, and C) Musa sub-catchment 133
Figure 31: Geochemical PCA plot (explaining 37.8% and 20.9% of variance) of soil samples and riverine sediment in the Ardai sub-catchment 139
Figure 32: δ^{13}-FA PCA plot (explaining 93.3% and 3.1% of variance) of soil samples and riverine sediment in the Ardai sub-catchment. 141
Figure 33: Boxplot of the a) geochemical BMM, b) δ^{13}-FA BMM, and c) integrated outputs, showing the estimated contributions of Bedrock incision (BedGul), Lowzone maize croplands (LowMaize), Lowzone open rangelands (LowRange), Midzone maize croplands (MidMaize), Midzone open rangelands (MidRange), Midzone bushlands (MidBush), Upzone mixed agriculture (UpAg), and Upzone forest (UpForest) 142
Figure 34: Geochemical PCA plot (explaining 32.5% and 17.6% of variance) of soil samples and riverine sediment in the Nanja sub-catchment 145
Figure 35: Geochemical PCA plot (explaining 49.6% and 19.0% of variance) of soil samples and riverine sediment in the Musa sub-catchment. 146
Figure 36: a) Boxplot of the Nanja BMM output indicating contributions of bedrock incision (BedGul), hillslope gullies (HillGul), lowzone surface soils (LowSur), midzone maize croplands (MidMaize), eastern midzone rangelands (MidRanE), and western midzone rangelands (MidRanW). b) Boxplot of the Musa BMM output indicating contributions of midzone hillslope gullies (MidGul),

midzone surface soils (MidSur), upzone mixed agriculture (UpAg), upland forest (UpFor), and upzone hillslope gullies (UpGul). 147
Figure 37: $^{210}Pb_{ex}$ profiles of the a) Naidosoito core and b) Nanja core. The constant rate of supply age-mass depth profile (CRS) and Mass Accumulation Rates (MAR) of the c) Naidosoito core and d) Nanja core. 149
Figure 38: PCA plot (explaining 42.2% and 24.7% of variance) visualising geochemical time trends in the Naidosoito core, related to changing dynamics of soil erosion and sediment transport. 151
Figure 39: The Nanja core A) geochemical PCA plot (explaining 36.2% and 12.8% of variance) and B) $\delta^{13}C$-FA PCA plot (explaining 78.4% and 9.5% of variance). 154
Figure 40: PCA plot (explaining 37.4% and 17.9% of variance) visualising geochemical trends in the Musa core. 156
Figure 41: Schematic representation of the dynamics of soil erosion and sediment transport in EARS, highlighting sediment connectivity as a link between the drivers (land pressures and precipitation), upstream impacts (hillslope soil erosion and hillslope connectivity), and downstream sedimentation. Source of livestock data for Tanzania is FAO (2019). 171

List of Tables

Table 1: Tributary hydrological properties: Drainage area in km2, the relief/length ratio (R/L), mean weighted bifurcation ratio (BR), and flow regime, as described in section 4.1. 68
Table 2: The selected land cover types, their broader classification and corresponding C-factor scores 72
Table 3: Percentages of the total catchment area (18372 km^2) per land cover type in 1988 and 2016, the total gains, losses, gross changes, swap and net changes (negative values have a net decrease). 73
Table 4: Estimated SDR (dimensionless), hillslope soil loss by surface erosion (E, in megatonnes per year), Sediment delivery (in megatonnes per year) and proportional sediment delivery in the different tributaries in 1988 and 2016. The changes in estimated hillslope soil loss by surface erosion (ΔE, in megatonnes per year), and sediment delivery (ΔSD, in megatonnes per year). 90
Table 5: The mean values and Gelman-Rubin diagnostics (Diag) outcomes from the two nesting levels of the Makuyuni sediment BMM. 124
Table 6: Overview of the RUSLE-SDR and $^{210}Pb_{ex}$-CRS sediment yield estimations on the different scales. CRS SY estimates for Manyara are an average between the lowest and highest values. 163

List of Appendices

Appendix A.1: Lake Manyara a) Bathymetry, b) Morphology, and c) Relative volume vs. relative area (Source: Deus et al. 2013, redistributed under the terms and conditions of the Creative Commons Attribution 3.0 license). 172
Appendix A.2: Pelicans resting on the boardwalk railing at Lake Manyara, which is normally 1.5-2 meters above the lake surface. 172
Appendix B.1: Yearly changes in annual precipitation (mm) measured at the Selian Agricultural Research Institute, Arusha, altitude: 1402m, coordinates 03°21'52" S 36°38'6" E (black) and at the Lake Manyara National Park headquarters, Mto Wa Mbu, altitude: 1006m, coordinates 03°22'7"S 35°50'31"E (blue). 173
Appendix C.1: Landsat image (February 2017) showing the overflow from the Tarangire-Burunge system to Lake Manyara. 173
Appendix D.1: Cross-tabulation table with the absolute values (in km^2) per land cover type of persistence (bold), transitions to other types, total area, losses and gains. 174
Appendix D.2: Tributary catchment (Dudumera, Endabash, Kirurumo, Makuyuni, Mto Wa Mbu, Simba, Tarangire) land cover percentages. 174
Appendix D.3: Confusion matrix with numbers and percentages of correct (diagonal), unsure and false classification per land cover type. 175
Appendix E.1: C-factor values from other RUSLE studies. 176
Appendix E.2: Erosion risk change map (red is increase, green decrease) overlaid with protected areas and delineation of the different sub-catchments to highlight the effect of land management and the spatial variability of the risk change. 177
Appendix E.3: Sensitivity analysis of the model output (Delta E= changes in surface erosion risk) with 10% random errors in the model inputs of a) the LS factor, b) R-factor and c) K-factor, while keeping the other factors stable, and d) the land cover error introduced in the C-factor. Note the high similarity in spatial risk distribution. 178
Appendix H.1: $^{210}Pb_{ex}$ and ^{137}Cs profiles of a) core1, b) core 4, and c) core 5 180
Appendix H.2: Mean and standard deviation (SD) of tributary sediment $^{210}Pb_{ex}$ activities. 180
Appendix I.1: Tracer element range tests between tributary sources (DUD, END, KIR, MAK, MWM, SIM, TAR) and the lake (MAN). In the box plots, median is shown by central line, interquartile range by box, range by whiskers with circles indicating outliers 182
Appendix I.2: Geochemical depth profiles of core 2 183
Appendix I.3: Geochemical depth profiles of core 3 184
Appendix I.4: Ordination plot of the two major principal components visualising the geochemical drivers of variance in A) Core 2 (explaining 37.5% and 19.2% of variance) and B) core 3 (explaining 39.6% and 15.9% of variance). Groups are as used for fixed categorical effect in the BMM. 185
Appendix J.1: The mean values and Gelman diagnostics (Diag.) of the Bayesian Mixing model runs for both 'global' and 'spatial' model builds. 186

Appendix J.2: The mean values and Gelman diagnostics (Diag.) of the Bayesian Mixing model output of core 2, specified for grouped core sections. 186
Appendix J.3: The mean values and Gelman diagnostics (Diag.) of the Bayesian Mixing model output of core 3, specified for grouped core sections. 186
Appendix K.1: Tracer element range tests between sub-tributaries (MS 1-8: Lesimingore A, Lesimingore B, Nanja, Lolkisale, Meserani Chini, Ardai, Meserani Juu, and Musa respectively), nested Makuyuni reaches (M1 and M2), and Meserani core (MC1). See Figure 1 for upstream connectivity. The median is shown by central line, interquartile range by box, range by whiskers with circles indicating outliers. 189
Appendix L.1: The mean values and Gelman diagnostics (Diag.) of the Bayesian Mixing model output, specified for grouped core sections. 190
Appendix M.1: an overview of selected tracers for soil-to-sediment BMM and core PCA. 190
Appendix N.1: Geochemical tracer range tests between soil sampling locations (APGul-OrRan), riverine sediment (River) and sediment core (Core) within the Ardai sub-catchment. Median is shown by central line, interquartile range by box, range by whiskers with circles indicating outliers. 193
Appendix N.2: δ^{13} FA tracer range tests between soil sampling locations (APGul-OrRan), riverine sediment (River) and sediment core (Core) within the Ardai sub-catchment. Median is shown by central line, interquartile range by box, range by whiskers with circles indicating outliers. 195
Appendix N.3: Geochemical tracer range tests between soil sampling locations, riverine sediment and sediment core within the Nanja sub-catchment. Median is shown by central line, interquartile range by box, range by whiskers with circles indicating outliers. 198
Appendix N.4: Geochemical tracer range tests between soil sampling locations, riverine sediment and sediment core within the Musa sub-catchment. Median is shown by central line, interquartile range by box, range by whiskers with circles indicating outliers. 201
Appendix N.5: Composite PCA plot (explaining 29.4% and 23.7%) of soil samples and riverine sediment in the Ardai sub-catchment 201
Appendix O.1: Mean values and Gelman-Rubin diagnostics (diag.) from the separate A) geochemical BMM, and B) δ^{13}-FA BMM, in the Ardai sub-catchment. 202
Appendix O.2: Mean values and Gelman-Rubin diagnostics (diag.) from the soil-to-sediment BMM in the A) Nanja sub-catchment, and B) Musa sub-catchment. 202
Appendix P.1: Geochemical tracer profiles of the Naidosoito core. 203
Appendix P.2: Geochemical tracer profiles of the Nanja core 204
Appendix P.3: Geochemical tracer profiles of the Musa core. 205
Appendix P.4: δ^{13}C-FA profiles of the Nanja core. 206

Appendix Q.1: Boxplot of SOM content (% of total) and Aggregate stability (% aggregates remaining after 60 runs of 30 seconds on 30 mm/hr intensity rainfall) in different land use types / catchment zones combinations. 206
Appendix R.1: Exposed plant root evidence of >2cm topsoil removal on rangelands by sheet erosion (Lat: -3.333751°, Lon: 36.360225°), and evidence of surface crusting and rill erosion (Lat: -3.410499°, Lon: 36.407072°). Photos by William Blake. 207
Appendix R.2: Gully incision on deeply weathered hillslope soils (saprolites, Lat: -3.334067°, Lon: 36.360801°). The gully was >7m deep at some places and still did not hit the bedrock. Photo by Carey Marks. 207
Appendix R.3: Repeated aerial photography showing recent rapid gully formation, deepening and hillslope progression (Lat: -3.334067°, Lon: 36.360801°). The yellow line corresponds with 100m (Source: Google Earth). 208
Appendix R.4: Interlinking of sheet erosion with lateral and upslope progression of gullies leading to badland formation. Exposed roots indicate over 50cm of soil removal (Lat: -3.316011°, Lon: 36.423080°). Photo by Maarten Wynants. 208
Appendix R.5: Degraded hillslope that has turned into badland (Lat: -3.339357°, Lon: 36.354331°). Photo by Carey Marks. 209
Appendix R.6: Hillslope terrace collapse after abandonment of agricultural soil conservation practices (Lat: -3.344074°, 36.521724°). Photo by Carey Marks. 209
Appendix R.7: Soil conservation practices with contour terraces that are buffered by permanent vegetation strips (Lat: -3.301534°, Lon: 36.519732°). Photo by Carey Marks. 210

List of Abbreviations

Al_2O_3: Aluminium oxide

Ba: Barium

BMM: Bayesian Mixing Model

CaO: Calcium oxide

Ce: Cerium

Cl: Chlorine

Co: Cobalt

Cr: Chromium

CSIA: Compound Specific Stable Isotope Analysis

Cu: Copper

DS: Deposited Sediment

EARS: East African Rift Systems

FRNs: Fallout radionuclides

F: Fluorine

FA: Fatty Acid

Fe_2O_3: Iron oxide

Ga: Gallium

K_2O: Potassium oxide

La: Lanthanum

LUCC: Land use and land cover changes

MgO: Magnesium oxide

Mn: Manganese

Na_2O: Sodium oxide

Nb: Niobium

Nd: Neodymium

Ni: Nickel

P_2O_5: Phosphorus pentoxide

Pb: Lead

Rb: Rubidium

PCA: Principal Component Analysis

RUSLE: Revised Universal Soil Loss Equation

RVL: Rift Valley Lake

SDR: Sediment Delivery Ratio

SiO_2: Silica

SO_3: Sulphur trioxide

SOM: Soil Organic Matter

Sr: Strontium

SS: Suspended Sediment

SY: Sediment Yield

Th: Thorium

Ti: Titanium

Y: Yttrium

Zn: Zinc

Zr: Zirconium

Chapter 1. Introduction

1.1 Problem analysis

Soil resources in East Africa's Rift Systems (EARS) are rapidly being depleted by erosion, threatening food-, water- and livelihood security in the region (Cobo, Dercon & Cadisch, 2010; Lal, 2001; Oldeman, 1992). A loss of permanent vegetation is causing an acceleration of surface and gully erosion on the agricultural and pastoral landscapes (Maitima *et al.*, 2009). While soil and land resources are progressively being depleted, the demand for the services they provide is increasing. The human population in East Africa's inter-lacustrine countries of Burundi, Kenya, Rwanda, Uganda and Tanzania has experienced an exponential growth from an estimated 6-12 million in the 1920s (Anderson, 1984; Trewartha & Zelinsky, 1954), 24 million in the 1950s, 56 million in the 1980s to 173 million in 2017 (UNDESA, 2017). Alongside population, its requirements for livelihoods, food, fibre, and other resources are growing rapidly (FAO, 2019). However, scapegoating this problem to overpopulation and overexploitation of natural resources fails to explain the complex human-environment interactions driving increased rates of soil erosion (Kiage, 2013; Lambin *et al.*, 2001). More than half of East Africans are still living in extreme poverty, having to survive with less than $1.8 a day (FAO, 2019; The World Bank, 2017). While the region is experiencing rapid economic growth in its urban centres (Devarajan & Kasekende, 2011), there is a lack of intensification and diversification in the agro-pastoral systems (Korotayev & Zinkina, 2015). As a result, increasing numbers of farmers are seeking land to establish agricultural operations, causing a marked shift from natural vegetation towards agricultural land (FAO, 2019; Salami, Kamara & Brixiova, 2010). This scramble for land is pushing them to areas that

are often unsuitable for agriculture and lack infrastructure (Jayne *et al.*, 2014; Odgaard, 2002). The conversion to privately owned farms has excluded pastoralists from large tracts of previously communal grazing lands. In addition to policies of sedentarisation and confinement within administrative boundaries, this exclusion is impeding the mobility of previously nomadic pastoralist communities (Homewood, Coast & Thompson, 2004). Moreover, pastoral communities are also experiencing internal pressures due to a growing population, dwindling importance of indigenous customs, and increased competition over grazing resources (Rufino *et al.*, 2013). A combination of all these factors have led to a tripling of the livestock numbers in the last 50 years (FAO, 2019) and is raising densities of domestic grazers, leading to overgrazing and trampling of the soil (Little, 1996; Ruttan *et al.*, 1999). Furthermore, the high reliance on natural vegetation as a source of fuel and fodder in both the urban and rural populations is causing massive exploitation pressures on forests and woodlands (Hiemstra-van der Horst & Hovorka, 2009). The conjunction of these multiple land pressures has been hypothesised to increase rates of soil erosion and sediment transport (Thornes, 1990). Furthermore, these processes are potentially amplified by natural rainfall variations (Ngecu & Mathu, 1999) and projected increases in extreme climatic events (Nearing, Pruski & O'neal, 2004; Shongwe *et al.*, 2011).

Increased soil erosion has a wide range of intractable detrimental impacts with potential positive feedback loops that push the agro-pastoral systems to degradation (Lal, 2001). However, the threats of land degradation to the food-, water- and livelihood security are nowhere as pressing as in East Africa (Tengberg & Stocking, 1997). First of all, the erosion mediated loss of soil and nutrients lowers the productivity of the land (Pimentel & Kounang, 1998).

Continued loss of productivity and arable land would be catastrophic for the agricultural sector in East Africa, which currently employs about 75% of the working population and is the foundation on which East African economies are build (Devarajan & Kasekende, 2011; FAO, 2019; Salami, Kamara & Brixiova, 2010). Furthermore, the majority of East Africans are directly dependent on soil productivity for their basic caloric uptake through subsistence agriculture or pastoralism (Sanchez, 2002; Tengberg & Stocking, 1997). Latest estimates classify about 30% of the East African population as malnourished. About one-fifth of the children are underweight and the prevalence of anaemia in reproductive women and stunted growth in children is very high (FAO, 2019; Tengberg & Stocking, 1997). While in some East African countries, there is a hopeful trend of decreasing numbers of malnourished people, in others the percentages and total numbers are still increasing (FAO, 2019; Korotayev & Zinkina, 2015). If erosion rates remain far beyond rates of soil production, people will lose their main source of livelihood and the per capita food production will decline even further. Communities eventually will be compelled to either adopt agricultural methods that sustain the soil or face increasing competition over a shrinking land- and resource base (Montgomery, 2007; Sanchez, 2002; Scherr, 1999; Tengberg & Stocking, 1997). The latter has the potential to destabilise the political situation, cause conflicts and increase migration out the region (Homer-Dixon, 1991; Homer-Dixon, 1994).

Besides these on-site impacts, increased soil erosion and downstream sediment transport also has major detrimental effects on aquatic ecosystems, water quality and energy security (Pimentel, 2006). East Africa's Rift Valley Lakes are some of the largest and most ecologically diverse aquatic systems in the world, supporting millions of people with water, food and livelihoods (Odada *et al.*, 2003).

Furthermore, rivers are often a vital source of water for both agro-pastoral communities and the world-renowned East African terrestrial ecosystems (Mango *et al.*, 2011). Given that ecotourism is another vital part of the economy, land- and ecosystem degradation is expected to additionally affect the livelihoods of many East Africans (Christie *et al.*, 2014). In addition, hydropower is a major part of East Africa's energy provision. Rapid siltation of reservoirs is diminishing the productive power of hydroelectric plants, thereby threatening the energy security and economic development of the region (Ndomba, 2007; Verhoeven, 2013).

It is thus clear that there is an urgent need for science-based land and water management strategies in EARS to achieve sustainable intensification of agro-pastoral production. However, there is still a lack of understanding on the complex drivers and feedbacks of increased soil erosion in the agro-pastoral systems of East Africa (Ananda & Herath, 2003; Blaikie & Brookfield, 2015; Kiage, 2013). Furthermore, a historical dearth in environmental data impedes the spatial and temporal assessment of the dynamics in land cover, soil erosion and catchment sediment transport. This complicates the development and application of sustainable land and water management strategies (Blake *et al.*, 2018b).

1.2 Aims and objectives

In the context of this wicked problem of soil degradation, the overall aim of this project is to further the understanding of the complex dynamics of increased erosion and sediment transport in EARS. An attempt will be made to answer some pressing questions. What are the main drivers of increased soil erosion? Are there internal feedback mechanisms in place? How does increased erosion affect downstream sedimentation? How does the sediment move through the system? How do land use and land cover changes (LUCC) and rainfall variability influence sediment connectivity on the basin scale?

The objective of the first literature review chapter (Chapter 2) is to provide a general background to the processes that operate within the natural soil-sediment continuum in East African Rift Lake catchments. The second, more analytical, literature chapter (Chapter 3) aims to position the problem in its complex social, economic and environmental context, by performing a detailed historical and contemporary analysis of the drivers and impacts of increased soil erosion in East Africa's agro-pastoral landscapes. Subsequently, the characteristics of the Lake Manyara catchment system in Tanzania are described (Chapter 4) with the objective to demonstrate its value as a microcosm of East Africa's diverse socio-ecological systems. The original research chapters of the project (Chapters 5-9) apply state-of-the-art environmental diagnostic tools with the aim to fill the identified scientific caveats in soil erosion and sediment transport in EARS. Each chapter has a specific research objective, which are summarised here:

- Chapter 5: Use satellite images to quantify and map temporal land cover changes over the past few decades in the wider Lake Manyara catchment.
- Chapter 6: Integrate land cover outputs with other remotely sensed data in a RUSLE model to pinpoint areas of increased erosion risk and estimate changes in soil erosion and tributary sediment delivery between 1988 and 2016.
- Chapter 7: Apply sediment geochronological techniques to assess changes in the sedimentation rate of Lake Manyara over the past century. Use geochemical tracing coupled with Bayesian Mixing Models (BMMs) to attribute dominant tributary sources of sediment to Lake Manyara and link changes over time to patterns of sedimentation.

- Chapter 8: Deconvolute sediment fluxes to the sub-tributary level with special attention to the role of sediment capture and -connectivity for downstream sedimentation.
- Chapter 9: Apply composite fingerprinting (i.e. biochemical and geochemical tracers) to assess the dominant land use, catchment zone, and erosion processes of current sediment fluxes. Combine composite fingerprinting with sediment geochronological techniques to understand the changing dynamics of increased soil erosion and sediment transport under LUCC.

By integrating these complementary evidence bases, this project ultimately aims to demonstrate links between LUCC, soil erosion, land degradation and the downstream aquatic impacts, thereby contributing to targeted management interventions to maintain soil health and water quality.

Chapter 2. The soil-sediment continuum in East African Rift Lake catchments

Terrestrial landscapes are naturally moulded by soil erosion, sediment transport and deposition processes, all taking part in a natural conveyor belt towards the oceans where material is continually recycled in the Earth's crust as the tectonic plates spread apart and collide to form new mountains (Montgomery, 2007; Morgan, 2005). Erosion is the result of two major processes: weathering of the bedrock material into soil particles and the detachment and transport of these particles by the elements. These processes are internally structured by separate smaller processes, which are generally classified by their particular mechanisms (Kirkby, 2008). In stable environments, hillslope soils develop over time towards a balance between erosion and soil production via weathering, where soils have their characteristic thickness for a particular climate and geological setting. As a result, soils and ecosystems evolve together through a mutual interdependence on the balance between soil erosion and soil production (Lowdermilk, 1953).

Bearing this in mind, EARS catchments naturally have high sediment yields (SY) as illustrated in Figure 1, which is largely due to the interaction between the semi-arid climate with high rainfall erosivity and disequilibrium vegetation, prevalence of fragile soils, tectonic activity and a distinct topography (Vanmaercke *et al.*, 2014; Walling & Webb, 1983). In this chapter, a background on the natural processes and influencing factors of soil erosion, sediment transport and sedimentation will be framed in the specific East African context.

2.1 Detachment and transport processes

There are numerous modes of detachment and transportation, which are often grouped based on the dominant processes. The rate of transport can be limited

by the transporting capacity of the process or limited by the supply of suitable material for transport (Gale & Haworth, 2005). Even though wind and gravity are important agents of erosion (Goudie, 1989; Selby, 1982), this project focusses on physical processes of water erosion and transport because of the dominant role it plays in soil erosion and sediment transport dynamics in EARS catchments, especially in the context of human-exacerbated soil erosion (Kirkby, 2008).

Figure 1: A global overview of SY, clearly showing the higher yields in semi-arid and mountainous regions (Walling & Webb, 1983).

Water can detach fragments of rock or soil in three ways: (i) water permeating a fine-grained deposit and converting it into a mixture of water and sediment which moves as a thick slurry (Iverson, 1997), (ii) detachment by raindrop impact (Poesen, 1985; Poesen, 1992), and (iii) flow of water over the surface picking up material (Shields, 1936). The first process is called fluidisation, and is able to carry large masses of material in debris flows (Iverson, 1997). Even though these rapid mass movements occur in small numbers and have a slower return time, the quantity of sediment they transport can be far in excess of that contributed by other processes (Morgan, 2005; Temple & Rapp, 1972). The main difference is

that during fluidisation, water is the agent reducing the frictional resistance of the soil mass and gravity is the main transporting force, while during raindrop impact and water flow processes, water is directly exerting the force for transport on the individual particles (Poesen, 1992; Selby, 1982). In the next two subsections, a distinction will be made between wash processes active on the soil surface (e.g. surface erosion: rainsplash, overland flow and rill erosion) and erosion resulting from the incision of the water in the soil (e.g. subsurface erosion: gully- and river bank erosion).

2.1.1 Surface erosion

Material is detached from the soil surface in two ways, by raindrop impact and flow traction, and transported either by jumping through the air or in a flow of water. Combination of these modes of detachment and transport give rise to the three different processes: rainsplash, rainwash and rillwash (Kirkby, 2008; Poesen, 1985; Poesen, 1992).

Rainsplash constitutes erosion from raindrop impact on the soil surface that detaches soil particles or small aggregates (Farres, 1987; Mutchler & Young, 1975; Poesen, 1985). Transportation through the air, usually in a series of hops, projects the particles in all directions, however the dominant direction is influenced by the impact direction of the raindrops and the slope of the area (Moeyersons, 1983; Poesen, 1985). The total rate of detachment is dependent on the energy of the raindrops, size of the particles and the stability of the soil aggregates (Farres, 1987; Gabet & Dunne, 2003; Pedersen & Hasholt, 1995; Poesen, 1985). If the rainfall intensity is higher than the infiltration in the soil, the water will start running off the hillslope as overland flow (Govers & Poesen, 1988). During the process of **rainwash,** the flow of water is not deep enough to absorb all the rain energy so that the soil still gets dislodged by rain impact and the

turbulence it creates (Palmer, 1963), but at the same time the tractive stress of the flowing water is still too low for dislodgement by the flow (Shields, 1936). Material dislodged by raindrop impact is subsequently transported by this rainwash and is moved much further and more rapidly than by aerial rainsplash (Govers & Poesen, 1988; Govers & Rauws, 1986). Once the exerted tractive stress by flowing water on the soil is sufficient to overcome the frictional and cohesion resistance of soil particles, they get dislodged (Savat, 1982; Shields, 1936). This process is called **sheetwash** and the rate of dislodgement is dependent on the shear velocity of the flow and the unit of discharge (Govers & Rauws, 1986). Rills are incised flow convergence lines that are initiated at a critical distance downslope, where sheet wash flow becomes channelled. These rills eventually converge into larger and larger rills and the increase in discharge intensifies particles movement, whereby small channels or trenches are cut by scouring (Merritt, 1984). Further downstream, these rill channels join up into bigger and bigger channels, eventually ending up in gullies, with head-cutting processes enlarging channel size, or the permanent channel network (Parsons, Abrahams & Luk, 1990). Coarser soils are more resistant to detachment because the larger particle weight results into a higher frictional resistance. However, the level of cohesion between soil particles is negatively correlated with grain size, making finer soils resistant to detachment as well (Savat, 1982). As a result, the most vulnerable group to rainsplash and flow detachment are intermediate grain sizes such as the silt loams, loams, fine sands and sandy loams as illustrated in Figure 2 (Kirkby, 2008; Poesen, 1992; Savat, 1982). In reality, the resistance to detachment is influenced by many other soil factors depending on the local environmental context. For example, Abrahams, Parsons and Hirsch (1992) found that plant cover and the microtopographic form of the soil surface are more

important in controlling particle detachment in semi-arid grasslands. In some cases, grain size effects may explain as little as 5 percent of the total resistance to detachment.

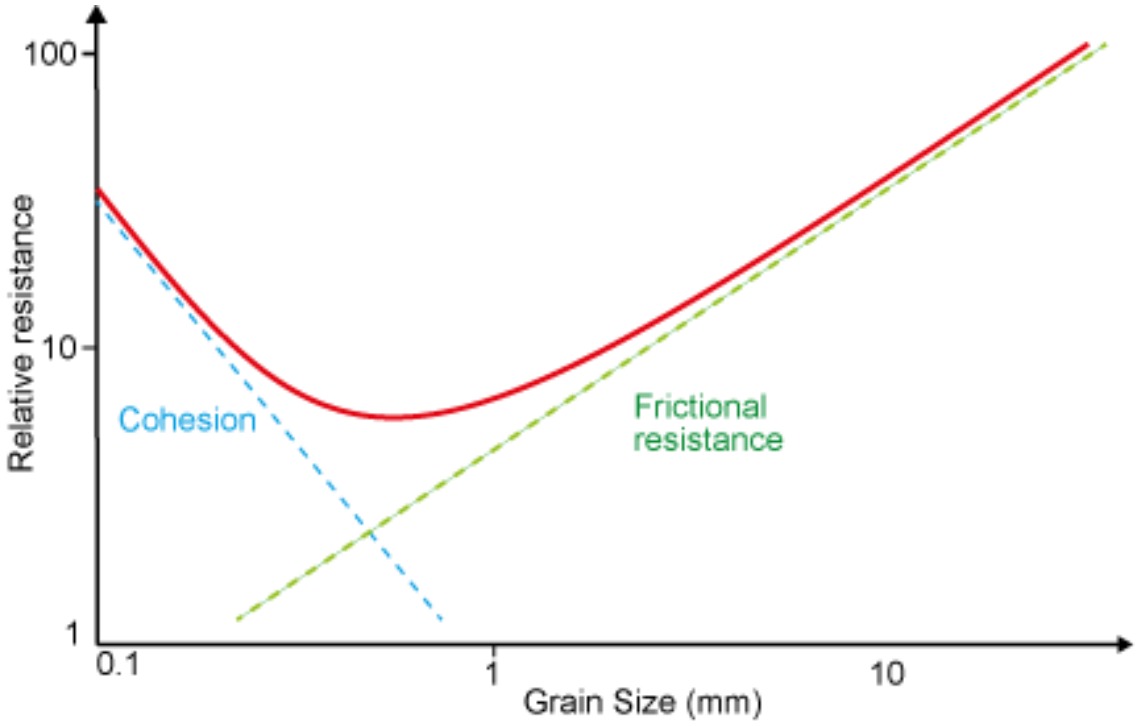

Figure 2: Simplified relation between the combined functions of cohesion (blue dashed) and friction (green dashed) effects resulting in the specific relative resistance (red full) of soil particles to detachment with the lowest resistance to detachment in intermediate grain fractions. Adapted from Kirkby (2008).

2.1.2 Subsurface erosion: gully- and riverine erosion

Gullies are relatively permanent steep-sided watercourses that experience ephemeral flows during rainstorms. A widely recognized definition used to separate gullies from rills is that they have a cross-sectional area greater than 1 m^2, although there are also process-related differences that relate to gullies being largely formed by head-cutting processes and rills being formed by flow convergence (Heede, 1975; Poesen, 1993; Valentin, Poesen & Li, 2005). Gullies have a greater depth and smaller width than river channels, carry larger sediment loads, are less stable and display very erratic behaviour (Poesen, 1993; Poesen, 2011). While gullies are often related to human-induced land use change, they are intrinsically natural and a common geomorphologic phenomenon in semi-arid

East Africa (Castillo & Gómez, 2016; Poesen *et al.*, 2003; Valentin, Poesen & Li, 2005). The main cause of gully formation is a disequilibrium between the amount of water runoff and stabilising vegetation, a condition that may be brought about by natural variations in climate and vegetation (semi-arid areas) as will be explained in sections 2.2.3 and 2.2.4.

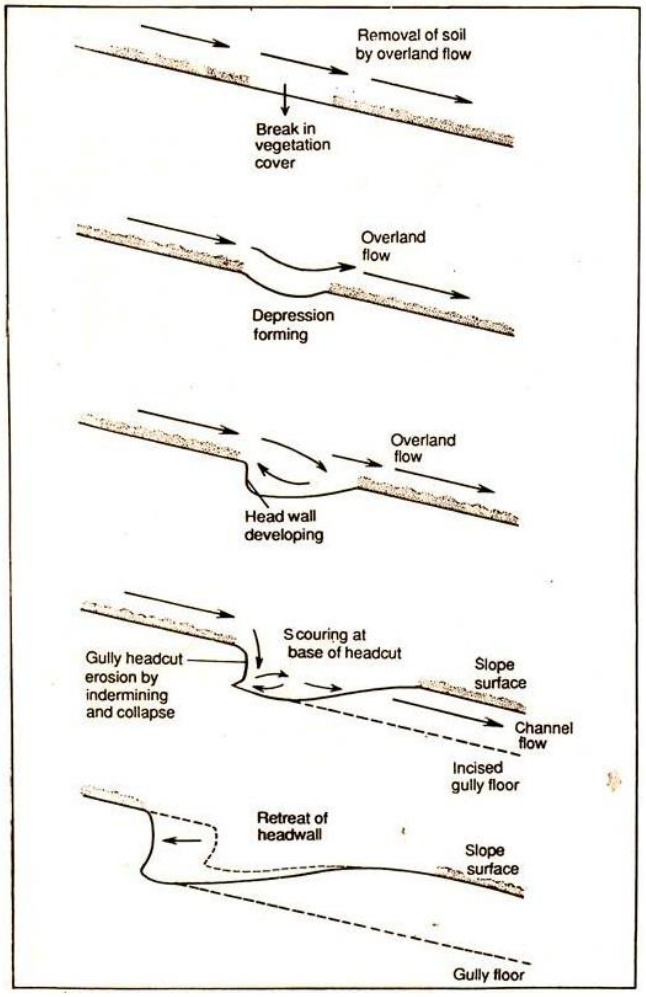

Figure 3: Stages in gully development on a hillslope (Leopold, Wolman & Miller, 2012).

However, more recently increased gullying in East Africa has been linked to climate change and LUCC (Poesen, 1993; Poesen *et al.*, 2003; Valentin, Poesen & Li, 2005). Deforestation, unsustainable agricultural practices, burning of the vegetation and overgrazing can all result in higher amounts of runoff. If the velocity or tractive force of the runoff exceeds a threshold, gullies will be formed (Castillo & Gómez, 2016; Poesen *et al.*, 2003; Schumm, 1979; Valentin, Poesen

& Li, 2005). The initiation of gullies is a complex process (Figure 3) starting in natural or human-made depressions on hillslopes (Castillo & Gómez, 2016; Leopold, Wolman & Miller, 2012; Prosser & Winchester, 1996; Valentin, Poesen & Li, 2005). Run-off concentrates in these depressions and enlarges them until several of them merge and an incipient channel is formed. Erosion is concentrated at the headcuts of the depressions, where steep, almost vertical, scarps develop, over which supercritical flow occurs. Most erosion happens by scouring at the base of the scarp, which deepens the channel, but also undercuts the headwall, resulting into collapse and retreat of the scarp upslope. The scouring action of the water flowing through the gullies and slumping of the banks also creates bank erosion, dislodging sediment further down the gully (Leopold, Wolman & Miller, 2012; Valentin, Poesen & Li, 2005). Hillside gullies may be continuous, which means they discharge into the river channel downstream, or discontinuous, fading out into a depositional zone and not reaching the river. Once formed, they can both grow upslope by headward retreat, and downslope, by incision of the channel floor (Leopold, Wolman & Miller, 2012; Morgan, 2005). Gullies can also form on the valley floor, when increased runoff concentrates in these topographic swales during heavy rains (Poesen, 1989). Even though individual gullies can remove vast quantities of soil, their contribution to the total soil loss is dependent on the gully density in the region, which is often low in natural conditions (Poesen *et al.*, 2003). However, in fragile and extremely disturbed environments, high rates of gully erosion may evolve the landscape badlands (Bryan & Yair, 1982; Castillo & Gómez, 2016; López-Bermúdez & Romero-Diaz, 1989; Prosser & Winchester, 1996; Valentin, Poesen & Li, 2005). The relative contribution of sheet wash and gully erosion depends on many environmental factors, is dynamic and often difficult to determine given the

relative invisibility of sheet wash erosion compared to gully erosion (Ben Slimane *et al.*, 2016).

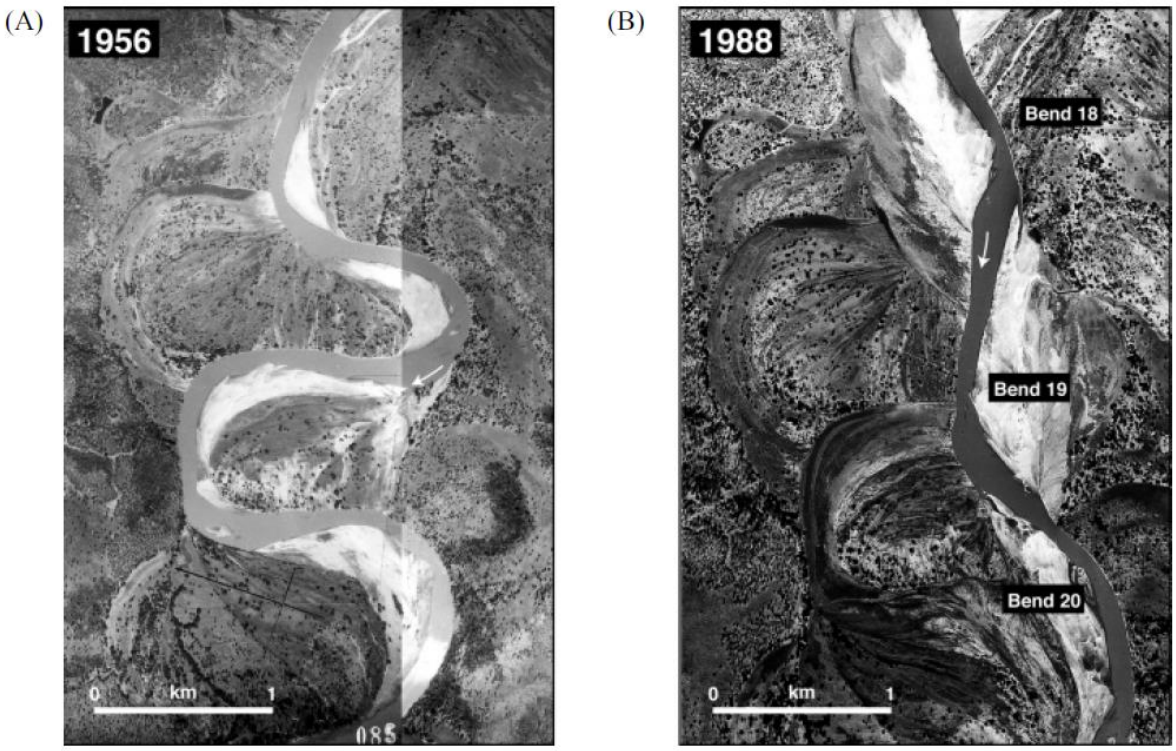

Figure 4: Channel planform change and meander development over a thirty year period in the semi-arid Luangwa River, Zambia (Gilvear, Winterbottom & Sichingabula, 2000).

The catchment river system constitutes of a continuous network of **river channels**, which are permanent geomorphological features that can widen or deepen by flowing water, or filled in by sediment deposition (Kirkby, 2008). These permanent channels can be fed by rain-, spring- and groundwater or a combination. Nevertheless around their stream banks, erosion occurs naturally from the powerful action of the adjacent moving water (Ashbridge, 1995; Hooke, 1979). The intensity and processes of erosion is largely dependent on the river gradient, bedrock material, riverbank characteristics, discharge volume and flood dynamics (Rosgen, 1994). The latter two are ultimately controlled by run-off dynamics upstream and how the water cascades down the catchment. Upstream run-off dynamics, hydrological connectivity and river gradient thus control downstream riverine erosion (Bracken & Croke, 2007; Heritage *et al.*, 2004;

Hooke, 1979). Little research has been done on river hydrology and -erosion in East Africa, therefore it is useful to evaluate evidence from river systems in similar semi-arid environments. Nonetheless, there is a great diversity in river channel types due to the dynamic and diverse climate and topography (Kaaya, 2015). Almost all East African river systems are characterised by seasonal discharge regimes and many are completely ephemeral, which means they respectively have a low or no flow during the dry season and can experience rapid flood peaks after rainstorms (Kaaya, 2015; Maingi & Marsh, 2002; Unesco, 1969). The flow intensity during these flood events can be very high, leading to high levels of bank- and bed erosion (Erskine & Warner, 1999; Yu *et al.*, 2017). These high erosion events gives semi-arid rivers distinct morphologies, which in turn influences the flow characteristics and downstream sediment transport and erosion processes (Bull, 2002; Heritage *et al.*, 2004; Powell *et al.*, 2012). Highland areas in East Africa are, even though the presence of rainfall seasonality, often permanently wet, giving rise to permanent fast flowing rivers (Kaaya, 2015). In general, these rapid flowing rivers will be dominated by erosion over deposition because of the high kinetic energy of the water and quick transport downstream. This gives rise to supply limited river channels, characterised by straight and deeply incised valleys developed on bedrock material (Rosgen, 1994). When rivers, both permanent and ephemeral, enter low-sloped areas, their flow will slow down, lowering the transport capacity of particles in the water. This gradual decrease in transport capacity gives rise to higher levels of in-channel deposition (Croke, Fryirs & Thompson, 2013). Nonetheless, erosional processes remain very important (Ashbridge, 1995), especially in the context of seasonal flood peaks typical for East Africa (Maingi & Marsh, 2002). This balance between erosion and deposition creates a wide variety of river

channel types depending on river gradient, discharge seasonality, riverbank and –bed characteristics and sediment supply (Gilvear, Winterbottom & Sichingabula, 2000; Heritage *et al.*, 2004; Montgomery & Buffington, 1998; Rosgen, 1994). Lowland river channels are thus often spatially dynamic, constantly migrating over the floodplain where new channels are eroded, while other channels deactivate and are filled in with sediments as illustrated in Figure 4 (Croke, Fryirs & Thompson, 2013; Gilvear, Winterbottom & Sichingabula, 2000). Increased discharge following LUCC disrupts the balance by increasing erosion intensities and decreasing deposition, often leading to channel widening and/or deepening, especially in rivers developed on alluvial sediment (Dagnew *et al.*, 2015; Montgomery & Buffington, 1998; Simon & Rinaldi, 2006). This reworking of earlier deposited floodplain sediment adds complexity to the source-to-sink dynamics in river catchments, which will be further explored in sections 2.3 and 2.4.

2.2 Natural controlling factors of soil erosion processes

In the previous section, the theoretical background of the different erosion processes was discussed. However, the intensity and prevalence of these erosion processes depends on the location and characteristics of the catchment. The areas close to the catchment divide in catchments are only subject to rainsplash, which feeds into areas, some disconnected, with thin films of water where rainflow is dominant (Govers & Poesen, 1988; Morgan, 2005). These areas in turn provide sediment to the eroding channels where rillwash is actively detaching material and enlarging the channels (Govers & Poesen, 1988). The process of water erosion is closely related to the pathways taken by water in its movement through the vegetation cover and over the ground surface. While not all run-off ends in permanent channels, the water that ends up in gullies and river channels influences erosion and sedimentation processes (Valentin, Poesen &

Li, 2005). Differences in geology, slope, soil, climate and vegetation, influence the erosion and runoff dynamics and intensities (Morgan, 2005; Morgan, Martin & Noble, 1987). In an East African context this creates a complex patchwork, where the interlinking of these factors will create site- and catchment specific erosion and run-off dynamics (Jacobs *et al.*, 2018), demonstrating the importance of considering catchment connectivity.

2.2.1 Topography and geology

A meta-analysis of Vanmaercke *et al.* (2014) showed that the high SY in East Africa are mainly explained by its high geological activity. High geological activity leads to high levels of soil erosion and sediment transport by earthquakes and volcanic tremors that trigger landslides (Hovius *et al.*, 2011), seismic weakening of rocks due to fracturing (Koons, Upton & Barker, 2012), but most importantly an increased rate in slope erosion processes and river incision as a response to catchment uplift (Whittaker, Attal & Allen, 2010). Slope influences erosion mostly through its gradient and length, which influences erosion and run-off processes (Kirkby, 2008; Morgan, 2005). To start, neutral soil movement processes, such as wetting expansion, biological mixing and rainsplash, create a net downward movement due to the influence of gravity (Benedict, 1976; Moeyersons, 1983; Roering *et al.*, 2002). More importantly though, precipitated water has less time to infiltrate the soil on steep slopes, giving rise to higher amount of run-off, which can transport dislodged material rapidly downstream and has a higher energy to erode the land due to the more rapid flow (Govers, 1992; Poesen, 1992). Slope length is important because it influences the upslope contributing area and thus amount of run-off discharge. Longer slopes usually generate higher amounts of run-off, which in turn has a higher energy to erode the land (Govers, 1992). Therefore, rill erosion increases substantially more with increasing slope gradient

and -length than interrill erosion (Fox & Bryan, 2000; Govers & Poesen, 1988). Globally, sloped areas thus have higher erosion rates than flat regions as shown by a meta-analysis of Montgomery (2007), which found an increase in geological erosion rates from gently sloping lowland landscapes (<10^{-4} to 0.01 mm/yr), to moderate gradient hillslopes (0.001 to 1 mm/yr) and steep tectonically active alpine topography (0.1 to >10 mm/yr) (Figure 5).

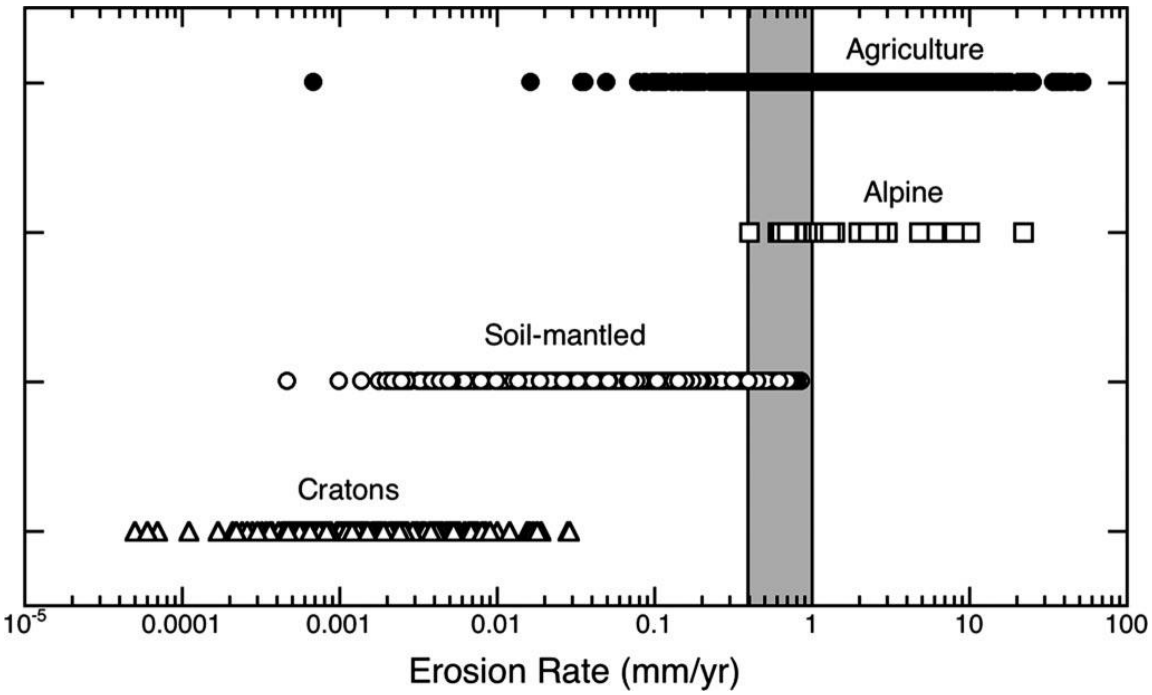

Figure 5: Comparison of soil erosion rates (in mm yr^{-1}) from agricultural fields under conventional agriculture and natural erosion rates from low gradient continental cratons, soil-mantled landscapes, and alpine terrain. Note that soil erosion rates from agricultural fields in all terrains is similar to natural rates in alpine regions. Shaded area represents range of the USDA standards (0.4-1.0 mm yr^{-1}) for tolerable soil loss (Montgomery, 2007).

Soil erosion on different slope gradients shows several features, although with many exceptions according to local conditions and history. While slope is necessary to create the forces for erosion, e.g. gravity and water flow, the interplay with other factors such as soil, climate and vegetation controls the intensities and dynamics of soil erosion and run-off processes (Kirkby, 2008). For example, Hudson and Jackson (1959) found that the effect of slope is stronger under semi-arid conditions, where rainfall is more intense, indicating the importance of climate. Moreover, Quinn, Morgan and Smith (1980) and Lal (1976)

found evidence that variations in vegetation cover have an exacerbated effect in sloped areas (McDonald, Healey & Stevens, 2002).

2.2.2 Soil characteristics

Differences in soil characteristics naturally influence the erosion vulnerability of an area, because they define the drainage capacity and resistance of the soil to both detachment and transport. This erodibility varies with soil texture, aggregate stability, shear strength, infiltration capacity and organic and chemical content (Morgan, 2005). As explained in subsection 2.1.1, the soil texture partly influences the resistance to detachment, as bigger particles have higher weights and smaller particles have stronger cohesive bonds (Poesen, 1992). Moreover, organic and chemical constituents of the soil are important because of their influence on aggregate stability (Evans, 1980). In general, permanent natural vegetation improves the soil structure by bioturbations and increasing the Soil organic matter (SOM) content through input of litter (Gyssels *et al.*, 2005; Sombroek, 1993). Furthermore, the drainage capacity of different soils is influenced by texture, organic matter content and structural development. Poorly-drained soils generate more run-off water than well-drained soils, increasing the wash potential downstream (Morgan, 2005). In semi-arid Africa, the impact of raindrops on exposed soil aggregates do not only lead to detachment but also consolidation in the form of a **surface crust** (Mutchler & Young, 1975; Tarchitzky *et al.*, 1984). As raindrops strike the surface, the impact energy can break aggregates down to their constituent grains and smaller aggregates. Moreover, some water is forced into aggregates, compressing air inside them, causing them to explode in a process known as slaking (Farres, 1987). The loose grains are subsequently washed into pore spaces around intact aggregates, creating and impermeable seal (Tarchitzky *et al.*, 1984). This crust creates an impermeable

surface that limits infiltration and increases runoff from subsequent rains (Casenave & Valentin, 1992; Luk & Cai, 1990; Tarchitzky *et al.*, 1984). The actual crusting response of a soil depends on its moisture content and, therefore, structural state (Bissonnais, 1990; Tarchitzky *et al.*, 1984) and the intensity of the rain (Poesen & Govers, 1986). Moreover, crustability decreases with increasing contents of clay and organic material since these provide greater strength to the soil. In general, loams and sandy loams are the most vulnerable to crust formation. An exception to this rule are cracking clay soils, which are widespread in East Africa. When these soils are wetted by the rain, they start to swell, creating an impermeable soil crust as well (Bissonnais, 1996; Casenave & Valentin, 1992; Morgan, 2005; Tarchitzky *et al.*, 1984). In conclusion, the soils in the semi-arid landscapes of East Africa have a natural high erodibility due to a combination of low SOM content, weak structural development and a high vulnerability to soil crusting or cracking (Mati & Veihe, 2001; Morgan, 2005; Veihe, 2002).

2.2.3 Climate

The effect of climate is closely linked with the rainfall amount and intensity. As explained in previous section of detachment and transport processes, precipitation influences erosion both directly by rainsplash erosion and indirectly through run-off mediated wash processes (Morgan, 2005). Most areas in East Africa are characterised by a distinct seasonality in precipitation with a dry season and one or two wet seasons. As most rainfall comes down in seasonal high intensity rains, the rainfall erosivity can be much higher than in temperate areas (Moore, 1979; Nicholson, 1996). Furthermore, during these high intensity rains, higher amounts of Hortonian overland flow is generated because the rate of rainfall on the surface generally exceeds the rate at which water can infiltrate the

ground (Horton, 1941). This high amount of run-off production also generates a high wash erosion potential through the kinetic energy of flowing water.

The most important climatic factor controlling erosion in East Africa is thus not the total rainfall amount but the frequency of high intensity rainfall events (Hudson, 1981; Rapp *et al.*, 1972). Hudson (1981) emphasized this by his research in Zimbabwe, where he found that about 50 per cent of the annual soil loss occurred in only two storms and that during one year even 75 per cent of the erosion took place in ten minutes. Another important factor for climate driven soil erosion in East Africa is linked to the high inter-annual variability in rainfall (Ngecu & Mathu, 1999), which is driven by an interplay of multiple global and local factors of which the exact details are still largely unknown (Nicholson, 1996; Souverijns *et al.*, 2016). One important phenomenon driving this variation is the El-Nino southern oscillation (Ropelewski & Halpert, 1987; Wolff *et al.*, 2011). The extreme rainfall during the 1998 El Nino triggered landslides and general higher erosion rates in East Africa (Ngecu & Mathu, 1999). Given all these climatic effects on erosion it is uncertain how climate change will alter the erosion dynamics in East Africa (Nearing, Pruski & O'neal, 2004; Pricope *et al.*, 2013). First, there is a lot of uncertainty about the extent of the climate changes in different parts in East Africa. A study by Souverijns *et al.* (2016) predicts a decrease in precipitation in the Ethiopian highlands, Sudan and the great lakes, and an increase in Tanzania, Uganda, Kenya and Somalia. However, due to the complex interplay between climate, vegetation, topography, geology and soil it is hard to tell how the erosion dynamics will respond (Nearing, Pruski & O'neal, 2004). For example, in East Africa precipitation is often linked to altitude, leading to an interesting synergy of high rainfall erosivity and slope effects, characterised by higher amounts of rainsplash erosion, but also run-off and wash erosion (Hudson & Jackson, 1959;

Moore, 1979). Models predicting the change in soil erosion therefore often have conflicting outcomes under different climate change scenarios and in different regions of the world (Correa *et al.*, 2016; Dabney, Yoder & Vieira, 2012; Zhang *et al.*, 2012). The multiple and complex interactions between vegetation and climate will be discussed in next subsection.

2.2.4 Vegetation

Vegetation influences the erosional vulnerability of the soil in numerous ways (Greenway, 1987; Thornes, 1990). The roots of trees and other plants act as a natural anchor by increasing the frictional resistance of soil particles, increasing slope stability and ultimately keeping the soil from moving (Greenway, 1987; Gyssels *et al.*, 2005; Reubens *et al.*, 2007). Moreover, vegetation cover directly buffers the impact energy of rain, reducing the rainfall erosivity (Hudson & Jackson, 1959; Morgan, 2005). Furthermore, vegetation and their roots physically obstruct run-off, decreasing the flow energy, while simultaneously promoting infiltration. Fauna and flora also promote infiltration by enhancing the soil structure through bioturbations and the addition of SOM (Greenway, 1987; Temple, 1982; Thornes, 1990). Last of all, vegetation cover and SOM dramatically reduces crust formation (Rhoton, Shipitalo & Lindbo, 2002; Thornes, 1990). All previous factors cause a very strong relationship between vegetation, runoff generation and erosion (Thornes, 1990).

However, the effect of vegetation is strongly linked to climate, more specifically rainfall amounts and seasonality. This interplay between precipitation, which promotes erosion but at the same time promotes vegetation growth which buffers that erosion, creates a clear global trend in SY as illustrated in Figure 1 (Walling & Kleo, 1979; Walling & Webb, 1983). East Africa's tropical and Afromontane zones are characterised by a more constant high amount of precipitation and thus

also a constant high potential for rainfall and wash erosion. However, these wet regions also allow the development of tropical forests that constantly buffer the run-off and erosion processes (Prins & Loth, 1988). East Africa's semi-arid regions are characterised by a long dry season and one or multiple rainy seasons (Nicholson, 1996). In these seasonal conditions, vegetation cover responds to monthly changes in rainfall with some delay. Due to this delayed response of the vegetation, there is nothing to buffer the erosional energy of the first rains. This causes the wash erosion potential to be very high in the beginning of the rainy season as illustrated by Kirkby (1980) in Figure 6a.

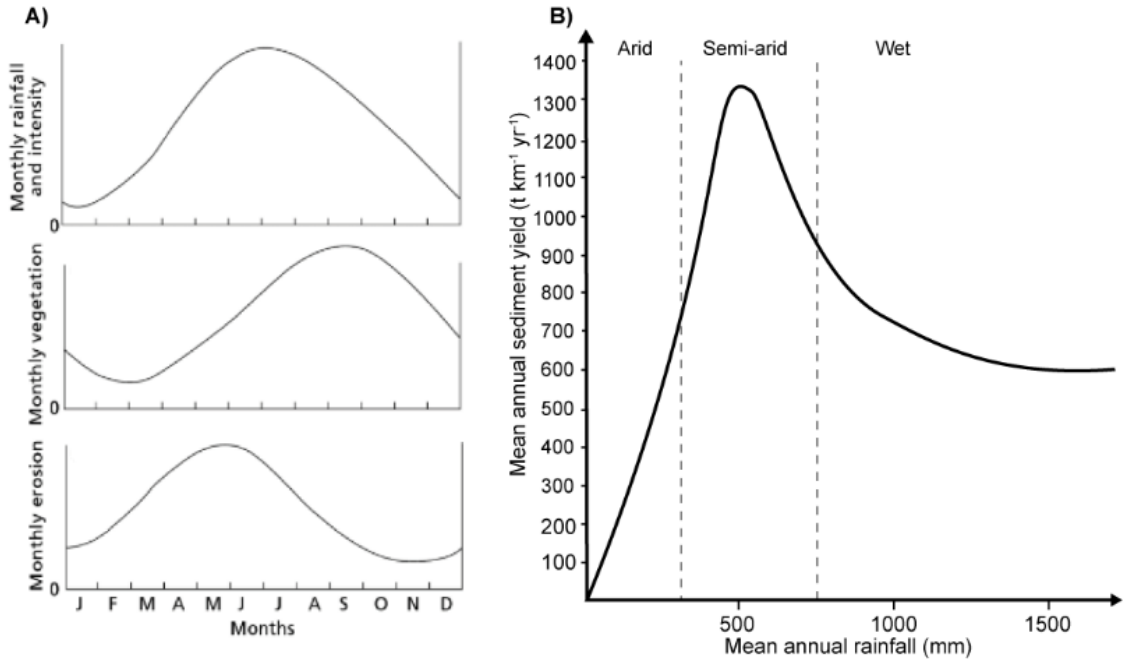

Figure 6: A) Seasonal cycle of rainfall and response of vegetation cover and erosion in a semi-arid climate (Kirkby, 1980), and B) the simplified relationship between SY and mean annual precipitation, adapted from Langbein and Schumm (1958).

Besides intra-annual seasonality, the East African climate is also characterised by high inter-annual variability and unpredictability, with dry and wet years or periods (Nicholson, 1996). Combined with the high prevalence of other disturbances such as grazing and wildfires, it is argued that East Africa's semi-arid ecosystems are in a constant disequilibrium, where concepts of climax vegetation and carrying capacity do not apply. These disequilibrium ecosystems

are naturally much more vulnerable to soil erosion due to the discrepancies between stabilising vegetation and rainfall (Kiage, 2013; Little, 1996; Ngecu & Mathu, 1999; Sullivan & Rohde, 2002). Therefore, catchments in semi-arid areas are globally observed to have higher mean annual SY than tropical catchments (Langbein & Schumm, 1958; Walling & Webb, 1983) as illustrated in Figure 6b.

2.3 Sediment connectivity

In previous sections, the processes of erosion and run-off generation and their influencing factors were described in detail. However, to illustrate the dynamic movement of sediment particles through the catchment, an understanding of the concept of sediment connectivity is required. It describes the potential for eroded soil particles to move through the system, and can also be used to address spatial and temporal variability in sediment delivery and storage (Bracken & Croke, 2007; Croke, Fryirs & Thompson, 2013; Fryirs, 2013; Hooke, 2003).

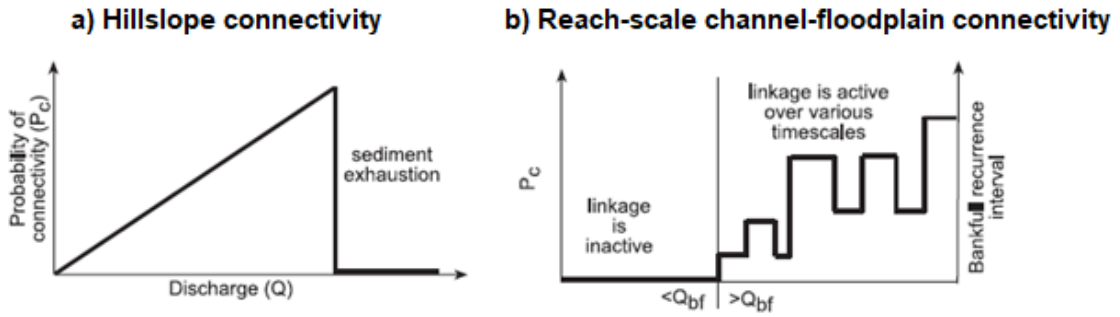

Figure 7: Croke, Fryirs and Thompson (2013) conceptual representation of a) hillslope connectivity where the probability of connectivity increases linearly with increasing discharge until sediment exhaustion occurs and b) reach-scale/channel-floodplain connectivity where the probability of connectivity only goes up after reaching a treshhold of flow (Q_{bf}) and after varies as a function of bankfull recurrence interval.

The sedimentological connectivity in catchments is largely controlled by hydrological connectivity, and is dependent on six major factors: (1) climate, (2) hillslope runoff potential, (3) delivery pathway, (4) lateral buffering, (5) landscape position, and (6) sediment propagation (Bracken *et al.*, 2013; Bracken & Croke, 2007). First, **climate** is an important factor because it influences rainfall extent,

duration and intensity, as well as the antecedent conditions in the catchment. As explained during previous section, semi-arid East Africa is characterised by seasonal torrential rains producing runoff through Hortonian overland flow (Horton, 1941). These torrential rains are often localised to specific areas in the catchment. Runoff-producing areas in East Africa are thus patchy by nature and do not necessarily relate to the downstream channel network, resulting in a mosaic of ephemeral channel floods (Jacobs *et al.*, 2018). It is more difficult for connectivity to be achieved in semi-arid catchments because of the interaction and response of this mosaic of patches to rainfall (Ambroise, 2004). Secondly, hillslopes, as the major landscape unit, are spatially variable in hydrological properties due to complex geological, pedalogical and management histories (Fitzjohn, Ternan & Williams, 1998). Many factors influence **hillslope runoff**, including the slope gradient, surface roughness, soil characteristics, vegetation type and density, land use and many more (Auzet *et al.*, 1993; Lal, 1990a; Puttock *et al.*, 2013; Singer & Le Bissonnais, 1998). In general, the sedimentological connectivity on hillslopes varies as a linear function of increasing runoff production until sediment exhaustion occurs as visualized in Figure 7a (Croke, Fryirs & Thompson, 2013). Human land use can both increase hillslope connectivity by increasing run-off following vegetation removal (Guzha *et al.*, 2018), or decrease connectivity by installing terraces and planting vegetation strips (Saiz *et al.*, 2016). The third major influencing factor of sediment connectivity is related to the **delivery pathway** of sediment from hillslope to river channel. Broadly speaking, runoff flowpaths can be subdivided into dispersive flows and channelized flows, the latter having a much higher probability of connectivity to the drainage line (Bracken & Croke, 2007) and thus transporting the sediment further downstream. Again, the delivery pathway is highly

dependent on previously discussed factors such as topography, surface roughness, vegetation and land use (Auzet *et al.*, 1993; Jacobs *et al.*, 2018; Montgomery, 1994). **Lateral buffering** is an important factor in the physical decoupling of hillslope to channels, limiting sediment delivery to the channel as illustrated in Figure 8a (Michaelides & Wainwright, 2002). This decoupling can be achieved by the presence of wetlands, swamps or riparian vegetation (Figure 8b) that act like a buffer to the runoff coming from hillslopes (Bracken & Croke, 2007; Tabacchi *et al.*, 2000). Research by Harvey (1996) and Michaelides and Wainwright (2002) has revealed important differences in catchment response when hillslopes are directly connected to a drainage line or are decoupled.

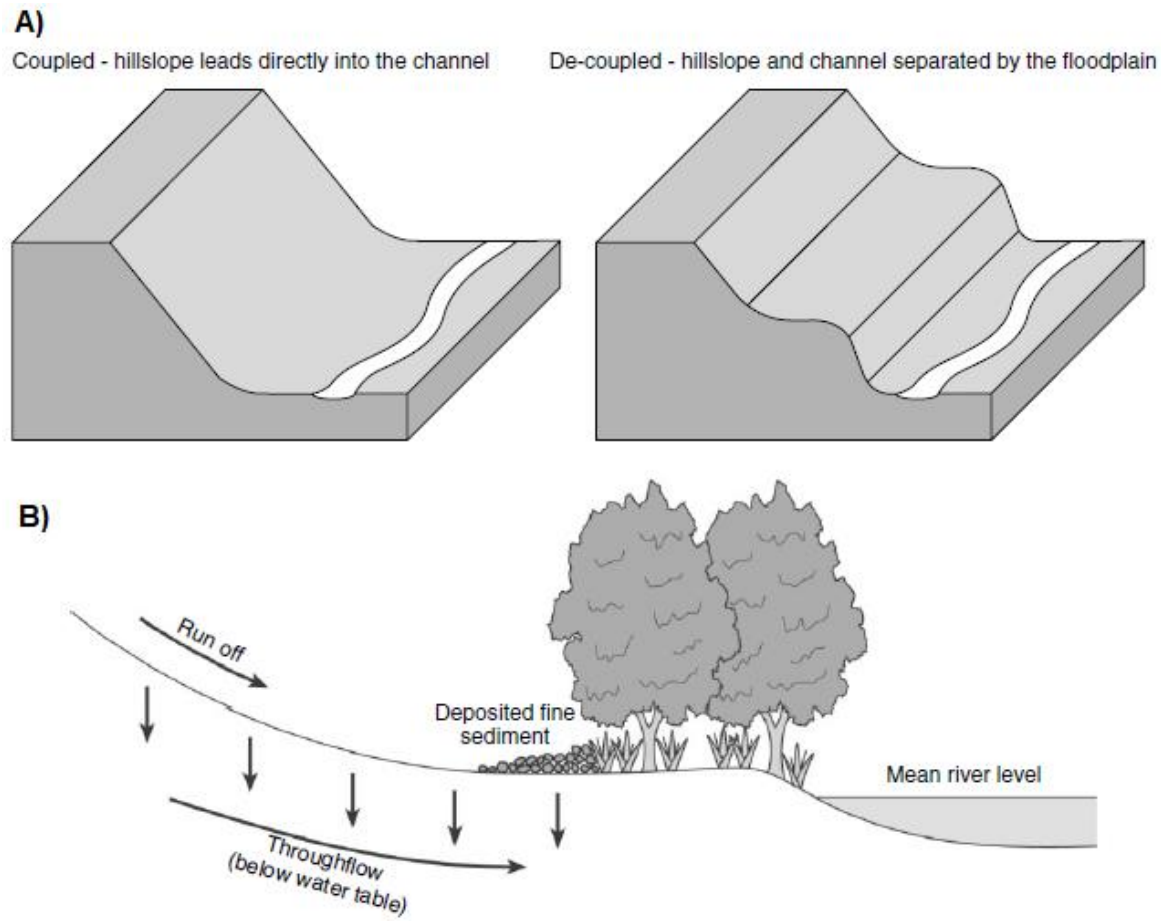

Figure 8: A) Illustration of connected and disconnected hillslope-channel systems (Michaelides & Wainwright, 2002) and B) riparian vegetation buffering the runoff and leading to sedimentation (Bracken & Croke, 2007).

The effect of **landscape position** in context of sedimentological connectivity is the distance from sediment source to the outlet (Bracken & Croke, 2007).

Intuitively, the connectivity will be higher as the distance to the stream or outlet is smaller, but as previously discussed, many factors can complicate this relationship (Bracken & Croke, 2007; Lal, 1990a). This leads us to the last factor of sediment connectivity in catchments, regarding **sediment propagation** in the river system. Again, many factors influence the dynamics of connectivity in river systems, such as transmission losses, catchment topography (influencing river gradient, -type and presence of floodplains), and many more (Fryirs, 2013; Hooke, 2003), which will be discussed in detail during next section. Humans can also increase river connectivity by straightening and embanking rivers or decrease connectivity by installing check dams and slowing down river flow.

Ultimately, connectivity is dependent on the combined effects of all these factors over the entire catchment. This leads to dynamic interactions of runoff generations between different zones, their propagation through the catchment and ultimately to large-scale response of catchments to produce floods (Bracken & Croke, 2007; Fiedler *et al.*, 2002). For example, Ambroise (2004) found that runoff can occur over a large proportion in the catchment, while none of this runoff is connected to the downslope outlet. The connectivity thus depends on the rainfall extent, duration and intensity being high enough to allow transmission of water over hillslopes and into channels, and then to propagate down channels overcoming transmission losses to connect whole catchments (Ambroise, 2004; Bracken & Croke, 2007; Lavee, Imeson & Sarah, 1998). Hillslope and sub-catchments can thus be spatially isolated from the rest of the catchment (Fryirs, 2013). However, there is limited understanding of the range of temporal scales over which disconnectivity occurs, and the changes necessary to reactivate sediment connectivity at a certain location in the catchment (Fryirs, 2013; Harvey, 2012). Important to realise is that sediment (dis)connectivity in East Africa's

disequilibrium systems isn't static but driven by short and long term variations in certain factors such as rainfall and vegetation, possibly connecting areas which are normally isolated or vice versa (Ambroise, 2004; Croke, Fryirs & Thompson, 2013; Heckmann & Schwanghart, 2013).

2.4 Sedimentation and storage

Sedimentation is the process, where the kinetic energy of the water flow is lowered to an insufficient level for entraining the particles in the flow, leading to its deposition (Meyer & Wischmeier, 1969). The systematic deposition of sediment particles in particular areas leads to sediment accumulation. Sedimentation is a dynamic process, which cannot be considered in isolation from erosion and transportation (Kirkby, 2008). Areas with a higher rate of erosion over sedimentation are called **source areas** because they have a net movement of soil particles away from the site. Vice versa, areas with higher rates of sedimentation over erosion, will have a net deposition. These **sink areas** will thus increase in soil volume over time, until the dynamics change (Borselli, Cassi & Torri, 2008). A sediment budget can be used to quantify the amount of storage over a certain period of time (Smith & Dragovich, 2008). Previous research has however indicated the dynamicity of storage by finding that sediment sources, sinks, and fluxes vary widely over time and space (Smith & Dragovich, 2008; Trimble, 1983; Trimble, 1999). Movement of sediment within the catchment should thus be described as a soil-sediment continuum (Croke, Fryirs & Thompson, 2013). Almost all of the sediment loss from the suspended river flows is attributed to overbank flow and deposition, with only very small amounts of sediment deposited within channel flow (Croke, Fryirs & Thompson, 2013; Lambert & Walling, 1987; Walling, Bradley & Lambert, 1986). During high flow events, sediment-laden river water spills out over the floodplain, slows and

eventually becomes almost stationary over large areas. This reduction in velocity leads to widespread deposition, as the water can no longer maintains the sediment in suspension (Ashbridge, 1995).

Deposition thus only occurs when thresholds for bankfull channel capacity have been exceeded and floodplain inundation occurs as shown in Figure 7b (Croke, Fryirs & Thompson, 2013). In following flood surges or changes in river course, the deposited sediments can be remobilized and transported further downstream (Foster, 1995). This produces stochastic sediment transfer and phased (dis)connectivity over various temporal scales (Reid *et al.*, 2007a; Reid *et al.*, 2007b). The length of time that sediment is stored in intermediate locations within the catchment will vary from location to location and from catchment to catchment (Walling & Webb, 1983). In general, larger catchments are more spatially variable, have more opportunities for intermediate floodplain storage and a decrease in slope and channel gradient, resulting in a more complex journey for sediment particles from source to the end of the catchment (Meade *et al.*, 1985; Walling, 1983). Furthermore, spatial variability in channel-floodplain connectivity leads to disconnectivity in the downstream transfer of sediments between reaches and affects sediment storage on adjacent floodplains (Croke, Fryirs & Thompson, 2013). On a big enough scale, the end of the catchment will almost always be an ocean or lake and when the river reaches them, the sudden decrease in flow also initiates deposition (Foster, 2010; Foster, Boardman & Keay-Bright, 2007; Foster, Dearing & Appleby, 1986; Meade, 1972). In the cases where freshwater comes into contact with saline water from oceans or saline lakes, flocculation is also an important factor promoting sedimentation (Droppo & Ongley, 1989; Meade, 1972). The continuous succession of depositions creates a slow cumulative vertical aggradation, which can be displayed as a sedimentary record (D'Haen,

Verstraeten & Degryse, 2012; Foster, 2010; Foster, Boardman & Keay-Bright, 2007; Trimble, 1983; Trimble, 1999). Disruption of the catchment soil-sediment continuum by increased erosion, climate change or other anthropogenic factors that affect connectivity thus lead to changes in sedimentation (Bracken *et al.*, 2013; Croke & Mockler, 2001; Lavee, Imeson & Sarah, 1998), which in turn can have detrimental impacts on downstream systems (Pimentel, 2006). Knowledge of the source-to-sink dynamics in catchments is thus important for investigating the relationship between on-site disturbances and off-site response (Bracken & Croke, 2007).

Chapter 3. Drivers, impacts and feedbacks of increased soil erosion in East Africa's agro-pastoral landscapes

Even though soil erosion is a natural part of the sediment conveyor belt, anthropogenic pressures are increasingly influencing erosional processes in East Africa. Studies and government reports are highlighting an acceleration of surface and gully erosion, which is mainly attributed to the loss of permanent vegetation through LUCC (Fleitmann *et al.*, 2007; Maitima *et al.*, 2009; Mati *et al.*, 2008). While LUCC are portrayed as a root cause of soil erosion, they are actually a symptom of wider social, economic and political factors, which are diverse, dynamic and rooted in historical disruptions to East Africa's socio-ecological systems (Kiage, 2013; Lambin *et al.*, 2001). The dynamics of LUCC and increased soil erosion depend on complex interactions between the natural, social and economic domains (Ananda & Herath, 2003; Kiage, 2013) as illustrated in Figure 10. Nonetheless, when the rate of soil erosion exceeds that of soil production, the soil base and all the services it provides will gradually disappear, inevitably leading to a decrease in agro-ecological productivity (Montgomery, 2007). To understand this wicked problem in East Africa's socio-ecological systems, a holistic understanding of the drivers, impacts and feedbacks of soil erosion is needed. This chapter starts with a description of LUCC in East Africa, followed by how this drives increasing rates of soil erosion. This will be succeeded by an in-depth discussion on the impacts and feedbacks of increased soil erosion on socio-ecological systems that potentially push the system to a degraded state. Subsequently, an in-depth historical analysis of the disruptions to East Africa's agro-pastoral systems will be given, followed by an overview of the contemporary social, economic and political drivers of unsustainable land use and soil erosion. Finally, some of the detrimental off-site

effects of increased soil erosion and runoff such as siltation, eutrophication and pollution will be discussed.

3.1 Land use and land cover change

Natural land cover is disappearing with an alarming rate in East Africa, due to increasing anthropogenic pressures. In general, a distinction can be made between two types of LUCC. The first type is a deliberate conversion of natural ecosystems, such as forest and savanna, to anthropogenic systems, such as agricultural and urban landscapes. The second type is the change in land cover due to the overharvesting of vegetation as a resource (Foley *et al.*, 2005). It is estimated that in the last 50 years, 10% of the land has been converted to agriculture , alongside with decreases in natural forests and savanna grasslands (FAO, 2019). By replacing natural vegetation with less permanent crop- or rangelands, the buffer between the soil and the elements will disappear (Kirkby, 1980; Thornes, 1990) and changes in land use are currently widely recognized the main driver behind the global accelerating soil erosion crisis (Foley *et al.*, 2005; Montgomery, 2007). The hillslope erosional reaction after LUCC depends on numerous factors such as the original vegetation, the slope, method of land cover change and eventual land use (Morgan, 2005). Several studies have demonstrated drastic increases in soil erosion following deforestation in East Africa (Barber, Thomas & Moore, 1981; Greenland & Lal, 1978; Rapp *et al.*, 1972). The severity of the erosional effects is dependent on the means and scale of deforestation, as well as the following farming system (Lal, 1996; Roose, 1986).

While the process of land use change often boosts the erosion rates, the continued cultivation of these changed landscapes is an important factor in maintaining this accelerated erosion (Montgomery, 2007). Myers (1993) estimated that on a global scale, erosion on agricultural lands is about 75 times

greater than in naturally forested areas. Montgomery (2007) performed a global meta-analysis comparing natural erosion rates with agricultural ones under different environmental conditions. The study found that under conventional agriculture, the rates of soil erosion overshoot the soil production with a factor of 10 to 100 (Figure 5). This discrepancy between soil erosion and -production implies an average net loss of soil under conventional agriculture, the magnitude depending on a combination of different environmental factors (Montgomery, 2007). Borrelli *et al.* (2017) estimated an especially grave increase in soil erosion in sub-Saharan Africa driven by cropland expansion and natural vulnerability (Figure 9).

While the deliberate conversion of natural cover types to anthropogenic types is clear and quantifiable, the effects of overexploitation on natural or semi-natural ecosystems on soil erosion dynamics are less straightforward. For example, the growing demand for wood as building material or fuel is one of the main drivers of loss of vegetation cover in East Africa (Hiemstra-van der Horst & Hovorka, 2009; Rudel *et al.*, 2009). Furthermore, in the past 50 years the livestock numbers in East Africa have increased by about 130%, while the available grazing lands are steadily decreasing due to privatisation and reduced mobility, leading to a more than doubling of livestock densities on both natural and semi-natural grasslands (FAO, 2019). The state of these agro-ecosystems is a function of the interaction between grazing and vegetation, which in turn depends on many factors, including the climatic conditions, the season, vegetation characteristics, duration of stocking, composition of domestic herds, and presence of non-domestic herbivores (Little, 1996; Ruttan *et al.*, 1999). While East Africa's semi-arid savanna grasslands are in constant state of disequilibrium due to the unpredictability of the climate and wildfires (Sullivan & Rohde, 2002), increasing

grazing pressures significantly impact rangeland ecosystems, in particular on the medium and long term (Fynn & O'connor, 2000; Illius & O'Connor, 1999; Le Houerou, 1984; Sinclair & Fryxell, 1985). The effects of overgrazing in East Africa's rangelands are thus time and site specific as different environmental conditions allow different grazing intensities (Campbell *et al.*, 2006; Fernandez-Gimenez & Allen-Diaz, 1999). Hein (2006) found that high grazing pressures are especially detrimental during dry periods and in drier areas. Nonetheless, when grazing pressures reach a critical point, the vegetation cannot recover anymore and only patches of unpalatable plants remain (Medina-Roldan, Huber-Sannwald & Arredondo, 2013). This process of overgrazing creates big areas of land without vegetation covering the soil, ultimately exacerbating the natural vulnerability to erosion of grassland ecosystems (Hein, 2006; Little, 1996; Reynolds *et al.*, 2007).

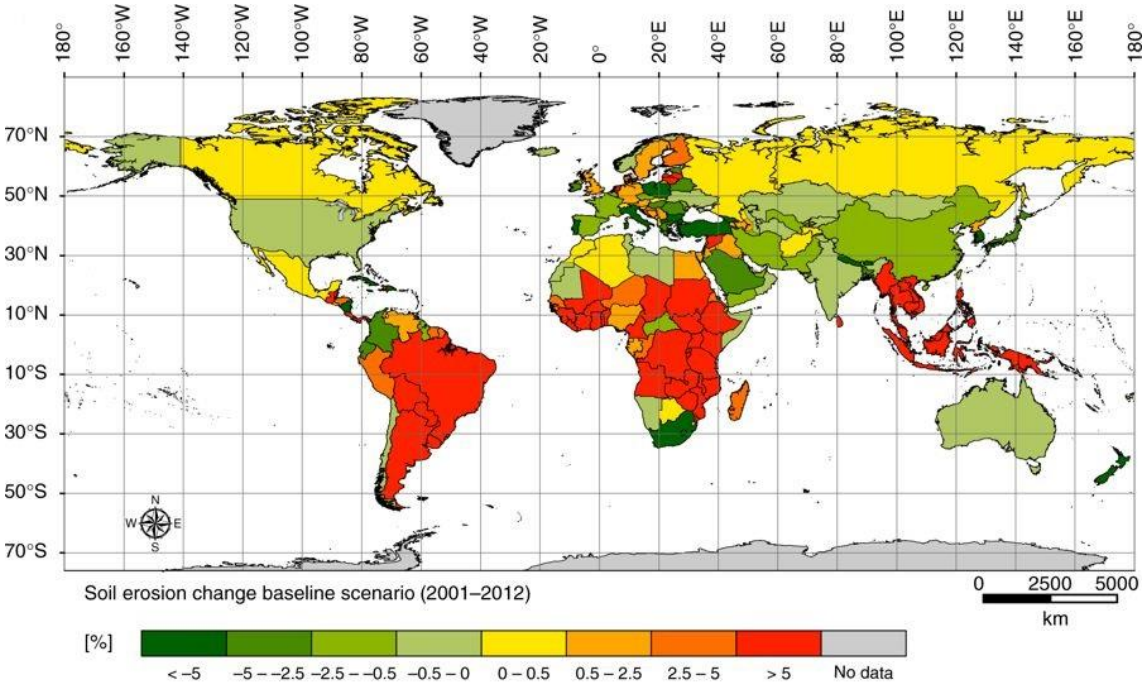

Figure 9: Country-specific percentages of increase or decrease of the annual average soil erosion rates between 2001 and 2012 obtained by comparing the pixel-based LUCC and agricultural inventory data of every country (Borrelli *et al.*, 2017).

3.2 Increased soil erosion and land degradation

Land degradation is the reduction or loss of biodiversity, ecosystem health, social value and economic productivity from socio-ecological systems. To grasp the

complexity of land degradation processes, it is essential to understand that it is driven by positive feedbacks set in motion by LUCC and climate changes (Schlesinger *et al.*, 1990). Drivers and effects of increased soil erosion and land degradation thus interact and exacerbate each other making it difficult to separate one from another. Therefore, general trends, feedback mechanisms and regime shifts will be discussed here.

3.2.1 Nutrients, organic matter, biodiversity and productivity

Besides the direct loss of soil, some processes during soil erosion exacerbate the loss of productivity. First of all, both wind and water erosion selectively removes the fine clay, silt and organic particles in the soil (Chepil, 1946; Poesen, 1992). As these particles bind the most nutrients, eroded soil disproportionally carries away vital plant nutrients such as nitrogen, phosphorus, potassium, and calcium (Quinton, Catt & Hess, 2001). Typically, eroded soil contains about 3 times more nutrients than the remaining soil due to this particle size enrichment (Troeh, Hobbs & Donahue, 1991; Young, 1989). Several studies have also demonstrated that removed soil is 1.3 to 5 times richer in SOM than the remaining soil (Allison, 1973; Lal, 1990b). SOM is key for nutrient recycling, productivity and decreasing erosion vulnerability through promotion of structural development and water infiltration (Langdale *et al.*, 1992). Furthermore, plants and soil biota require soils of adequate depth for optimal growth and functioning (Pimentel *et al.*, 1995; Wardle *et al.*, 2004). When soil depth is substantially reduced by erosion, plant root space is minimal, and plant production is significantly reduced (Thornes, 1990). Previously described processes influence the productivity substantially. For instance, nutrient deficient soils produce 15 to 30% lower crop yields than uneroded soils (Olson & Nizeyimana, 1988; Schertz *et al.*, 1989). Moreover, the reduction of SOM from 1.4 to 0.9% lowered the yield potential for grain by 50%

(Sundquist, 2000). In addition to decreased productivity, reductions in soil nutrient content, soil depth, SOM and available water adversely affect the overall species diversity and abundance within the soil ecosystem (Heywood & Watson, 1995; Walsh & Rowe, 2001). As these biological agents also have a vital impact on soil structure, nutrient recycling and erosion control, their loss may further speed up the process of soil and nutrient loss (Heywood & Watson, 1995; Lazaroff, 2001; Walsh & Rowe, 2001). Lastly, erosion of the topsoil can remove most of the seed bank, which prevents the vegetation to regenerate naturally (Cerdà & Garcıa-Fayos, 2002).

3.2.2 Runoff and water availability

Healthy soils with an extensive vegetation cover are much better in absorbing water from rainfall (Dunne, Zhang & Aubry, 1991; Temple, 1982; Thornes, 1990). Some studies have estimated that moderately eroded soils absorb from 10-300 mm less water per hectare per year from rainfall, which represents a decrease of 7 to 44% in the amount of water available for vegetation growth (Murphree & McGregor, 1991; Wendt, Alberts & Hjelmfelt, 1986). Evans, Cassel and Sneed (1991) calculated that when soil water availability for an agricultural ecosystem is reduced between 20-40% in the soil, plant biomass productivity is reduced between 10-25%, where the exact response depends on multiple other factors. Moreover, heavy machinery on cropland and trampling of pasture land by high densities of livestock can cause compaction of the soil (Donkor *et al.*, 2002; Hamza & Anderson, 2005). During compaction the soil is packed to a much higher density, reducing the infiltration capacity (Hamza & Anderson, 2005). Furthermore, the aggregate stability and crusting vulnerability of soils are also directly dependent on vegetation cover and SOM (Bissonnais, 1996). Crusting and compaction of the soil results in a further decrease in rainfall infiltration and

thus a greater runoff response (Du Toit, Snyman & Malan, 2009; Hiernaux *et al.*, 1999). Not only will there be less water available for plant production, the increased water run-off in turn also strengthens the erosional energy downslope, incising the landscapes with gullies (Poesen *et al.*, 2003; Valentin, Poesen & Li, 2005). This increase in gully density subsequently promotes hydrological connectivity in the landscape, rapidly channelling the water from the hillslope to the river network (Dunne, Zhang & Aubry, 1991; Fitzjohn, Ternan & Williams, 1998; Lal, 1996). Guzha *et al.* (2018) linked the decrease in permanent vegetation cover in East Africa with increases in surface runoff, river discharge and peak flows. However, the study also showed that the response is complex and dependent on other factors such as the slope, original and eventual land use system. Nonetheless, the risk of flooding after high precipitation events will be increased due to increased peak discharge and volume, and decreased time to peak (O'Driscoll *et al.*, 2010; Suriya & Mudgal, 2012; Swan, 2010). Besides the obvious risks for human infrastructure (Istomina, Kocharyan & Lebedeva, 2005), flood peaks also have a much higher energy, increase river bank erosion, and rapidly transport high amounts of sediment downstream (Croke, Fryirs & Thompson, 2013; Grove, Croke & Thompson, 2013).

3.2.3 Regime shifts

As discussed in section 2.2.4, natural vegetation acts as a buffer to the climatic drivers that supports its growth. The high variability in climate and intensity of disturbances has resulted in many East African ecosystems being in constant disequilibrium, making it more challenging to define 'natural' levels of soil erosion and anthropogenic land degradation in these systems. Notwithstanding, long-term observance or reconstruction (decades, centuries) of interactions between climate, vegetation and soil erosion do allow an assessment of land degradation

by soil erosion. In this context, land degradation in semi-arid East Africa can be seen as the shift of high-value system to a degraded state by progressive, continuous and/or abrupt anthropogenic disturbances strong enough to overcome internal stabilising feedbacks (Reynolds *et al.*, 2007; Scheffer *et al.*, 2001; Schlesinger *et al.*, 1990). Ultimately, depletion of nutrients, SOM, soil depth, biodiversity, seed banks and water availability in hillslope soils decreases vegetation growth and regeneration, which in turn further increases the run-off and erosion potential (Lal, 1990b; Pimentel *et al.*, 1995). Soil erosion and land degradation thus operate in tandem, where the effects of soil erosion lead to land degradation and land degradation leads to increased vulnerability to soil erosion (Hein, 2006; Schlesinger *et al.*, 1990; Thornes, 1990). This negative spiral of ever increasing erosion has already destroyed a lot of East Africa's once arable land. Around 80% of sub-Sahara Africa's pasture and rangeland areas are classified as moderately to extremely degraded (Oldeman, 1992; Pimentel, 2006; Ruttan *et al.*, 1999). Furthermore, it is estimated that average losses in productivity of cropping land in sub-Saharan Africa are in the order of 0.5–1% annually, suggesting productivity loss of at least 20% over the last 40 years. Continued loss of productivity has resulted in the abandonment of large areas of agricultural land across East Africa as they do not allow a subsistence anymore (Conte, 1999).

While these feedbacks are pushing productive system towards a degraded state, the most detrimental feedback is located on the interface between the natural and human world. As land, soil- and biological resources are disappearing due to land degradation, the pressures on the remaining productive systems will further increase, especially under a projected continued increase in population and little livelihood diversification outside agro-pastoralism (Ananda & Herath, 2003; Korotayev & Zinkina, 2015). East Africa is home to some of the most biodiverse

and valuable ecosystems (Little, 1996; Stoner *et al.*, 2007) and degradation of these systems would be a catastrophe for the biodiversity they harbour and the communities they sustain (Heywood & Watson, 1995; McClanahan & Young, 1996; Myers, 1990). Increasing competition for a dwindling resource base is increasing conflicts between stakeholder groups, but also between humans and wildlife, which is associated with the rapidly declining wildlife numbers in East Africa (Bhola *et al.*, 2012; Ogutu *et al.*, 2009; Stoner *et al.*, 2007; Western, Groom & Worden, 2009). As degraded lands are kept in their state by internal feedbacks, overcoming these to recover the lands back to a productive state needs substantial inputs of energy (Barrow, 1991). Natural recovery of the degraded lands by succession can take centuries or even millennia, and often human disturbances already return before full recovery, as the degraded state becomes the new normal (Montgomery, 2012). Recovery can be sped up by input of soil and nutrients, planting of vegetation, and building physical barriers for trapping water and soil, but this is labour- and cost intensive. Furthermore, recovered ecosystems will require adaptive management as dynamic, resilient systems that can withstand stresses of climate change, habitat fragmentation, and other anthropogenic effects (Chazdon, 2008; Suding, Gross & Houseman, 2004).

3.3 Disruption pathways to degradation

As highlighted in previous sections, human societies are an integral part of the balance between soil erosion and soil production. So even though soil erosion is a physical process, its underlying causes are firmly rooted in the social, economic and institutional environment in which land users make decisions (Ananda & Herath, 2003; Blaikie & Brookfield, 2015; Boardman, Poesen & Evans, 2003). On the most direct level of interaction between anthropogenic and biophysical factors, prime locations and modes of farming in East Africa coincide with areas of high

vulnerability. One example is that precipitation and soil fertility are often linked to altitude, with more suitable areas for agriculture in sloped highlands (Kurukulasuriya & Mendelsohn, 2008; Trapnell & Griffiths, 1960). Moreover, farmers often solely depend on rain for watering their crops, whereby they time the planting during the beginning of the rainy season (Barron *et al.*, 2003; Trærup & Mertz, 2011), leaving the fields exposed to the full force of torrential rains (Ngwira *et al.*, 2013).

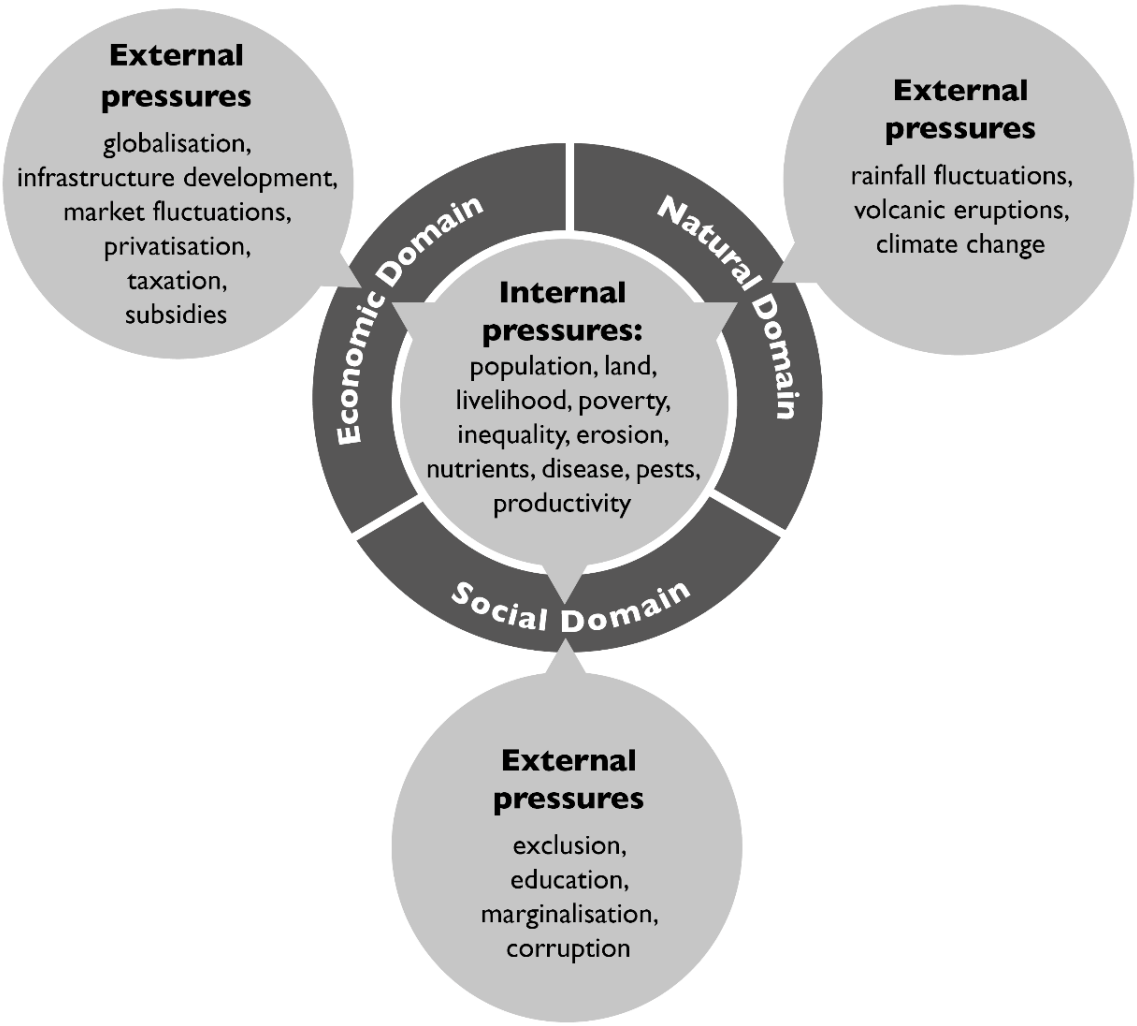

Figure 10: A schematic representation of East Africa's agro-pastoral systems structured by internal interactions between social, economic and natural domains, which are in turn influenced by external pressures, possibly altering the balance in the system.

However, East Africa's agro-pastoral systems are shaped by millennia of co-adaptation, reciprocal influencing and feedback mechanisms between communities and ecosystems. It is argued that agro-pastoral communities could

only persist by developing systems that were able to conserve or improve the soil properties (Gual & Norgaard, 2010; Lang & Stump, 2017; Widgren & Sutton, 1999). In this section, the East African land degradation problem is studied through the lens of the three domains of sustainable development: natural, social and economic (Brundtland, 1987; Griggs *et al.*, 2013), and their interactions in complex adaptive agro-pastoral systems (Berkes, Folke & Colding, 2000; Gual & Norgaard, 2010; Liu *et al.*, 2007) as illustrated by Figure 10. The natural domain can be bluntly described as Earth's life support system (Griggs *et al.*, 2013). For the purpose of this study, it is specified to describe the interlinking of soils and vegetation in ecosystems providing regulatory, supporting and provisioning services to the communities (Costanza *et al.*, 1997). The social domain in agro-pastoral systems is arguably the most complex as it is used as an umbrella term to describe social, cultural and governance structures. In this study it is described as environmental and agronomic knowledge, education, mobility, social networks, culture and norms, but also how and to what degree these factors are embedded in adaptive resource management and governance structures through political representation (Berkes, Colding & Folke, 2000; Pretty, 2003; Rammel, Stagl & Wilfing, 2007). The economic domain constitutes human-produced goods, which in this context of agro-pastoral systems mostly refers to crops and livestock outputs aimed for the market. It thus also represents communities' access to land, fertilisers, seeds and livestock varieties and agricultural technologies needed for the production of those goods. Furthermore, it also comprises infrastructure and access to market structures to exchange the produced goods for capital, which communities can use to increase wellbeing or invest in increasing productivity (Kelly *et al.*, 2015; Tittonell & Giller, 2013). The sustainability of agro-pastoral systems is dependent on how these domains interact. Changing internal and

external shocks and pressures influence the balance between the natural, economic and social domains. By describing the situation as unsustainable (e.g. the natural domain is degrading), both a thorough understanding the history of internal and external disruptions to those domains leading to the current degraded state (Koning & Smaling, 2005; Montgomery, 2012; Stump, 2010), are needed. East Africa is a diverse region with a complex history, and this study does not aim to generalise. Instead, an overview of the disruption history in the region is given without losing the importance of specific local conditions and outcomes.

3.3.1 Indigenous agro-pastoral systems

The first European explorers of the savanna plains and tropical highlands of East Africa describe ‘pristine’ natural environments, where ‘primitive’ human societies were ‘in the defensive’ against forces of nature on which they had little impact (Stanley, 1889; Thompson, 1887; von Höhnel, 1894). Contrary to those reports, pre-colonial East African systems were characterised by millennia of reciprocal influencing and co-evolution between human societies and ecosystems. Humans had a substantial influence on their environment, which does not mean that pre-colonial agro-pastoral systems never collapsed through human or natural disasters (Marchant *et al.*, 2018; Stump, 2010; Widgren & Sutton, 1999). Additionally, the division of the African population into static tribes or ethnic groups is a colonial construct rather than something inherent to African societies. The tribal structures known today are in reality conglomerates of peoples, who had previously been carriers of different cultural identities (Klopp, 2001; Lema, 1993; Spear & Waller, 1993). Instead, the history of the region is characterised by the spread and changing influence of major African groups, Arabic sultanates, trading networks and slave trade, which influenced land use, politics, culture and

economy. Some of these cultures developed into kingdoms and even empires, with dynamic spheres of influence. These population movements and the amalgamation of different peoples have taken place in East Africa since time immemorial (Iliffe, 1979; Mamdani, 2018; Marchant *et al.*, 2018). Agro-pastoral systems in East Africa thus not only had to adapt to changing environmental conditions but also to changing pressures from externally imposed governance systems, migration, trade and culture (Jones, 1980; Leach & Mearns, 1996; Spear & Waller, 1993; Stump, 2010). Therefore, communities will be described by the terminology 'indigenous' and by specifying modes of land use and –tenure. What is 'indigenous' is thus not static but a fluid concept of thousands of years of co-evolution between dynamic societies and a dynamic environment (Bruce, 1988; Reij, Scoones & Toulmin, 2013).

Most pre-colonial agricultural zones developed in naturally forested areas, but due to the strong dependence on forest ecosystem services, indigenous communities developed a 'conservation ethos', where natural ecosystems were valued for provision, regulating and supporting services. This often led to communal usage and conservation of those ecosystems with strong local controls to safeguard continued services (Conte, 1999; Haugerud, 1989; Lawi, 2002; Tengö & Hammer, 2003; Thornton, 1980). In response to the challenging East African conditions, farming systems developed in a way to build and sustain productive soils (Lang & Stump, 2017; Widgren & Sutton, 1999). For example, intercropping in fertile and wet areas, where a permanent and extensive cover with multiple crop types protected the soil from erosion and regenerated the productivity, as well as providing farmers a more diverse output secure from crop failures. Farmers also improved and conserved the soil base and water availability by investing labour to build terraces, cut-off drains, contour ploughing,

applying manure, mulching, rotating crop types and selecting crop types suitable for the specific location (Reij, Scoones & Toulmin, 2013; Snyder, 1996; Tengö & Hammer, 2003; Widgren & Sutton, 1999). In these areas of permanent production, households usually had customary rights to plots of land, which was transferable to sons (Bruce, 1988; Migot-Adholla *et al.*, 1991; Snyder, 1996). Shifting cultivation was dominant in less fertile areas, where there was a need to shift the location of farm plots in order to regenerate soil fertility naturally by periods of fallow. In these shifting cultivation systems with lower fertility and higher land abundance, indigenous tenure systems leaned more towards communal control but even then, farmers typically had secured use and inheritance rights through investment of labour or capital, even on the fallow lands (Bates, 1986; Bruce, 1988; Migot-Adholla *et al.*, 1991; Morgan, 1969). Only in areas unsuitable for cultivation due to environmental unpredictability, such as the savanna grasslands, complete communal usage of land was beneficial, as communities needed large areas for grazing and mobility to adapt to changing climatic conditions. In these pastoral systems, communities often adapted a nomadic existence following the rains with their herds (Little, 1996; Warren, 1995). Evidence suggests that these pastoral communities nonetheless developed elaborate management strategies for the communal lands, which were enforced through strict social norms and cultural traditions (Darkoh, 1989; Fratkin, 1986; Lawi, 2002; Migot-Adholla *et al.*, 1991; Niamir-Fuller, 2000; Roth, 1996). In all cases, social networks were a vital part of indigenous communities to buffer for droughts, labour or capital shortages. (Migot-Adholla *et al.*, 1991; Odgaard, 2002; Tengö & Hammer, 2003; Widgren & Sutton, 1999). Additionally, the indigenous land use- and tenure systems were not static but adapted to changing conditions, both natural as anthropogenic, from inside or outside the agro-pastoral system (Bruce, 1988; Cohen, 1980; Migot-

Adholla *et al.*, 1991). Historical analyses suggest that land tenure and -use demonstrated remarkable flexibility in adapting to new farming technologies, climate fluctuations, land opportunities, population increase or methods of exchange long before the colonial period (Bates, 1986; Haugerud, 1989; Jones, 1980; Morgan, 1969; Ruthenberg & Jahnke, 1985; Snyder, 1996). Indigenous agro-pastoral systems in East Africa thus have to be characterised as dynamic points along a continuum depending on the local environmental, social and economic conditions influencing the extent and patchwork constitution of settlements with permanent intercropping and/or shifting cultivation areas, natural or human-created grasslands, primary forest and recovering secondary forest. Even though it is generally accepted now that these early European reports were motivated by racial and political prejudices, they nonetheless formed the justification of the colonial policies of intervention in human-environment relations in East Africa (Coulson, 1981; Leach & Mearns, 1996; Stump, 2010).

3.3.2 The colonial disruption

The colonial rule subjected all of the inter-lacustrine East African countries from the end of the 19th century continuing for the greater part of the 20th century. While the policies were not static and greatly differed between the territories, they had in all cases major impacts on indigenous farming and pastoral systems (Anderson, 1984; Blaikie, 2016; Kjekshus, 1996). The major driver behind these changes was that the colonial state acted to alter human-environmental relationships within western systems of market-led agricultural and resource management. Colonial policies were enforced from a centralised power structure, replacing the more localised indigenous management (Anderson, 1984; Smith, 1989). While the indigenous land use and -tenure systems were flexible and dynamic, the new colonial rules imposed rigid legal systems distinguishing between private, public

and government land (Bruce, 1988; Haugerud, 1989; Migot-Adholla *et al.*, 1991). Colonial powers also altered indigenous power structures by using chiefs and royals to coerce communities into certain land use, livestock and crop types. Farmers and pastoralists entered the modern economy as producers, but were also forced to pay taxes and buy certain goods and services (Anderson, 1984; Coulson, 1981; Glazier, 1985; Mackenzie, 1989; Smith, 1989; Tosh, 1973). Combined with coerced changes in land use was the large-scale exclusion out of previously communal forest and grazing lands, which were repurposed for private farming, conservation, hunting reserves or forestry. The most productive land was attributed to the state and European settlers, implementing large-scale plantations and monocultures for export. In the process, local smallholder farmers were forced to move to less productive land or work on the plantations (Conte, 1999; Kjekshus, 1996; Sandford, 1919; Sorrenson, 1968). Both policies led to a large-scale shift to 'cash crops' of interest to the colonial powers, such as coffee, cotton, rubber and tea, replacing the more diverse selection of food-crops (Jones, 1980; Kjekshus, 1996; Smith, 1989). A direct consequence of the centralised agricultural intensification in the diverse and dynamic East African agro-pastoral systems was that areas under years of monocropping regimes and intense grazing were experiencing soil exhaustion, declining fertility and severe erosion (Anderson, 1984; Coulson, 1981). Indigenous farmers and pastoralists were shunted and confined to marginal areas where they struggled to adapt to the unfamiliar and constricted ecological space, often leading to land degradation and famine (Homewood, 1995; Kjekshus, 1996; Little *et al.*, 2008; Rutten, 1992). Another, indirect, result of this exclusion from previous communally managed pasture and forest land, was a shift from communal land tenure to permanent cultivation as a way to stake claim, where no dispute of ownership was possible.

As this process often involved clearing the land of trees and other ecosystem goods deemed valuable for the colonial state, exclusion out of forest and nature reserves thus had the perverse effect of crushing any indigenous impetus towards conservation and often led to increased land degradation outside these conservation centres (Conte, 1999; Homewood, 1995; Rutten, 1992). Perversely, these effects of exclusion were in turn used to argue and implement further exclusion and stricter regulations (Anderson, 1984; Blaikie, 2016; Hodgson, 2011; Sendalo, 2009).

From an economic development perspective, the instalment of an export-based economy also opened up opportunities to link certain cash-crops to the global market, where farmers could build up economic capital and invest that into better practices. Additionally, the introduction of pesticides, high-yield crop and livestock varieties, mineral fertilisers (post WW2) and agricultural technologies also offered opportunities to increase the productivity (Boserup, 2017; Jones, 1980; Migot-Adholla *et al.*, 1991; Ruthenberg, 1968; Smith, 1989). Whether regions are argued to have developed or have been exploited by colonial rule, the enormous impacts it had on agro-pastoral systems in East Africa cannot be ignored. Historical evidence suggest massive shifts in social organisation, political power balances, agricultural production, land tenure and economic systems, ultimately leading to changing interactions between humans and the environment (Botte, 1985a; Botte, 1985b; Cochet, 2003; Hydén, 1980; Kjekshus, 1996; Rodney, 1972; Smith, 1989).

3.3.3 Post-independence disruption

Many of the post-independence issues regarding unsustainable land management can be attributed to the erosion of indigenous social structures during the colonial period, combined with the sudden release from the strict

colonial rules into the chaotic new nation-states as illustrated in Figure 11a. Good examples of this come from the Usumbara mountains in Tanzania, described by Conte (1999) and Enfors and Gordon (2007), where the process of losing the 'indigenous' conservation ethic during colonial time, combined with increasing population pressures and a sudden release from colonial forest enforcement, led to uncontrolled exploitation and encroachment in the years following independence. As the farmers demand for arable land was a major rallying point during independence struggles, the newly found Tanzanian state (then still known as the republic of Tanganyika, but referred to as Tanzania throughout this chapter for simplicity) had difficulties refusing claims for agricultural land. Reports following this conversion of forest to cropland in Usumbara describe rapid decreases in soil quality, increases in sheet erosion and more extreme hydrological conditions with droughts and flash floods. These resulted into rapid degradation of the new farmland, where the farmers often abandoned their newly gained plots after a couple of years (Conte, 1999; Lundgren, 1978; Lundgren & Lundgren, 1979). Other examples are related to soil conservation measures, such as terraces, mulching and tree cover, which were enforced by the colonial government and subsequently formed the basis of 'nationalist' movements in Kenya, Uganda and Tanzania. In the early years after independence, most farmers were not willing to adopt these soil conservation measures because political officials denounced them during independence struggles, which made it difficult to enforce soil conservation in the new nation. As a result, agricultural systems aimed for soil conservation started to break down, leading to systematic degradation and loss of agricultural land (Anderson, 1984; Cliffe, 1970; Mung'ong'o *et al.*, 1995; Throup, 1987).

Fundamentally, post-independence issues regarding unsustainable land management have their roots in the colonial period because the new nation-states were built on colonial laws, policies, borders and western notions of economic growth. Just as the colonial governments, the post-independence centralised policies lacked the complexity and adaptability of local co-evolved agro-pastoral systems, often leading to economic growth strategies that degraded the natural resources (Hydén, 1980; Kjekshus, 1977; Lane & Pretty, 1990; Ruthenberg, 1968; Smith, 1989) as illustrated in Figure 11b. One of the most interesting cases comes from the Tanzanian 'Ujamaa Vijiji' (villagisation) policy, where people of previously different identities were forced to live in a village nucleus with communal production to build up the Tanzanian national identity and economy (Hydén, 1980; Kikula, 1997; Kjekshus, 1977; Lawi, 2007). When enforced these policies disrupted the locally co-adapted agro-pastoral systems greatly. The poor location of many villages regarding water provision, soil productivity and grazing capacity prohibited the instalment of sustainable agricultural practices. Additionally, the forced sedentarisation of previously nomadic pastoralists increased the grazing pressures enormously around the village nucleus. Moreover, lack of any land tenure security halted the production of perennial cash-crops and capital investments in farms. A lot of studies found that due to the complete imbalance between the newly formed 'Ujamaa' communities and the alien environment, systems often spiralled towards land degradation (Coulson, 1981; Ellman, 1975; Hydén, 1980; Kikula, 1997; Kjekshus, 1977; Lawi, 2007; Sendalo, 2009). The antipode to 'Ujamaa vijiji' are the effects of liberalisation and globalisation of the markets, which happened in all East African countries but on different timelines and scales (Bryceson, 2002). East African governments have continued the exclusion of smallholder farmers and

pastoralists from their land, which are being repurposed for game reserves and private agricultural enterprises under the guise of conservation and economic development (Bluwstein *et al.*, 2018; Desta & Coppock, 2004; Homewood, Coast & Thompson, 2004; Lane & Pretty, 1990). Combined with the enforcement of administrative boundaries and sedentarisation policies, this has led to a decrease in the mobility of pastoralist communities, disrupting systems of rotational grazing and adaptability to rainfall fluctuations (Fratkin & Roth, 2006; Homewood, 1995; Little *et al.*, 2008; Sendalo, 2009).

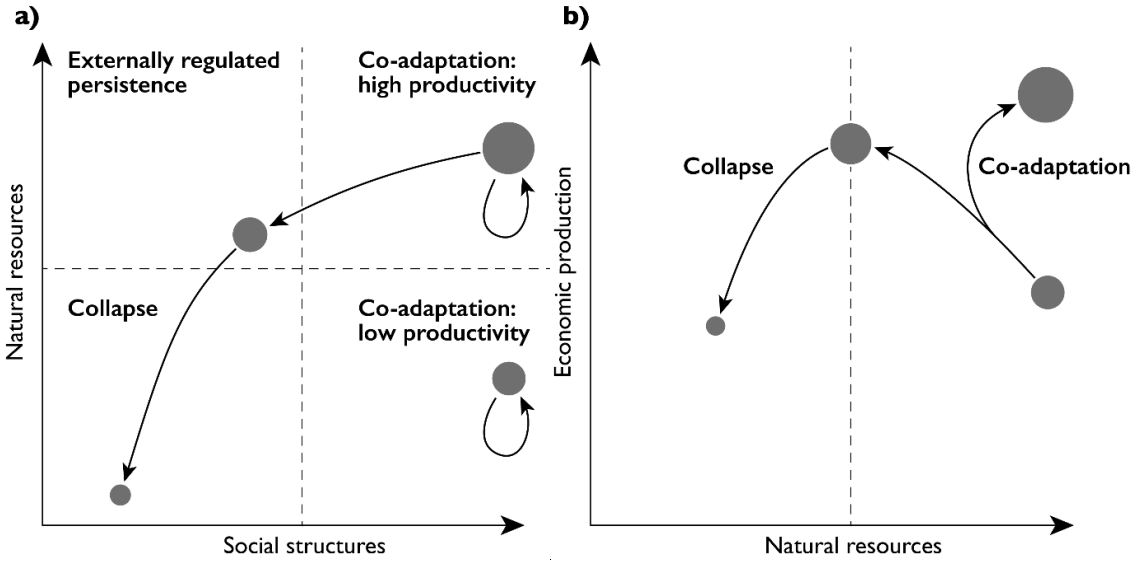

Figure 11: Conceptual pathways of degradation and co-adaptation in East Africa's agro-pastoral systems. Circle sizes illustrate the benefits generated for the agro-pastoral systems by the interactions of the domains. a) Collapse of natural resources is preceded by a gradual erosion of social structures necessary for sustainable resource management. The horizontal dashed line illustrates the ecological tipping point and the vertical dashed line the hypothetical social threshold where after communities lack the social structures to internally manage natural resources and co-adapt to external pressures. The different starting points represent natural differences in productivity. The circular arrows illustrate the adaptive capacity of systems with a well-developed social domain to higher or sustained high productivity. b) Interaction between the natural and economic domains. If economic production is increased by degrading natural resources, ecosystems will move towards a tipping point, after which both collapse. Communities with a well-developed social domain can however, sustainably intensify production without degrading the natural domain, as illustrated by the co-adaptation arrow.

This systematic erosion of social and economic structures in agro-pastoral communities through loss of access to land and natural resources, social organisation, knowledge, and mobility often led to increased pressures on the available resources. Overexploitation of vegetation and soil resources combined

with the lack of nutrient input and time to recover have contributed greatly to increased rates of soil erosion and ultimately land degradation (Ruttan *et al.*, 1999). Exactly as during the colonial period, the latter is being used as an argument to intensify policies of exclusion and coercing change (Fratkin & Roth, 2006; Hodgson, 2011; Homewood, 1995; Rutten, 1992).

3.4 Contemporary drivers of increased soil erosion

During the previous section, an overview on the historical disruptions to East Africa's agro-pastoral systems is given, where it is argued that indigenous social and economic structures gradually eroded following external disruptions. This section will explore how underdeveloped social and economic domains in East Africa drive the increasing rates of soil erosion, where a distinction is made between four major pressures: i) poverty ii) population growth iii) governance and political representation and iv) land rights and -access.

3.4.1 Poverty

Africa's rural poor are heavily dependent on natural resources for survival, have limited access to capital, fertilisers and technology and thus cannot invest in improved land management. Hence, *poverty* is a major driver of soil degradation (Boserup, 2017; Tittonell & Giller, 2013). One example is that poor East African farmers tend to raise row monocrops, such as maize, because of the low investment, quick return and predictable market values, even though the soil is highly susceptible to erosion under these cover types (Barron *et al.*, 2003; Blaikie & Brookfield, 2015; Salami, Kamara & Brixiova, 2010). Another example is that most of the rural poor rely on wood and crop residues for building, fodder and fuel. This results in the overharvesting of biomass from natural and agricultural ecosystems, which otherwise would protect the soil from erosion (Barrow, 1991;

Enfors & Gordon, 2007; Hiemstra-van der Horst & Hovorka, 2009). In addition to the rural areas, the growing demand for charcoal in East Africa's urban areas is driving degradation of forests and woodland in the entire region (Hofstad, 1997). However, what constitutes poverty in East Africa is beyond modern notions of income, expenditures and monetary capital, especially for pastoralist communities. Defining poverty in East Africa's agro-pastoral communities needs better understanding of the changing assets available to households, which can be tangible such as livestock or land, but also non-tangible such as social networks and mobility (Little *et al.*, 2008). Poverty can thus better be described as the lack of assets available to households to obtain a satisfactory standard of living, and is often a result of the underdevelopment of both the social and economic domains in communities. This often forces communities to have an unsustainable reliance on the available natural resources. In the next subsections a further exploration into the wider factors that contribute to this underdevelopment will be done.

3.4.2 Population growth

Linked to poverty are the effects of population growth, which often operate in tandem. An increasing population results in more mouths to feed, but also more livelihoods to find (Korotayev & Zinkina, 2015). A distinction is made between two possible responses to population growth: an unsustainable population-led and a sustainable intensification response. Which of these responses will dominate depends on the local interactions between the natural, social and economic domains in agro-pastoral systems (Ananda & Herath, 2003; Boserup, 2017; Lele *et al.*, 1989) as illustrated by Figure 10 and Figure 11. The *population-led response* locks growing communities into a continuous spiral of increasing exploitation of soil resources, which ultimately prohibits development of

sustainable agro-pastoral systems. Currently, an estimated 75% of East Africans are dependent on agriculture or pastoralism and without livelihood diversification, the next generation will be forced to find their livelihood in these sectors as well (Jayne *et al.*, 2014; Korotayev & Zinkina, 2015). There is ample evidence for the population-led response where increased competition for land following a population boom pushes farmers to smaller and/or unsuitable farming areas and increases grazing pressures on rangelands. This disrupts systems of nomadic pastoralism, shifting cultivation and intercropping towards more unsustainable practices with low investment and quick reward (Bryceson, 2002; Fratkin & Roth, 2006; Kiage, 2013; Odgaard, 2002; Rufino *et al.*, 2013; Western, Groom & Worden, 2009). In communities with underdeveloped social and economic domains, population increase is thus a major driver of increased rates of soil erosion (Tittonell & Giller, 2013). Vice versa, in the *sustainable intensification response*, population pressure promotes more favourable technological and organisational innovation that not only increases productivity but also preserves other ecosystem services (Ananda & Herath, 2003; Bernard & Lux, 2017; Boserup, 2017). Examples from sustainable intensification responses in African systems demonstrate communities' potential to adapt to increasing population pressure by investing in soil conservation methods, allowing a sustainable increase in productivity and revenues (Barbier, 1998; Matlon & Spencer, 1984; Tengö & Hammer, 2003; Tiffen, Mortimore & Gichuki, 1994; Turner, Hydén & Kates, 1993). Even though the latter examples of community-driven sustainable intensification highlight the adaptive capacity when the social and/or economic domains are well developed, it is argued that in areas of East Africa where the population-led response dominates, the only way to escape this poverty and population driven degradation is by external intervention aimed at decreasing

human fertility through family planning, compulsory secondary education and rise of the legal marriage age (Korotayev & Zinkina, 2015), combined with increasing agricultural productivity, market access and diversifying the livelihood possibilities outside agriculture (Koning & Smaling, 2005; Pretty *et al.*, 2006).

3.4.3 Governance and political marginalisation

This call for external intervention to escape the poverty and population trap leads us to the role of governance, whereby the rate of institutional adaptability relative to environmental dynamics is crucial regarding land and soil management (López, 1997). If population driven environmental change dominates institutional dynamics, then soil erosion will be exacerbated, while if it's the other way around, new institutions that protect the land will emerge (Ananda & Herath, 2003; López, 1997). This means that strong governments (either local or centralised) have to impose regulations in order to adapt to the increasing pressures without damaging the soil. When this does not happen because of spatial and/or temporal mismatches between policy development and the environmental dynamics, irreversible damage to the land base can occur (López, 1997). In that aspect, the centralised governments in most of East Africa's young and developing nation-states haven't managed to develop and/or implement adequate land management strategies to safeguard the soil base in comparison to the local 'indigenous' systems (Ananda & Herath, 2003; Blaikie, 2016). However, powerful institutions can also have a perverse effect, when they only focus on increases in productivity and fail to consider the 'damage costs' of certain farming practices. When institutions distort the market by subsidies, tax exemptions, guaranteed prices or protectionist policies, farmers respond to these changing price incentives by changing their crops. Some of these encouraged farming practices or crops may have an inherently high risk in terms of generating runoff and

erosion (Boardman, Poesen & Evans, 2003; Koning & Smaling, 2005; Myers & Kent, 2001; Ostrom, 2009). Furthermore, this simplistic classification of weak or strong institutions fails to describe the intricacies of the contemporary East African political systems, which are plagued by corruption and the apparent lack of democratic responsibility to provide services that are deemed central to the modern state (Chabal, 2013; Hodgson, 2011; Klopp, 2001). Top-down exploitation of producers by the bureaucratic and political elite creates a negative impetus towards any form of investment in sustainable growth, as the rewards will be taken away (Blaikie, 2016; Lopez & Mitra, 2000). Moreover, the lack of access to basic state services, such as roads, education, technology and electricity, prohibits communities to develop (Ananda & Herath, 2003). Democratic involvement and *political representation* is thus a key element in protecting or developing strong social and economic structures. Due to the lack of accountability of the political system towards certain communities, some policies are downright exploitative, increasing poverty, inequality and food insecurity (Chabal, 2013; Homewood, Coast & Thompson, 2004). Even when government intervention has noble intentions, the lack of local involvement in the process of formulating and executing land management strategies may have perverse effects, often leading to management solutions incompatible with the local environment. The political marginalisation of local communities is therefore one of the main drivers of increased rates of soil erosion and environmental degradation in East Africa (Blaikie, 2016; Homewood, Coast & Thompson, 2004; Klopp, 2001).

3.4.4 Land rights and –access

Conflicts regarding land rights and –access are on the rise in East Africa. The different post-independence nation-states in East Africa have pursued different

directions in land policy. For example in Kenya, private property rights were gradually introduced from 1956, while in Tanzania, all land is state-owned, where individuals use land as tenants and the purchase, sale and rental of land is limited within boundaries of the state (Pinckney & Kimuyu, 1994). Multiple studies in East Africa have set out to test the effects of these different land tenure systems on agricultural development and inequality but found little or no impact of land titling on investment, nor increased land inequality (Atwood, 1990; Bruce, 1988; Haugerud, 1989; Migot-Adholla *et al.*, 1991; Pinckney & Kimuyu, 1994). However, they did find that agricultural communities have held on, in different degrees, to indigenous land tenure arrangements, which both provide community control, as well as security for investment and have strong impacts on land markets, even when the latter are no longer in effect according to the law (Haugerud, 1989; Migot-Adholla *et al.*, 1991; Odgaard, 2002; Pinckney & Kimuyu, 1994). Due to the introduction of modern land tenure laws combined with the partial conservation of indigenous tenure systems, East African communities currently have a complicated mixture of both indigenous (customary) and formal (modern) land rights (Haugerud, 1989; Migot-Adholla *et al.*, 1991; Odgaard, 2002; Pinckney & Kimuyu, 1994). Under increasing land-scarcity, conflicts of land are increasing between individuals who obtained land rights through the different mediums. Often the most powerful and educated people can best navigate the complex maze of bureaucracy and customary rights, leading to increased inequality. In these cases, land conflicts through the presence of two tenure systems decreases land security, which in turn decreases capital and labour investments on farmland. That way decreasing land security can contribute to unsustainable management of soil resources in agricultural areas (Bluwstein *et al.*, 2018; Odgaard, 2002).

While agricultural systems are under pressure, communal usage of land and resources, which is vital for pastoral communities, is heavily threatened by policies of privatisation and exclusion justified by misconceptions on common land management (Bluwstein *et al.*, 2018; Homewood, Coast & Thompson, 2004; Western, Groom & Worden, 2009). Degradation of *communal lands* is often portrayed as a classic example of 'the tragedy of the commons', where an ever increasing competition between the users of these lands drives its degradation. In these shared-resource systems, individual users act independently according to their own self-interest and thus behave contrary to the common good of all users by depleting that resource through their collective action (Hardin, 1968; Ostrom, 2000). However, as argued in previous chapter, historical evidence suggests that indigenous pastoral communities developed effective systems of managing common resources in the long-term interest (Ellis & Swift, 1988; Niamir-Fuller, 2000; Ruttan *et al.*, 1999; Spear & Waller, 1993; Sullivan & Rohde, 2002). Additionally, there are multiple contemporary examples of successful common land management, if the institutions governing these lands are successful in imposing regulations (Feeny *et al.*, 1990; Ostrom, 2000). Pastoral livelihood strategies co-evolved with the unpredictable East African environment where mobility and a sufficient livestock herd acts as a buffer against droughts (Niamir-Fuller, 2000; Roth, 1996; Spear & Waller, 1993). External imposed limits to livestock numbers and mobility thus threatens pastoral livelihood- and food security (Little *et al.*, 2008; Rufino *et al.*, 2013; Ruttan *et al.*, 1999). The problem starts when these indigenous managing systems are disrupted due to internal and external pressures such as population growth, migration, sedentarisation, marginalisation, privatisation and exclusion (Anderson, 1984; Fratkin & Roth, 2006; Homewood, Coast & Thompson, 2004; Western, Groom & Worden, 2009).

Therefore, it is argued that when indigenous local arrangements lost influence and/or were replaced by centralised government, the common land tenure regimes gradually converted into open access in which the rule of capture drove each to grab as much as possible before others did. The reality of overgrazing of communal lands can thus best be described as the 'tragedy of open access' rather than 'tragedy of the commons' (Darkoh, 1989; Lawi, 2002; Migot-Adholla *et al.*, 1991; Roth, 1996). Similar, deforestation following the disappearance of indigenous communal conservation regimes and the collapse or lack of strict state enforcement can be explained as a tragedy of open access (Conte, 1999; Enfors & Gordon, 2007).

3.5 Siltation, eutrophication and pollution

Increasing amounts of soil lost from East Africa's agricultural and pastoral lands will often also end up in lakes and rivers, where it can have a range of detrimental effects (Pimentel, 1997). First of all, heavy sedimentation can lead in some cases to river and lake flooding (Myers, 1993). Siltation of reservoirs and dams reduces water storage, increases the maintenance cost of dams, and shortens the lifetime of reservoirs (Pimentel *et al.*, 1995). As East Africa is highly dependent on hydro-energy, erosion potentially threatens energy security and economic development in the region (Ndomba, 2007; Verhoeven, 2013). Furthermore, the deposited sediment shallows lakes, causing the water to spread out over a larger surface, increasing the evaporation. This is most of all a problem in shallow lakes where an increase in evaporation can cause the lake drying and decrease the water quality (Bonython & Mason, 1953; Vallet-Coulomb *et al.*, 2001). Increased turbidity due to the higher amount of suspended solids following siltation can decrease primary production by limiting the availability of light (Bilotta & Brazier, 2008; Newcombe & MacDonald, 1991) and decrease the habitat quality of fish

(Alabaster & Lloyd, 2013), resulting into altered food web structures and lower fish harvests (Lemmens *et al.*, 2017; Teffera *et al.*, 2017).

In addition to the direct effects of siltation, fine sediment is also an important diffuse source pollutant in surface waters due to its role in governing the transfer and fate of many substances, which makes sediment a multiple stressor in terms of water pollution (Walling & Collins, 2008). Fine clay, silt and organic particles in the soil have high specific surface areas and charge densities, increasing the adsorption of nutrients, agrochemicals and heavy metals onto the transported sediment. As a result, nutrients, trace metals and other potentially harmful pollutants are mobilised and enriched through soil erosion processes (Cadwalader *et al.*, 2011; Harrod, 1994; Quinton & Catt, 2007). High levels of nutrients adsorbed onto sediment can be released in water flows where they become biologically available. The nutrient limitation subsequently disappears from those ecosystems, which increases the dominance of certain fast growing species, who outcompete less competitive species for light, leading to their disappearance (Codd, 2000; Hautier, Niklaus & Hector, 2009). This process is called eutrophication and often causes algal blooms that produce toxins, or create anoxic water layers by reducing the oxygen in the water (Codd, 2000; Smith, Tilman & Nekola, 1999). Decreasing water quality decreases both aquatic biodiversity by affecting the habitat quality as well as terrestrial and avian biodiversity by poisoning the sources of food and water (Clark, 1987; Codd, 2000; Smith, Tilman & Nekola, 1999). For example, Lugomela, Pratap and Mgaya (2006), and Nonga *et al.* (2011b) have found evidence that cyanobacteria blooms and the toxins they produce are responsible for the mass mortalities of lesser flamingos in northern Tanzania's alkaline lakes (Koenig, 2006a). The combination of water pollution by sediment particles, the nutrients and pollutants

they carry, and indirect pollution by the toxic by-products of algal blooms, destabilises aquatic ecosystems and decreases the availability of drinkable water for wildlife, livestock and humans (Clark, 1987; Codd, 2000; Pimentel *et al.*, 1995).

Chapter 4. Study site: The Lake Manyara catchment

Lake Manyara is a shallow (Appendix A.1) rift lake located in in the Northern Tanzanian Rift Valley. The lake's only output of water is through evaporation, giving it a naturally high salinity and alkalinity. Rainfall in the Lake Manyara catchment is highly seasonal as highlighted in Appendix B.1. The short rains occur from November to early January. These are interrupted by a short dry season in January and February. The long rains occur between February and May. The dry season from June to October is consistent through the years and lengthens if the short rains fail (Prins & Loth, 1988). Besides intra-annual variability, the area also experiences high inter-annual variability through the interlinking of multiple global and local climatic phenomena such as the El Nino Southern Oscillation (Nicholson, 1996). Due to these variations in rainfall, the lake size and depth are also highly variable (Appendix A.2), with a recorded maximum around 480 km² and minima that reduced the lake to smaller disconnected pools (Deus, Gloaguen & Krause, 2013; Kiwango, 2012). While these conditions create a unique aquatic ecosystem, they also make Lake Manyara extremely vulnerable to anthropogenic changes in input of water, sediment and pollutants (Deus, Gloaguen & Krause, 2013; Yanda & Madulu, 2005). The lake is central to the Lake Manyara National Park, which is a biodiversity hotspot and since 1980 one of the four Tanzanian UNESCO Biosphere reserves (UNESCO, 2015). Furthermore, the Lake Manyara catchment also comprises the Tarangire national park, parts of the Ngorongoro conservation area, multiple forest- and game reserves, and Wildlife management areas. Additionally, many of the unprotected areas in the catchment are vital wildlife habitats and corridors on their own (African Wildlife Foundation, 2003). As part of the iconic savanna systems of Northern Tanzania, the Lake Manyara

catchment generates much-needed direct (tourist visits) and indirect (the service sector and trade) tourism revenues (Kahyarara & Mchallo, 2008). The wider Lake Manyara catchment system is characterised by distinct volcanic landscapes and a high social and environmental diversity (African Wildlife Foundation, 2003). Moreover, it is vital for food and livelihood security in northern Tanzania in terms of fisheries, (irrigation) agriculture and pastoralism. The increasing anthropogenic pressures in the wider catchment area impose serious threats for the ecosystem services needed to support its status as a socio-ecological system of high value (Nonga *et al.*, 2010; Rohde & Hilhorst, 2001; Shechambo, 1998; Yanda & Madulu, 2005). Studies and management reports of Lake Manyara voice concern regarding decreasing water depths, pollution, eutrophication, toxic cyanobacteria blooms and biodiversity decrease (Kiwango, 2012; Koenig, 2006b; Nonga *et al.*, 2011a). Furthermore, many parts of the wider catchment system are described by environmental studies and government reports to experience land degradation, increased surface and gully erosion, and siltation of water bodies (Kiunsi & Meadows, 2006; Maerker *et al.*, 2015; Meindertsma & Kessler, 1997; Muyungi, 2007).

The closed nature of the lake concerning sediment transport, combined with the high environmental diversity and socio-economic challenges typical for EARS makes the Lake Manyara catchment the ideal study site for investigating erosion and sediment dynamics under changing land use pressures. However, uncertainties surrounding the unique and dynamic hydrology in the Lake Manyara catchment need clarification before erosion and sediment dynamics can be studied.

4.1 Mapping the hydrological network

The first step of the project was to delineate the Lake Manyara catchment and map its hydrological network. Multiple 1 arc second resolution SRTM images (Farr *et al.*, 2007) were selected so that they covered the entire catchment area as expected from previous studies (Deus, Gloaguen & Krause, 2013). After projecting the images to the UTM 37S projection with 30m resolution, they were mosaicked into one Digital Elevation Map (DEM) containing elevation information about every cell. This allowed the analysis of the total Manyara watershed and drainage network, which was done in QGIS 2.14.8 (QGIS Development Team, 2009) using the 'Catchment Area', 'Channel network' and 'Watershed basins' tools following the hydrological analysis protocol (Olaya, 2014). The threshold of contributing area before the river network was set at 90000 m^2 (Tarboton, Bras & Rodriguez-Iturbe, 1991). The output maps provided a detailed delineation of the total Lake Manyara catchment area, as well as its sub-basins and their river networks. Ground surveys and analysis of (historical) scientific reports, Google Earth and Landsat images were used to correct for errors in lower sloped areas due to the course resolution (30m). Furthermore, this information was also used to describe complex hydrological phenomena in the river systems, such as the flow regime, sinks and intermittent connectivity. Moreover, the resulting hydrological output could be used to calculate tributary specific hydrological properties (Roehl, 1962), such as the drainage area, the relief-length ratio (R/L: the ratio of the difference between highest and lowest elevation and the sum of mean lengths of each river order), and the weighted mean bifurcation ratio (BR: amount of river streams of order n+1 divided by the amount of river stream of order n).

4.2 Catchment characteristics

Figure 12 shows the detailed hydrological network of the total Lake Manyara catchment and its location within Africa. Lake Manyara has a catchment area of roughly 18,372 km² with elevations ranging between 938 m and 3633 m above sea level. Nine major river systems drain the Manyara catchment, with different land cover (Appendix D.2), highly variable discharge regimes, catchment areas and environmental characteristics as summarised in Table 1. Besides inflow from these major rivers, there is also direct inflow from smaller drains and springs surrounding the lake. Figure 13 shows the spatial distribution of the rainfall, soil types and lithology in the catchment.

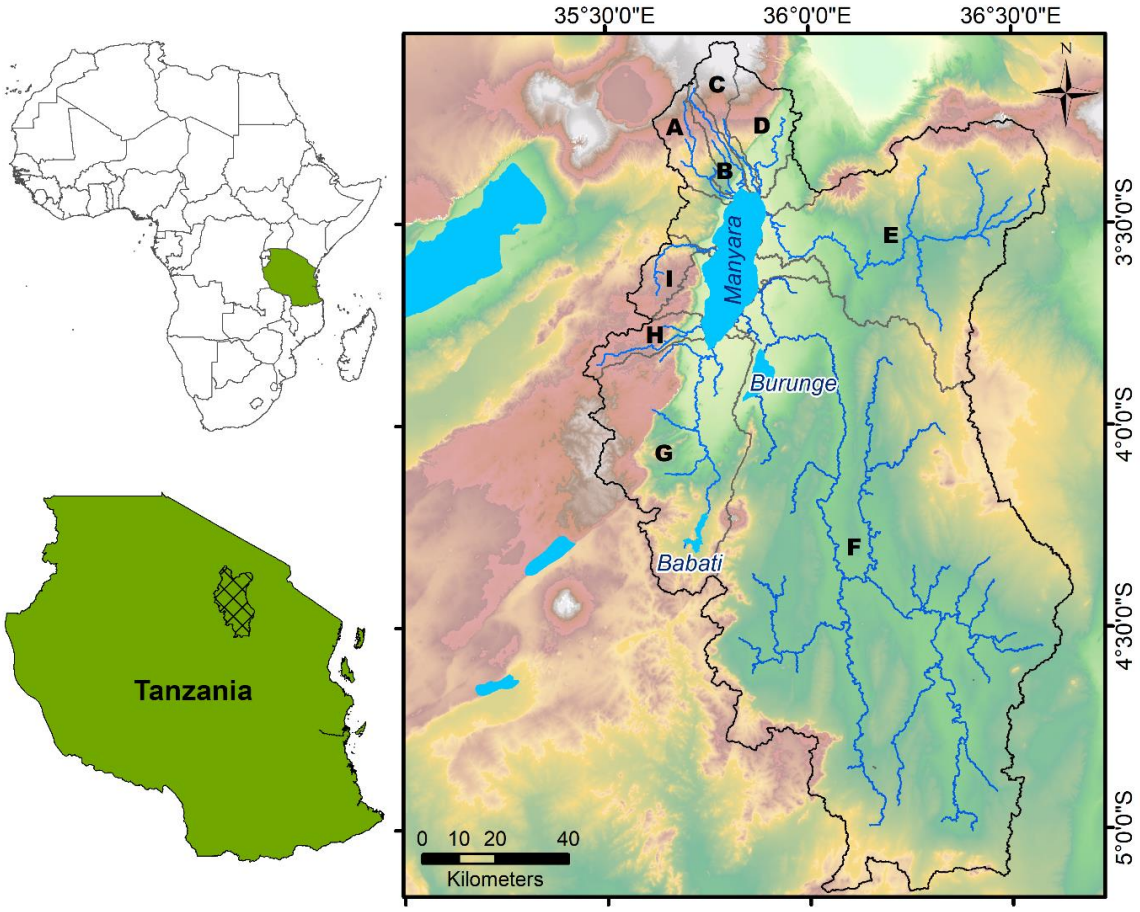

Figure 12: Location of the Lake Manyara catchment within Africa. Detailed topographic map of the Catchment with its major tributary systems: A) Marera, B) Kirurumo, C) Simba, D) Mto Wa Mbu, E) Makuyuni, F) Tarangire, G) Dudumera, H) Magara, I) Endabash.

The northern river systems of **Marera, Kirurumo, Simba and Mto wa Mbu** all originate on the Ngorongoro Highlands and all except Mto Wa Mbu rapidly flow

to the lake. Mto wa Mbu moves over the rift valley, where the flow slows down creating floodplains, currently mostly used for irrigation agriculture. The soils in the uplands are mostly Leptosols and Nitisols that are developed on young volcanic deposits. Due to the more permanent wet nature of the Ngorongoro highlands and the presence of springs, these rivers are perennial. However, they all still experience a high seasonality with peak flows during the rainy season. The land cover is dominated by forest and agriculture in all of the catchments, with a significant proportion of alpine grasslands in the Simba catchment. In the Mto Wa Mbu catchment, there is a substantial percentage of seasonal grazing areas in the drier rift valley and a small pocket of irrigation agriculture.

To the east, the **Makuyuni River** system is more complex, originating on the Monduli, Lesimingore and Lepurko volcanic highlands (dominated by Andosols and Chernozems) to the north and on the semi-arid Maasai steppe (Luvisols developed on older metamorphic rocks) in the south and east. Rainfall is highly variable and localised in the catchment, but in general, most of the water originates from the highlands. Connectivity between reaches is often not accomplished due to the larger catchment area and the presence of sinks between upland areas with the main river. This gives the Makuyuni a typical ephemeral character, not having a flow during most of the dry season and experiencing seasonal flooding during the rainy season when the rainfall exceeds a limit where connectivity can be reached between the different reaches of the river. The main river moves from the northern and southern reaches over the drier Maasai steppe and during peak discharge the river flows rapidly towards Lake Manyara. Locally, the river occasionally spills into flood plains. Savanna grasslands (24.2% permanent and 22.5% seasonal), bushlands (15.9%), agriculture (19.2%), and bare land (10.9%) dominate the land cover. Smaller

pockets of forest and riparian vegetation are confined to the uplands and floodplains respectively.

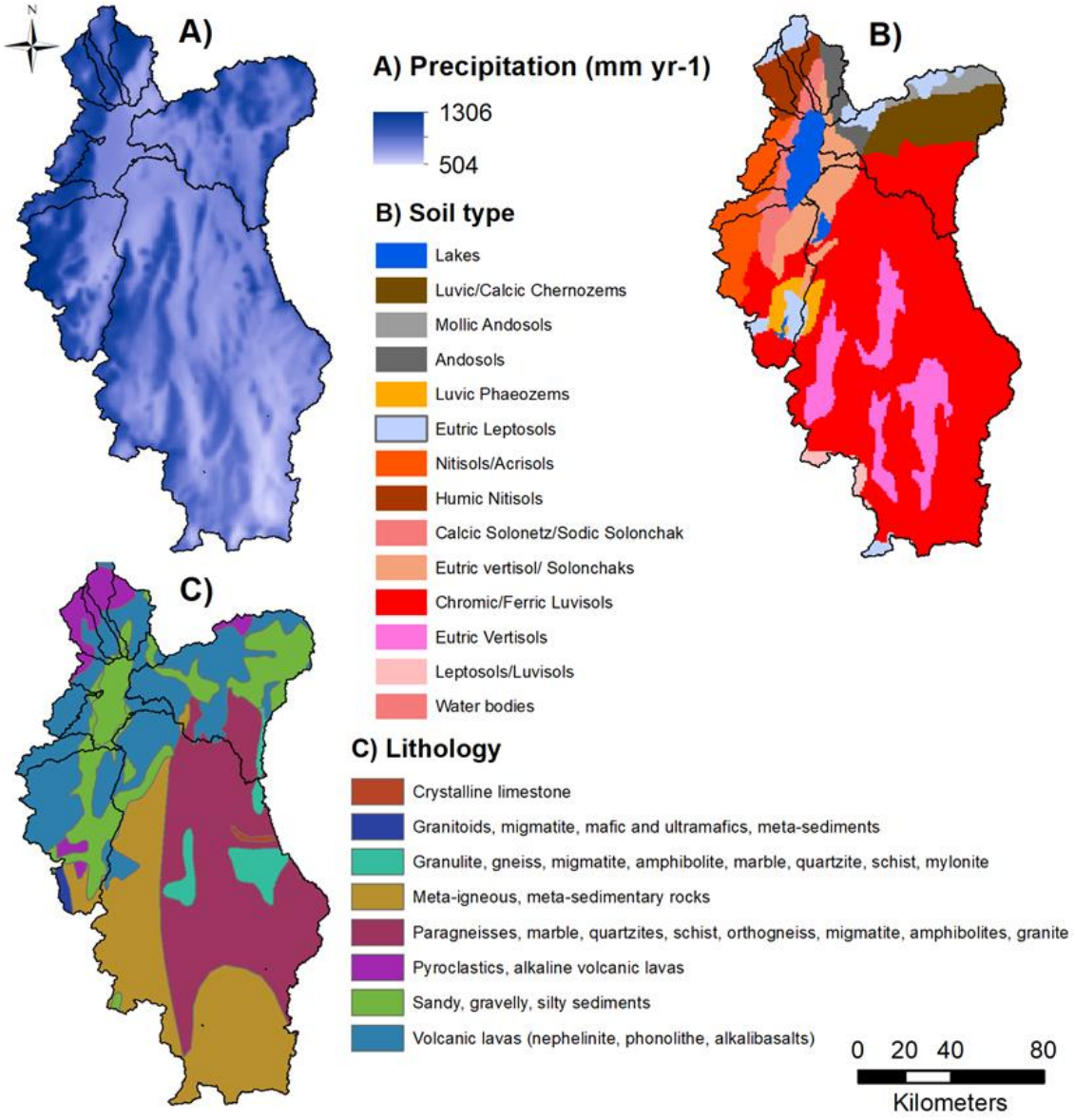

Figure 13: Spatial distribution of A) precipitation (Source: CHELSA model), B) soil types (Source: Harmonised world soil database), and C) Lithology (Source: Tanzanian Geological Survey).

The **Tarangire River** drains the southeastern part of the Manyara basin. This is by far the largest sub-basin and big parts, especially around the main river, have a national park status. Beside some smaller pockets of wetter highland, most of the basin is semi-arid savanna and bushland. The main river is characterised by natural depressions, which act like buckets that need to overflow in the next part of the river for it to continue, creating large natural wetlands. Luvisols, developed

on older metamorphic rocks, and Vertisols in the natural depressions, are the dominant soils types. Due to these wetlands and the large catchment size, the Tarangire River has a more permanent flow than Makuyuni, however, is still strongly seasonal, has localised connectivity and regularly dries out. Furthermore, it does not directly drain into Lake Manyara but flows into Lake Burunge first instead. Because a lot of the water evaporates here, the outflow from Lake Burunge to Lake Manyara is dependent on a longer period of high rainfall and is thus seasonal and sometimes even inter-annual. When Lake Burunge reaches full capacity, the Tarangire River overflows near its inflow into Burunge and connects with local drainage networks in the Kwakuchinja corridor as shown in Appendix C.1. The land cover is dominated by permanent grassland (43.3%), bushland (22.3%) and agriculture (25.8%). To the south of the lake, the **Dudumera River** system is both perennial and seasonal. The river originates from the Mbulu highlands to the west (dominated by Nitisols developed on younger volcanic lavas) and the Babati highlands to the south (dominated by Luvisols developed on older metamorphic rocks). The most southerly reaches first flow into Lake Babati, which only overflows during the wet season (Gerden *et al.*, 1992). The main river subsequently flows over the rift valley, where the flow slows down giving rise to extensive floodplains, which are currently almost all used for irrigation agriculture. The land cover is a mixture of agriculture (26.3%), irrigation agriculture (17.9%), mosaic (13.3%), forest (18.3%) and bushland (10%).The ephemeral **Magara and Endabash rivers** originate on the horst plateau, west of the rift valley, and are highly responsive to rainfall. They subsequently rapidly drain down the rift into Lake Manyara. The dominant soil type are Nitisols, developed on younger volcanic lavas, while the dominant land cover type is forest and agriculture.

Tributary	Area (km^2)	R/L	BR	Flow regime
Dudumera	2066.5	0.011	4.308	Permanent
Endabash	228.8	0.026	4.221	Ephemeral
Kirurumo	170.6	0.060	4.442	Permanent
Magara	245.9	0.040	4.775	Ephemeral
Makuyuni	2915.9	0.009	4.113	Ephemeral
Marera	283.3	0.036	3.889	Permanent
Mto wa Mbu	407.3	0.033	4.437	Permanent
Simba	237.6	0.045	4.426	Permanent
Tarangire	10817.9	0.005	4.467	Ephemeral

Table 1: Tributary hydrological properties: Drainage area in km2, the relief/length ratio (R/L), mean weighted bifurcation ratio (BR), and flow regime, as described in section 4.1.

Chapter 5. Quantifying and mapping land cover changes using Landsat images

5.1 Introduction

Unlike topography, which is relatively stable over centuries, land cover is subject to rapid changes due to a combination of ecological, climatic and anthropogenic factors. This dynamic nature of land cover often makes it the major driver behind the recent observed changes in soil erosion intensities (Thornes, 1990; Vanacker *et al.*, 2014; Walling, 1999). Spatial and temporal assessment of land cover in river catchments is thus a vital part of any soil erosion study (Renard, Meyer & Foster, 1997; Thenkabail & Lyon, 2016). However, the lack of long term scientific data about land cover change in East Africa impedes the assessment of its impacts on soil erosion dynamics. A possible solution to fill this caveat in scientific information can be the use of Landsat imagery to document the changes in land cover (Zhu & Woodcock, 2014). The Landsat thematic mapper has been orbiting earth since 1972 and scans the earth surface, measuring the reflectance strength of different electromagnetic spectral wavelength bands. Landsat data constitute the longest record of global-scale medium spatial resolution earth observation data and is therefore a good tool for investigating land cover changes (Hansen & Loveland, 2012; Wulder *et al.*, 2016). Using Landsat for land cover classification assumes that each land cover type has its unique spectral reflectance, which shows in a signature of different strengths of the electromagnetic wavelength reflectance bands. By informing remote sensing software of the reflectance signatures of known land cover areas, it can extrapolate the classification for a larger area. That way it is possible to map and quantify different land cover classes in large river catchments and detect potential changes (Franklin *et al.*, 2015; Hansen & Loveland, 2012; Zhu & Woodcock, 2014).

In this chapter, a detailed methodology for assessing land cover changes in EARS is given. The methodology is applied to the Lake Manyara catchment and observed changes are discussed within the specific social, economic and environmental setting. Furthermore, an evaluation of the challenges and solutions related to land cover reconstructions in the dynamic East African landscapes will be presented. Herein the objective lies in providing a template for future studies assessing changes in land cover over the past decades in EARS and other areas where there is lack of long-term land cover or soil erosion monitoring schemes.

5.2 Material and methods

All the raw input images, data and model outputs can be accessed online for reproductive purposes: http://dx.doi.org/10.17632/fmyz53987t.3.

5.2.1 Land cover classification and validation

Ortho-rectified and geometrically corrected Landsat images were obtained from USGS Earth Explorer and selected on the lack of interfering cloud cover. To highlight the effect of seasonal drying on vegetation, which is important regarding soil erosion dynamics (Kirkby, 1980), high quality images at the end of the dry season from two time periods were used. For the recent land cover ‘Landsat 8’ files obtained on 22/10/2016 (east) and 16/02/2016 (west) were used, while for the historic land cover ‘Landsat 4-5’ files obtained on 01-10-1988 (east) and 15/02/1987 (west) were used. These dates allowed the reconstruction of almost three decades of land cover change in the area. During multiple field campaigns, a comprehensive documentation of the land cover spectrum was obtained using geo-tagged photos and field notes. The efforts focused close to accessible roads with additional on foot surveys in more remote areas. Overall, with the knowledge

gained from these campaigns, coupled with the available high resolution satellite imagery from Google Earth, the major land cover types in the area were delineated and used to build signature files. The conversion of the Landsat imagery to a land cover classification was done using the supervised method in ArcMap, wherein the expert-build signature files were extrapolated over the entire catchment. In addition, the unsupervised classification was used to check for potential reflectance differences within land cover groups that could influence the classification. Signature files were further optimised by comparison with ground and high-resolution data, and when necessary, land cover groups were split. Following the previous steps, 23 land cover classes were used for the supervised classification that were grouped into 11 major classes post-classification (Table 2). Even with the high amount of land cover classes, false classifications were unavoidable due to reflectance differences in the same cover type, which can be caused by other factors such as soil type or wetness. Vice versa, different cover types are potentially classified as one because of reflectance similarities. The last step in the land cover reconstruction was to visually detect and correct those false classifications, which was done by manually selecting the incorrect areas and giving them the right land cover class. Additionally the limited cloud cover classifications were replaced with the dominant surrounding land cover. Land cover change analysis was performed following Pontius Jr, Shusas and McEachern (2004), accounting for the gross changes, net changes, persistence and swap.

The land cover classes were validated by stratified randomised sampling, where the output raster was overlaid with 300 random points, evenly spread per land cover class. For each point the classified cover type was checked with high resolution Google Earth images and when possible ground surveys. Three

possible validation types were possible: ‘Correct’, ‘False’ and ‘Grey’. The latter was included because in some cases the actual cover was in an intermediate zone (for example between ‘permanent savanna’ and ‘bushland’). The validation results were portrayed in a confusion matrix (Appendix D.3) wherein the amount of wrong classification and the confused land cover type were highlighted .

Land cover type	Broad type	C-factor	Land cover type	Broad type	C-factor
Highland forest	Forest	**0.05**	Afroalpine grassl.	Savanna	**0.20**
Lowland forest	Forest	**0.05**	Seasonal grassl.	Seasonal grassl.	**0.40**
Riverine forest	Forest	**0.05**	Saline grassl.	Saline grassl.	**0.25**
Seasonal agr.	Agriculture	**0.50**	Wetland veg.	Wetland/Riparian	**0.03**
Highland agr.	Agriculture	**0.35**	Lake delta	Wetland/Riparian	**0.03**
Grassy agr.	Agriculture	**0.40**	Riparian veg.	Wetland/Riparian	**0.03**
Irrigation agr.	Irrigation	**0.25**	Burned sav.	Savannah	**0.20**
Bare agr.	Agriculture	**0.60**	Degraded	Bare	**0.80**
Mosaic	Mosaic	**0.20**	Bare	Bare	**0.80**
Bushland	Bushland	**0.15**	Mud flats	Water bodies	**0**
Permanent sav.	Savanna	**0.20**	Water bodies	Water bodies	**0**
Floodplain grassl.	Savanna	**0.20**	Clouds	Surrounding cover	**/**

Table 2: The selected land cover types, their broader classification and corresponding C-factor scores

However, the biggest challenge was to classify the 1988 Landsat imagery because of a lack of information on land cover and high resolution satellite imagery for that period. The key solution for this issue was to select signature files with land cover delineation in areas where it was more or less known that the land cover had remained stable (National parks, reserves, etc.) and/or to select areas where the land cover in 1988 could be predicted with a high certainty (distinct spectral reflectance signature). As a post-classification accuracy assessment was not possible, it had to be assumed that the accuracy of the 1988 land cover classification was similar to that of 2016.

5.3 Results and discussion

5.3.1 Land cover changes

The land cover changes are visualised in Figure 14 and summarised in Table 3. The cross-tabulation with absolute values can be found in Appendix D.1 and gives information about the values of persistence and conversion of specific land cover types to others. The most distinctive trends are the net decreases in 'bushland', 'permanent savanna' and 'seasonal grassland', which would be traditionally used as common grazing areas for pastoralist (Lane & Pretty, 1990). At the same time, substantial net increases in 'Agriculture' and 'Irrigation' and a minor increase in 'Mosaic' can be observed. Another alarming shift is the substantial net increase in 'bare/degraded land', which is mostly limited to the Makuyuni sub-catchment and is largely caused by degradation of grazing lands. This development highlights the negative spiral of land degradation, as these bare lands will be even more vulnerable to soil erosion, hence degrade further.

Land cover type	**1988**	**2016**	**Gain**	**Loss**	**Gross change**	**Swap**	**Net change**
Agriculture	10.7	24.8	16.7	2.6	19.4	5.3	14.1
Bare/Degraded	0.4	2.0	1.8	0.2	2.0	0.4	1.6
Bushland	26.2	17.6	6.4	15.1	21.5	12.8	-8.6
Forest	6.8	7.0	1.4	1.1	2.5	2.3	0.2
Irrigation	0.3	2.5	2.3	0.1	2.4	0.3	2.1
Mosaic	1.2	1.7	0.7	0.2	0.9	0.5	0.5
Permanent savannah	33.9	30.3	10.9	14.4	25.3	21.7	-3.5
Saline grassland	1.7	1.5	0.8	1.0	1.9	1.6	-0.2
Seasonal grassland	14.0	7.9	3.9	9.9	13.8	7.7	-6.1
Water bodies	2.4	2.7	0.3	0.0	0.4	0.1	0.3
Wetland/Riparian	2.4	2.1	1.6	1.9	3.6	3.2	-0.3

Table 3: Percentages of the total catchment area (18372 km^2) per land cover type in 1988 and 2016, the total gains, losses, gross changes, swap and net changes (negative values have a net decrease).

Other notable trends are the decrease in wetland coverage and the slight increase in ‘forest’ cover, the first being converted among others to irrigation agriculture and grazing areas and the latter probably due to a better protection of the forest reserves. The decrease in saline grassland is linked to the increase in the area of Lakes Manyara and Burunge, which are dynamic in size and engulf parts of the surrounding grassland during wetter periods.

Even though the net changes are already very distinct, the gross changes and swap between the different land cover types are much higher, indicating that the system is highly dynamic and that some land cover types have a low persistence. The highest percentages of swap are found between ‘Permanent Savanna’, ‘Bushland’ and ‘Seasonal grassland’. Besides being the main source of agricultural land, these cover types thus also seem to shift between each other. However, the drivers behind previously described net and gross changes are not straightforward. Land cover change is driven by both environmental- and land use change, the latter in term is a result of complex social, political and economic transitions as discussed in chapter 3.

Validation of the recent land cover classification described 89% of the random points as ’correct’, 7% as ‘grey’ and 4% as ‘false’. The accuracy of the land cover reconstruction is high compared to other studies, and above the recommended 85% level (Foody, 2002; Gómez, White & Wulder, 2016; Olofsson *et al.*, 2014). This can be partly explained by the relative ‘small’ size of the study area, the detailed distinction between land cover groups and high number of ground observations. Moreover, the demonstrated optimisation of the supervised classification with random unsupervised classes and detailed knowledge of the study area was a good strategy to decrease classification errors. However, the

accuracy of the classification differed between the classes, which is summarised in the confusion matrix (Appendix D.3).

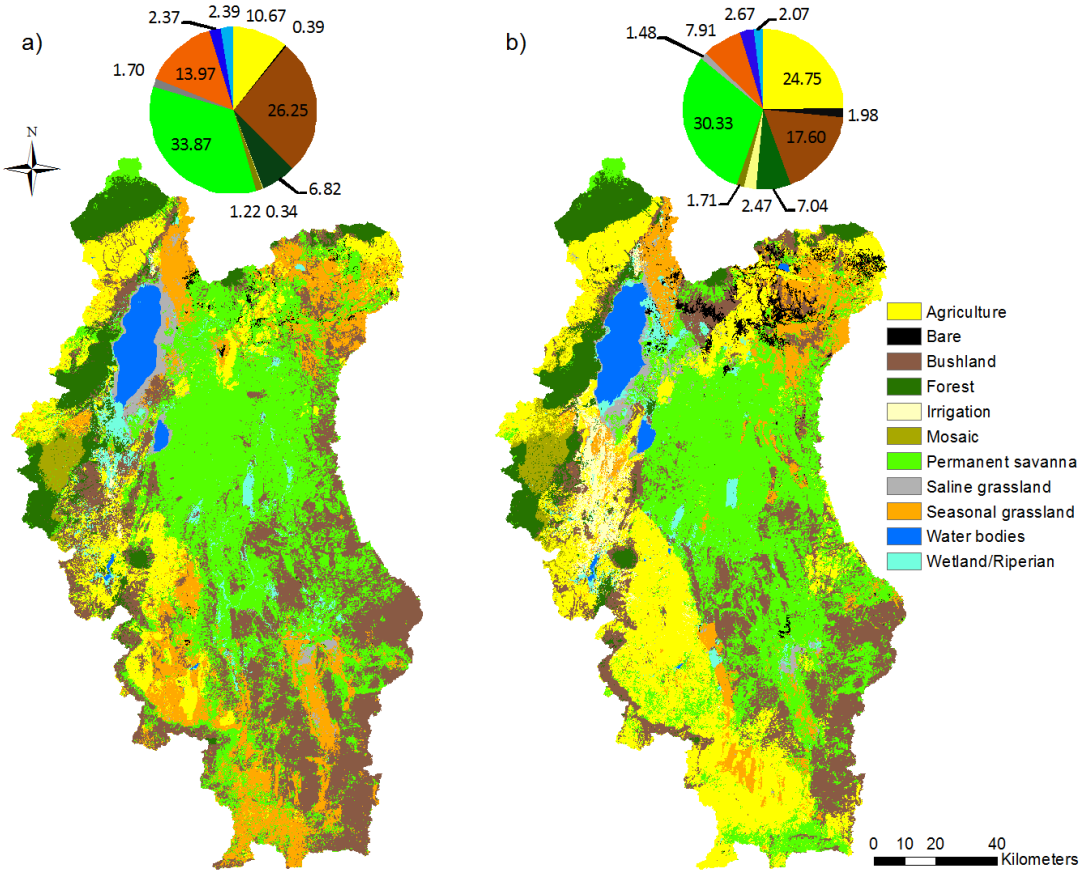

Figure 14: Land cover maps and percentages of land cover types derived from Landsat imagery of a) 1988 and b) 2016.

'Bare/degraded land' and 'Wetland/Riparian vegetation' had, with respectively 71.5% and 72.4%, the lowest percentages of correct classifications. 'Agriculture' and 'Irrigation' also had slightly lower percentages with 81.5% and 85.2% respectively. The confusion matrix allowed an evaluation of the false positives and false negatives for these specific land cover types. The results showed that 'bare/degraded land' is mostly overestimated at the expense of 'bushland' and 'agriculture'. 'Irrigation' and other cover types were incorrectly classified as 'wetland/riparian vegetation', but vice versa, 'wetland/riparian vegetation' was also often classified as other cover types (mostly irrigation). Wrong 'agriculture' classifications were mostly at the expense of 'seasonal grasslands' and 'permanent savanna'. Vice versa, 'agriculture' was often classified as other land

cover types. The high rates of both false positives and false negatives in ‘agriculture’ is not surprising given its high diversity and dynamicity. Nonetheless, it is apparent that besides ‘agriculture’, all of the major land cover types have a very high accuracy, which indicates that overall the results are a good representation of the land cover dynamics in the Lake Manyara catchment.

5.3.2 Limitations and future possibilities

The application of Landsat images for land cover change detection also poses some risks and challenges (Congalton *et al.*, 2014; Hansen & Loveland, 2012; Olofsson *et al.*, 2014). First, false classifications of land cover are unavoidable, especially in open cover types without extensive foliage cover. Differences in factors not related to vegetation, such as soil type or wetness, can lead to reflectance differences in the imagery. Vice versa, different cover types can be classified as the same because of reflectance similarities. Additionally, the medium resolution of Landsat imagery makes it difficult to expertly detect and correct for false classifications (Gómez, White & Wulder, 2016; Hansen & Loveland, 2012). The use of high-resolution images, such as mosaicked aerial photographs available on Google Earth, can complement this method by allowing better remote expert classification (Giri *et al.*, 2013; Olofsson *et al.*, 2014). Performance of accuracy assessments of medium-resolution Landsat land cover reconstruction using these high-resolutions satellite images allows the quantification of errors and evaluation of the representability of the technique as demonstrated in this study (Cihlar, 2000; Congalton *et al.*, 2014). Another risk for land cover change detection, especially in semi-arid areas, is the fact that potential seasonal or inter-annual variability in climate and land cover can be interpreted as land cover change, while in reality the land cover has remained stable. Only two years were used in this study, prohibiting the inclusion of rainfall

variability, which is tightly linked to vegetation dynamics. This problem was partly overcome by selecting images captured in the same period. However, the only way to truly disentangle anthropogenic land cover changes with interannual variability is by opting for continuous change detection. (Franklin *et al.*, 2015; Kennedy, Yang & Cohen, 2010; Olofsson *et al.*, 2014). In this aspect, the amount of high quality Landsat data available for many locations, including the Lake Manyara catchment, is less than desirable. Especially in persistently cloudy areas, the number of available images may be inadequate for analysis (Hansen & Loveland, 2012; Roy *et al.*, 2010), which can be partly overcome by selecting and mosaicking the best available observations subject to user defined criteria (Gómez, White & Wulder, 2016; Griffiths *et al.*, 2013; White *et al.*, 2014). Moreover, multiple processes can result into similar observed changes, making it difficult to evaluate the actual drivers of land cover change. Furthermore, more subtle disturbance dynamics, such as within-cover modifications, are more challenging to quantify using this method and often go undetected (Hansen & Loveland, 2012; Pfeifer *et al.*, 2012). A key example of this relating to East African systems is the increased grazing pressures on rangelands, which is a critical factor in soil erosion dynamics, but is difficult to monitor using Landsat imagery (Hein, 2006; Lambin & Geist, 2008). While this challenges the assessment of subtle dynamics between land cover classes, it does not affect the detection of land cover changes that can only be the result of changes in land use. As the main outcome of this specific exercise is the detection of major conversions to agricultural land, previously discussed limitations do not curtail the relevance of the results. Finally, Landsat images only go back a couple of decades in time, which is not a very tangible baseline in the Lake Manyara area. Possibilities to extend the period of land cover reconstruction by using old colonial aerial

photographs would permit the assessment of transformative historic events on the land cover such as the end of the Colonial period.

5.4 Conclusion

Evaluation of land cover data in the present study highlight that the major land cover types are highly dynamic and offers strong evidence of large-scale conversion from natural or semi-natural cover to agricultural land in the Lake Manyara catchment. Specifically, the biggest net declining cover types were found to be ‘bushland’, ‘seasonal grassland’ and ‘permanent savanna’, which have reduced by 8.7, 6.1 and 3.5 % respectively. While the Landsat based land cover reconstruction has many limitations, the evaluation of the accuracy and distinctiveness of the results make the outcomes of this chapter highly relevant.

Chapter 6. Pinpointing areas of increased soil erosion risk following land cover change

6.1 Introduction

In previous chapter, the temporal and spatial dynamics of land cover were assessed. However, the extent and impact of vegetation changes on the soil erosion dynamics depend on other less dynamic factors in the areas of change (Renard, Meyer & Foster, 1997; Wischmeier & Smith, 1978). Hence, land cover reconstruction can form the base for erosion risk maps together with slope, soil and precipitation data (Leh, Bajwa & Chaubey, 2013; Vrieling, 2006). There are numerous models to convert information about these factors to actual predictions of the soil erosion dynamics (Vrieling, 2006), but many are based on the Revised Universal Soil Loss Equation (Renard, Meyer & Foster, 1997), which calculates the mean annual soil loss rates by sheet and rill erosion. Each of these factors can be estimated using remote sensed and/or open access information and that way predictive models for soil erosion dynamics can be remotely developed (Oliveira *et al.*, 2015; Sepuru & Dube, 2018; Vrieling, 2006). While the original development of RUSLE models was aimed for estimating the quantities of soil loss in small agricultural catchments (Renard, Meyer & Foster, 1997), regional and global studies are approaching the method as qualitative tool for mapping areas of high soil erosion potential (Angima *et al.*, 2003; Claessens *et al.*, 2008; Ligonja & Shrestha, 2015; Panagos *et al.*, 2015b).

Catchment specific hydrological and geomorphological characteristics also influence the sediment connectivity and downstream sediment transport (Hoffmann, 2015). The sediment delivery ratio (SDR) indicates the percentage of the eroded sediment that reaches the tributary outflow. Empirical evidence on annual soil erosion and, to a lesser extent, annual sediment yield is hard to obtain,

especially in larger catchments. Therefore, SDR models have been developed that draw upon known correlations between sediment connectivity and catchment characteristics (Roehl, 1962; Walling, 1983) or upon landscape-based indices of connectivity (Borselli, Cassi & Torri, 2008; Heckmann & Vericat, 2018). The latter are limited to a smaller catchments, while in the former, catchment area is a factor itself. SDR models can be used either to estimate values of annual catchment erosion from known annual SY or to estimate values of annual SY from an estimated annual total catchment erosion. While SDR modelling requires many assumptions, it is a very useful concept to model catchment scale sediment delivery processes (Lu, Moran & Prosser, 2006).

By integrating land cover change maps from the previous chapter with RUSLE modelling, qualitative maps can be produced that pinpoint areas of increased soil erosion risk following land cover change. Furthermore, the combination of quantitative estimations of hillslope erosion and SDRs allow an estimation of tributary sediment delivery to Lake Manyara. In this chapter, a novel step-by-step methodology will be presented that allows the spatial and temporal assessment of changes in surface erosion risk and sediment delivery due to land cover changes in the Lake Manyara catchment. The output from the models are discussed in their social, economic and environmental setting with attention to limitations and wider potential applications of this methodology. Herein a template is provided for assessing increases in erosion risk and sediment delivery over the past decades in EARS catchments and other areas with a lack of long-term soil erosion and sediment delivery monitoring. In this context, the goal of this chapter is to pinpoint locations for targeted land management interventions in order to combat soil erosion and land degradation, as well as safeguard food- and water security, ecosystem health and local livelihoods.

6.2 Material and methods

All the input data and model outputs can be accessed online for reproductive purposes: http://dx.doi.org/10.17632/fmyz53987t.3.

6.2.1 Erosion risk mapping and comparison

Erosion risk modelling was performed using ArcGIS' 'modelbuilder' and is based on the RUSLE model (Renard, Meyer & Foster, 1997; Wischmeier & Smith, 1978), which calculates the mean annual soil loss rates by sheet and rill erosion by following equation:

$$E = R \times LS \times K \times C \times P \quad (1)$$

Where E: annual average soil loss (t ha^{-1} yr^{-1}), R: rainfall erosivity factor (MJ mm ha^{-1} h^{-1} yr^{-1}), K: soil erodibility factor (t ha h ha^{-1} MJ^{-1} mm^{-1}), C: cover-management factor (dimensionless), LS: slope length and slope steepness factor (dimensionless), and P: support practices factor (dimensionless).

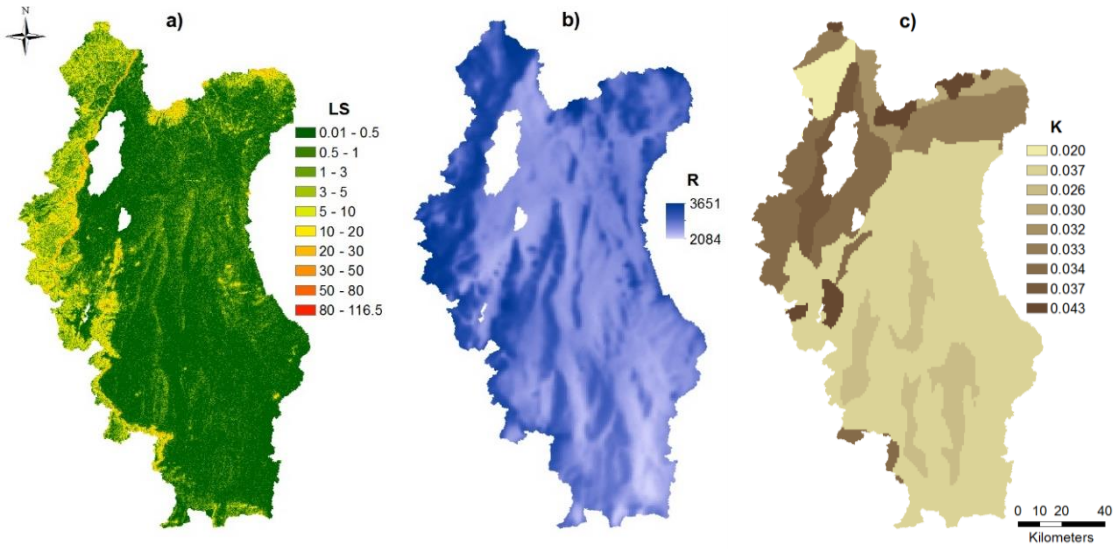

Figure 15: The model input maps of the a) dimensionless slope length and slope steepness factor LS, b) Rainfall erosivity factor R (in MJ mm ha^{-1} h^{-1} yr^{-1}), and c) Soil erodibility factor K (in t ha h ha^{-1} MJ^{-1} mm^{-1}).

The **slope factor (LS)** is a proxy for the soil erosion vulnerability of an area regarding the slope angle and length and its distribution in the catchment is shown in Figure 15a. For the calculation of LS in ArcGIS from the DEM (Farr *et*

al., 2007) the LS-tool developed by Zhang *et al.* (2013) was used, which is based on McCool *et al.* (1989) and Desmet and Govers (1996):

$$LS = L \times S \tag{2}$$

$$L_{ij-in} = \frac{[(A_{ij-in} + D^2)^{m+1} - \left(A_{ij-in}\right)^{m+1}}{(D^{m+2}) \times \left({x_{ij}}^m\right) \times \ (22.13)^m} \tag{3}$$

$$m = \frac{\beta}{1+\beta} \tag{4}$$

$$\beta = \frac{(\sin\theta)}{[3 \times (sin\theta)^{0.8} + 0.56]} \tag{5}$$

$$S = 10.8 \times si\,n\,\theta + 0.03 \; if \; \theta < 9\% \tag{6}$$

$$S = 16.8 \times \sin\theta \ \ - 0.05 \; if \; \theta > 9\% \tag{7}$$

Where: m is the variable length-slope exponent, β is the ratio of rill vs. inter-rill erosion, θ is the slope angle, A_{ij-in} is the contributing area at the inlet of the grid cell with coordinates (i,j) in m^2, D = grid cell size (m) and $X_{ij} = (\sin\alpha_{ij} + \cos\alpha_{ij})$. Flow accumulation was used as a proxy representing the contributing area for each cell (A). A threshold unit of 90000m^2 was inserted as the point where flow accumulates into the river network and changes from hillslope surface erosion to riverine- or gully erosion. This number is a generalisation set to match the hydrological mapping from section 4.1. In reality, the threshold contributing area for channel incision is spatially and temporally variable depending on climate and catchment characteristics (Dewitte *et al.*, 2015; Ijjasz-Vasquez & Bras, 1995; Montgomery & Dietrich, 1992).

In terms of **rainfall erosivity**, the intensity and frequency of high intensity rainfall events are more predictive than the total rainfall amount. However, this information was not available for our study site. For East Africa, however, there is a high correlation between the Kinetic energy of the high intensity storms and the mean annual precipitation, as almost all rainfall in the area happens in

seasonal intensive events (Moore, 1979). The mean annual rainfall (MAR) data was obtained from the global "CHELSA" dataset (Karger *et al.*, 2017), which is based on 34-year of climate data (1979-2013) combined with numerous other predictive inputs. This dataset was chosen because of its high resolution and inclusion of orographic factors that provide a better prediction of precipitation patters compared to other datasets in areas with a distinct topography. Using Moore's (1979) regressions, the kinetic energy of the rains (KE) and ultimately the rainfall erosivity factor (R) was calculated using equations 8 and 9 respectively and is shown in Figure 15b.

$$KE = 3.96 \times MAR + 3122 \quad (8)$$

$$R = 17.02(0.029 \times KE - 26.0) \quad (9)$$

The **soil erodibility factor** was calculated from soil information obtained from the Harmonized world soil database (Nachtergaele *et al.*, 2008), complemented with field information regarding soil texture, and organic carbon content (Appendix P.1). Based on the dataset, the basin was divided into 16 different soil regions, which could be split into 5 textural classes for the basin: Heavy clay, Clay, Clay loam, Sandy clay loam and Loam. Together with the topsoil organic carbon content (% of weight) of each soil region, this information was used to calculate the soil erodibility factor (Figure 15c) following the simplified table of Stewart, Wischmeier and Woolhiser (1975), accounting for the conversion to SI units by multiplying with 0.1317.

The **cover-management factor** reflects the effects of plant- and root cover and soil disturbing activities, which are included when giving the erosion vulnerability scores of different cover types (Wischmeier & Smith, 1978). The presence of soil conservation practices was mostly related to the type of agriculture, which is why it was chosen to integrate the **support practice factor** in the cover-management

score, resulting in one score. The risk scores were attributed per land cover type (displayed in Table 3) using expert knowledge from field and satellite observations, and ecological and agronomic information. The scores considered four facets, adapted from Renard, Meyer and Foster (1997). The first facet was the permanency of the land cover: from permanent forest to seasonal grassland, or perennial crops (such as coffee) to seasonal crops. The second facet was the extent of the cover: from 100% soil cover in the forests, to a more patchy vegetation distribution in the seasonal grasslands and a constant bare surface on the bare lands. The third facet was the depth of the cover: from multiple layers with a well-developed root zone in forests compared to one layer in grasslands. The fourth facet was the prevalence of large-scale soil disturbances: from rare in natural cover to annual ploughing in agricultural land cover. In agricultural cover types, additional soil conservation practices, such as terracing and length of the growing seasons, were also included as a facet. Each land cover type (based on results of section 5.3.1) was given a relative C-factor score between 0 (full cover) and 1 (no protection). Maps of the C-factor were created for both 1988 (Figure 16a) and 2016 (Figure 16b). The C-factors were compared with literature examples shown in Appendix E.1 (Angima *et al.*, 2003; Gelagay & Minale, 2016; Ligonja & Shrestha, 2015; Mati, 1999; Panagos *et al.*, 2015a).

All of the previously described factor maps were subsequently used as input parameters for the RUSLE modelling (equation 1) and the resulting output provide an estimation of the annual soil loss rates by sheet and rill erosion in the Lake Manyara basin in 1988 (Figure 17a) and 2016 (Figure 17b). However, the ultimate goal of this study was not to estimate the soil loss quantities in the catchment, but to map the on-site changes in soil erosion risk. By subtracting the map of 2016 (E_{2016}) with that of 1988 (E_{1988}), a risk change map (ΔE, Figure 17c)

was obtained, which shows the spatial distribution of erosion risk increases and decreases in the Manyara catchment:

$$\Delta E = E_{2016} - E_{1988} \quad (10)$$

6.2.2 Model sensitivity analysis

A sensitivity analysis was performed to test the model's response to potential omission or commission errors in the model inputs. Following the literature estimations of errors in each of the model inputs (Farr *et al.*, 2007; Karger *et al.*, 2017; Nachtergaele *et al.*, 2008), it was decided to test the model's sensitivity for a 10% potential error to the slope-, soil- and precipitation data. This was done by creating a random raster with values ranging from 0.9 to 1.1 and multiplying it with the selected model parameter, while keeping the other parameters constant. For the sensitivity analysis to land cover errors, the results of the land cover validation (Appendix D.3) were used. A raster was created wherein the percentage of land cover found to be correctly classified was randomly translated to a percentage of cells given the value 0. The percentage of land cover found to be grey was randomly translated to a percentage of cells and given a value ranging from -0.05 to 0.05 (as the errors are minor). The percentage of land cover found to be classified falsely was randomly translated to a percentage of cells given a value ranging between -0.30 to 0.30 (as the errors are major). The resulting sensitivity analysed model outputs were subsequently compared with each other to assess the potential impact of errors on the results. The potential effect of supply limitation on steep and rocky hillslopes was evaluated by comparing the model outcomes above 500 tonnes ha^{-1} yr^{-1} with high resolution imagery on Google Earth to check the soil status. Furthermore, a checked model was run, where the K value in areas with a slope >40° was set to 0.001. The

differences between the original and the checked model were subsequently evaluated.

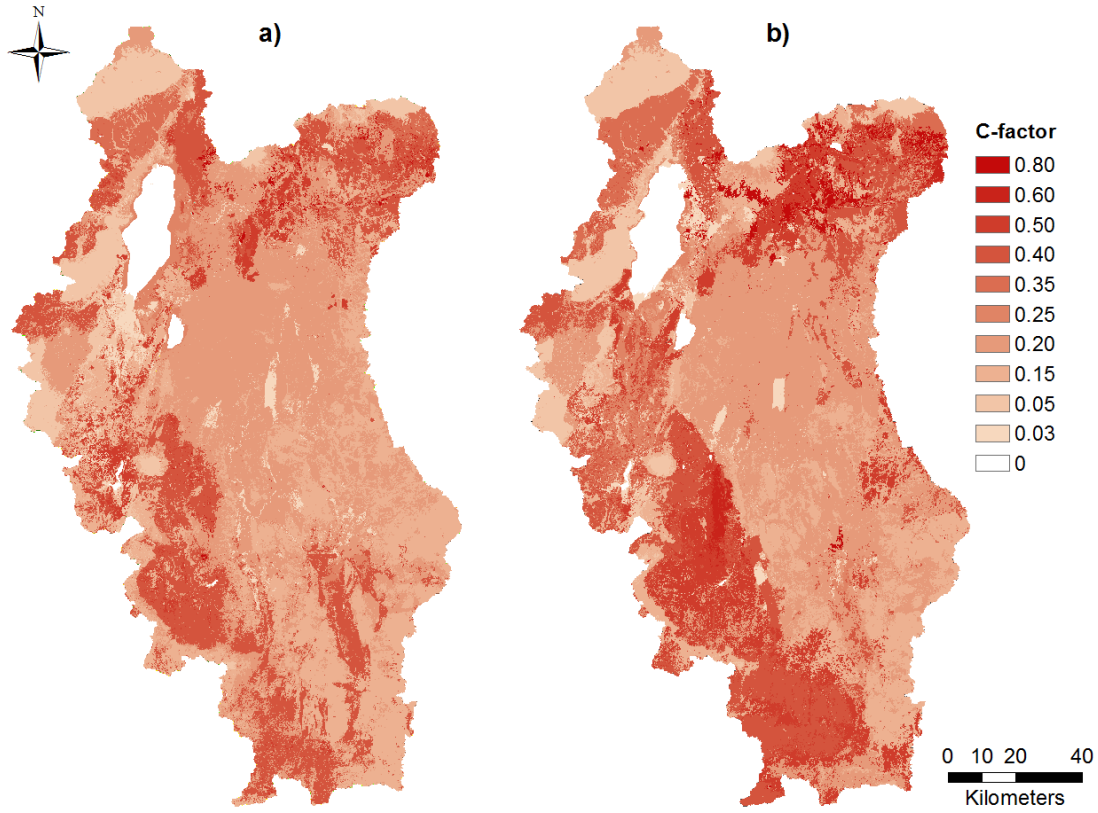

Figure 16: The dimensionless land cover erosivity factor input maps for a) 1988 and b) 2016.

6.2.3 Modelling tributary sediment delivery

The sediment delivery ratio (SDR) of the tributary catchments was calculated using the model by Roehl (1962). This model was chosen because of its emphasis on differences in catchment characteristics (versus differences in landscape connectivity), which fitted better to the research objective to estimate differences sediment contribution to Lake Manyara from the different tributaries. The catchment characteristics are relatively easy to calculate from DEMs as demonstrated in section 4.1 (Table 1):

$$Ln\ SDR_e = 4.50047 - 0.23043\ log10\ W - 0.51022\ ln\ \frac{1}{\frac{R}{L}} - 2.78594 \ln BR \qquad (11)$$

Where W is the drainage area of the tributary (in square miles), R/L is the ratio of the relief (highest elevation – lowest elevation) and the river length (sum of mean lengths of each river order), and BR is the weighted mean bifurcation ratio (amount of river streams of order n+1 divided by the amount of river stream of order n). This means that the SDR is lower for bigger catchments, with low stream gradients, and higher level of bifurcation. While both modelled erosion rates and modelled SDR make major assumptions of tributary hydrology, they can provide an estimate of the absolute amount of sediment delivered to Lake Manyara from each catchment. Multiplication of the catchment specific estimations of the yearly gross hillslope surface erosion and SDR allows an estimation of the total yearly sediment delivery from the tributaries to Lake Manyara. Furthermore, this also permits the evaluation of changes in SY of the tributaries between 1988 and 2016.

6.3 Results and discussion

6.3.1 Erosion risk change

An evaluation of the estimated total amounts of soil loss by surface erosion indicates that over the entire catchment there is a trend of increased surface erosion risk (Table 4). The total yearly catchment surface erosion is estimated to have increased by 2.54 megatonnes from 23.25 megatonnes yr^{-1} in 1988 to 25.79 megatonnes yr^{-1} in 2016. The average erosion in the catchment similarly increased from 12.7 tonnes ha^{-2} yr^{-1} (ranging between 0 and 1700.8) to 14.1 tonnes ha^{-2} yr^{-1} (ranging between 0 and 1848.4). These outputs correspond with smaller scale modelling exercises in Kenya (Angima *et al.*, 2003) and Tanzania (Ligonja & Shrestha, 2015). The upper range of the modelled values are likely to be overestimations as there might not be much soil to erode in these areas.

However, erosion plot studies by Kimaro *et al.* (2008) (bounded 1.2 x 20 m plots) under maize monocrops in the Uluguru Mountains, Tanzania, and by Angima *et al.* (2002) (bounded 9 x 2.5 m plots) in the central Kenyan highlands, found soil erosion rates up to 500 tonnes ha^{-1} yr^{-1}. These results indicate that the modelled estimations are not unrealistic on the longer slopes.

Analysis of the spatial distribution shows that the erosion risk changes are grouped in spatially distinct areas representing erosion hotspots (Figure 17c). However, it also indicates that the increase in erosion risk is not ubiquitous, including areas evidencing risk decrease. The most distinct increases in surface erosion risk are observed in the Dudumera, Makuyuni, Mto Wa Mbu and Tarangire sub-catchments. These results highlight that a lot of land conversion is happening in naturally vulnerable areas, giving rise to spatially distinct areas of anthropogenically-enhanced surface erosion risk. This fits with the existing research, stating that the effect of land cover change on soil erosion dynamics is highly dependent on the environment where the change occurs (Foley *et al.*, 2005; Montgomery, 2007). Most of the protected areas are characterized by stable or decreasing erosion risk, further highlighting the importance of land management (Appendix E.2).

Sensitivity analysis suggests that introducing errors in the separate factors had minor effects on the eventual quantitative predictions of the surface soil erosion risks, mostly affecting the outlier values. Introducing a K-factor of 0.001 for areas with a slope higher than 40° (assuming they were rocky), slightly lowered the total erosion estimation with 0.3 megatonnes to 23.0 and 25.5 megatonnes in 1988 and 2016 respectively. Regarding the spatial distribution of risk change, there was no observable effect when introducing error in any of the model inputs (Appendix E.3), nor when running the checked model for steep slopes.

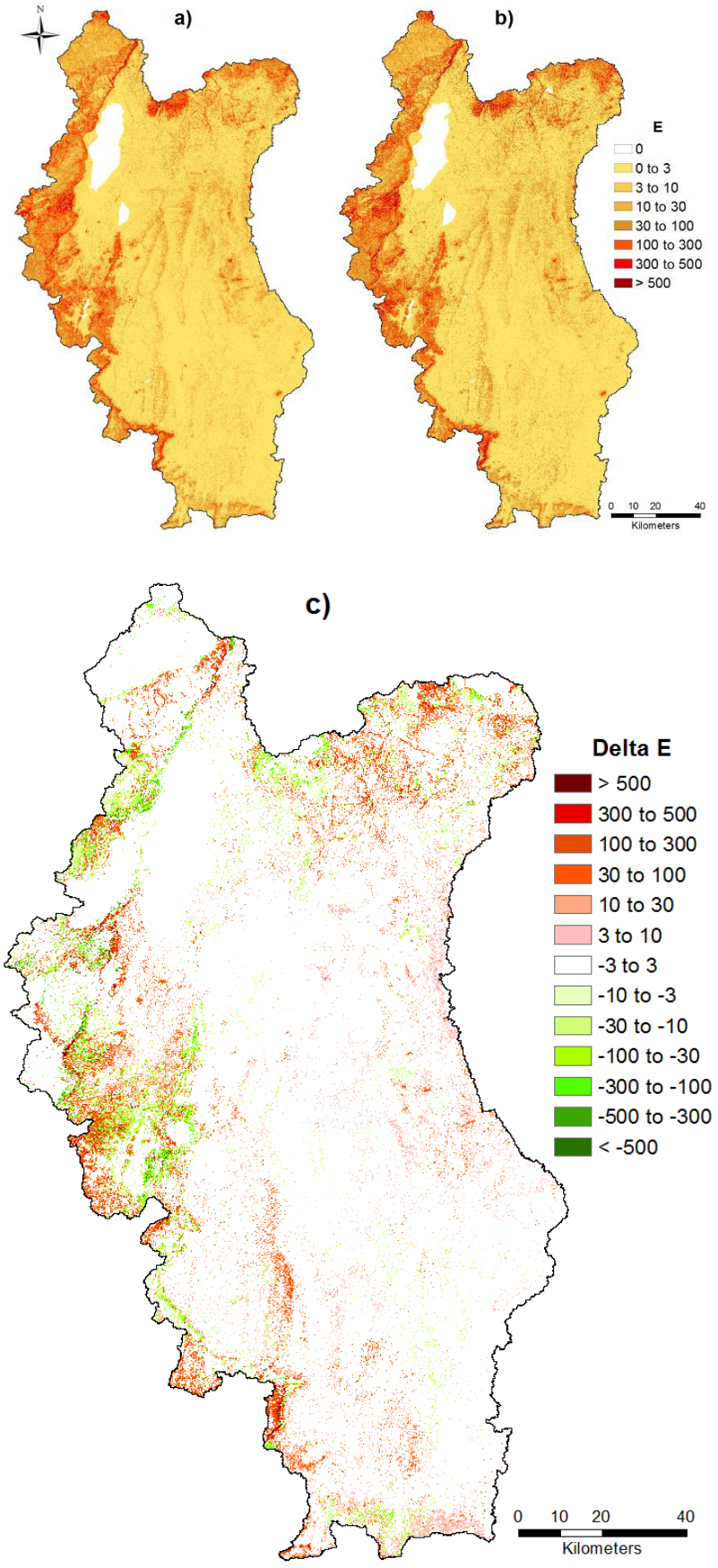

Figure 17: Modelled output maps of the annual average soil loss E (in t ha-1 yr-1 or as qualitative proxy for erosion risk) for a) 1988 and b) 2016. With c) the predicted changes in erosion risk (Delta E) following land conversion between 1988 and 2016. In the green areas erosion risk has decreased, while in the red areas it has increased.

The extreme soil erosion rates were mostly located at the downslope of the rift wall and steep mountain valleys. It is safe to assume that in these areas the soil is naturally thin or absent, which would mean that these values are an overestimation. However, as demonstrated with the checked model, these extreme values only have a minor influence on the total and mean erosion estimations. Moreover, some of the areas with modelled extreme soil erosion rates clearly demonstrate that the soil is rapidly being eroded/incised into badlands. This indicates that in East African environments, changing land cover can rapidly lead to extreme rates in soil erosion. Introducing errors in the model parameters thus only led to minor changes in the quantitative predictions and the spatial distribution of erosion hotspot zones remained the same. This observation is particularly promising, as the main goal of this study is to pinpoint hotspots of increased erosion risk.

6.3.2 Tributary sediment delivery

		1988			2016				
Catchment	SDR	E	SD	Proportion	E	SD	Proportion	ΔE	ΔSD
Dudumera	0.078	6.80	0.53	27.6%	7.45	0.58	27.5%	0.65	0.05
Endabash	0.160	0.93	0.15	7.8%	0.92	0.15	7.0 %	-0.01	0.00
Kirurumo	0.222	0.32	0.07	3.7%	0.32	0.07	3.4%	0.00	0.00
Magara	0.142	1.16	0.16	8.6%	1.25	0.18	8.4%	0.02	0.02
Makuyuni	0.079	4.42	0.35	18.3%	5.27	0.42	19.8%	0.85	0.07
Marera	0.234	0.62	0.15	7.6%	0.65	0.15	7.2%	0.03	0.00
Mto Wa Mbu	0.150	1.05	0.16	8.2%	1.24	0.19	8.8%	0.19	0.03
Simba	0.186	0.62	0.12	6.1%	0.60	0.11	5.3%	-0.02	-0.01
Tarangire	0.039	6.01	0.23	12.1%	6.92	0.27	12.7%	0.91	0.04

Table 4: Estimated SDR (dimensionless), hillslope soil loss by surface erosion (E, in megatonnes per year), Sediment delivery (in megatonnes per year) and proportional sediment delivery in the different tributaries in 1988 and 2016. The changes in estimated hillslope soil loss by surface erosion (ΔE, in megatonnes per year), and sediment delivery (ΔSD, in megatonnes per year).

The modelled changes in total E between 1988 and 2016 amount to an increase in total yearly sediment delivery of 0.20 megatonnes per year (9.65%) from the

major tributaries to Lake Manyara. The estimated values for 1988 and 2016 and changes in estimated tributary sediment delivery and proportional contribution are summarised in Table 4. While the total sediment delivery increases for every tributary except Endabash and Simba, these increases are not ubiquitous. This accounts for the observed minor changes in the estimated proportional contributions of the different tributaries to the total sediment delivery. Especially, the Makuyuni tributary seems to have a disproportional increase in sediment delivery.

6.3.3 Limitations

There are numerous limitations with risk change modelling based on RUSLE and remotely sensed data (Claessens *et al.*, 2008; Sepuru & Dube, 2018; Vrieling, 2006). One of these is the focus on surface erosion (interrill and rill erosion), and not accounting for other forms of erosion (e.g. streamline incision processes), which are potential contributors to net soil export and land degradation in the Manyara catchment. It is thus important to acknowledge that this modelling only represents one aspect of the total soil erosion spectrum. Possibilities lie in the coupling of these models with models mapping vulnerability to other erosion processes (e.g. mass movements, gully-, riverine- and wind erosion), which would give a better representation of the total erosion vulnerability (Aksoy & Kavvas, 2005). Additionally, these models do not account for sediment supply limitation and overland flow initiation dynamics, which are important factors for erosion dynamics as well. For example, areas highlighted as having a high erosion risk might have never developed a soil due to a natural overshoot of soil erosion over formation, and thus cannot actually deliver the eroded soil that the model predicts. Another limitation lies with the resolution of the data (30m), which excludes the effects of microtopographic landforms such as terraces that divide

the hillslope in small plateaus and that way impact slope factors. Moreover, the scoring process of land cover types arguably lacks the complex interaction of land cover with erosion. For example, overgrazing and trampling of rangelands due to overstocking would increase in erosion risk even though land cover remained stable. The estimation of the C-factor is also dependent on the expert, making comparison between studies difficult. A limitation specific to the semi-arid nature of the study site is that the rainfall erosivity is based on the mean annual precipitation of a 30-year period and does not consider the potential effects of interannual variation in precipitation. For example, Vrieling, Hoedjes and van der Velde (2014) have demonstrated that in semi-arid Africa, the rainfall erosivity can be 2-3 times higher in wet years compared to the mean. Furthermore, this rainfall variability is tightly linked to vegetation dynamics, which in turn influences the C-factor. For example, a wet year following a dry year will increase the C-factor as the vegetation will have desiccated in the dry period, creating an extra high vulnerability of soil erosion in the wet period (Kirkby, 1980).

The major issue related to SDR modelling is that it is based on static assumptions of catchment characteristics (Roehl, 1962; Walling, 1983). However, the complexity and dynamicity of hydrological and geomorphological factors challenges the identification of the dominant controls on catchment sediment response and on catchment-to-catchment variability (De Vente *et al.*, 2013). On the hillslope scale, this relates to the high impact of increasing gully incision, land cover dynamics and extreme rainfall variations (Croke & Mockler, 2001). On the catchment scale, sediment connectivity also has a potential non-linear response to rainfall and discharge due to channel bed and floodplain sediment deposition and reactivation (Croke, Fryirs & Thompson, 2013; Parsons *et al.*, 2006). The SDR estimations in this study thus do not account for sediment transport

dynamics under natural and/or anthropogenic dynamics (Hoffmann, 2015) and the resulting sediment delivery estimates cannot be interpreted as accurate representations. Therefore, they have limited value for informing management interventions on their own (Parsons *et al.*, 2006).

6.4 Conclusion

The soil erosion risk assessment presented here provides an important framework to assess changing soil erosion risk and support land management decisions. Model outputs indicate that a lot of land conversion has occurred in areas that are naturally vulnerable due to topography, soil type and rainfall patterns, seriously increasing the soil erosion risk. Quantitative estimation of soil loss can be a useful tool in smaller agricultural catchments but is less accurate in large and diverse catchments such as Lake Manyara. In this regard, the strength of this approach lies in 1) the estimation of catchment specific changes in surface erosion risk and tributary sediment delivery, and 2) spatially qualitative proxy maps of erosion risk changes following land conversion. This information is particularly useful to pinpoint hotspots of increased soil erosion risk that 1) supports targeting these areas for more detailed investigation of controls on erosion processes, and 2) guides stakeholders and policy makers in land management decisions of soil conservation measures and possible action.

Chapter 7. Determining tributary sources of increased sedimentation in Lake Manyara

7.1 Introduction

As highlighted in chapter 4, a lack of continuous monitoring in Lake Manyara and its tributaries impedes the assessment of sediment dynamics and hampers its coupling with upstream land degradation processes. Moreover, these processes are potentially influenced by natural rainfall variations (Ngecu & Mathu, 1999) and amplified by projected increases in extreme climatic events (Nearing, Pruski & O'neal, 2004; Shongwe *et al.*, 2011). The application of sediment tracing and -dating techniques as synergistic environmental diagnostic tools has the potential to fill this knowledge gap in Lake Manyara's sedimentation dynamics (Mukundan *et al.*, 2012; Walling, 2013).

Sediment apportionment applications assume the geochemical fingerprint of riverine sediment is a result of the amounts and geochemical composition of the various source soils (Haddadchi *et al.*, 2013; Walling, 2013). Differences in geology, climate, land cover and pedogenesis, give the resulting soils a characteristic geochemical composition (Motha *et al.*, 2002). Hydrological processes transport eroded soils from different catchment areas into the channel network, where after they are mixed and transported downstream as a composite parcel of sediment particles. The geochemical composition of downstream lake sediment thus depends on the relative contributions and geochemical fingerprint of different tributaries (Haddadchi *et al.*, 2013; Walling, 2013). Integrating source and mixture geochemical fingerprints within a BMM framework allows the proportional attribution of the tributary sources to the lake sediment (Blake *et al.*, 2018a). Furthermore, by taking sediment cores in the lake, the yearly cumulative vertical aggradation of sediment can be derived (Baskaran *et al.*, 2014). The

fallout radionuclides (FRNs) ^{210}Pb and ^{137}Cs are valuable tools for dating recent sediment deposits (<150 years) due to their known radioactive decay and unique origins resulting in fallout on the sediment surface layers (Appleby, 2008). While $^{210}Pb_{ex}$ is naturally (and continuously) formed in soils, the peak deposition of ^{137}Cs on sediment deposits in the southern hemisphere is generally being agreed to have occurred in 1965 and results from nuclear weapons testing (Cambray *et al.*, 1989; Walling & He, 2000). This known peak typically allows independent dating of sediment layers (Appleby, 2002), but is complicated, however, by low ^{137}Cs fallout in tropical Africa (Walling *et al.*, 2001; Walling & He, 2000). Hydrological and volcanic events can also lead to distinct geochemical peak depositions in sediment layers that can be used for independent dating of sediment layers, if corresponding dates are known (Arnaud *et al.*, 2006; Łokas *et al.*, 2010).

Against this background, the aim of this chapter is to evaluate the application of a complementary set of sediment dating and –tracing techniques in EARS to meet the requirements for targeted management interventions. First, the methodological challenges and results of sediment dating and sedimentation modelling in the Lake Manyara study site are evaluated. Second, geochemical fingerprints of sources and mixture are integrated within a BMM context to quantify spatial tributary apportionment in Lake Manyara. Third, the novel application of BMM on previously dated sediment deposits is assessed to quantify changes in tributary contributions over time. Finally, these multiple evidence bases are integrated to link changing sedimentation rates with specific changes in tributary sediment delivery, permitting evaluation of wider land use- and climatic factors.

7.2 Material and Methods

7.2.1 Sampling strategy

Riverine transported sediment was gathered from the lower reaches of seven of the nine major tributaries (Dudumera, Endabash, Kirurumo, Mto Wa Mbu, Makuyuni, Simba and Tarangire) (Figure 18), wherein specific sampling locations were subject to accessibility, necessary permits and safety. By sampling as close to the mouth of the inflow as possible, it was assumed that the transported sediment was a composite mixture of eroded sediment from the entire tributary catchment. Deposited sediment (DS) was collected from all riverbeds by taking between 10 and 20 composite samples, each composed of 15 sub samples of material from depositional features with clear indication of deposition by water. Samples were taken over a reach length of about 200 m to account for random spatial variability in riverine sediment deposition (Gellis & Noe, 2013; Wilkinson *et al.*, 2013). If the rivers happened to be flowing at the time of sampling, suspended sediment (SS) samples were also collected for the purpose of testing potential differences in fingerprint between SS and DS (Phillips, Russell & Walling, 2000). SS was sampled by collecting buckets of river water and transferring them in 1.5L bottles. The sediment was settled out overnight, where after the water was decanted and the remaining sediment dried. 3-5 SS samples were collected for the Makuyuni, Mto Wa Mbu and Simba rivers. The SS samples were only used for comparative purposes but were not included in the further analysis. In East African catchments, location and time specific rainfall can create temporal differences in active source areas to the mixed sediments transported in a river (Ambroise, 2004). Therefore, storm (Lizaga *et al.*, 2019), seasonal (Walling *et al.*, 2001) and annual (Phillips, Russell & Walling, 2000) variability was integrated in sediment fingerprints through multiple sample periods of DS over

three years. Lake bed sediment was retrieved by diving to collect grab samples. To account for localised sedimentation effects on the sediment fingerprint (Thevenon *et al.*, 2011), 44 samples were taken in 4 different areas of the lake: northeast, northwest, southeast and southwest (Figure 18).

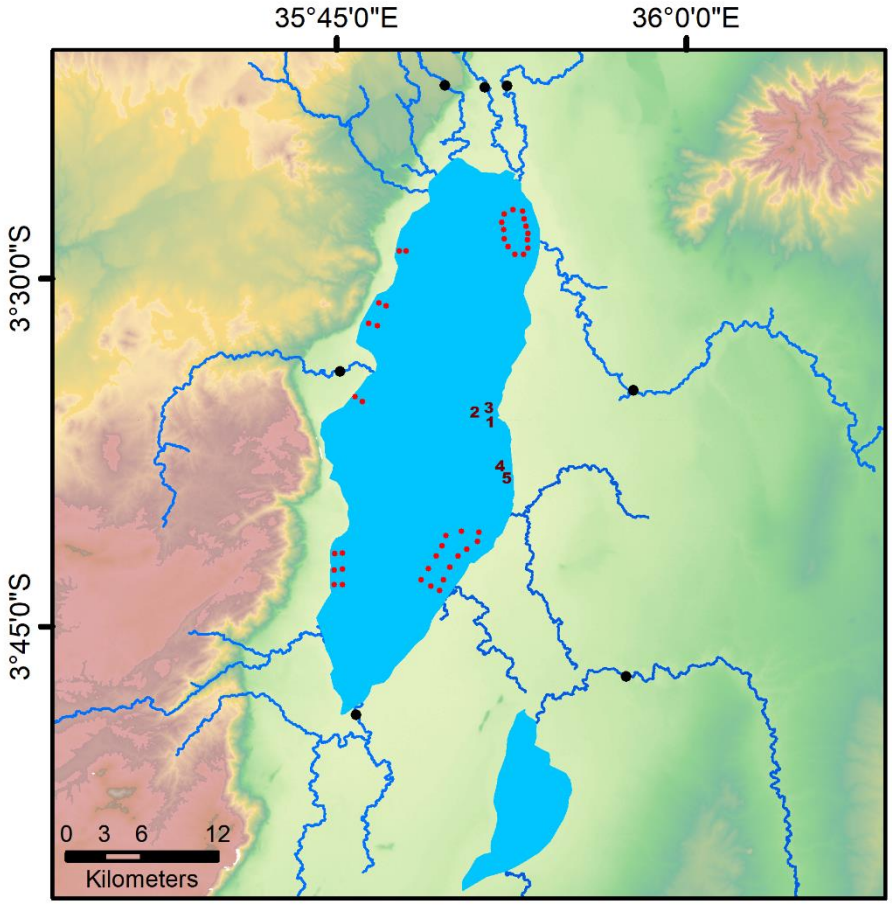

Figure 18: Riverine sediment sampling locations (black circles). Focus of Lake Manyara with locations of the sediment grabs (red circles) and cores (numbers correspond with core numbers).

While a gridded approach to lake sampling is preferable (Haddadchi *et al.*, 2019), this was not possible due to logistical challenges. First, Lake Manyara has an area of over 400 km^2 but had to be sampled by wading because of the shallowness and alkalinity of the lake, which is unsuitable for outboard engines. Second, the lake has limited access points for vehicles due to the difficult terrain and lack of roads. Third, hippo populations and other wildlife along the western side of the lake impeded safe sampling. The selected sites (Figure 18) cover all major river inlet areas and are therefore deemed to be representative of

sedimentation around the lake shores. In addition to the surface sediment samples, five cores (with respective depths of 44, 21, 32, 28, and 49 cm) were taken in southeastern Lake Manyara (Figure 18) between 2017-2018. A corer, internally fitted with pvc tubes, was manually pushed in the sediment. The pvc tubes were subsequently removed from the corer and opened sideways, after which the cores were sectioned in 1 cm intervals.

7.2.2 Laboratory Analysis

Sediment and core sections were either oven-dried at 40°C or freeze-dried and subsequently disaggregated using a mortar and pestle.

Radioactivity Determinations: Sediment core sections and tributary samples were packed into metal containers and sealed for a minimum of 21 days to allow equilibration between ^{214}Pb and its progenitor ^{226}Ra. Activity concentrations of the radionuclides were measured at the University of Plymouth ISO9001: 2018-certified Consolidated Radioisotope Facility (CoRiF) using low background EG&G Ortec planar (GMX50-83-LB-C-SMN-S) and well (GWL-170-15-S) HPGe gamma spectrometers. $^{210}Pb_{ex}$ was calculated by subtracting ^{226}Ra activity, measured using ^{214}Pb gamma emissions at 295 and 352 keV, from the total ^{210}Pb, measured by its gamma emissions at 46.5 keV ($^{210}Pb_{ex} = {}^{210}Pb_T - {}^{214}Pb$). ^{137}Cs was measured using its gamma emission at 662 keV. Count times were typically 24 hours, although a few sediment samples of low mass were counted for 48 hours, and the results quoted with a 2σ counting error. The calibration of the gamma spectrometer was performed using a natural homogenised soil, with low background activity, spiked with a radioactive traceable standard solution (80717-669 supplied by Exckart & Ziegler Analytics, Georgia, USA). Geometry-specific calibration relationships were determined using GammaVision software.

Analytical performance was assessed by participation in IAEA worldwide proficiency using example soils (IAEA-CU-2009-03 and soil IAEA-TEL-2012-03).

Geochemical determinations: Samples were analysed for major and minor element geochemistry by Wave Length Dispersive X-Ray Fluorescence (WD-XRF, PANalytical Axios Max; OMNIAN application) as pressed pellets. Prior to analysis all samples were sieved to <63µm to overcome particle size effects (Laceby *et al.*, 2017; Motha *et al.*, 2002) and because of the general focus on the detrimental fine sediment in the SS load (Walling, 2013). The sieved <63 µm fraction was further homogenised by milling it for 20 minutes at 300 rpm in order to prevent shadowing effects and preferential analysis of finer particles (Willis, Turner & Pritchard, 2011). Measurements were validated using stream sediment certified reference material (GBW07318, LGC, UK). Triplicates were made of randomly selected samples to assess the analytical variability and sample homogeneity. Instrument drift was assessed following internal quality control procedures using a multi-element glass sample. Only those elements returning measurements above the limit of detection for >75% of the samples and with triplicate variability <5% were used in further analysis.

7.2.3 Sediment dating and mass accumulation rates

^{210}Pb originates from the in-situ decay of particle-bound ^{226}Ra and ^{210}Pb fallout resulting from the decay of ^{222}Rn gas. Because of the fallout of $^{210}Pb_{ex}$ on the sediment surface layers, they contain a higher ^{210}Pb activity than what is expected from the equilibrium. The rate of change in $^{210}Pb_{ex}$ activity with mass depth in a sediment core provides the base for an age-depth relationship and for estimating sediment mass accumulation rates (MARs) (Goldberg, 1963; Krishnaswamy *et al.*, 1971; Robbins, 1978). The relatively long half-life of ^{210}Pb ($t_{1/2}$=22.23 years) makes it possible to measure time-series processes up to 5-6

half-lives, i.e. ~100 years. Different models have been developed for this purpose, making specific assumptions about the dynamics of sedimentation and $^{210}Pb_{ex}$ flux (Sanchez-Cabeza & Ruiz-Fernández, 2012). As demonstrated in Chapters 4-6, Lake Manyara has a large and diverse catchment, which is experiencing catchment-wide environmental changes. The constant rate of supply (CRS) model was used, which was specifically developed by Appleby and Oldfield (1978) to include changes in sedimentation rates and initial $^{210}Pb_{ex}$ activity concentration in the sediment and is described in detail Appendix F.

While the CRS model includes changing lake sedimentation rates and initial $^{210}Pb_{ex}$ activity, it assumes a constant rate of $^{210}Pb_{ex}$ supply to the sediment (Appleby & Oldfield, 1978). This assumption might be problematic in Lake Manyara for two major reasons. Firstly, sediment from different tributaries has different $^{210}Pb_{ex}$ activities (Appendix H.2), which might be caused by natural variability in the geological prevalence of ^{238}U and/or differences in dominant erosion processes (He & Walling, 1997) within the catchment. Second, LUCC can alter the dominant erosion process within each sub-catchment over time. Changes in dominant processes of erosion within tributary can alter the proportion of topsoil versus subsoil material in the transported sediment, thus its $^{210}Pb_{ex}$ activity (Aalto & Nittrouer, 2012; Baskaran *et al.*, 2014; Du & Walling, 2012). When the sediment delivery from the tributaries and/or the dominant erosion within the tributary catchments varies over time, so will the secondary $^{210}Pb_{ex}$ activity linked to the DS delivered to the lakes. So even when the atmospheric $^{210}Pb_{ex}$ flux to the lake environment stays relatively constant over time, the incoming secondary $^{210}Pb_{ex}$ signature of DS might vary substantially. For this reason, CRS model outcomes were scrutinised by comparison with independent ^{137}Cs ($t_{1/2}$=30.17 years) peak fallout (Appleby, 2008). Because of

the low ^{137}Cs fallout in tropical Africa, the geochemical profiles of the cores were also scanned for distinct changes or peaks that could be linked to hydrological changes (Davies, Lamb & Roberts, 2015; Łokas *et al.*, 2010) using upstream soil analysis (section 9.3.1) or volcanic events (Arnaud *et al.*, 2006) using samples from nearby volcano 'Ol Doinyo Lengai'.

The southern hemisphere 1965 ^{137}Cs time marker was subsequently incorporated into the model using the fitting approach (CRS-fitted) as described in Appleby (2002) and Appendix G. Since this method fits the 1965 reference date to its corresponding ^{137}Cs peak depth, dates of points between the reference and surface are unlikely to be greatly in error. At the same time, this approach increases the uncertainty of the deeper sediment dates as the core inventory is estimated by extrapolation of the reference values (Appleby, 2008).

7.2.4 Bayesian mixing model for source apportionment

The output from the WD-XRF geochemical analysis represents each sediment sample as a multi-elemental concentration data point. The sediment fingerprints can subsequently be obtained by grouping the samples per tributary sources and lake mixtures in multivariate concentration matrices. The model draws upon these matrices to proportionally attribute different tributary sources to the lake sediment. A BMM was created for this purpose within the MixSIAR framework (Stock *et al.*, 2018; Stock & Semmens, 2016), which is implemented as an open-source R package (Stock & Semmens, 2017) and adapted by Blake *et al.* (2018a) for river basin sediment transport.

BMM generally assume that 1) all dominant sources contributing to the sediment are represented, 2) tracer values are known in both sources and mixture, 3) tracers are conserved through the mixing process, and 4) fingerprint variability

between sources is larger than within sources. These assumptions were partly met by spatial and time-integrated sampling of sources in combination with standardised sample analysis, as discussed in sections 7.2.1 and 7.2.2.

a. Tracer selection

For the model to meet assumptions 2 and 3 and accurately represent catchment erosion and siltation processes, tracer properties need to be conservative in their environmental behaviour over space and time (Blake *et al.*, 2018a; Motha *et al.*, 2002). This conservative behaviour implies that there are no processes during detachment, transport or after deposition that alters the tracer concentration (Belmont *et al.*, 2014; Koiter *et al.*, 2013; Laceby *et al.*, 2017). Adopting the simple tracer screening of Blake *et al.* (2018a) and Sherriff *et al.* (2015), the range between sources and mixture of all tracers was tested (Appendix I.1). When the mean tracer concentration of the mixture was found to be outside the mean concentrations of the different sources, enrichment or depletion processes are likely and the tracer was excluded out of the analysis. Furthermore, if the rangetest demonstrated intra-source variance to be higher than the inter-source variance for specific tracers, they were also removed. As the model assumes that mixture tracer data are normally distributed (Stock *et al.*, 2018), the individual tracer distributions in the lake mixture were subsequently assessed for normality using the 'Shapiro-Wilk test' and histogram plotting.

After removal of non-conservative elements, 19 elements remained for use in the BMM: Ba, Co, Cr, Cu, Fe_2O_3, Ga, Mn, Nb, Ni, Pb, P_2O_5, Rb, SiO_2, SO_3, Sr, Ti, Y, Zn, and Zr. When analysing sediment deposits, Cr, Y and Pb were additionally removed because they fell out of range between source and core, which can be caused by release spikes from unknown sources or vertical mobility within the sediment column.

b. Fingerprint analysis

Assumption 4 requires the difference between the different source fingerprints to be larger than the difference within each source fingerprint. In this context, a principal component analysis (PCA) was performed on the multi-elemental source fingerprints to reduce the dimensionality (D'Haen, Verstraeten & Degryse, 2012). This allowed an analysis of the temporal and spatial distinctiveness of the source fingerprints as demonstrated in Figure 19.

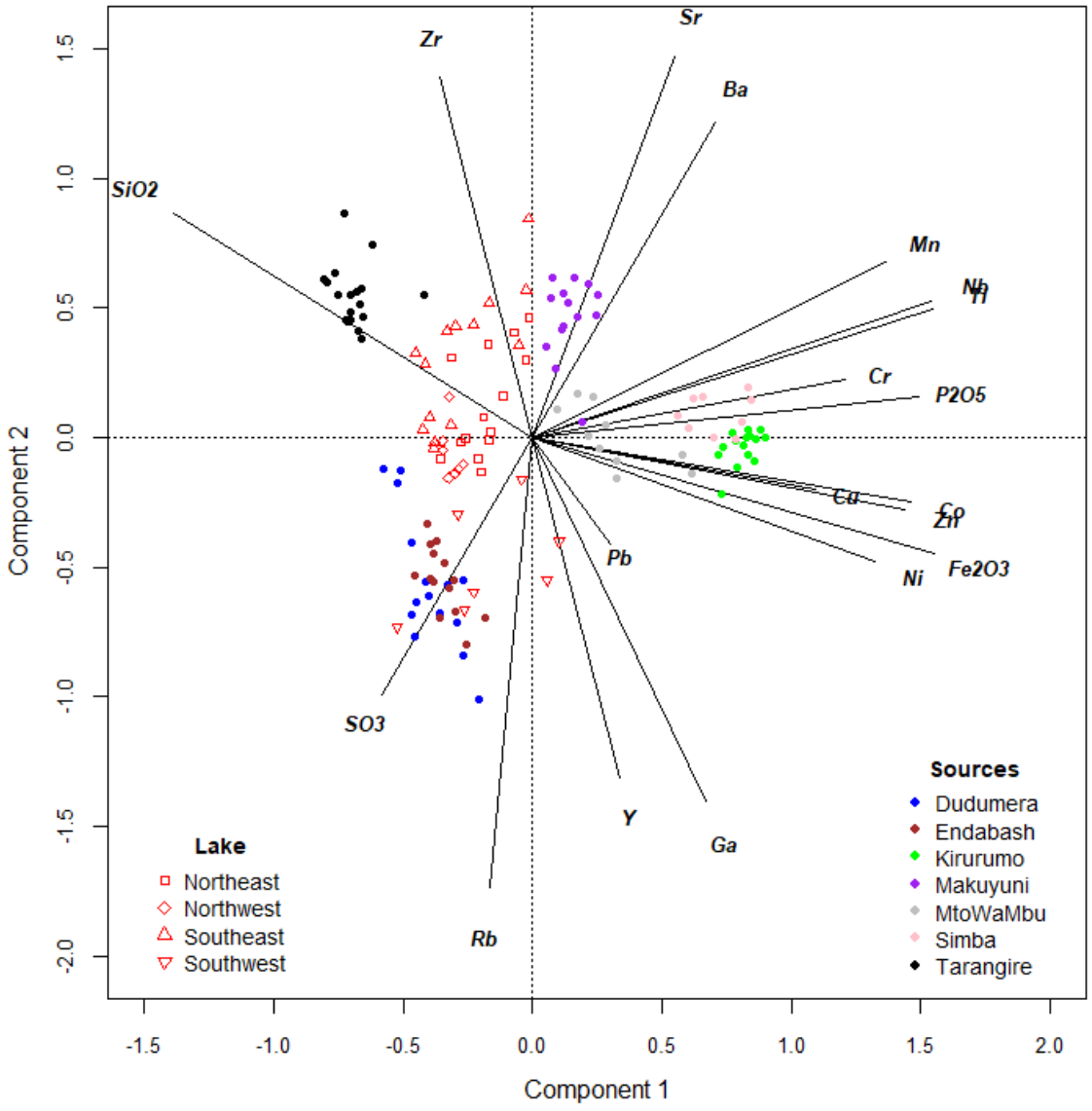

Figure 19: Ordination biplot visualising the geochemical drivers of variance in the DS fingerprint from different tributary sources and lake mixture using the two largest eigenvalues (explaining 47.6% and 21.2% of variance), with grouping of different lake areas.

If the tributary fingerprints occupy small niche spaces on the ordination plot and have low levels of overlap with each other, the model will be a strong tool for sediment attribution (Smith & Blake, 2014; Smith *et al.*, 2015). When fingerprints of different tributaries overlap, the model will struggle to distinguish them. In this case, the model robustness can be increased by a-priori grouping of sources based on the overlap in fingerprint (Stock *et al.*, 2018). If a-priori grouping is used in combination with geospatial information, it preserves the environmental representativeness. In this study, all tributaries formed distinct fingerprint clusters and a significant fingerprint overlap only occurred between Kirurumo and Simba tributaries (Figure 19), which is likely due to their similarities in catchment size, location, relief, geology, climate and land cover (Figure 18). Both tributaries were therefore grouped into one Ngorongoro class, meaning that the model will attribute the contribution from those two sources to one larger regional source.

The lake mixture is taking a central, but large, space on the ordination plot, indicating a high variability in Lake Manyara's surface sediment geochemistry. A focused PCA analysis of the lake sediment indicates clear geochemical grouping between the northeastern, northwestern, southeastern and southwestern sediment. This indication of localised sediment geochemical variability is not surprising given the lake's large size, shallow nature and high salinity, which induces flocculation of clay particles when they enter from freshwater rivers (Last & Schweyen, 1983). Location in the lake thus affects the geochemical fingerprint of the sediment, highlighting the importance of including spatial variability in the sampling strategy and the model build.

The PCA also allowed the assessment of assumption 2 by quantifying the differences between sampling time and method. No structural differences in DS fingerprint of tributary sediment were found between sampling moments.

However, minor differences were observed between DS and SS in some of the tributaries. Even though the differences between sampling methods in tributaries were minor in respect the differences between the tributaries, only the DS samples were included in the model due to their natural temporal integration of sediment compared to the more flashy nature of SS.

c. Mixing model build

One of the major advantages of BMMs is the flexibility in model structure. Depending on the specifications of 1) error formulation, 2) prior information, 3) tracer covariance, and 4) fixed and/or random effects, the model can be tailored to the specific data and research questions (Blake *et al.*, 2018a; Stock *et al.*, 2018).

1) Sediment mixing consists out of a dynamic flux of geochemically distinct sediment particles from tributaries to the lake. As it is impossible to capture the entire variability within sediment systems by sampling, a 'residual error' formulation has to be included in the model. The 'process error' was not included because the transport of sediment from rivers to the lake is random and constant (Stock *et al.*, 2018; Stock & Semmens, 2016).
2) A prior information file was built using the 2016 modelled sediment delivery output of each tributary (Section 6.3.2, Table 4). The modelled sediment delivery estimates were rescaled to the total number of sources as demonstrated by Stock *et al.* (2018). After rescaling, the following prior values were used: 1.95, 0.5, 1.41, 0.63, 0.62, and 0.9, corresponding with Dudumera, Endabash, Makuyuni, Mto Wa Mbu, Ngorongoro, and Tarangire rivers respectively. An uninformative prior (1, 1, 1, 1, 1, 1) was used for comparison and for the core BMM.

3) Due to the high number of tracers and their potential covariance, tracer redundancy can occur. By inserting the data points in raw form, the model can include this covariance between individual tracers (fully Bayesian) and thus reduce the effects of tracer redundancy. While this does not affect the actual model outcome, it increases model efficiency and thus the likelihood of convergence (Stock *et al.*, 2018).
4) Inclusion of fixed or random effects was tailored to the specific research questions and data structure. The lake mixture (42 samples) was firstly analysed without fixed or random effects to infer the contributions of the tributaries to the 'total' lake sediment. Subsequently, sampling 'location' in the lake was used as a fixed categorical effect of the sediment mixture to infer the contribution of different tributaries to the specified sampling areas in the lake. Changes in source attribution over time were investigated by using sediment cores as either separate or pooled mixtures and introducing two modes of covariate analysis. First, 'age' was introduced as a fixed continuous effect. Second, age and PCA fingerprint analysis were used to group the sediment cores into distinct classes that were subsequently included as fixed categorical effect. Model efficiency and outcomes were evaluated under different modes of covariate structure.

For all MixSIAR model runs, the Markov Chain Monte Carlo (MCMC) parameters were generally set as follows: chain length = 3000000, burn = 2700000, thin = 500, chains = 3. Convergence of model chain output was evaluated using the Gelman-Rubin diagnostics (Gelman *et al.*, 2013), rejecting model output if >5% of total variables was above 1.05 confidence interval, in which case chain length was increased or the model build was re-evaluated (Stock *et al.*, 2018). The outcomes of the changes in tributary proportional contribution were converted to

absolute changes in tributary sediment delivery by multiplying them with the MAR outputs.

7.3 Results and discussion

7.3.1 Sedimentation rates

Of the five sediment cores, only cores 2 and 3 showed a $^{210}Pb_{ex}$ profile that offered evidence of undisturbed stratigraphy (Figure 20a and 19b). Four potential processes could have caused profile mixing in cores 1, 4 and 5 (Appendix H.1), each having different implications regarding geochronological model applicability. The first process relates to high wind and/or biological/human activity in the shallow lake zone leading to vertical mixing of the sediment deposits and a flattening of the $^{210}Pb_{ex}$ profile. Second, periodical drying of the lake could have exposed the coring sites to periods of direct atmospheric $^{210}Pb_{ex}$ deposition and/or removal of sediment by wind erosion. Third, changing erosion and sediment transport dynamics in the catchment could have influenced $^{210}Pb_{ex}$ flux into the sediment (Appleby *et al.*, 2019) as discussed in section 7.2.3. Finally, accelerating sedimentation rates could have markedly diluted the $^{210}Pb_{ex}$ activities in recent sediment deposits, resulting in a lower activity then expected (Appleby, 2002). The ^{137}Cs activity in all of the cores is low, with most of the sections below the limit of detection. These findings correspond with the global predictions of ^{137}Cs fallout in tropical regions (Walling & He, 2000). Unfortunately, the low ^{137}Cs activities impedes the assessment of ^{137}Cs peak integrity and thus does not allow the unambiguous attribution of $^{210}Pb_{ex}$ flattening to sediment mixing or increases in sedimentation rate (Appleby, 2002). Due to this remaining uncertainty, only the results from cores 2 and 3 will be discussed here. Both cores have two $^{210}Pb_{ex}$ activity peaks, which is observed in lakes with accelerating

sedimentation regimes where dilution of fallout occurs (Appleby, 2008). The deepest detectable ^{137}Cs activities were found at mass depth 30 g cm^{-2} and 20 g cm^{-2} in cores 2 and 3 respectively. Due to the low activities in, and differences between, the core sections, in combination with the constant radioactive decay of ^{137}Cs isotopes, these oldest detectable layers were assumed to be the 1965 southern hemisphere peak deposition (Cambray *et al.*, 1989; Walling & He, 2000). However, the observed ^{137}Cs 'peak' might also be related to transport of naturally concentrated eroded particles to the lake, meaning that it could be younger than 1965 (Mabit, Benmansour & Walling, 2008). For these reasons, the ^{137}Cs dating in the Lake Manyara cores has a high level of uncertainty.

The CRS output from cores two and three (Figure 20c and 19d respectively) show a similar age-depth relationship. In both cores, the ^{137}Cs peak slightly lies above the curve, which could either be because of variations in the ^{210}Pb$_{ex}$ activity of the DS over time, or because of uncertainty around the ^{137}Cs peak. CRS model outputs are presented for both the standard and fitted (to ^{137}Cs) approaches and trends in sedimentation rate were found to be very similar. The main difference in both cores being the flattening out of the older MAR peaks in the CRS fitted approach. The MAR output of the **CRS-standard** approach starts out with 0.225 g cm^{-2} yr^{-1} from 1905-1920 in core three and 0.288 g cm^{-2} yr^{-1} from 1913-1926 in core two. The MARs decrease to 0.117 g cm^{-2} yr^{-1} for core three and 0.248 g cm^{-2} yr^{-1} for core two in the 1920s and 1930s. From this point, the MARs show a general trend of increasing sedimentation over time in both cores. A series of peaks are observed in core three in the 1950s and 1960s, the highest (0.852 g cm^{-2} yr^{-1}) in 1962, which might be related to high levels of deforestation and agricultural degradation following independence in Tanzania. In core two, a similar increase in sedimentation is observed in the 1950s and 1960s, however,

peaking (0.803 g cm^{-2} yr^{-1}) in 1972, about 10 years later then core three. The slight delay of the peak in core two might be due to spatial differences in sedimentation or higher uncertainties in the older sediment dates. In both cores, the MAR decreases again in the 1980s and 1990s, albeit to higher levels than original. The most recent peak is observed at 2010 in both cores. While the 2010 MAR peak (0.84 g cm^{-2} yr^{-1}) in core three is similar in height to the one in 1962, the peak in core two (1,813 g cm^{-2} yr^{-1}) is much higher.

The **CRS-fitted** approach of Appleby (2002), using the independently dated 1965 as a fixed date, did not cause substantial alterations in sediment dates of the shallower core sections as shown in Figure 20c and 19d. However, the differences were much larger in deeper core sections, attributing older dates to deeper core sections, which slightly impacted the calculated sedimentation rates. The lowest fitted MARs were in deeper core sections, starting out with 0.0714 g cm^{-2} yr^{-1} from 1890 in core two and 0.024 g cm^{-2} yr^{-1} from 1860 in core three. In both cores, the fitted MARs gradually increased until a small peak of 0.4233 g cm^{-2} yr^{-1} in 1952 for core two and of 0.423 g cm^{-2} yr^{-1} in 1943 for core three. For both cores, the fitted MARs stayed slightly higher from the 1950s until the early 1970s, after which they decreased to lower, albeit higher than original, levels from the late 1970s until the early 1990s. Both cores subsequently record an increase from the late 1990s with a distinct peak in 2010 of 1.550 g cm^{-2} yr^{-1} for core two and 0.745 g cm^{-2} yr^{-1} for core three. Considering the large size of Lake Manyara, the MAR outcomes of both approaches is very high, even in the older core sections. If the most recent peak values are extrapolated to the entire lake area (taken at 440 km^2), sedimentation quantity in Lake Manyara in 2010 estimates between 3.68 (core 3) and 7.95 (core 2) Megatonnes for the standard approach and between 3.27 (core 3) and 6.80 (core 2) megatonnes for the fitted approach.

However, as the lake cores were taken away from most river inlets, these estimates are probably on the lower end of the actual sedimentation in the lake. These high volumes of sediment transported to Lake Manyara from its catchment are comparable with measured SY in EARS (Vanmaercke *et al.*, 2014).

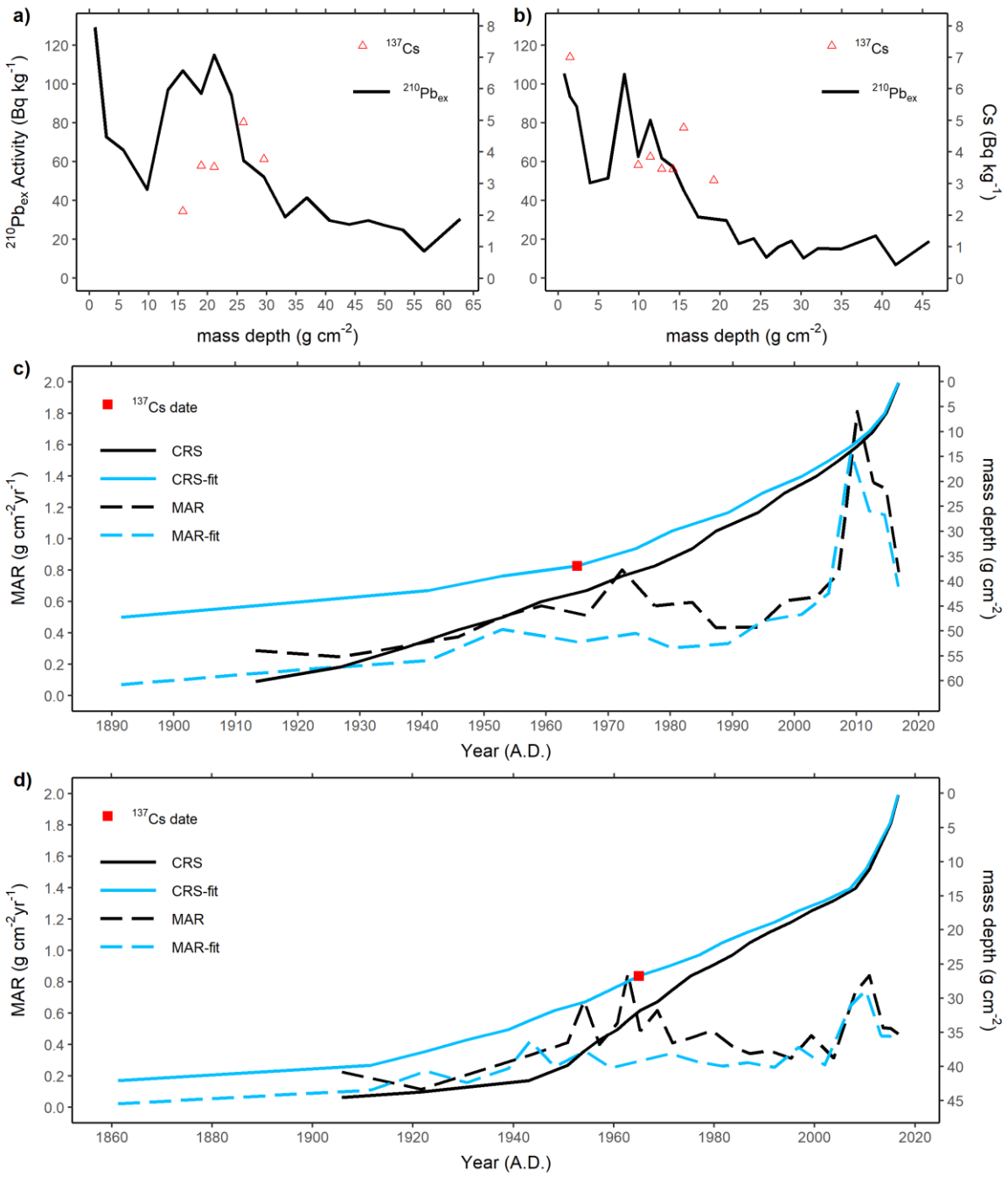

Figure 20: $^{210}Pb_{ex}$ and ^{137}Cs mass depth profiles of a) core two and b) core three. Age-depth relationship (full) and Mean Accumulation rates (dashed) using the standard CRS (black) and CRS-fitted (blue) approach for c) core two and d) core three.

Comparing the CRS output of both cores with their geochemical profiles allows independent confirmation of the output MARs. Interestingly, the most recent MAR

peaks of both cores exactly correspond with peaks in many elements linked to allogenic sediment origins (as will be shown in section 9.3.1) and minima in elements linked to autogenic aquatic origin (Appendix I.2 and Appendix I.3). In both cores the allogenic tracers: Al_2O_3, Fe_2O_3, Nb, Ti, and Zr, all have distinct maxima, while the autogenic tracers: K, MgO, Na_2O, Sr and Cl, have their minima at the same depth (9.73 and 3.95 g cm-2 for cores two and three respectively) as the MAR peak. This high correlation between geochemical deposition and sedimentation rates in both cores mutually confirms both evidence bases, making it highly likely that Lake Manyara recently experienced extreme sedimentation rates driven by increased erosion and sediment transport in the catchment. Comparison of the sedimentation rates with annual rainfall variations (Appendix B.1) do not reveal a direct correlation between rainfall and sedimentation peaks. This suggests that the observed increase in sedimentation in Lake Manyara is mainly driven by a complex interaction between increased upstream delivery and natural rainfall fluctuations through sediment connectivity.

7.3.2 Proportional tributary contribution

The BMM results of the sediment in Lake Manyara for both the ‘total’ and ‘spatial’ analysis are shown in Figure 21 and Appendix J.1. The results from the ‘total’ analysis are very distinct, attributing 58.2 % of the recently deposited lake sediment to the Dudumera tributary and 35.9% to the Makuyuni tributary. This corresponds with chapters 6 and 7 that highlighted both sub-catchments to have experienced widespread conversion of natural land cover to agricultural purposes, leading to increased risk of soil erosion risk. Furthermore, the Makuyuni sub-catchment is evidencing increasing levels of grazing, gully incision and land degradation (Blake *et al.*, 2018b). The other tributaries contribute only marginally to the total sediment load, both Endabash and Mto Wa Mbu rivers with

1.1%, the Ngorongoro region with 1.7% and Tarangire with 2.0%. The results of the 'spatial' analysis are more nuanced, demonstrating the importance of localised sedimentation in the lake. While the Dudumera river was dominating the overall lake sediment in the 'total' analysis, it has a smaller, yet still significant, contribution to all different lake locations. The Endabash river is dominating in the northwestern sediment, but only has minor contributions in the other areas. Interestingly, the Makuyuni river is dominating the northeastern lake system, while also significantly contributing to all other lake areas. Mto Wa Mbu river is the dominant contributor to the southwestern lake sediment but insignificant in other lake areas, which is surprising given the northern inlet in the lake. The Tarangire river has its inlet in the southeastern part of Lake Manyara and is also dominating the southeastern lake sediment, while being insignificant in other lake areas. The Ngorongoro region does not have any significant contribution to the sediment in any of the lake areas.

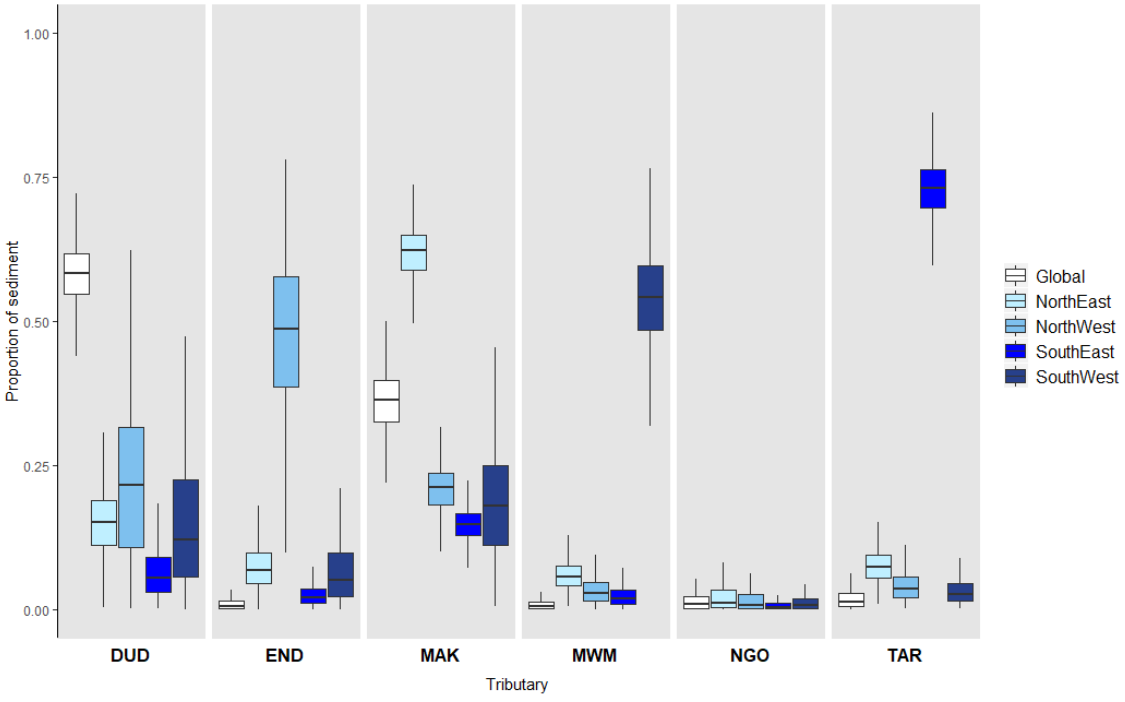

Figure 21: MixSIAR proportional sediment contribution of the tributary rivers (Dudumera, Endabash, Makuyuni, Mto Wa Mbu, Ngorongoro, and Tarangire) to the 'total' lake sediment (white) and different lake areas (blue shades). The density distributions are represented as boxplots with median shown by central line, interquartile range by box, and range by whiskers.

Overall, the lake sediment seems to be originating from the Dudumera and Makuyuni sub-catchments, which is highlighted by their dominance in the 'total' analysis and significant contribution to all lake areas in the 'grouped' analysis. However, even though the other tributaries were not identified by the 'total' analysis, they often dominate localised depositions as highlighted by the 'spatial' analysis. The Makuyuni river both dominates the northeastern sediment and significantly contributes to other lake areas, as well as being a major contributor of the 'total' lake sediment. The consistency of model output towards Makuyuni, in combination with reports indicating that lake sedimentation is especially grave northeastern lake area (Kiwango, 2010), highlights the overall importance of sediment contribution from this tributary.

7.3.3 Archived changes in tributary sediment delivery

The geochemical stratigraphic record of the sediment cores offer useful indication of changes in tributary sediment delivery to Lake Manyara over time. Model efficiency was higher under the BMM with 'grouped' core classes as a fixed categorical effect compared to the BMM with 'age' as a fixed continuous effect. This further confirms that sedimentation is not continuous in Lake Manyara, but experiences distinct episodes of high and low sedimentation that are linked to changes in tributary sediment delivery. The continuous BMM was not able to converge, even with extremely long chain lengths, and therefore only the results of the grouped BMM will be discussed. BMM outcomes for cores 2 and 3 are shown in Figure 22a and Figure 22b, and Appendix J.2 and Appendix J.3 respectively.

While both cores are dominated by the Dudumera fingerprint, the changes in proportional contribution differ slightly between them. In core 2, the proportional contribution of the Dudumera experiences three distinct dips followed by gradual

increases, albeit to lower levels then before. In core 3, the proportional contribution of Dudumera stays relatively stable, followed by a small but abrupt drop during the ‘50s and subsequent increase to a higher level in the ‘60s and ‘70s. From the ‘80s the Dudumera contribution start to decrease gradually, rapidly speeding up the last ten years dropping to its lowest level. In both cores, the Makuyuni is the second most important contributing tributary, and seems to behave opposite to Dudumera. In core 2, the changes in Makuyuni contribution are relatively small, with peaks in the ‘40s and 2010. In core 3, the Makuyuni contribution stays relatively stable up until the last 10 years, after which it increase rapidly. The Endabash tributary has a minor contribution in both cores with minor elevations during ‘50s-‘70s and ‘90s in core 2, and a distinct peak during the ‘50s in core 3. The Tarangire tributary only has a significant contribution in the older sections of core 3, wherein it stays stable until 1960, after which it drops to a low contribution. The increasingly significant contribution of the Ngorongoro system in core 2 and to a lesser extend in core 3 is surprising given its insignificant contribution to both ‘total’ lake sediment and ‘spatial’ lake zones, and might be a specific observation for this site. However, the most likely explanation for this anomaly lies with the specific fingerprint of the Ngorongoro sediment (Figure 19), which due to its volcanic geology and specific catchment characteristics is naturally typified by the same geochemical tracers that are related to increased allogenic sediment delivery to the lake (Appendix I.2 and Appendix I.3: Fe_2O_3, Nb, Ti, Zn). The observed increase in proportional contribution of the Ngorongoro system might thus actually represent the general increase in allogenic sediment delivery to the lake.

Especially with extreme increases in sedimentation, as observed in core 2, the quantitave sedimentation signal seems to overpower the spatial signal. BMM

outcomes of sediment deposits based on geochemical stratigraphic record should thus be interpreted with care in lakes that have experienced extreme changes in sedimentation. Furthermore, other lake areas might exhibit different trends in changing tributary contributions related to the demonstrated importance of localised sedimentation effects. Moreover, these changes are relative to the total sediment entering the lake, which is increasing as demonstrated by the CRS outcomes. Even though the proportional contribution of the Dudumera tributary has decreased in the last thirty years, its absolute sediment delivery actually increased as illustrated for core 3 in Figure 23. This further highlights that increased sedimentation in Lake Manyara is a catchment-wide issue, but seems to be disproportionally driven by increased delivery from the Makuyuni tributary.

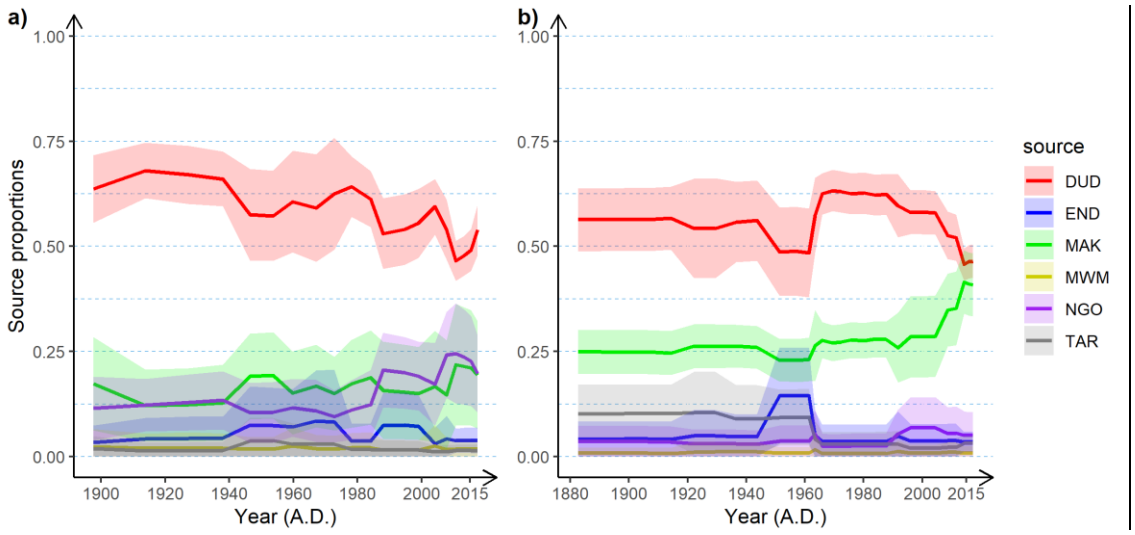

Figure 22: Changing proportional sediment contributions of tributary rivers over time to a) core 2, and b) core3.

7.4. Conclusion

Increased sedimentation of RVLs is threatening the provisioning of water, food and livelihoods in EARS. However, a lack of long-term data on sediment delivery dynamics and sedimentation rates hampers the development of science-based land and water management plans. In this context, this Lake Manyara case study demonstrates methods to overcome environmental challenges in sediment

tracing and -dating techniques and highlights their potential to fill knowledge gaps in EARS sediment source-to-sink dynamics. Low ^{137}Cs peak activity increases the uncertainty around radioactive dating and changes in sedimentation rates. This study demonstrates the potential of geochemical profile analysis as a valuable alternative for independent confirmation of extreme sedimentation rates. As evidenced from mutually confirming $^{210}Pb_{ex}$ dating, allogenic maxima and autogenic minima, Lake Manyara has experienced a general increase in rates of sedimentation over the last 150 years, with a distinct peak in 2010. These results confirm the concerns on increasing sedimentation in Lake Manyara raised by local land and water conservation authorities. No clear correlation was found between sedimentation peaks and annual rainfall, indicating complex dynamics of upstream sediment delivery and downstream sediment propagation.

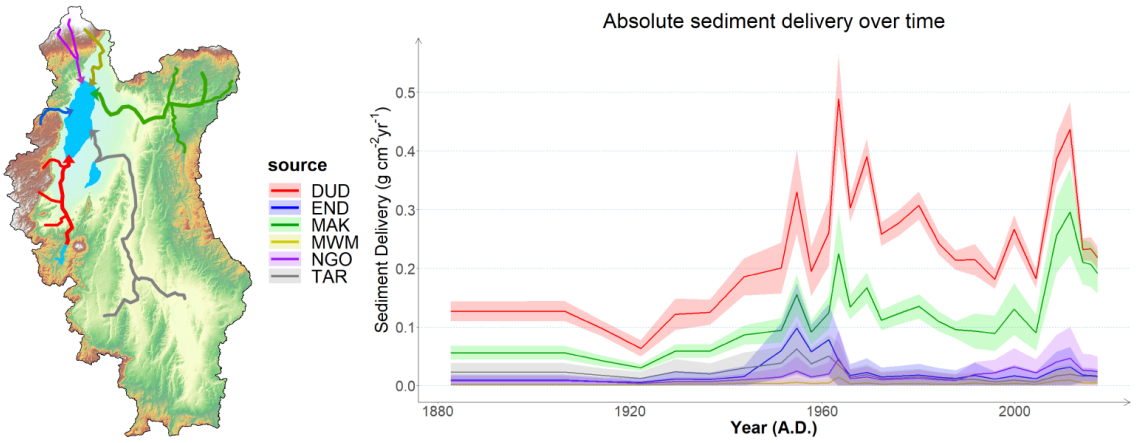

Figure 23: Changes in absolute sediment delivery from tributaries (DUD=Dudumera, END=Endabash, MAK=Makuyuni, MWM= Mto Wa Mbu, NGO= Ngorongoro, and TAR=Tarangire) to Lake Manyara over time as reconstructed from $^{210}Pb_{ex}$ dating and BMM of core 3.

The integration of geochemical fingerprinting within a BMM framework was proven a robust tool for attributing dominant contributing tributary sources to lake sediment. The 'total' model provided an estimate of the tributary sediment contributions to the entire lake and, in the case of Lake Manyara, pointed towards Dudumera and Makuyuni as the major sources. Both sub-catchments have

experienced widespread conversion of natural land cover to agricultural purposes and especially Makuyuni is evidencing increasing levels of grazing, gully incision and land degradation. However, with sedimentation being often highly localised in large RVLs, this study has shown the importance of using spatial factors as a fixed categorical effect in BMMs. Inclusion of localised sedimentation effects provided a fuller representation of spatially specific sedimentation issues and a deeper understanding of the driving processes within the catchment. Different tributaries dominate sediment delivery to different areas of Lake Manyara, with the Makuyuni being overall the largest source.

Furthermore, the novel application of BMMs to sedimentary geochemical data allowed the assessment of changes in source attribution over time. In parallel with $^{210}Pb_{ex}$ dating, changes in sedimentation rates over time were linked to changes in sediment delivery from specific tributaries. In this context, the sedimentation peak from 1950s to 1961 in Lake Manyara seems to be mostly driven by the Dudumera tributary and, to a lesser extent, the Endabash tributary and is potentially linked to uncontrolled deforestation in these naturally forest-dominated catchments following independence (as discussed in section 3.3.3). The current increasing levels of sedimentation are disproportionally driven by increased sediment delivery from the Makuyuni tributary. Even though the proportional contribution of the Dudumera tributary has recently decreased, its absolute sediment delivery continued to increase. However, this study also highlights a substantial challenge for the application of this technique, which results from the potential overlap between the geochemical signals of tributary contribution and increased sedimentation. Furthermore, due to previously highlighted localised sedimentation effects, the results from the historical sediment BMMs were difficult to extrapolate to the entire lake environment.

Predictions of changing sedimentation rates and source sediment contributions should thus be interpreted in their localised lake sedimentation context. Based on these limitations, future studies that aim to link changes in sedimentation with changes in tributary sediment delivery in RVLs should try to 1) minimise the conflict between the spatial source and quantitative sedimentation signals, and 2) include spatially integrated sediment coring in their study design. Nonetheless, the complementary nature of this set of sediment analysis tools has proved to be able to constrain siltation issues in impacted lake areas to specific tributary sources. This clears the way for targeted investigations into the dynamics of increased erosion and sediment transport, linking upstream land degradation processes with downstream ecosystem health.

Chapter 8. Deconvoluting sediment fluxes within the Makuyuni tributary.

8.1 Introduction

As demonstrated in chapter 7, geochemical fingerprinting in a BMM framework is a valuable tool in tributary attribution of lake sediment in large and environmentally diverse catchments. In that context, the Makuyuni tributary was pointed out as a major driver of recent increasing rates of sedimentation in Lake Manyara. Moreover, in chapter 6, large areas of increased erosion risk were highlighted in the Makuyuni catchment. While both evidence bases are valuable tools to constrain the sedimentation and erosion problems, they do not elucidate sediment flux dynamics within the Makuyuni tributary. In this chapter, a deconvolutional approach to BMM of riverine and floodplain sediment against upstream subtributaries will be implemented to 1) further constrain the dominant sediment sources to sub-tributary level, and 2) assess changing dynamics of sediment origins and transport in the Makuyuni system. This section of work is set against the same literature context as chapter 7.

8.2 Material and methods

8.2.1 Sample collection and analysis

Riverine transported sediment was collected from all of the major subtributaries of the Makuyuni system (Appendix K.1), including nested downstream samples along the Makuyuni river gradient as shown in Figure 24. The method of collection was done as described in section 7.2.1 but was highly dependent on the environmental and logistical constraints in the system. While a nested sampling approach with high temporal resolution is the most accurate representation of riverine source-to-sink dynamics (Blake *et al.*, 2018a), a combination of logistical

challenges and a highly complex system complicated the sampling strategy. First, the ephemeral nature of some of the Makuyuni subtributaries did not always allow the sampling of SS, in which case DS samples were taken from the exposed bed. Additionally, a lack of roads and presence of wildlife made it impossible to sample the middle channel reaches of the Makuyuni system during the wet season. Therefore, the middle reach nested samples (M3 and M4) result from one sampling event of DS undertaken during the dry season. This is potentially problematic as the high spatial and temporal variability in the Makuyuni system could lead to discontinuous connectivity between subtributaries and main river system. M3 and M4 thus only give a snapshot of the sediment dynamics in the Makuyuni system and it is not safe to assume that they provide an accurate representation of the yearly contribution of upstream tributaries to the total tributary system. The downstream nested sampling locations (M1 and M2) and most of the upstream subtributaries (M1-2, M5-M8) were easier to reach and therefore allowed a higher temporal resolution of sampling. Furthermore, the downstream location of M1 and M2 account for a natural integration of upstream sediment. All samples were collected over three sampling campaigns between 2016-2018. The potentially uncaptured temporal variability within sub-tributary (MS1-MS8) sediment fingerprint was therefore assumed lower than the captured spatial variability between them.

The mid-reach temporal issue was overcome by including a nested floodplain core that captured the changes in upstream sediment delivery over time. The floodplain location was selected depending on accessibility and spatial positioning to capture an integration of multiple upstream tributary systems (MC1, Figure 24). A 1m deep pit was dug and samples were collected directly at 3-5cm

interval depths. Sediment samples were analysed for major and minor element geochemistry by WD-XRF as described in section 7.2.3.

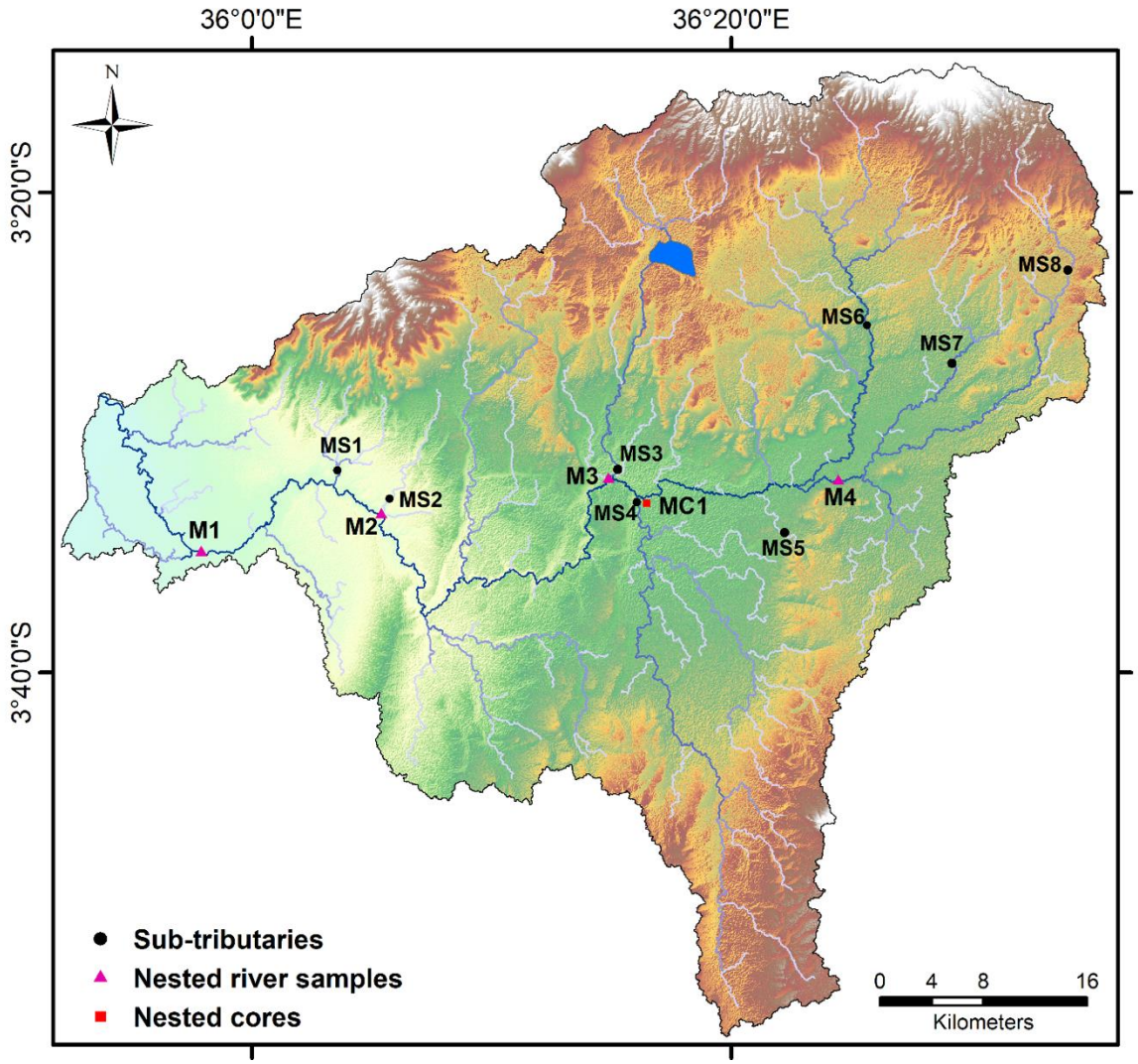

Figure 24: Sampling locations in the Makuyuni system. Four nested river samples: M1, M2, M3 and M4. Eight sub-tributaries: Lesimingore A (MS1), Lesimingore B (MS2), Nanja (MS3), Lolkisale (MS4), Meserani Chini (MS5), Ardai (MS6), Meserani Juu (MS7) and Musa (MS8). One nested floodplain core: Meserani floodplain (MC2).

8.2.2 Deconvolutional Bayesian mixing model

a. Tracer selection and fingerprint analysis

The simplified tracer selection process and PCA as described in section 7.2.5 were also applied in this context. For the nested BMM, twenty tracers were selected based on the outcome of range tests (Appendix L.1): Al_2O_3, Ba, CaO, Co, Cr, Cu, Fe_2O_3, Mn, Nb, Ni, P_2O_5, Pb, Rb, SiO_2, SO_3, Sr, Ti, Y, Zn, Zr. For the unmixing of the Meserani core sections, additional tracers: Ba, Fe_2O_3, P_2O_5, Rb,

SiO_2, Sr, Ti, and Y were removed because they fell out of the range. Ordination of the multi-elemental source and mixture fingerprints allowed both a spatial analysis of the subtributary source fingerprints and a temporal analysis of the floodplain sediment deposits (Blake *et al.*, 2018a; D'Haen, Verstraeten & Degryse, 2012).

b. Model build

The nested sampling approach and high hydrological complexity of the Makuyuni system required an adapted model structure. A partly deconvolutional approach with only two nesting levels was adopted. In the first nesting level, the “Makuyuni outlet” was taken as the mixture with the “Lesimingore” tributaries as the first source and the “Makuyuni Bridge” as the nested upstream source. In the second nesting level, the “Makuyuni outlet and Makuyuni Bridge” samples were pooled into one mixture with the “Ardai”, “Lolkisale”, “MeseraniChini”, “MeseraniJuu”, “Musa” and “Nanja” sub-tributaries as the sources. The upper nesting level was integrated within the first nesting level by multiplying the proportions, thereby obtaining the entire river basin sediment apportionment based on the approach described in Blake *et al.* (2018a).

The BMM to unravel the “Meserani floodplain core” was built by introducing covariate structure into the core mixture data either with ‘Depth’ as a continuous categorical effect or ‘Group’ as a fixed categorical effect. The latter grouping was based on trends in sediment fingerprint observed from the PCA plots of the sediment deposit (Figure 27). The sources were set as the upstream contributing rivers connected to the floodplain, which for the “Meserani floodplain core” were “Lolkisale”, “Meserani Chini”, “Ardai”, “Meserani Juu” and “Musa”. A non-informative prior (1,1,1,1,1) was used since there was no exisiting evidence to indicate dominance of any specific source.

For all MixSIAR model runs, the Markov Chain Monte Carlo (MCMC) parameters were generally set as follows: chain length = 3000000, burn = 2700000, thin = 500, chains = 3. Convergence of model chain output was evaluated using the Gelman-Rubin diagnostics (Gelman *et al.*, 2013), rejecting model output if >5% of total variables was above 1.05, in which case chain length was increased or the model build was re-evaluated.

8.3 Results and discussion

8.3.1 Deconvoluted riverine source apportionment

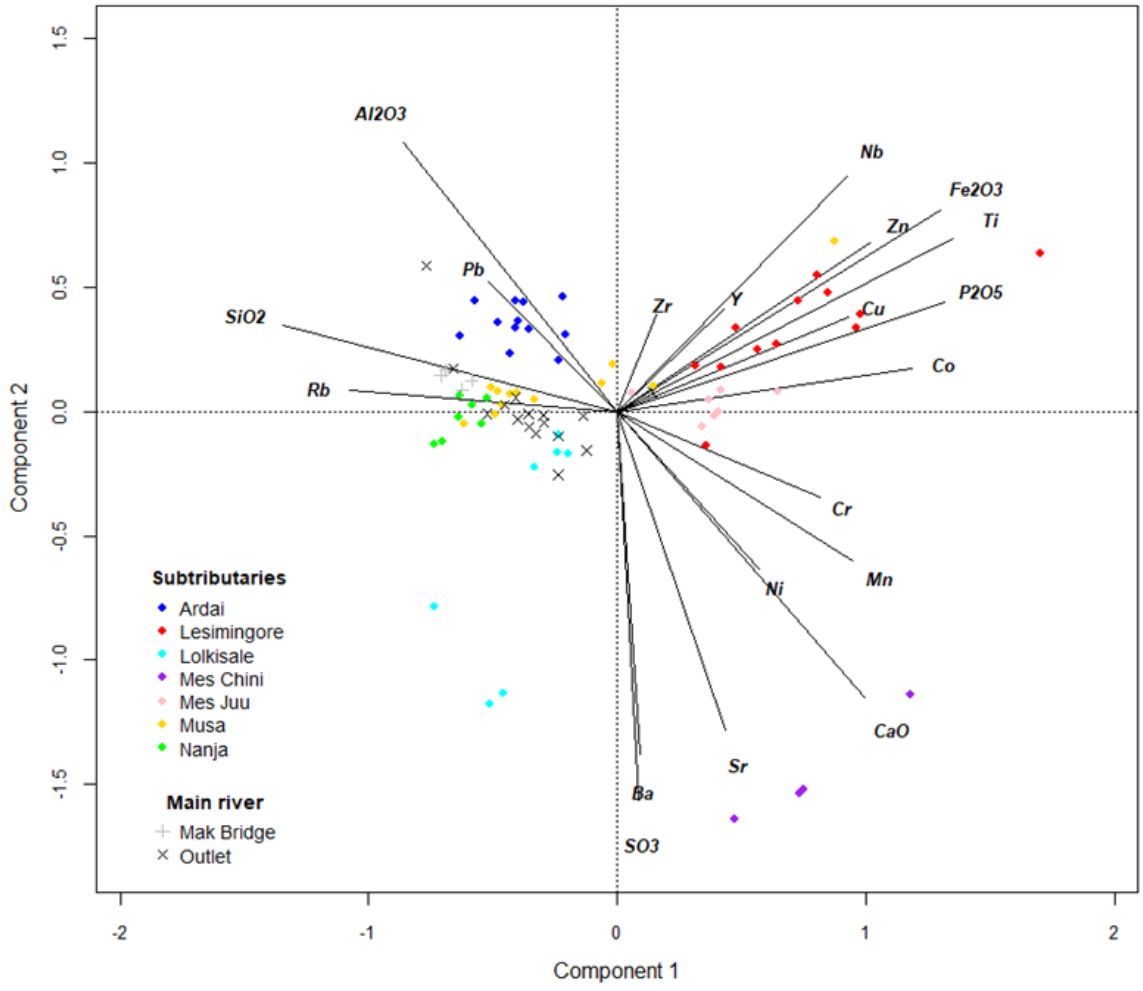

Figure 25: Ordination biplot visualising the geochemical drivers of variance in the fingerprint from upstream sub-tributaries and nested river samples using the two largest eigenvalues (explaining 35.3% and 21.3% of variance).

The PCA plot (Figure 25) of the sub-tributaries show a low level of fingerprint overlap, indicating a strong spatial distinction between the sub-tributaries.

Furthermore, the downstream nested riverine samples do not occupy a large niche space, indicating a low variability in the sediment mixture. The results from the deconvolutional unmixing of the Makuyuni riverine sediment are very distinct and have a low statistical uncertainty as summarised in Table 5. On the first nesting level, 1.9% of the sediment was attributed to the Lesimingore sub-tributaries, while 98.1% was attributed to the nested upstream source. Deconvolution of the second nesting level against the upstream subtributaries and integrating them within the entire Makuyuni sediment attributed 85.5% to Ardai, 2.8% to Lolkisale, 0.7% to Meserani Chini, 2.0% to Meserani Juu, 1.8% to Musa and 5.3% to Nanja subtributaries.

Nesting level 1

Lesimingore		**Mak. Bridge**	
Mean	*Diag*	*Mean*	*Diag*
0.019	1.03	0.981	1.03

Nesting level 2

Ardai		**Lolkisale**		**Mes. Chini**		**Mes. Juu**		**Musa**		**Nanja**	
Mean	*Diag*	*Mean*	*Diag*	*Mean*	*Diag*	*Mean*	*Diag*	*Mean*	*Diag*	*Mean*	*Diag*
0.872	1.00	0.028	1.00	0.007	1.01	0.020	1.00	0.018	1.00	0.054	1.00

Table 5: The mean values and Gelman-Rubin diagnostics (Diag) outcomes from the two nesting levels of the Makuyuni sediment BMM.

These results correspond to some extend with the output of chapter 6, which shows that the Ardai subcatchment has the largest hillslope erosion potential in the Makuyuni catchment and additionally highlights large areas of increased erosion risk due to land cover change. Nevertheless, the Nanja and Musa subcatchments also have a high hillslope erosion potential and large areas of increased erosion risk. However, these subtributaries are partly disconnected from the main Makuyuni channel by a lake and a dispersive floodplain respectively (Figure 26), which capture much of the upstream sediment. The disproportional dominance of the Ardai sediment delivery in the Makuyuni system thus indicates that sediment connectivity is an important factor to explain the

observed differences in downstream sediment delivery. A short-term solution to curb the high sediment delivery from the Ardai system could be by installing flow retardants, and –dispersants that stimulate sediment deposition and thus decrease connectivity. An example is the instalment of smaller check dams on lower order streams, which are already present in the area, but for water availability purposes. While this can protect downstream ecosystems from sedimentation, it does not solve the ultimate cause, which is increased hillslope erosion and runoff. Similarly, the Nanja and Musa systems also experience problematic levels of hillslope erosion and gully incision even though most of this sediment is captured in natural and/or man-made sediment sinks.

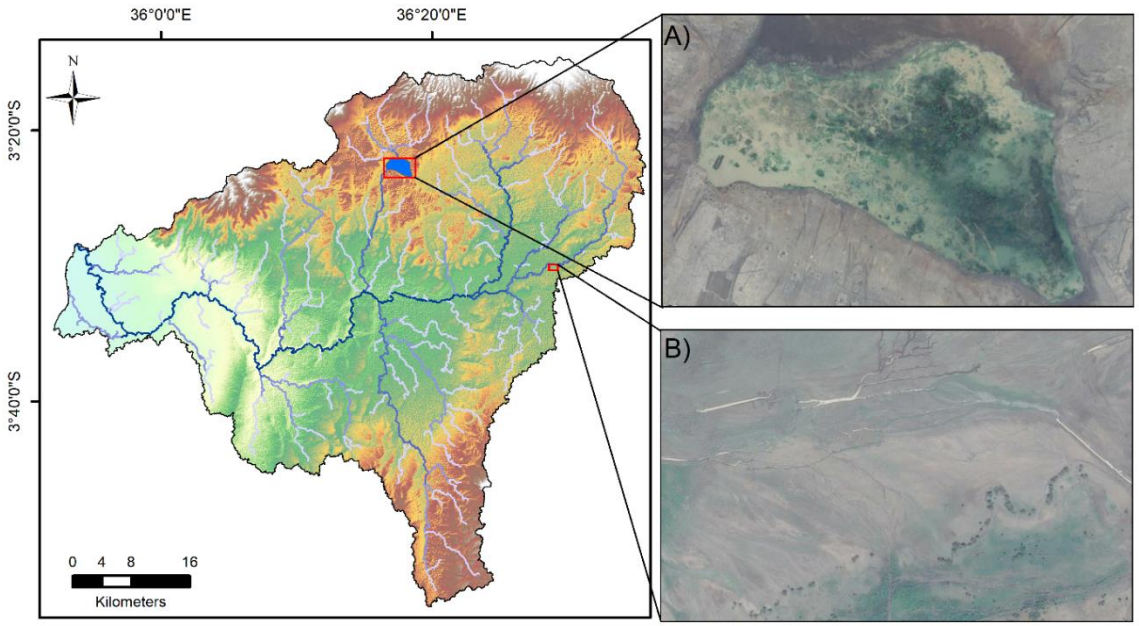

Figure 26: The location of A) Nanja lake and B) Duka Bovu Floodplain (image source: CNES/Airbus, Google Earth) that respectively disconnect the upstream Nanja reaches and the Musa sub-tributary with the main Makuyuni river.

Furthermore, while these results indicate that the partly deconvolutional BMM is a strong tool for constraining sediment sources in the mid-sized Makuyuni catchment, the high temporal variability in this system limits these results to being a snapshot in time.

8.3.2 Historical sediment fluxes from subtributaries

Downcore analysis of sediment deposits gives an indication of historical changes in riverine source contribution to floodplain deposits in the Makuyuni catchment. The PCA of the Meserani floodplain core shows a gradual change in sediment fingerprint over depth (Figure 27). However, an overlap between spatial and process signal complicated the unmixing of these sediment deposits against riverine sources. Notably, the range tests showed that tracers linked to subsurface erosion (Rb and SiO_2, owing to their relative resistance to weathering), have a higher concentration in the Meserani floodplain sediment, while the tracers linked to hillslope topsoil erosion (Fe_2O_3, P_2O_5, and Ti) have a lower concentration in the floodplain sediment, when compared to the riverine sediment (Appendix L.1). This skewed geochemical signal on the Meserani floodplain is probably because extreme rainfall and runoff events are both linked to higher amounts of subsurface erosion and higher probability of floodplain connection (Belmont *et al.*, 2014; Bracken & Croke, 2007). Moreover, this finding demonstrates the importance of extreme events in sediment source-to-sink dynamics and hence geochemical fingerprints of deposited material (Lizaga *et al.*, 2019). It is thus also important to keep in mind throughout this section that the floodplain only captures the sediment during larger events when overbank flow is happening. The potentially important cumulative effect of smaller flows are therefore excluded from the historical analysis.

Nonetheless, the presence of a ‘black box’ zone in the Makuyuni river system where spatial and process factors are both dynamic and important controls on resulting mixture fingerprints, can potentially result in conflicting outcomes from source apportionment (Bracken & Croke, 2007). While historical analysis of sediment fluxes is essential to understand source-to-sink dynamics in this zone,

it thus also requires the disentanglement of the process and the spatial signal from the total fingerprint. As the main interest in this chapter is to attribute sediment to spatial sources (sub-tributaries), dominant process tracers were simply removed from the analysis, assisted by the range analysis. However, individual tracers can be both dependent on process and space, and tracer selection for historical analysis of complex sediment source-to-sink dynamics is thus always a case specific exercise.

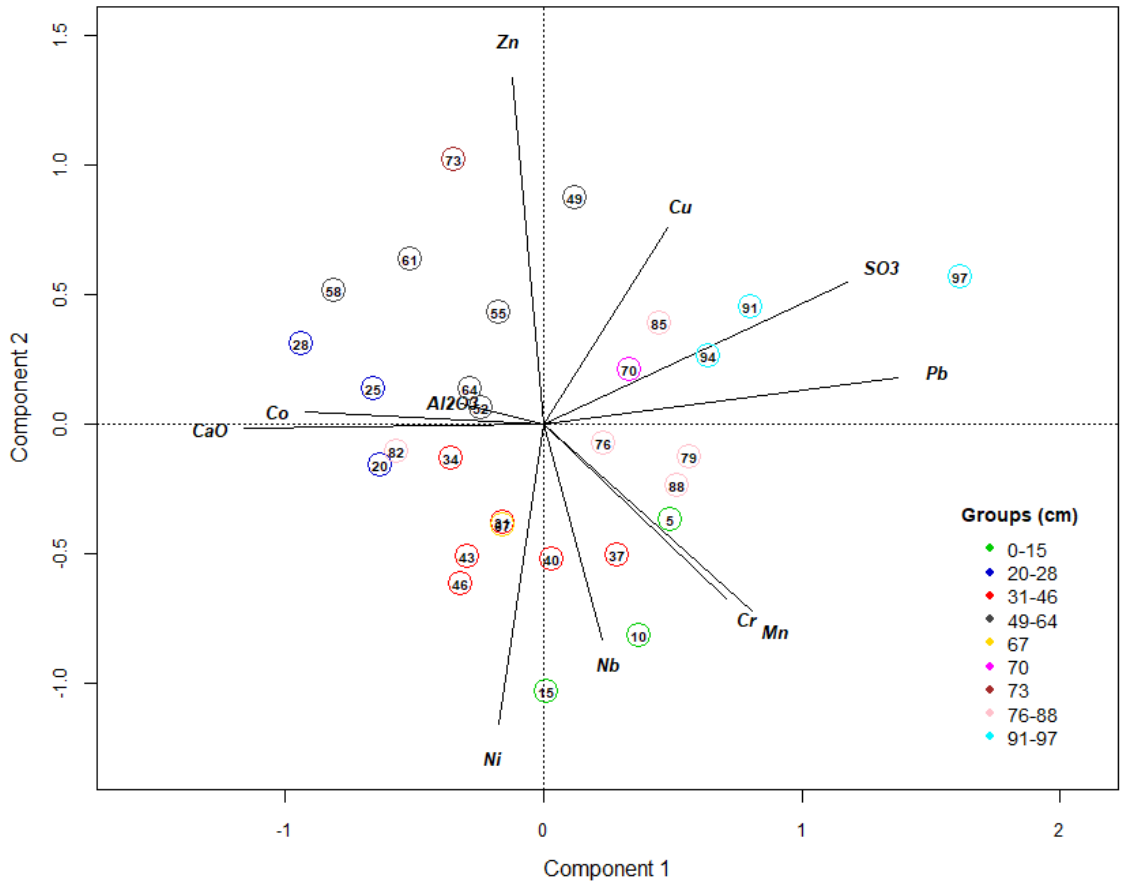

Figure 27: Ordination biplot visualising the geochemical drivers of variance in the Meserani core using the two largest eigenvalues (explaining 24.5% and 16.2% of variance), with depth groups in corresponding colours.

The BMM was not able to converge under 'continuous' depth analysis, therefore the results of the 'grouped' analysis only will be discussed. The Meserani core shows a consistent dominance of the Ardai tributary around 75% of floodplain contribution with one distinct drop to 60% at 67cm as shown in Figure 28 and

summarised in Appendix M.1. Moreover, the observed changes in Ardai contribution always correspond with changes in the Lolkisale tributary, which hovers around 20% contribution, beside distinct rise to 35% at 67cm. The contributions of the Meserani Juu, Meserani Chini and Musa tributaries are minor throughout the core. The dominance of Ardai and to a lesser extend Lolkisale is not surprising as they have large the biggest sub-catchment areas (Appendix K.1) and therefore high total hillslope erosion potentials. Moreover, sub-tributaries with larger sub-catchment areas can generally generate greater discharges that are subsequently more likely to spill into floodplains. At the same time, the relative stability of sub-tributary contribution is surprising, given the spatially distinct changes in surface erosion risk in the entire Makuyuni catchment. This indicates that the geochemical changes within the core are mostly resulting from changing dynamics of erosion and sediment transport within the Ardai and to a lesser extend Lolkisale sub-tributaries. However, as no sediment dating has been performed on the Meserani core, these findings cannot be linked with specific times and changing sedimentation rates.

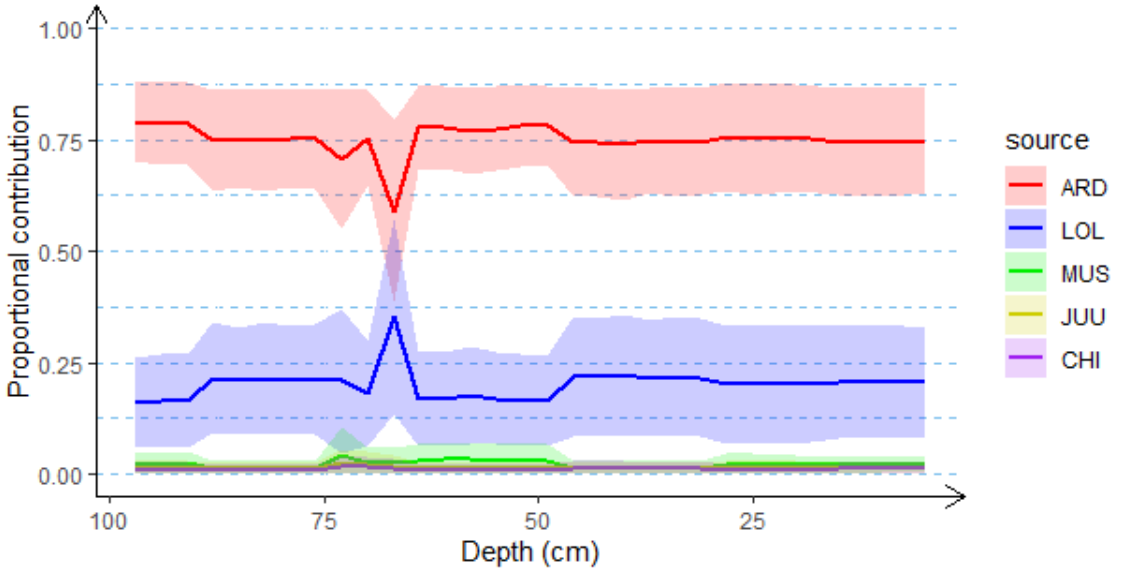

Figure 28: Changing proportional sediment contributions of sub-tributaries (Ardai=red; Lolkisale=blue; Musa=green; Meserani Juu=yellow; Meserani Chini=purple) over depth.

8.4 Conclusion

A partly deconvolutional approach was shown to be the most pragmatic method of constraining sediment fluxes to the sub-tributary level in the complex and logistically challenging Makuyuni tributary. The key finding of the BMM implicate the Ardai sub-tributary for contributing around 85% of the downstream sediment. Uncertainties resulting from uncaptured temporal variability in sediment fluxes were partly overcome by including a nested floodplain core in the analysis. However, overlap of spatial and process signals complicated the analysis of sediment deposits in the catchment 'black box' zone, which required the removal of process tracers from the core analysis. The Meserani core demonstrated a consistent dominance of the Ardai tributary around 80% with only minor fluctuations over depth. The results also highlighted that sediment connectivity is an essential aspect of sediment delivery in these catchment systems. First, sediment capture of the upper Nanja reaches and Musa sub-tributary explain their low contribution to the downstream Makuyuni sediment. Second, sub-catchment size influences the potential discharge amounts, which is important for downstream sediment transport and floodplain connection. A further exploration of hillslope soil-to-sediment dynamics in the Ardai, Musa, and Nanja subcatchments will be performed in chapter 9.

Chapter 9. Understanding the dynamics of increased soil erosion and sediment transport in the northern Makuyuni catchment.

9.1 Introduction

As demonstrated in chapter 7, sediment dating and geochemical fingerprinting are valuable tools for reconstructing changing lake sedimentation and tributary attribution. Moreover, geochemical fingerprinting allowed further deconvolution of sediment delivery to sub-tributary levels as demonstrated in chapter 8. Results from these chapters pointed to the Makuyuni catchment as a major source of increased sedimentation in Lake Manyara. Sediment delivery was further constrained to the Ardai sub-tributary as the consistent dominant source of Makuyuni sediment.

In addition to sediment attribution on large scales, these techniques can also be used to elucidate dynamics at the hillslope soil-to-sediment interface within specific sub-tributary catchments. However, in this context, additional difficulties arise, reflecting the complexity of source-to-sink dynamics. First, geochemical tracers can be both dependent on the source area and the dominant process of erosion, causing potential conflicting outcomes of sediment attribution models, especially because both are not stable in time and space (D'Haen, Verstraeten & Degryse, 2012; Walling, 2013). Catchment-specific sampling strategies capturing both the spatial and process variability in erosion are needed to allow the disentangling of both factors as drivers of increased erosion (Du & Walling, 2017; Smith *et al.*, 2015). The sampling procedure should thus include different source areas and nested soil depth profiles within each of those areas (Manjoro *et al.*, 2017; Zhang & Liu, 2016). While soil geochemistry is relatively stable over longer time periods, transported sediment is highly dynamic. Therefore, samples were

taken over multiple events to integrate temporal changes in dominant sources and erosion processes to the transported sediment (Mukundan *et al.*, 2012; Phillips, Russell & Walling, 2000).

Opposite to geochemical composition of the soil, which is influenced mostly by abiotic factors, the biochemical composition mostly results from the fauna and flora living in or on the soil (Blake *et al.*, 2012; Koiter *et al.*, 2013). Different ecosystems and land cover types have different (micro)biological compositions and thus deposit a specific biochemical signature in the soil (Gibbs, 2008; Reiffarth *et al.*, 2016). Biochemical soil and sediment fingerprinting is thus a potentially powerful tool for investigating the contributions of different land use types to the eroded sediment (Alewell *et al.*, 2016; Blake *et al.*, 2012). However, like geochemical tracers, these biochemical tracers need to be conservative over time and space. In this aspect, the $\delta^{13}C$ isotope signature of plant-derived, long chain (> C22), saturated fatty acids (FAs) has proved to be suitable (Alewell *et al.*, 2016; Upadhayay *et al.*, 2017). First of all, the $\delta^{13}C$ of FAs is not altered by volatilisation, dilution, dispersion and sorption, making it more stable over long timescales in soil and sediments (Blessing, Jochmann & Schmidt, 2008; Gibbs, 2008). Moreover, FAs are polar and have high abundances in soils, allowing them to adsorb to soil particles (Feakins *et al.*, 2016; Gibbs, 2008; Guzmán *et al.*, 2013), and disperse together with the sediment particles (Blake *et al.*, 2012; Laceby *et al.*, 2015). However, biological activity during the sediment transport cycle will always result in a higher $\delta^{13}FA$ variability than can be explained by the mixture of source signatures alone, requiring appropriate sampling and tracer selection strategies (Blake *et al.*, 2012; Reiffarth *et al.*, 2016; Upadhayay *et al.*, 2017).

In this chapter, soils and sediment in three of the northern Makuyuni sub-tributary catchments are both geochemically and biochemically fingerprinted with the aim

of proportionally attributing the source contributions at three levels of interest: catchment zone, erosion process and land use. Additionally, by combining sediment dating with integrated fingerprinting, the intractable and changing nature of land cover, catchment zone and erosion processes were disentangled to reconstruct historical dynamics of increased erosion and sediment transport.

9. Material and methods

9.2.1 Sampling strategy

Riverine sediment of the Nanja, Ardai and Musa sub-tributaries (Appendix K.1), of which the sampling strategy is discussed in section 8.2.1, were used as sediment mixture in this chapter. Soil samples were taken from 34 locations in the upper Makuyuni catchment (Figure 29), of which 20 in Ardai, 8 in Nanja, and 6 in Musa sub-catchment. Sampling locations in each sub-catchment were selected to represent the three levels of interest: land use, catchment zone and erosion process. In each catchment zone, the dominant land use types were sampled by taking 5-10 integrated surface soil samples (5 scoops per sample) along a 100m spatial transect. Additionally, at each sampling location, when gullies or rivers were present, subsurface soils were sampled. The gully and riverbank samples were taken just above the active scouring face at variable depths.

Cores were sampled using monoliths or root corers from the Nanja reservoir (5.99 km^2), the Naidosoito reservoir (0.31 km^2, part of the Ardai sub-tributary), and the Musa floodplain (Figure 29). Both monoliths and root cores were sliced on 1cm intervals and packed for further analysis. The Nanja core captures the upper-to-middle catchment zone (1384-2124m, 148.1 km^2) and is characterised by ‘open rangeland’, ‘bushland’, ‘maize cropland’, and smaller fragments of ‘upland forest’.

The Naidosoito core captures sediment from middle-to-lower catchment zone (1305-1506m, 35.1 km^2) and is characterised by 'open rangeland', with increasing area of 'maize cropland'. The Musa core captures sediment from an upper Musa reach (1551-2256m, 7.5km^2), which currently consist mainly of mixed 'upland agriculture' (coffee, wheat and maize) and 'forest'.

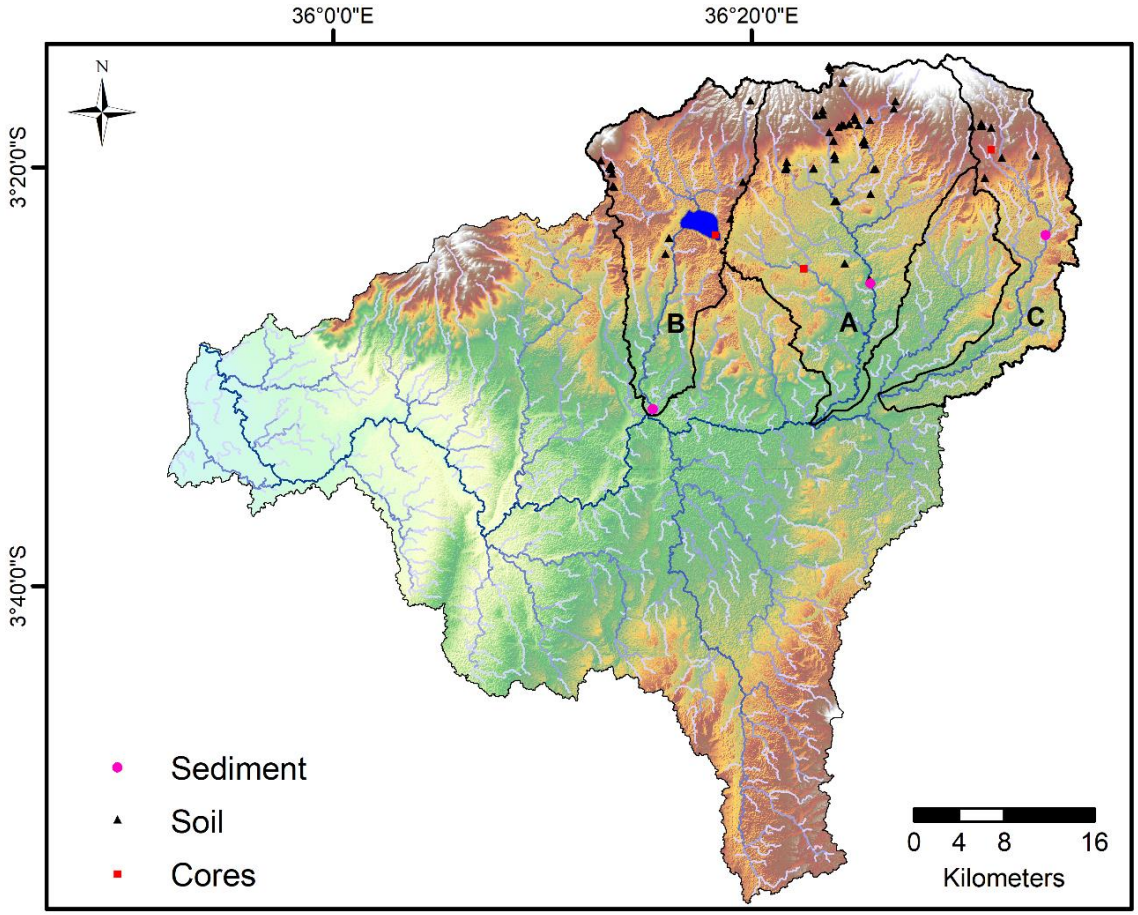

Figure 29: Overview map of Makuyuni catchment depicting the sampling locations of source soils (black triangles), riverine sediment (purple circles), and sediment cores (red squares) within the A) Ardai sub-catchment, B) Nanja sub-catchment, and C) Musa sub-catchment

9.2.2 Laboratory analysis

Sediment and soil samples were either freeze-dried or oven-dried at 40°C and subsequently disintegrated using a mortar and pestle. The SOM content was measured for a representative number of soil samples using the Loss of Ignition (LOI) method, whereby the weight loss after 24 hrs on 550°C was converted in percentage of organic matter in the soil. Geochemical analysis of soil samples

and sediment core sections was done by WD-XRF following the protocol described in section 7.2.3.

Due to a low $^{210}Pb_{ex}$ gamma activity, the $^{210}Pb_{ex}$ activity of the Nanja and Naidosoito core sections was analysed by alpha spectrometry (Mabit, Benmansour & Walling, 2008) at the University of Exeter following the slightly modified protocol of (Jia & Torri, 2007). Samples were first spiked with 1ml dilute ^{209}Po (93.87 mBq mL^{-1}). Per each gram of sediment, 2 mL of HNO3, 70% was added, after which the samples were evaporated on a moderate heat. Subsequently, 2 ml of 6M HCl was added per each gram of sediment after which the samples dry-damped again. Afterwards, 5ml of 6M HCl was added, and the samples were transferred to centrifuge tubes and centrifuged for 10min at 2500rpm. This step was repeated two times and the supernatant was transferred to a plating jar. Subsequently, silver planchets that were previously varnished on one side, were suspended in the supernatant, while it was being magnetically stirred. After 24 hrs the planchets were rinsed and dried. Alpha activity of the planchets was measured using a passivated implanted planar silicon detector and Genie-2000 spectroscopy system. Instrument calibration and yield determination were evaluated by comparison with ^{210}Po and ^{209}Po standard solution references supplied by the International Atomic Agency. $^{210}Pb_{ex}$ was yielded by subtracting the ^{210}Po from the ^{209}Po peak.

Compound specific stable isotope analysis (CSIA) of FAs was performed in the Isotope Bioscience Laboratory (ISOFYS) at Ghent University, Belgium, following the methodology described by Upadhayay *et al.* (2017). Due to the high labour and financial costs of CSIA, only soil samples from the Ardai sub-catchment, sediment from the Ardai river and sediment layers of the Nanja core were selected for analysis. Selected samples were first loaded in extraction cells and

a recovery standard (C17:0 FA, no natural occurrence) was added to allow evaluation of FA extraction efficiency. Total lipid was extracted from the samples using the 'accelerated solvent extraction' (ASE) with DCM:MeOH (9:1) as solvent. The FAs were purified from the total lipid using Aminopropyl columns and eluted from the columns by adding 2 x 2 ml of 2 % acetic acid in diethyl ether (Mottram & Evershed, 2003). Subsequently, the FAs were derivatised by adding 2mL of 14% BF3 in MeOH and heating the mixture to 60°C for 20 minutes. After cooling to room temperature, 1 ml of hexane and 1 ml of Milli-Q water was added, after which the mixture was vertexed and centrifuged for 2.5 min at 500g. The hexane layer was collected and ethylated C20:0 FA was added as internal standard. Fatty acid content was measured using 'gas chromatography with flame ionization detection' (GC-FID). FA contents were subsequently used to adapt the hexane volume for each sample and obtain an ideal concentration. Finally, the δ^{13}C-FA was measured using 'gas chromatography-isotope ratio mass spectrometry' (GC-IRMS). Schimmelman FAME mix reference was used for δ^{13}C calibration (after every 5 samples, 4 references are injected). The values were subsequently corrected for the MeOH group that was added during derivation using the measurements of the internal standard.

9.2.3 Data analysis

a. Bayesian source apportionment

First, conservative behaviour of tracers was tested with the simplified screening procedure, described in section 7.2.5, for each separate sub-catchment (Appendix O.1, Appendix O.2, Appendix O.3, and Appendix O.4). Ideally, individual tracers signal only one of the three interest levels: land use, catchment zone (up-to-low), and erosion process (gully vs. surface). However, as mentioned in chapter 8, individual tracers can have overlapping signals, which thus required

further scrutinising of tracer behaviour with range tests and PCA. Additionally, δ^{13}C-FA C16-C21 were removed because they are predominately produced by microorganisms and are thus more likely to be produced post-erosion. Furthermore, these shorter chained FAs are more susceptible to degradation and thus less conservative (Upadhayay *et al.*, 2017). Moreover, δ^{13}C-FA C25, C27, C29 and C31 were removed because they had a low abundancy resulting into higher uncertainties and missing values (Appendix N.1).

Soil samples were grouped into source classes that were based on a combination of geospatial information and visual interpretation of soil sample clustering on the PCA plot (Figure 30, Figure 31, and Appendix O.5 for Ardai, Figure 33 for Nanja, and Figure 34 for Musa). In the Ardai sub-catchment, a separate analysis of geochemical and δ^{13}C-FA fingerprints, and a composite fingerprint analysis was performed. Results were evaluated against each other. Likewise, in the Nanja sediment core both a separate and composite analysis was done. However, composite analysis proved to be challenging because of the high number of tracers with overlapping and conflicting signals, which made distinct source grouping almost impossible (Appendix O.5). Therefore, only the outcomes from the separate analysis will be discussed. As in chapters 7 and 8, the Bayesian MixSIAR framework (Stock *et al.*, 2018) was used to construct the BMM. Soil classes from each sub-catchment were used as source and the sub-tributary sediment as mixture (Blake *et al.*, 2018a). An uninformative prior (value 1 for each source) was used and no fixed effects were included. Model output was evaluated using the Gelman-Rubin diagnostics (Gelman *et al.*, 2013), after which the results were either accepted or the soil groups were restructured.

b. Landscape change analysis

$^{210}Pb_{ex}$ dating of the Naidosoito and Nanja cores, and reconstruction of their mean accumulation rates was based on the CRS model as described in Appendix F. MAR were converted to total sediment (tonnes yr^{-1}) by multiplying for reservoir area, and converted to SY (tonnes km^{-2} yr^{-1}) by dividing by drainage area.

The upstream sediment cores were not unmixed using BMM for two main reasons. First, non-conservativeness between sources and sediment core was observed for many process tracers (Appendix O.1, Appendix O.3, and Appendix O.4), which could be caused by fluvial sorting processes as explained in 8.3.2. However, unlike chapter 8 where the spatial signal was required, an understanding of dominant erosion processes is one of the main research goals in this chapter. Exclusion of these tracers from the core analysis would therefore result in the loss of the process signal. Second, potential dominance of certain source groups could hide more nuanced, but important, changes in the contribution of other sources. Therefore, the relative changes in processes and sources of erosion were explored using depth profile analysis of individual tracers and PCA of the multivariate core geochemical fingerprint. Specific tracers that signal either process, catchment zone, and land use were selected based on the PCA of soil samples (Figure 30, Figure 31, and Appendix O.5 for Ardai, Figure 33 for Nanja, and Figure 34 for Musa). Tracers for the core PCA were thus not selected based on conservative behaviour, but on the strength of their signal (Appendix N.1). Core PCA trends could subsequently be linked to increased contribution from certain source zones, processes and/or land use types.

9.3 Results and Discussion

First, a detailed account is given on the soil clustering analysis and proportional contribution from source soil groups to the sediment for the three sub-catchment systems. Second, based on results from the sediment core analysis, a narrative of changing erosion and sediment transport dynamics over time is constructed.

9.3.1 Hillslope soil to riverine sediment analysis

a. Ardai

Exploration of the separate geochemical soil fingerprint using PCA (Figure 30) revealed a complex soil system with variability on two levels of interest. First, the PCA plot indicated a clear zonal signal, e.g. lower, middle and upper catchment zones. The lower catchment soils are characterised by an evaporative signal (K_2O, Na_2O and MgO), probably due to their drier conditions. Furthermore, they have a partly overlapping signal with bedrock incision (SiO_2 and Rb), which is probably due the sandier soils in the lower parts of the catchment. The wetter upland soils have a distinct detrital signal P_2O_5 and SO_3 and are further characterised by high concentrations of CaO, Cl and Zn. Interestingly, the midslope samples formed two separate clusters, which is probably due to location specific pedogenic processes. The first group of midslope soil samples took a central location on the PCA plot that probably indicates the intermediate between the upper and lower geochemical signals. The second group of midslope soil samples are characterised by a clear weathering signal (Ti, Fe_2O_3, Co, Nb, Al_2O_3 and Zr). This group represent a catchment zone with deeply weathered soils and high clay content (Appendix S.2) and were grouped as a separate ‘saprolite’ class. Besides a zonal clustering, the PCA revealed a distinct process signal. Most of the gully bank samples were characterised by clear bed incision signals (SiO_2, Rb and Na_2O) and were therefore grouped separately.

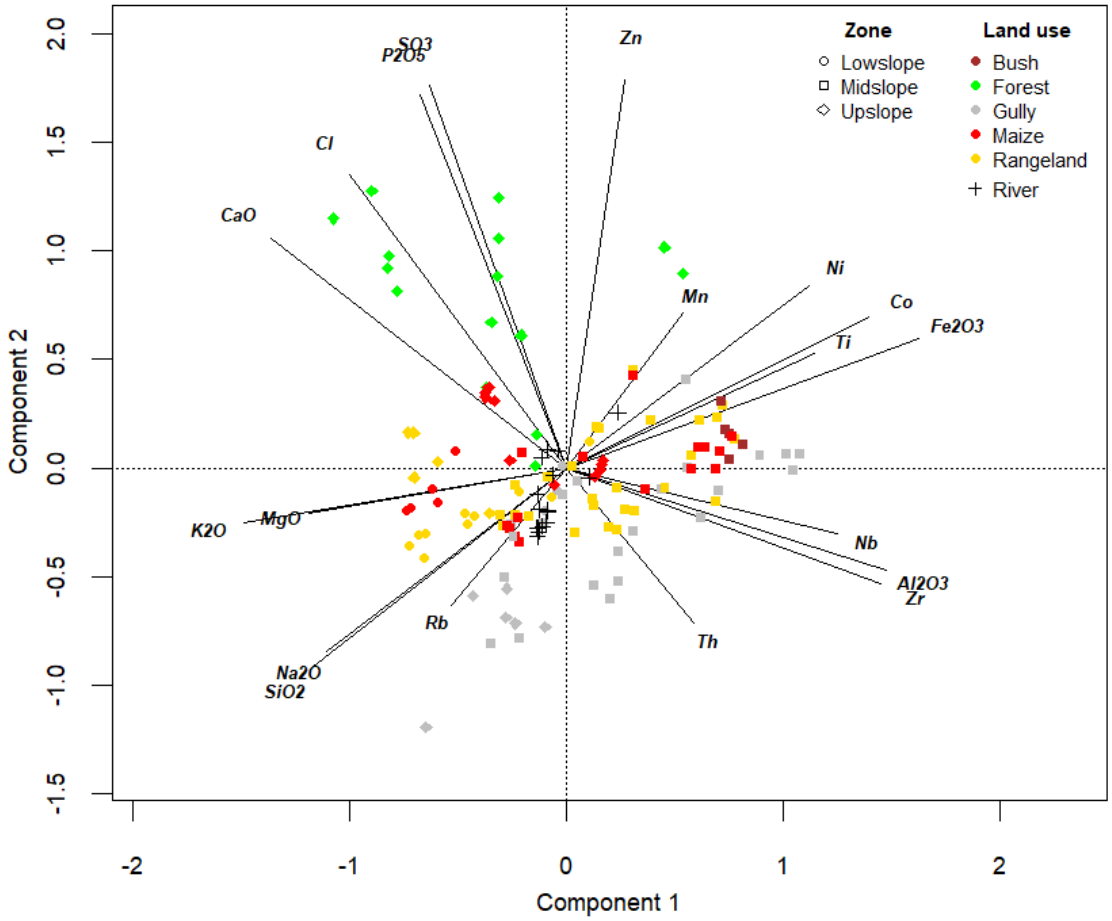

Figure 30: Geochemical PCA plot (explaining 37.8% and 20.9% of variance) of soil samples and riverine sediment in the Ardai sub-catchment.

However, some gully samples clearly fell within the midslope cluster groups, which can be explained by the deeply weathered soils on many of the mid elevation hillslopes. As the gullies incise the landscape, they cut into the saprolite instead of the bedrock and thus have a strong weathering signal. This complicates the eventual attribution of eroded sediment into source processes. At the same time, this outcome also highlights the complex nature of gully incision. While hillslope gullies and valley gullies often have similar geomorphological characteristics and are both greatly influenced by human disturbances, they result from different hydrological processes and can lead to different geochemical signatures. Increased hillslope gullying is ultimately caused by the same processes and often even a direct result of increased rates of hillslope surface erosion (Poesen, 2011; Valentin, Poesen & Li, 2005). Therefore,

gullies with a weathering signal were classified within their respective hillslope class.

Exploration of separate soil δ^{13}-FA PCA plot (Figure 31) reveals one dominating trend that is driven by the specific East African environment and associated plant carbon fractionation. While woody C3 plants with lower δ^{13}C dominate upland wetter zones, grassy C4 plants with higher δ^{13}C values dominate the drier lowland zones (Osborne, 2008). As maize is also a C4 plant, soils under continued cropping will incorporate a C4 signal (Christensen *et al.*, 2011). This finding accentuates that in East African systems with a strong altitude-rainfall gradient, the δ^{13}-FA fingerprint in the soil will be mainly driven by the C3 vs. C4 gradient, whereby more nuanced differences in fingerprint between land use types are potentially lost. Nonetheless, as dominant land use types also often correspond with rainfall, CSIA is still a robust tool for land use attribution to the sediment as is evident from the distinct clustering on the PCA plot (Figure 31). The most distinct cluster consists of 'upland forest' samples, which is mostly characterised by low δ^{13}-FA (C3 dominated vegetation). Interestingly, another distinct cluster consist mainly of the 'upland agriculture' and are characterised by slightly higher δ^{13}-FA values (especially for the heavier C28-C32) then forest. This could be due to the mixture of the dominant maize crop with a residual forest signal, crop rotations with C3 types, the general wetter conditions allowing C3 weed growth, and/or the presence of threes on the terrace boundaries (Appendix S.7). Partly overlapping with both the upland forest and agriculture groups was a cluster of 'bushland' and rangeland, which probably signals an intermediate rainfall zone consisting of a mixture of woody and grassy vegetation. The fourth and fifth cluster are respectively characterised by 'maize cropland' and 'open rangeland' samples. The soil fingerprint of 'open rangelands' and 'maize croplands' thus still

slightly diverges, highlighting the strength of using compound specific FA fingerprinting compared to bulk $\delta^{13}C$ or $\delta^{15}N$. However, substantial overlap is still evident between these two groups, which might be due to the dynamic nature between these two land use types. As demonstrated in chapter 5, the rangelands are the major source of new maize cropping land and this can leave a residual signal in the soil. Vice versa, maize crops are often abandoned and return to rangeland. Moreover, the maize growing season is short and even during the growing season it is highly likely that the plots are re-colonised by natural grassland plants. Last, CSIA of the gully samples proved very challenging. Due to the lack organic content, they had a very low FA concentrations and thus unreliable δ^{13}-FA values. Therefore, the gully samples were excluded from the separate δ^{13}-FA fingerprint analysis.

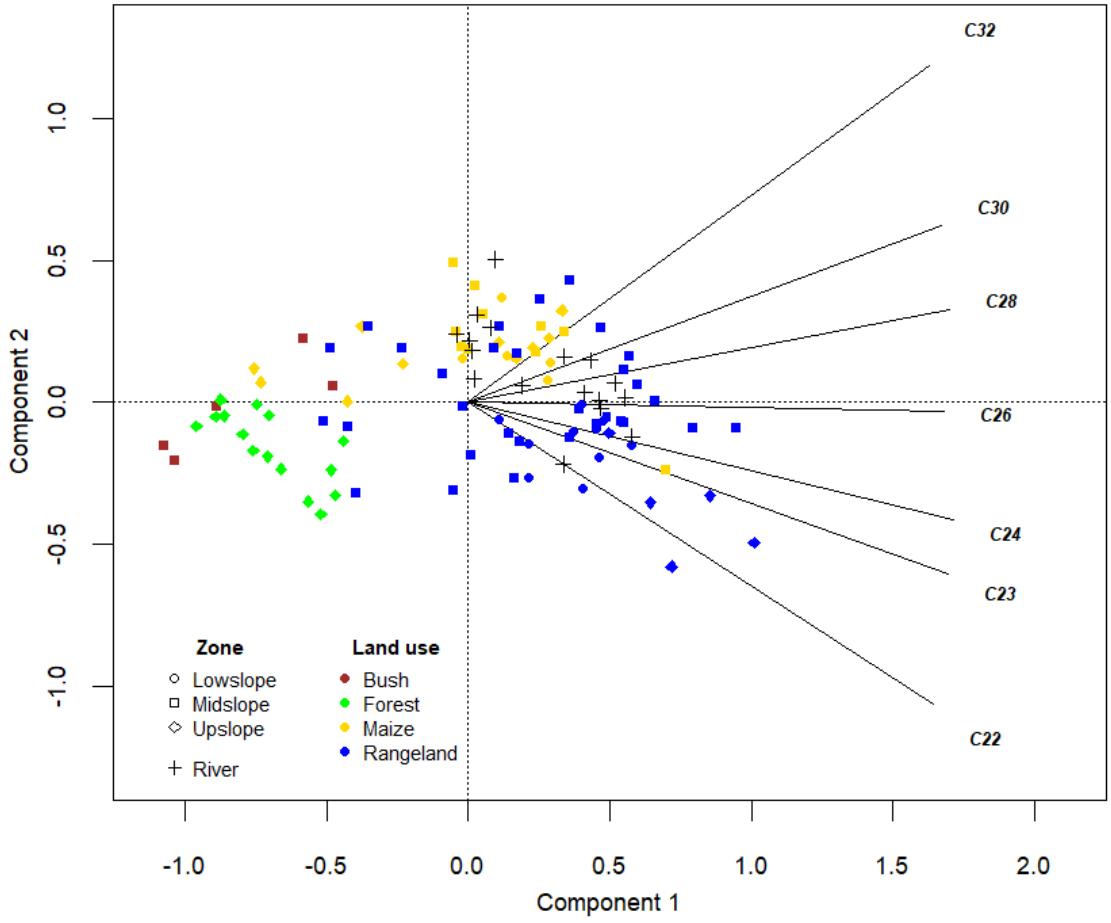

Figure 31: δ^{13}-FA PCA plot (explaining 93.3% and 3.1% of variance) of soil samples and riverine sediment in the Ardai sub-catchment.

Output from the δ^{13}-FA BMM (Figure 32b and Appendix P.1) points towards two major land use sources of sediment: 'open rangeland' with 63.6% and 'maize cropland' with 24.7%. 'Upland agriculture' contributes 5% of the sediment, while 'bushland' and 'upland forest' respectively contribute 4.3% and 2.4% to the Ardai riverine sediment.

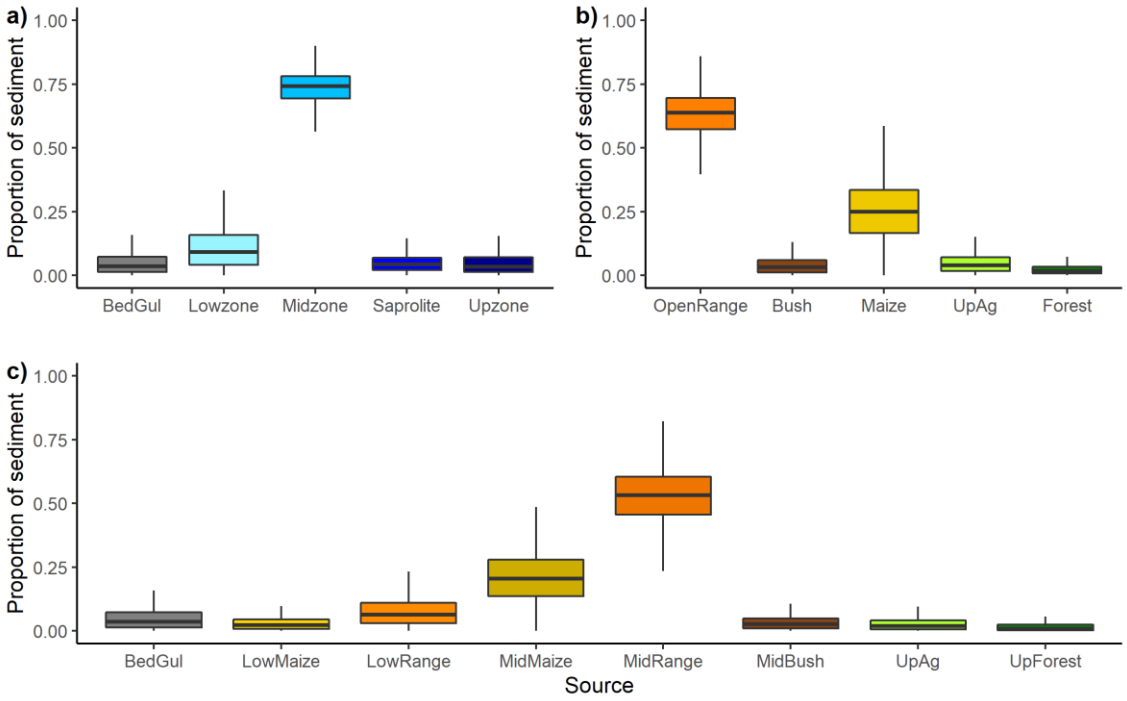

Figure 32: Boxplot of the a) geochemical BMM, b) δ^{13}-FA BMM, and c) integrated outputs, showing the estimated contributions of Bedrock incision (BedGul), Lowzone maize croplands (LowMaize), Lowzone open rangelands (LowRange), Midzone maize croplands (MidMaize), Midzone open rangelands (MidRange), Midzone bushlands (MidBush), Upzone mixed agriculture (UpAg), and Upzone forest (UpForest).

Integration of the geochemical and biochemical evidence bases was possible because the land use types are more or less constrained to specific catchment zones. The land use contributions were rescaled per zone and subsequently multiplied with the zonal contribution to build the zonal land use groups. Lower zone results were integrated with maize and open rangeland. Upper zone results were integrated with the upland agriculture and forest outcomes. Middle zone and saprolite hillslopes were combined and integrated with maize, open range and

closed range. Bedrock incision was kept separate, as it is process based and independent from land use and catchment zone.

The outcome of the integration (Figure 32c) illustrates that hillslope erosion (both surface and subsurface) on the ‘midzone rangelands’ and ‘midzone maize croplands’ are the major sediment sources (52.4% and 21.4%) in the Ardai sub-tributary. This corroborates with chapter 6 wherein the middle-catchment zone in the northern Makuyuni is highlighted as the area with the highest increase in erosion risk. Moreover, the observed domination of ‘maize cropland’ and ‘open rangeland’ matches visual evidence of hillslope degradation in the study area (Appendix S.1, Appendix S.4, Appendix S.5, and Appendix S.6). The ‘open rangelands’ in the middle and lower catchment zone have a seasonal vegetation cycle, making them naturally vulnerable for erosion in the start of the rainy season. More importantly, increasing grazing pressures on these vulnerable ecosystems is rapidly degrading the soil resources (Appendix R.1) as discussed in chapters 3-5. Moreover, the high contribution of ‘open rangeland’ could also be partly explained by their clearance for conversion into ‘maize croplands’. The mid and lower zone ‘maize croplands’ in the Makuyuni catchment are solely dependent on rainfall and are cleared for planting at the start of the rainy season (Trærup & Mertz, 2011). Furthermore, they only provide cover for a short period in the year and their superficial root system and row planting does not provide a solid buffer from erosion (Ngwira *et al.*, 2013). Moreover, field observations evidenced low SOM (Appendix R.1) and a lack of soil conservation practices on most of these ‘maize croplands’ in this catchment zone, even on sloped plots (Appendix S.6). The higher contribution of ‘open rangelands’ compared to ‘maize croplands’ could be partly explained by the bigger area it still constitutes (Figure 14), but partly also because gullies are kept in check on private farms, while they

remain uncontrolled on the common rangelands. The observed lower contribution of ‘upland agriculture’ can be explained by longer growing seasons, a more diverse crop selection with better soil cover, higher SOM content (Appendix R.1), and the presence of terraces and permanent vegetated buffer strips (Appendix S.7). Moreover, the lower contribution of ‘bushland’ and ‘upland forest’ proves that natural vegetation remains the best buffer for soil erosion and sediment transport, especially if you consider that these land use types are currently constrained to the steepest areas in the sub-catchment.

b. Nanja

PCA of the Nanja soil samples indicated clear clustering by catchment zone, and to a lesser extent erosion process and land use (Figure 33). A slight distinction was observed between the eastern (Lepurko) and western (Arkaria) open rangelands. The ‘western midzone open rangeland’ soils overlapped with ‘western bushland’ soils and were therefore grouped into one class. Furthermore, the ‘midzone maize cropland’ samples clustered together nicely and were therefore kept in their own separate class. In the lower sub-catchment zone, the surface ‘maize cropland’ and surface ‘open rangeland’ soil samples showed substantial overlap and were therefore grouped into one ‘lowslope surface’ class. Furthermore, shallow gully samples (30 cm) from the lower zone were integrated within this cluster. Even though they demonstrated a high geochemical variability, other gullies could be grouped into two major classes. Bed gullies were characterised by a clear incision signal from SiO_2 and Rb, and hillslope incision were characterised by a weathering signal.

The BMM output (Figure 35a and Appendix P.2) from the Nanja sub-catchment points to the rangelands in the eastern midzone as the major source (82.6%) of sediment of the downstream Nanja river. While this corresponds with the results

from the Ardai system and hotspot areas of increased erosion risk (chapter 6), these results are still surprising given the presence of Lake Nanja disconnecting sediment transport to the downstream river. While Lake Nanja captures vast amounts of upstream generated sediment, enough seems to get transported downstream in order to dominate the riverine fingerprint. The domination of the eastern mid-catchment zone could be due to more accentuated terrain and potentially higher land use pressures compared to the western side.

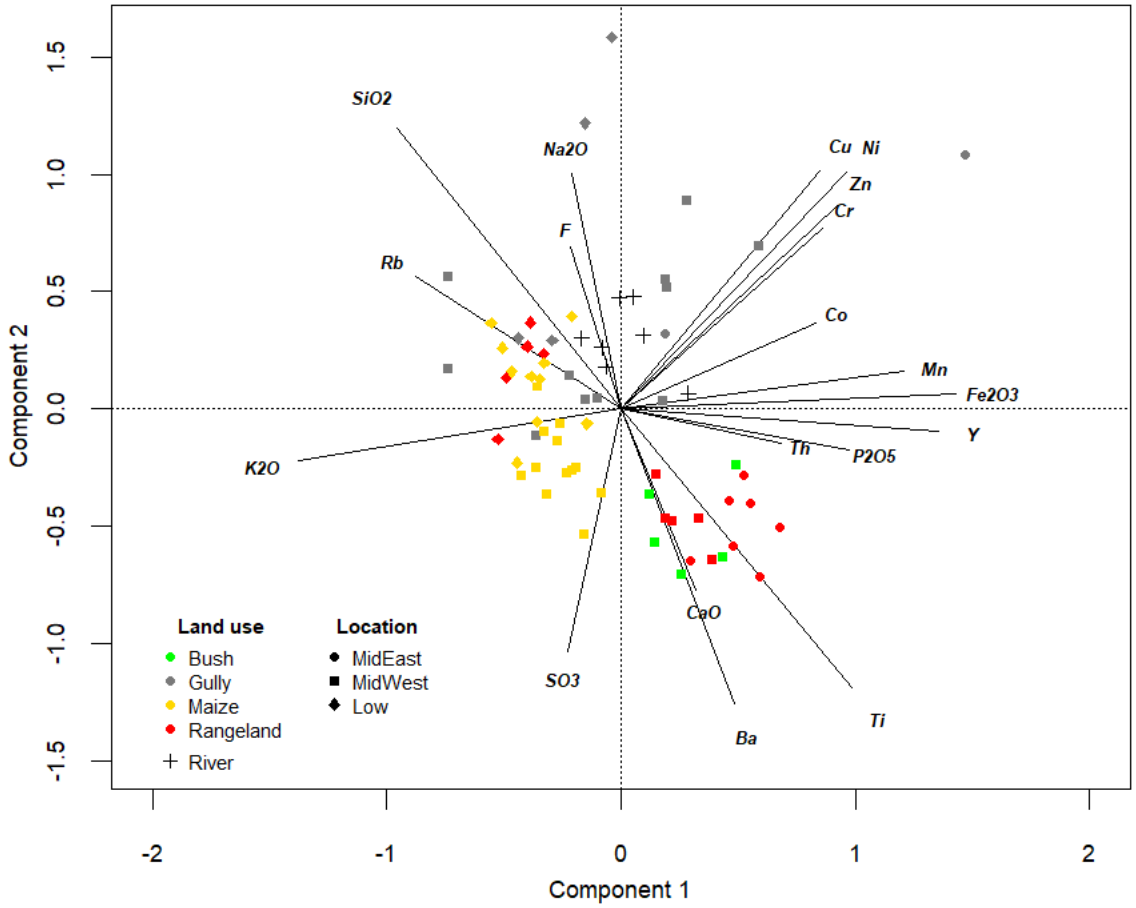

Figure 33: Geochemical PCA plot (explaining 32.5% and 17.6% of variance) of soil samples and riverine sediment in the Nanja sub-catchment.

c. Musa

The PCA plot (Figure 34) indicates distinct clustering that seems to be mainly driven by geochemical differences between erosion processes on the one hand and catchment zone on the other. The upzone surface soils are characterised by a distinct detrital signal with high concentrations of P_2O_5 and SO_3, as well as high

concentrations of Br and CaO. The forest fingerprint slightly diverges from the upper agricultural fingerprint and has two distinct outliers that seem to be driven by a weathering signal. Furthermore, the forest soils have higher concentration of SO_3, while the agricultural soils have a higher concentration of SiO_2, which could be a site-specific indication of a higher sand content in the latter.

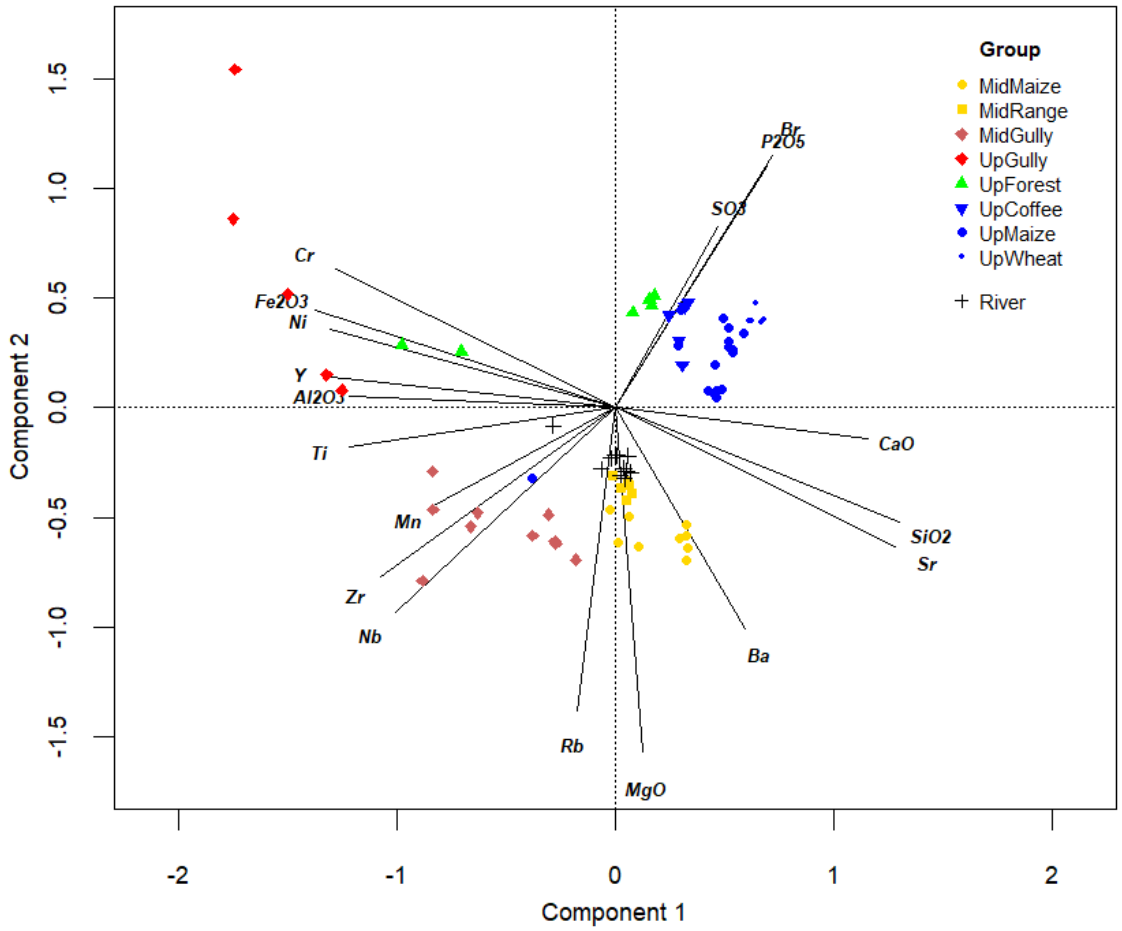

Figure 34: Geochemical PCA plot (explaining 49.6% and 19.0% of variance) of soil samples and riverine sediment in the Musa sub-catchment.

The upper agricultural soils form a distinct cluster with smaller sub-clusters between the different agricultural practices that slightly overlap. The midzone surface soils also group into one distinct cluster with two sub-clusters of rangeland and maize cropland. These soils are mainly characterised by MgO, Sr and Ba, potentially signalling drier conditions compared to the upper zone. At the same time, the midzone (older) soils have higher concentrations of some of the weathering tracers (Zr, Nb and Mn) compared to the upslope (younger) soils, but

lower compared to the gullies. The upslope and midslope gullies group into separate distinct clusters. Interestingly, both seem to be characterised by a distinct weathering signal: Fe_2O_3, Ti, Y, Ni, Cr, Al_2O_3, Zr, Nb and Mn. The midslope gullies have slightly lower concentrations of some of the weathering tracers and at the same time signal bedrock incision with Rb. The characterisation of subsurface erosion by weathering tracers is counterintuitively, however, as discussed in the the Ardai subsection, soils in East Africa are often deeply weathered. Gully incision into these saprolites can thus increase the hillslope weathering signal (weathering signal is not diluted with an organic or evaporative signal in these deeper soil layers).

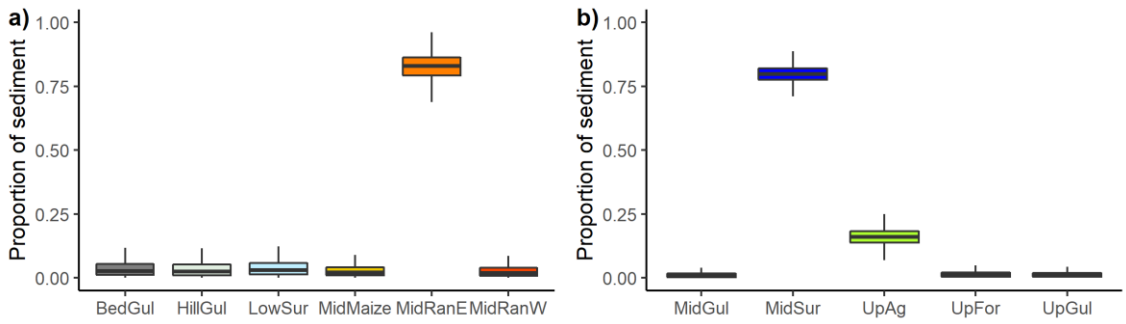

Figure 35: a) Boxplot of the Nanja BMM output indicating contributions of bedrock incision (BedGul), hillslope gullies (HillGul), lowzone surface soils (LowSur), midzone maize croplands (MidMaize), eastern midzone rangelands (MidRanE), and western midzone rangelands (MidRanW). b) Boxplot of the Musa BMM output indicating contributions of midzone hillslope gullies (MidGul), midzone surface soils (MidSur), upzone mixed agriculture (UpAg), upland forest (UpFor), and upzone hillslope gullies (UpGul).

Based on the PCA cluster analysis, the dataset was grouped into five source classes: 'upzone forest', 'upzone mixed agriculture', 'midzone surface' (rangeland + maize), 'upzone gullies', and 'midzone gullies'. The BMM produced highly distinct source attributions of these classes into the Musa river (Figure 35b and Appendix P.2). Nearly 80% of the riverine sediment was attributed to sheet erosion from the 'midzone maize- and rangelands'. The second major source to the riverine sediment was found to be 'mixed upland agriculture' with about 15%. The contributions of 'upzone forest', 'upzone gullies', and 'midzone gullies' was

minimal with 1.6%, 1.4%, and 1.3% respectively. The dominant contribution of 'midzone maize- and rangelands' further confirms the outcomes from the Ardai and Nanja systems, as well as the results of chapter 6. Furthermore, this outcome also matches with results from chapter 5 and with visual evidence that indicates increasing bare and degraded areas in the Musa sub-catchment (Appendix S.1, Appendix S.4, Appendix S.5, and Appendix S.6). While the distinction between the sampled gully and surface fingerprints are very distinct in this sub-catchment, only two gully systems were sampled. Younger or shallower gullies might have a different, transitional, fingerprint. Similar to the previous two sub-catchments, the 'sheet erosion' section is likely to include hillslope incision processes.

9.3.2 Changing landscape dynamics

In the previous section, it was shown that sediment in the Makuyuni river mainly originates from 'maize croplands' and 'open rangelands' on the midzone hillslopes. However, these results are a snapshot in time and do not necessarely represent long-term contribution. Furthermore, this contemporary analysis, does not allow an evaluation of the changing dynamics of soil erosion and sediment transport under increasing land use pressures. Therefore, three upstream cores were scrutinised for changing sedimentation dynamics and sediment origins.

a. Naidosoito core

As shown in Figure 36a, the Naidosoito $^{210}Pb_{ex}$ profile has two distinct peaks and the deepest core sections are radioactively dated to end of the 19th century. Moreover, reconstruction of the MAR indicates an exponential increase in sedimentation, with two distinct drops (1981 and 2009-2012) to values that, however, are still much higher than in older sections. While a lack of ^{137}Cs measurements does not allow the traditional confirmation of CRS dates, the

smaller sub-catchment area makes that the potential variations in rate of $^{210}Pb_{ex}$ supply are probably minor anyway (Appleby, 2002).

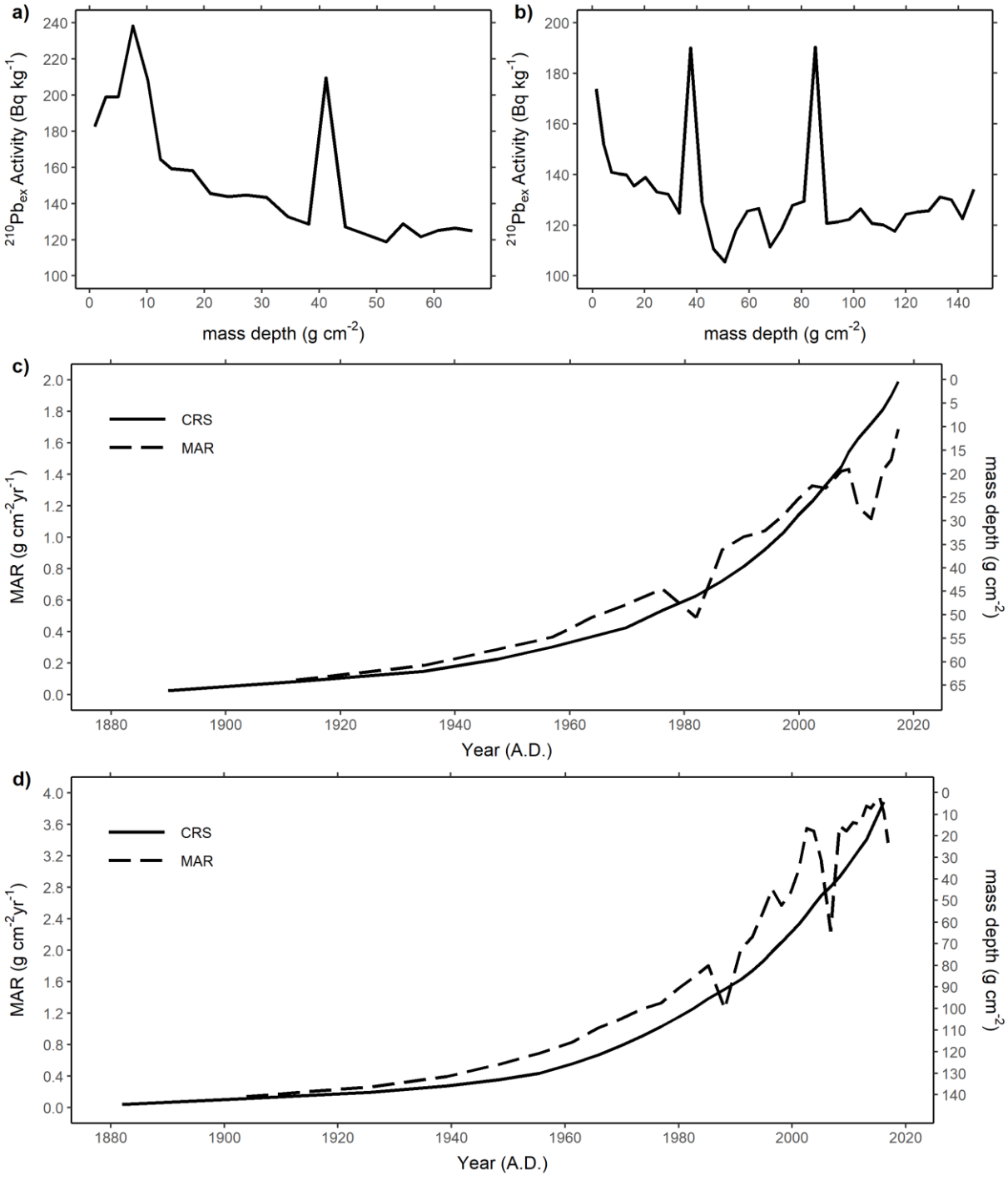

Figure 36: $^{210}Pb_{ex}$ profiles of the a) Naidosoito core and b) Nanja core. The constant rate of supply age-mass depth profile (CRS) and Mass Accumulation Rates (MAR) of the c) Naidosoito core and d) Nanja core.

Moreover, the explicit output from the model means that even larger variations in the rate of ^{210}Pb supply would not change the observed trend of exponentially increasing sedimentation. The drops in MAR correspond to some extent with

periods of decreased rainfall (Appendix B.1), providing some indication of climatic driven variations in soil erosion rates and sediment transport. However, a lack of rainfall monitoring in the sub-catchment area, in combination with apparent spatial differences in interannual rainfall variability, makes a clear comparison of rainfall and sedimentation rates extremely challenging. Nonetheless, if climate were to be the main driver of increased erosion and sediment transport, a more punctuated MAR profile would be expected. Ultimately, the exponential increase in sediment delivery to the reservoirs can only be explained by consistently accelerating rates of soil erosion and sediment transport through unsustainable land use practices. Converting these values to SY shows an increase from 8 to 149 t km^{-2} yr^{-1}.

Processes and sources of erosion were explored using profile analysis of individual tracers (Appendix Q.1) and PCA of the multivariate geochemical fingerprint (Figure 37). The main trend in the core is an increase in importance of the allogenic hillslope tracers and a linked decrease in the autogenic tracers (K_2O, Na_2O, MgO and Sr). This indicates an increasing input of terrestrial soils to the lake sediment and thus independently confirms the CRS output of increasing sedimentation in the reservoir. The oldest core sections (1875-1987) evidence a long stability and are characterised by higher concentrations of SiO_2 and Rb, which indicate a higher importance of bedrock incision processes. A distinct shift is recorded from ca. 1990 onwards and seems to indicate increasing importance of topsoil contribution to the reservoir evidenced by P_2O_5, SO_3, Cl, Ti, Nb, Y, Ba, CaO, Sr and Mn. This situation of increased surface contribution remained stable for about 20 years, after which the core records a rapid shift characterised by a weathering signal: Fe_2O_3, Zr, Zn, Ni, Y and Al_2O_3. This could indicate increasing

gully incision in the hillslope soils that 1) increases direct subsurface soil contribution, and 2) rapidly funnel eroded hillslope soils downstream.

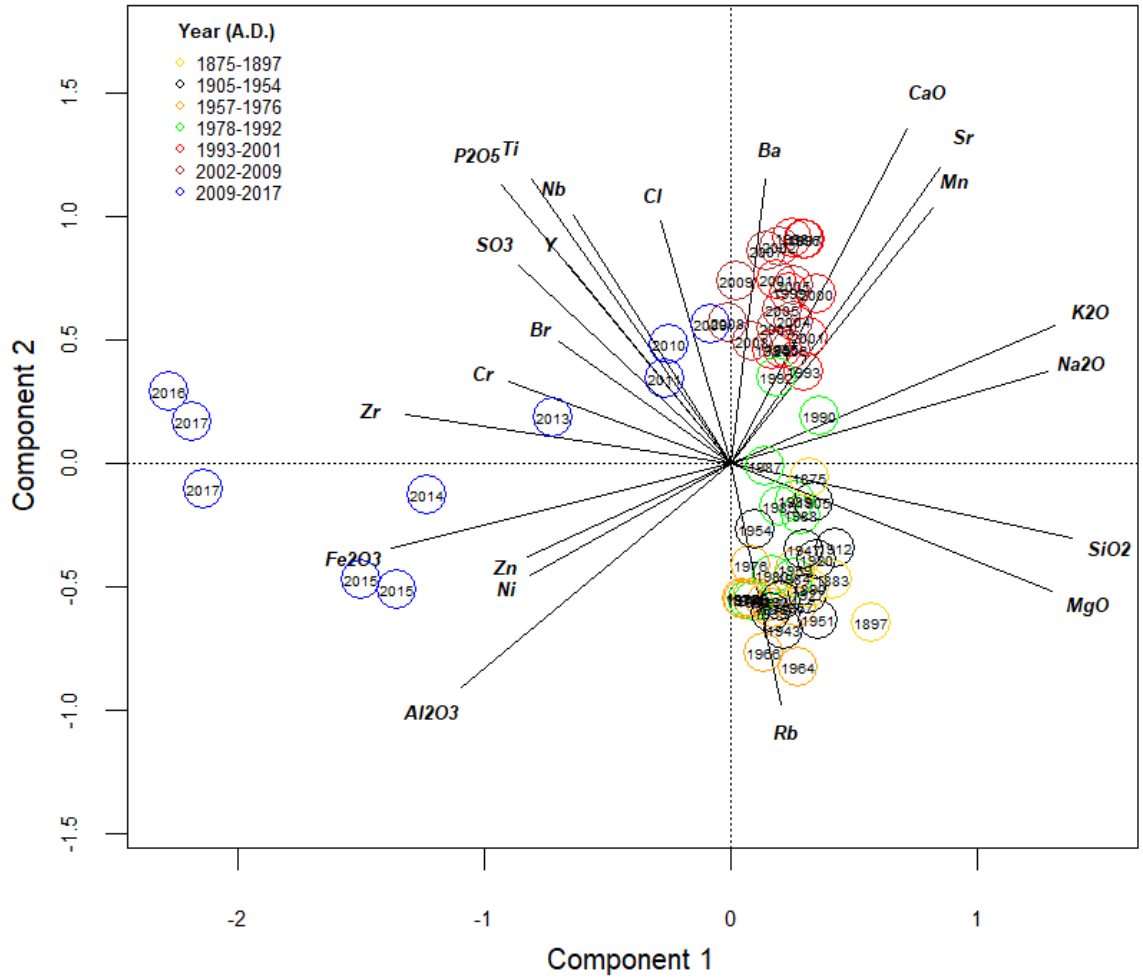

Figure 37: PCA plot (explaining 42.2% and 24.7% of variance) visualising geochemical time trends in the Naidosoito core, related to changing dynamics of soil erosion and sediment transport.

b. Upper Nanja

Like the Naidosoito core, the Nanja $^{210}Pb_{ex}$ profile has two distinct peaks and its deepest core sections are dated to the end of the 19th century (Figure 36b). Moreover, CRS output indicates an exponential increase in MAR with two distinct drops in 1988 and 2006 and a smaller recent drop. Converted to SY shows an increase from 57 t km^{-2} yr^{-1} in the oldest sections to nearly 1600 t km^{-2} yr^{-1} in 2015. The small differences in age of the sedimentation drops between the Naidosoito and Nanja core could be due to uncertainties related to the $^{210}Pb_{ex}$ dating, or due to sub-catchment differences. The SY are about tenfold higher in the Nanja

drainage area compared to Naidosoito, which is probably due the steeper terrain. Nonetheless, the high similarity of sedimentation changes with the Naidosoito core (± 4 years difference) adds evidence to the landscape change narrative. While rainfall variations are important, the only possible explanation for the observed extreme increase in sedimentation is a corresponding extreme increase in soil erosion rates through unsustainable land use.

Analysis of the geochemical profiles (Appendix Q.2) and multivariate PCA plot (Figure 38A) allows the reconstruction of landscape change in the upper Nanja catchment. The first main trend is a decreasing concentration of autogenic tracers (MgO, Sr, F, Na_2O), combined with an increase in concentration of allogenic hillslope elements (Ti, P_2O_5, SO_3, Fe_2O_3, Nb), which independently confirms the increasing sedimentation rates from CRS analysis. Like in the Naidosoito core, the oldest core sections are characterised by higher concentrations of SiO_2 and Rb, indicating a higher importance of bedrock incision processes. From the 1950s, the core records gradually increasing concentrations of CaO, Ba, Co and Mn, and lower concentrations of SiO_2, Rb and Al_2O_3, indicating a shift to increasing contribution of topsoil from the upper catchment zone. This situation remained relatively stable from 1982-2004, while experiencing a parallel increase in allogenic sediment delivery. The core records a distinct jump in 2005 back to increasing levels of SiO2, Rb and Al_2O_3, followed by rapid increases in Ti, P_2O_5, SO_3, Fe_2O_3, Nb. This indicates increasing bedrock and hillslope gully incision that rapidly funnel eroded hillslope soils downstream through the increasingly connected landscape.

As shown in previous section, the open rangelands and maize croplands have a higher $\delta^{13\text{-}}$FA compared to the upland forests, agriculture and bushland. Analysis of the $\delta^{13\text{-}}$FA profiles (Appendix Q.4) and PCA plot (Figure 38B) evidence distinct

historical shifts in contributions from soils of different land use types to the sediment. The oldest sections of the Nanja core take a central position on the PCA plot, indicating a balance between sediment contribution from the drier rangelands and wetter forest. From 1956-1985 the core records a decrease in δ^{13}C-FA, indicating an increase in the contribution from the upper zone forest and bushland with a distinct peak in 1961. This peak in 1961 corresponds with Tanzanian independence, which led to a period of uncontrolled deforestation as described in chapter 3. From 1995 to 2010 the core sways to increased δ^{13}C-FA, indicating increased contribution from drier maize and rangelands. Interestingly, the most recent core sections (2014-2017) indicate a subsequent higher contribution again of upper zone soils, albeit to slightly lesser extent than the 1956-1985 section. This latest increase in upper zone soil contribution could be due to overharvesting of woody vegetation, but is more likely due to the higher connectivity between the upper catchment zone and the river network caused by gully incision.

Linking both tracer analyses paints a complex history of landscape change in the upper Nanja catchment, however, with increasing levels of erosion and sediment delivery as a consistent trend. Increases in sediment delivery to Lake Nanja during the late 1950s and 1960s seem to originate from upper surface soils and is probably linked to increased deforestation. Subsequent rises in sediment delivery originate from the mid-to-lowslope range and maize lands and are probably caused by progressively increasing grazing pressures and agricultural transitions. A subsequent switch to increased subsurface erosion points towards a regime shift where the gradual weakening of the soils combined with a high rainfall period rapidly incised the landscape through gully formation.

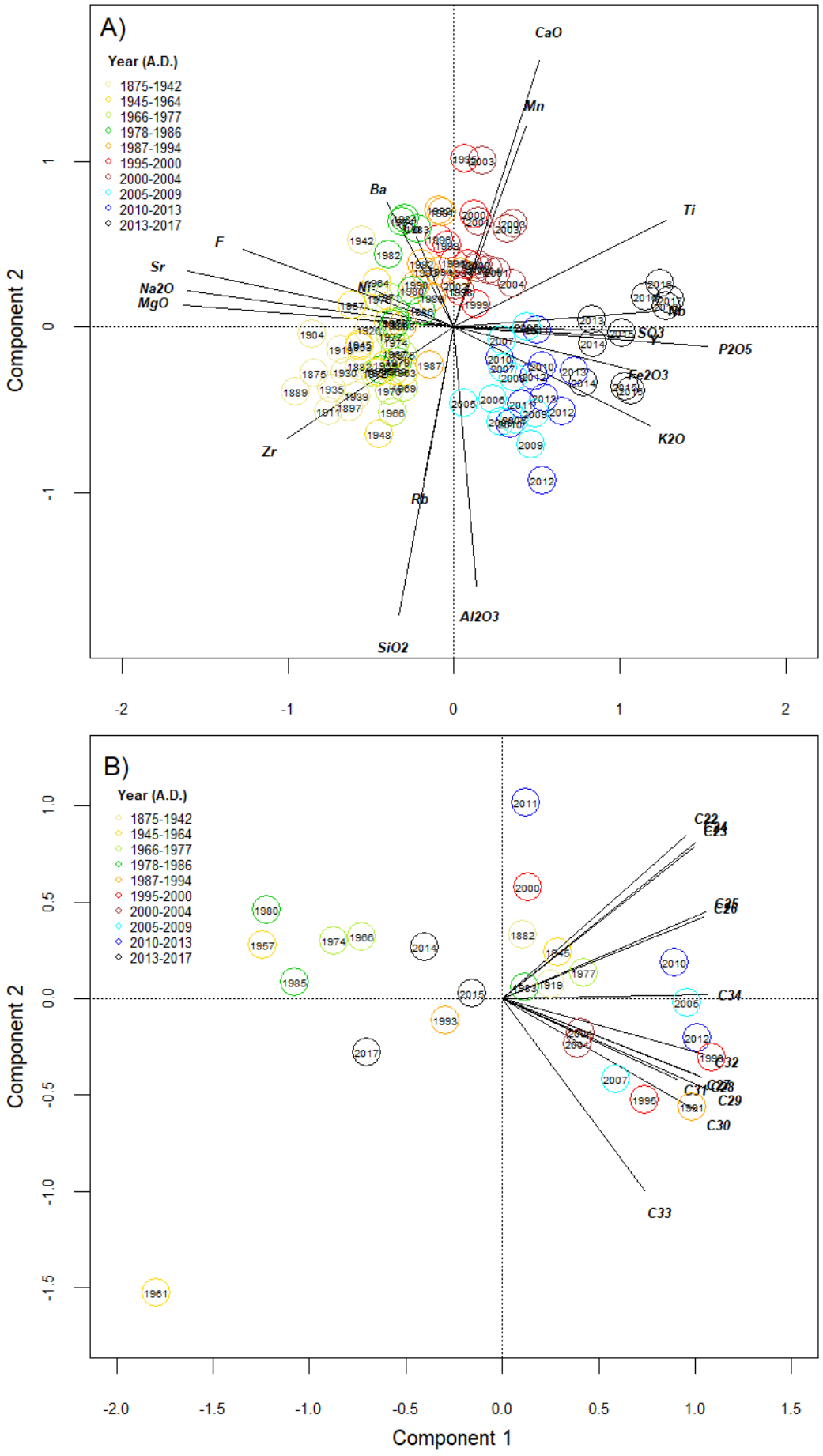

Figure 38: The Nanja core A) geochemical PCA plot (explaining 36.2% and 12.8% of variance) and B) δ^{13}C-FA PCA plot (explaining 78.4% and 9.5% of variance).

The current situation constitutes a highly connected landscape, where high amounts of eroded soils from all over the catchment, including the upper zone, are rapidly transported downstream.

c. Upper Musa core

The elemental profiles and multivariate PCA plot of the Musa core are shown in Appendix Q.3 and Figure 39 respectively. Like the other cores, the main observable trend is decreasing concentrations of autogenic tracers (Na_2O, Cl, and K_2O) and increasing concentrations of allogenic hillslope tracers (Fe_2O_3, Ti, Mn, Nb, Al_2O_3) and thus seems to be related to increasing rates of sediment delivery. Moreover, the deepest sections of the Musa core are characterised by a SiO_2 and Rb signal that indicates an original higher proportional contribution of bed incision erosion. The core subsequently records a punctuated detrital signal (71-76 cm) with increased concentrations of SO_3, CaO and P_2O_3, that probably indicates deforestation and increased contribution of upper zone soils. As no $^{210}Pb_{ex}$ dating was performed on this core, it is not possible to correspond this with a specific time period, however, it is highly likely that similar to the Nanja system this corresponds with the early '60s period of uncontrolled deforestation. From 70cm depth the core gradually shifts towards increasing importance of Fe_2O_3, Ti, Mn, Nb, Al_2O_3, pointing towards a general increase in erosion and sediment delivery. However, this could also indicate incision into deeply weathered soils and/or continued erosion of already topsoil depleted soils. Moreover, some of the deeper core sections lie further on the axis then expected, possibly marking high erosion events. The Musa floodplain core thus tells a story of a punctuated deforestation driven increase in soil erosion and subsequent continued increased sediment delivery originating from farmed surface hillslope soils. Overall, the recorded changes are less distinct compared to the Naidosoito

and Nanja cores. This can be partly explained by the smaller drainage area, but also by more established soil conservation practices on the agricultural lands in the upper Musa sub-catchment zone (Appendix S.7).

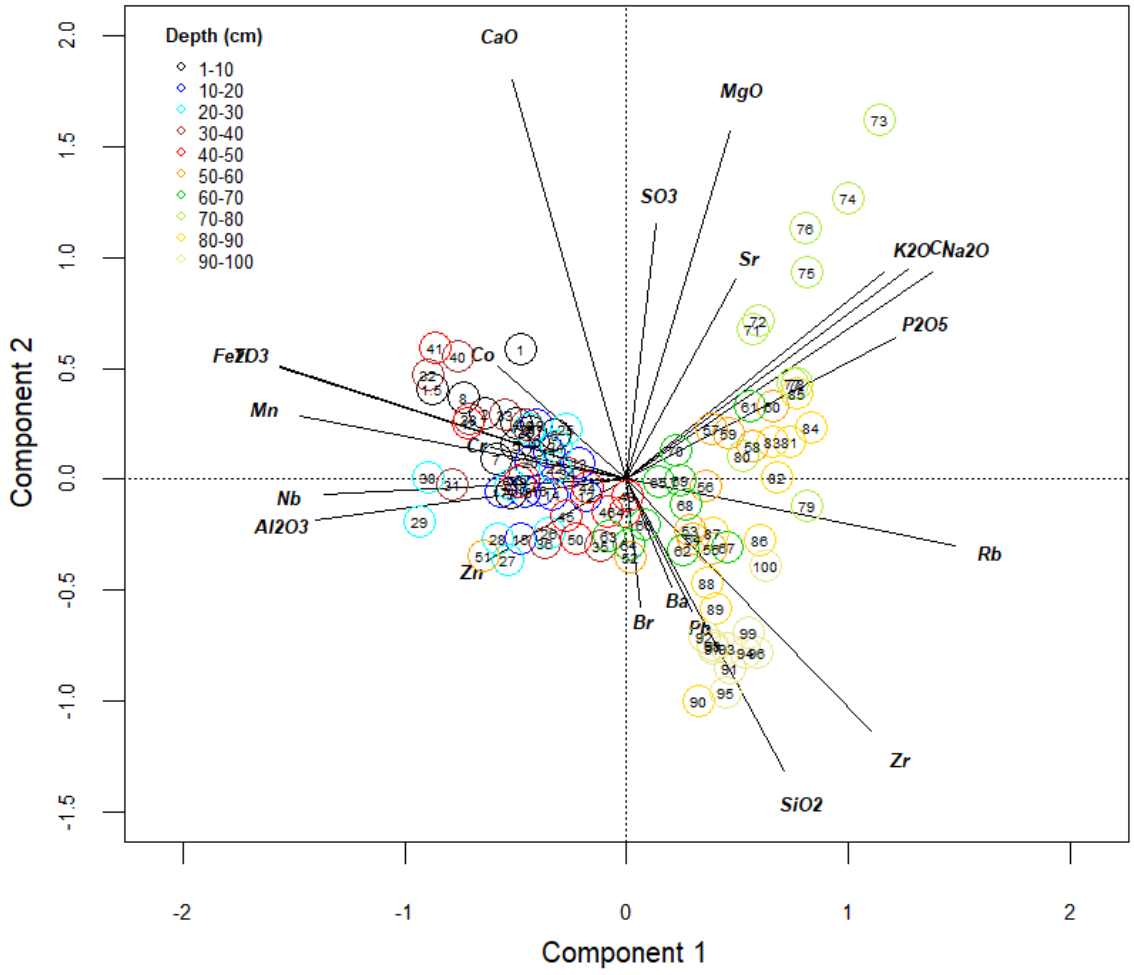

Figure 39: PCA plot (explaining 37.4% and 17.9% of variance) visualising geochemical trends in the Musa core.

9.4 Conclusion

Analysis of the soil and sediment fingerprints in the Ardai, Nanja and Musa sub-catchment revealed a highly complex and variable soil system. Geochemical fingerprinting was demonstrated as a robust tool for distinguishing catchment zone and to a lesser extent land use. However, because gully formation is not a uniform process and thus did not have a singular geochemical signal, erosion process classification proved to be challenging. The δ^{13}C-FA biochemical fingerprinting was dominated by a wetness gradient between the upper (C3

plants) and lower (C4 plants) zone. However, specific $\delta^{13}C$ for the different FA still made it possible to pick up nuanced differences between fingerprints, such as ‘maize cropland’ and ‘open rangeland’. The inability to fingerprint subsurface soils is a major limitation of erosion process attribution in tropical areas. Deeply weathered soils and low ^{137}Cs fallout prohibits the use of typical geochemical and fallout radionuclide fingerprinting. Moreover, organic compounds are absent from deeper subsurface layers, while using concentration of those compounds as tracers is not conservative. Another limitation in the methodology relates to the limited spatial extend of soil and gully samples in the sub-catchments, which was due to logistical constraints. If logistically possible, future studies should adhere to a grid-based approach to soil sampling, which would allow the geospatial analysis of soil fingerprints and has been demonstrated to increase the determinative strength of sediment sources (Haddadchi *et al.*, 2019).

The combination of $^{210}Pb_{ex}$ dating with integrated geochemical and biochemical signals greatly improved the understanding of the highly complex historical landscape dynamics in the northern Makuyuni catchment. Results from these complimentary diagnostic tools on sediment cores evidenced drastic changes in the soil erosion and sediment transport dynamics over the past 130 years. The common trend over the entire northern catchment is the exponential increase in sediment yield. However, further inspection revealed distinct changes in source zones, land use types and erosion processes. All three sediment cores evidenced a seemingly stable landscape in their older sections that was characterised by a higher importance of bedrock incision processes and surface erosion on the semi-arid rangelands and steep upper zones. Post-independence uncontrolled deforestation and transition to agriculture led to an increase in sediment delivery from the newly exposed soils in the upper catchment. Subsequently, the

exponentially increasing sediment delivery gradually transitioned into domination by ‘open rangelands’ and ‘maize cropland’ sources from the middle and lower catchment zones. This is probably related to the progressively increasing grazing pressures and conversion to maize farming systems. A marked switch to increased subsurface erosion, followed by rapid increases in hillslope sediment delivery points towards a regime shift of rapid hillslope collapse. This rapid degradation likely resulted from the continued weakening of soils through years of vegetation removal and surface erosion (Appendix S.1) that interlinked with an extreme rainfall event to cause rapid and massive hillslope incision (Appendix S.3) or even complete collapse (Appendix S.4 and Appendix S.5). The current situation constitutes a highly connected landscape, where high amounts of eroded soils from all over the catchment, including the upper zone, are rapidly transported downstream. Current extreme amounts of sediment transport are dominated by hillslope erosion (both sheet and gully incision) from the middle catchment open rangeland and maize croplands.

Chapter 10. Conclusions, challenges and future research

The application of a complementary set of environmental forensic tools has been demonstrated to fill scientific caveats in land use and land cover change, soil erosion and sediment transport dynamics in East African rift systems. First, the reciprocal integration of multiple evidence bases has proved to increase the explanatory power and predictive capacity of diagnostic tools and independently confirm scientific outputs, thereby reducing uncertainty and increasing confidence in interpretations. Second, the complementary nature of the multiple evidence bases has allowed quantification and interlinkage of spatial changes in land cover, soil erosion and sediment transport. Third, through targeted application of these tools, a detailed temporal reconstruction of complex dynamics of environmental change was possible, furthering the understanding of the intractable nature of the driving processes behind observed changes. Fourth, this study exposed challenges related to the used environmental diagnostic tools in East African rift systems and identified blueprints on how to overcome these in future research studies. Altogether, the demonstrated integration of environmental forensics in East African rift systems will provide valuable support for future development and implementation of sustainable land- and water management plans.

10.1 Quantifying temporal changes in land cover, soil erosion and sediment delivery

Evaluation of land cover data in this study offers strong evidence of the role of large-scale conversion from natural or semi-natural cover to agricultural land in enhanced soil erosion and sediment transfer. Much of this land conversion is

happening in areas that are naturally vulnerable, giving rise to notable increases in erosion risk. While an exact quantification of soil loss and sediment yield is constrained by limitations of the RUSLE approach and sediment delivery calculations in large and diverse catchments, this work has shown that the approach does allow the temporal assessment of catchment specific changes in surface erosion risk and sediment yield in East African Rift Systems lakes basins. In the Lake Manyara catchment, the total yearly hillslope surface erosion is estimated to have increased by 2.54 megatonnes (11%) over the entire catchment from 23.3 megatonnes in 1988 to 25.8 megatonnes in 2016. Furthermore, integration with tributary-specific connectivity indices estimated that the modelled increase in hillslope erosion amounts to a 9.6% increase in total yearly sediment delivery (from 1.91 to 2.11 megatonnes per year) to Lake Manyara.

As evidenced from mutually supportive $^{210}Pb_{ex}$ dating and geochemical profiles, Lake Manyara has experienced a general increase in rates of sedimentation over the last 120 years, reaching a peak in 2010 that is 4 to 6 times higher than the levels in the beginning of the 20th century. Extrapolated for the entire lake these sedimentation rates amount to total sediment delivery to Lake Manyara in 2010 between 3.3 (lowest estimate) and 7.9 (highest estimate) Megatonnes. On the sub-catchment scale, $^{210}Pb_{ex}$ dating and geochemical profiles of sediment deposits evidenced an exponential increase in sediment yield over the northern Makuyuni catchment leading to a current peak of about 130 t km^{-2} yr^{-1} for the lower sloped areas and 1600 t km^{-2} yr^{-1} for the higher sloped areas (Table 6). The exponential increase and lack of clear correlation with annual rainfall, implicates increasing land use pressures as the major driver of the observed increases in soil erosion and sediment transport as summarised in Figure 40.

10.2 A multiscalar comparison of RUSLE-SDR and $^{210}Pb_{ex}$-CRS sediment yield estimations

The application of two different methodologies of sediment yield estimation provided a unique opportunity for a multiscalar comparison of the results (Table 6). On the largest scale (Manyara), SY estimates from both methods lie remarkably close to each other. The CRS model shows a bigger increase in SY between the years compared to the RUSLE model. In the smaller sub-catchments, the RUSLE estimations lie further off the CRS estimates, which is surprising since it was originally designed for smaller catchments. Interestingly, in the more complex Nanja sub-catchment, the RUSLE model underestimated the SY, especially in 2016, while in the lower-sloped Naidosoito sub-catchment, the RUSLE-model overestimated the SY. It is hard to predict if these discrepancies are due to differences in total erosion estimations or differences in the SDR. Most likely, the effect of hillslope gullying caused both an underestimation of the total eroded sediment (RUSLE only measures surface erosion) and SDR (increased connectivity following hillslope incision). It is also important to note that Lakes Nanja and Naidosoito have an outflow in the rainy season and therefore the CRS-based SY are probably underestimations. Low levels of gullying and higher levels of sediment outflow might explain the lower CRS-SY values in the lower-sloped Naidosoito sub-catchment. The more distinct increases in estimated SY from the CRS model in the Manyara and Nanja catchments highlight the limited ability of remotely sensed models to pick up punctuated changes in soil erosion or sediment delivery in complex catchments. The high seasonal and interannual variability in rainfall and vegetation create complex hillslope erosion dynamics that are difficult to capture with limited time points. More importantly, the sediment delivery model used in this study assumes

sediment connectivity is dependent on static catchment characteristics only and thus has no spatial or temporal dimension. In reality, hillslope sediment connectivity is highly dynamic, especially under increasing gully incision. Moreover, catchment sediment connectivity has many non-linear responses to upstream environmental and landscape changes. The closer match between both models in Lake Manyara indicates that when including the contribution of multiple larger catchments, calculating the SDR based on catchment characteristics can be appropriate. Conversely, SDR estimations based on indices of functional landscape connectivity might be more suitable on the smaller scales (Hamel *et al.*, 2017; Heckmann & Vericat, 2018). Despite the differences in SY estimations from the RUSLE and CRS models, they both independently confirm the concerns on increasing sediment yield on all the scales. Observed increases in hillslope erosion and sediment yield highlight the urgent need for management interventions.

While $^{210}Pb_{ex}$ sedimentation models provide more reliable and dynamic sediment yield estimates, they require field sampling and laboratory analysis, both being timely and costly, limiting the widespread application in East Africa. $^{210}Pb_{ex}$ dating also requires the assumption of constant $^{210}Pb_{ex}$ supply to the sediment, which inevitably results in some uncertainty, especially in the dynamic East African environment. Furthermore, with a limited number of cores, the spatial sedimentation patterns in the lake remain unknown, making the extrapolation of sedimentation rates to total lake sediment delivery also uncertain. Remote sensing techniques for estimating sediment yield are much cheaper (many satellite images and GIS-software packages are free) and more widely accessible (no need for state-of-the-art laboratories). For these reasons, future developments to increase the monitoring of soil erosion and sediment transport

dynamics will inevitably tilt towards remote sensing techniques. However, as thoroughly discussed before, remote sensed models require many assumptions of the processes of soil erosion and sediment transport leading to high uncertainties around the quantitative sedimentation estimations. Comparisons like this can provide important guidance to increase the representability of remote sensed soil erosion and sediment delivery models.

Catchment	Size (km^2)	Lake (km^2)	Year	SY (RUSLE ; tonnes km^{-2} yr^{-1})	SY (CRS ; tonnes km^{-2} yr^{-1})
Manyara	18372	438.47	2016	114.8	144.7
			1988	104.1	85.8
Nanja	148	5.97	2016	626.3	1490.5
			1988	563.5	683.4
Naidosoito	36	0.31	2016	467.5	132.7
			1988	357.3	83.1

Table 6: Overview of the RUSLE-SDR and $^{210}Pb_{ex}$-CRS sediment yield estimations on the different scales. CRS SY estimates for Manyara are an average between the lowest and highest values.

On the small catchment scale, multiple integrative soil erosion and sediment connectivity models have been developed that include environmental factors as weights for sediment connectivity calculations and thereby allow the evaluation of environmental change on landscape connectivity (Borselli, Cassi & Torri, 2008; Hamel *et al.*, 2017; Heckmann & Vericat, 2018; Lane, Reaney & Heathwaite, 2009; Lizaga *et al.*, 2018). Future advancements in integrative soil erosion and sediment connectivity modelling should focus on upscaling these models to complex catchment systems and on allowing temporally continuous data integration. This can be done by adaptable modules that allow the inclusion of 1) high temporal resolution environmental factors, 2) gully and riverbank erosion with dynamic and multifactorial thresholds, 3) gully incision effects on hillslope sediment connectivity, 4) supply limitation on rocky slopes, and 5) non-linear

processes of catchment sediment connectivity. Ultimately, remote sensed models should allow a high-resolution evaluation of historical and future changes in erosion and sediment delivery under LUCC and climate changes.

10.3 Pinpointing areas of increased erosion risk and spatial sources of increased sediment delivery

The integration of land cover change mapping within RUSLE models allowed spatially qualitative proxy maps of erosion risk changes following land conversion. This information is particularly useful to pinpoint distinct hotspot areas of increased risk. In the Lake Manyara catchment, these are mostly, but not exclusively, located on the middle zone hillslopes of the Makuyuni and Dudumera catchment, which both have experienced conversion of natural and semi-natural land cover to cropland.

The demonstrated application of geochemical fingerprinting data within a Bayesian mixing model framework has proved to be a robust tool for attributing dominant contributing tributary sources to lake sediment. The ‘global’ model provides an estimate of the tributary contributions to the entire lake and, in the case of Lake Manyara, points towards Dudumera and Makuyuni tributaries as the major contributing systems. However, the approach also highlighted that localised sedimentation effects are very important in large Rift Valley Lakes. Location specific sedimentation issues is highlighted by distinct differences in source attribution for different lake areas. In this study, the domination of the Makuyuni river in the northeast of Lake Manyara, in combination with its significant contribution in all other regions, further highlight the importance of this particular system for recent sedimentation in the entire lake.

The novel application of Bayesian Mixing Models on sediment inventories in parallel with $^{210}Pb_{ex}$ dating allowed a coupled assessment of historical changes in sedimentation and tributary sediment delivery. The 1961 peak in increased sedimentation in Lake Manyara are mostly driven by increased sediment delivery from the Dudumera tributary. The current increasing levels of sedimentation are caused by a disproportional increase in sediment delivery from the Makuyuni tributary. However, increased upstream hillslope erosion can generate a process specific geochemical signal, which can push the source attribution to a tributary with a natural presence of the same signal. This study thus highlights a risk in the application of this technique that results from the potential presence of overlapping geochemical signals between tributary contribution and increased sedimentation.

Further deconvolution of the Makuyuni river sediment revealed a consistent dominance of the Ardai sub-tributary. The results also highlighted that sediment connectivity is an essential aspect of sediment delivery within catchment systems. The larger sub-catchments (Ardai and Lolkisale) seemed to be able to generate larger discharge volumes, increasing their connectivity, while sediment capture of the upper Nanja reaches and Musa sub-tributary explains their low contribution to the downstream Makuyuni sediment. On the sub-catchment scale, sediment of the Ardai, Nanja and Musa sub-tributaries mainly originates from hillslope soils on the open rangelands and maize croplands from the middle catchment zone.

However, while both the RUSLE and Bayesian mixing models indicate certain dominant sources of eroded sediment, the results are not wholly unambiguous. Increased erosion risk is spread over the catchment and different tributaries dominate different lake zones, indicating that increased soil erosion and sediment

delivery ultimately is a catchment-wide problem. Nonetheless, the complementary nature of this set of spatial soil erosion and sediment analysis tools has provided detailed evidence of hillslope-to-sink dynamics in river catchments and independently confirmed the contribution of high-risk areas to downstream ecosystems. First, hotspot areas of increased soil erosion risk were pinpointed. Second, siltation issues in impacted lake areas were constrained to specific tributary and sub-tributary sources. Third, dominant zonal contributions within sub-tributaries were highlighted. Fourth, temporal increases in sedimentation quantities were linked with increased contribution from spatially distinct tributary sources. These evidence bases can guide stakeholders and policy makers for spatially targeted land- and water management interventions.

Limitations of remote sensing models in mind, using them to fine-tune sediment tracing mixing models is particularly promising as was demonstrated in Chapter 7. Future applications of BMMs for sediment apportionment can improve their predictive capacity by integrating remote sensed estimations of soil erosion risk and sediment delivery as prior information. Furthermore, in large lakes, spatial factors should be included in the model structure as a fixed categorical effect to account for localised sedimentation effects. This also allows a targeted investigation into the sediment provenance of particularly impacted lake areas. Furthermore, future sediment tracing studies that want to constrain tributary sources of increased sedimentation should, to the extent possible, 1) account for the overlap between source fingerprints and increased sedimentation signals, and 2) include sediment cores from different lake areas in their study design. Deconvoluting the sediment flux of human impacted rivers with a high intra- and interannual variability will be one of the key challenges for the sediment connectivity and –tracing community in the next years. Future studies would

benefit from including multiple floodplain cores along the different river zones to reconstruct zonal changes in sediment flux and –connectivity.

10.4 Understanding processes of increased erosion and sediment transport

While previous evidence bases show that sediment delivery from certain catchment areas is increasing rapidly, there is a need to understand how land cover change is driving increased erosion and downstream sediment transport. Results from complimentary environmental diagnostic tools on the sediment cores evidenced drastic changes in the soil erosion and sediment transport dynamics over the past 130 years. As highlighted in 10.1, sedimentary evidence clearly points to an exponential increase in upstream SY. However, further inspection also revealed distinct changes in source zones, land use types and erosion processes, over time. The northern Makuyuni sub-catchments seemingly experienced relatively stability from the late 19th century until the 1950s, which was characterised by natural rates of bedrock incision and surface erosion on the semi-arid rangelands and steep upper zones. Uncontrolled deforestation and transition to cropland initiated the first stage of soil degradation and led to a punctuated increase in sediment delivery from the newly exposed soils in the upper catchment. Over the latter part of the 20th century, increasing grazing pressures and conversion to maize farming systems in the middle and lower catchment zone led to gradually increasing rates of sheet erosion and sediment contributions from open rangelands and maize cropland sources. This also resulted into decreased capacity of hillslope soils and ecosystems to buffer extreme rainfall events. From about 2006, a marked increase in gully incision was followed by rapid increases in hillslope sediment delivery. This rapid acceleration in soil erosion and sediment transport implies a regime shift that

resulted from constant weakening of soils through years of vegetation removal and surface erosion. A circumstantial extreme rainfall event or wet year was probably enough to cause massive hillslope incision or even complete collapse. The current situation constitutes a highly connected landscape, where high amounts of eroded soils from all over the catchment, including the upper zone, are rapidly transported downstream. This rapid movement of water and soil particles away from terrestrial soils, along with the nutrients and plant seeds they carry, make it harder for the vegetation to recover naturally. This positive feedback has the potential to further degrade hillslope soils and can ultimately lead to formation of badlands, where only a deeply incised and unproductive landscape remain (Appendix S.5). While it was hard to quantify the proportion of hillslope gullies to the total transported sediment, their effect on sediment connectivity and land degradation is evident. Furthermore, increased hillslope connectivity also resulted into increased flood peaks that have major downstream impacts on river incision, sediment transport and siltation, threatening vital infrastructure and downstream ecosystems.

The evidence thus clearly demonstrates that hillslope soil systems are degrading rapidly and upstream reservoirs are silting up exponentially. However, Lake Manyara seems to be partly sheltered from upstream degradation by the presence of sediment sinks in tributary catchments (Figure 26). On the lake basin scale, sub-tributary disconnections are only overcome during the wettest years, giving rise to distinct peaks in lake sedimentation with a more continuous increase on the background. Sediment connectivity thus takes a central role in linking upstream degradation with downstream sedimentation as summarised in Figure 40. A combination of a rapid sequence of wet years in the 1960s, combined with a period of uncontrolled deforestation, led to the 1961 SY peak in Lake Manyara.

A period of less distinct precipitation peaks between the 1980s and 1990s explain why only recently, the extreme rates of upstream soil erosion and hillslope connectivity have translated into another, more pronounced, downstream SY peak. In the context of future climate change, increasing runoff peaks and continuing land pressures, it is expected that these temporary connections will become more and more frequent, posing a major threat for the ecosystem health and functioning of Lake Manyara.

The complex interactions between land use and soil erosion processes and the spatial and temporal dynamics of sediment connectivity are still not fully understood. In the context of the major global challenges ahead, future research should focus on the synergies between changing rainfall dynamics and LUCC as drivers of both upstream degradation and downstream sediment propagation. Especially the role of gully incision as a positive feedback loop in the hillslope degradation and sediment connectivity processes requires more attention. This study also highlighted the need for reliable tracers that can pick up gully erosion signatures from deeply weathered soils in tropical areas.

10.5 Multifaceted drivers of soil erosion

While increasing land use pressures and the removal of permanent vegetation is the main environmental driver of increased soil erosion, it is actually a symptom of wider socio-ecological changes. Temporal and spatial mismatches between centralised land policies and the divers and dynamic East African environment often directly led to soil exhaustion, decrease of productivity, increased rates of erosion and ultimately the depletion of soil resources. More importantly, indigenous communities were and still are politically marginalised and systematically excluded out of vast areas repurposed for large-scale agriculture,

private ranches or conservation under the guise of development. These policies gradually eroded the indigenous social and economic structures and post-independence East African nation-states are struggling to provide access to key services that are needed to (re)develop them. Impacted communities are struggling to adapt to changing external pressures and the increasing demands of a booming population. Exemplary to this is the absence of growth in agricultural productivity and livelihood options outside agriculture, which forces communities to degrade and overexploit natural resources. A shrinking natural resource base further increases social and economic pressures on ecosystems and this positive feedback locks the system in a pathway to degradation.

Ultimately, sustainable management plans need to be tailored to the specific socio-ecological and constitutional context. The integrity of locally adapted systems, in which management practices and knowledge are embedded, needs to be protected, but not isolated, from external driving forces. Agro-pastoral communities need to adjust to the demands of population increase, commercialisation and modernisation by building upon, not abandoning, existing linkages between the natural, social and economic domains. At the same time, locally adapted management practices need to be integrated in regional, national and supra-national institutions, enabling regional development of sustainable agro-pastoral systems that safeguard ecosystem health, food- and livelihood security. While soil erosion research has until now mostly focussed on defining the problem, future research projects need to move towards an interdisciplinary investigation into the required marriage between local tailor-made management and state structures.

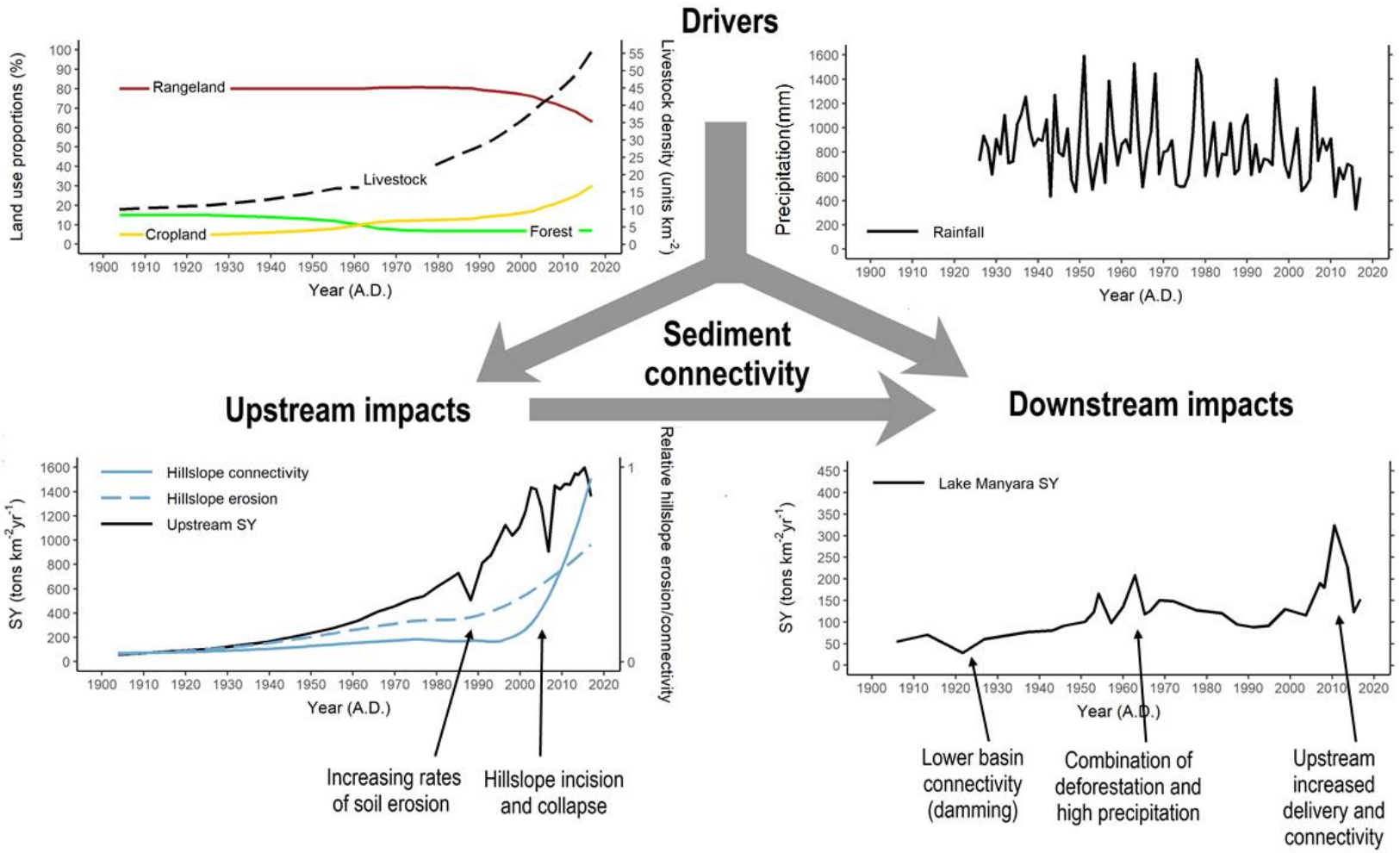

Figure 40: Schematic representation of the dynamics of soil erosion and sediment transport in EARS, highlighting sediment connectivity as a link between the drivers (land pressures and precipitation), upstream impacts (hillslope soil erosion and hillslope connectivity), and downstream sedimentation. Source of livestock data for Tanzania is FAO (2019).

Appendices

A. Lake Manyara bathymetry

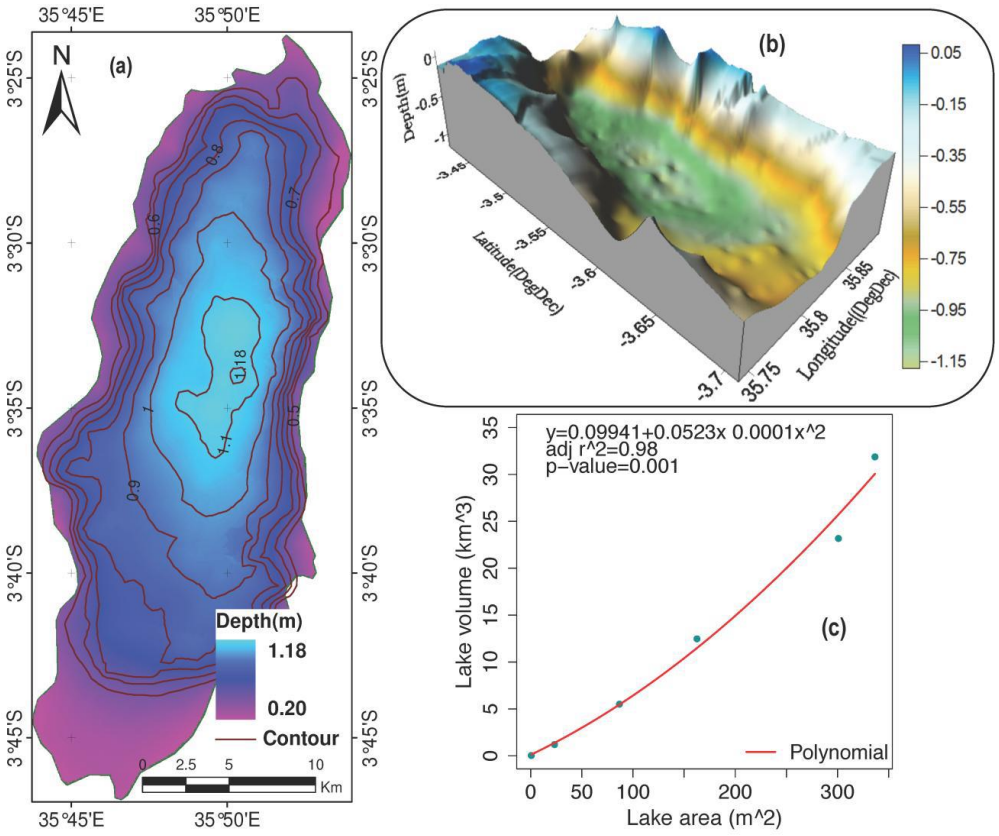

Appendix A.1: Lake Manyara a) Bathymetry, b) Morphology, and c) Relative volume vs. relative area (Source: Deus et al. 2013, redistributed under the terms and conditions of the Creative Commons Attribution 3.0 license).

Appendix A.2: Pelicans resting on the boardwalk railing at Lake Manyara on 01/04/2020, which is normally 1.5-2 meters above the lake surface.

B. Rainfall fluctuations

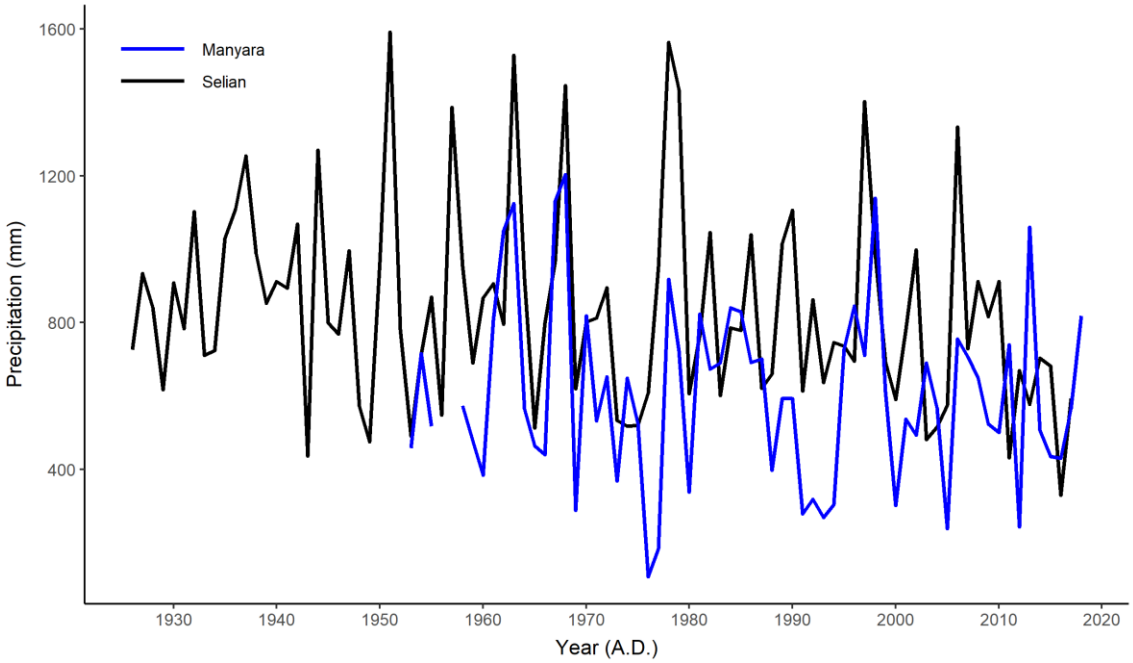

Appendix B.1: Yearly changes in annual precipitation (mm) measured at the Selian Agricultural Research Institute, Arusha, altitude: 1402m, coordinates 03°21'52" S 36°38'6" E (black) and at the Lake Manyara National Park headquarters, Mto Wa Mbu, altitude: 1006m, coordinates 03°22'7"S 35°50'31"E (blue).

C. Satellite evidence of Tarangire-Manyara connectivity

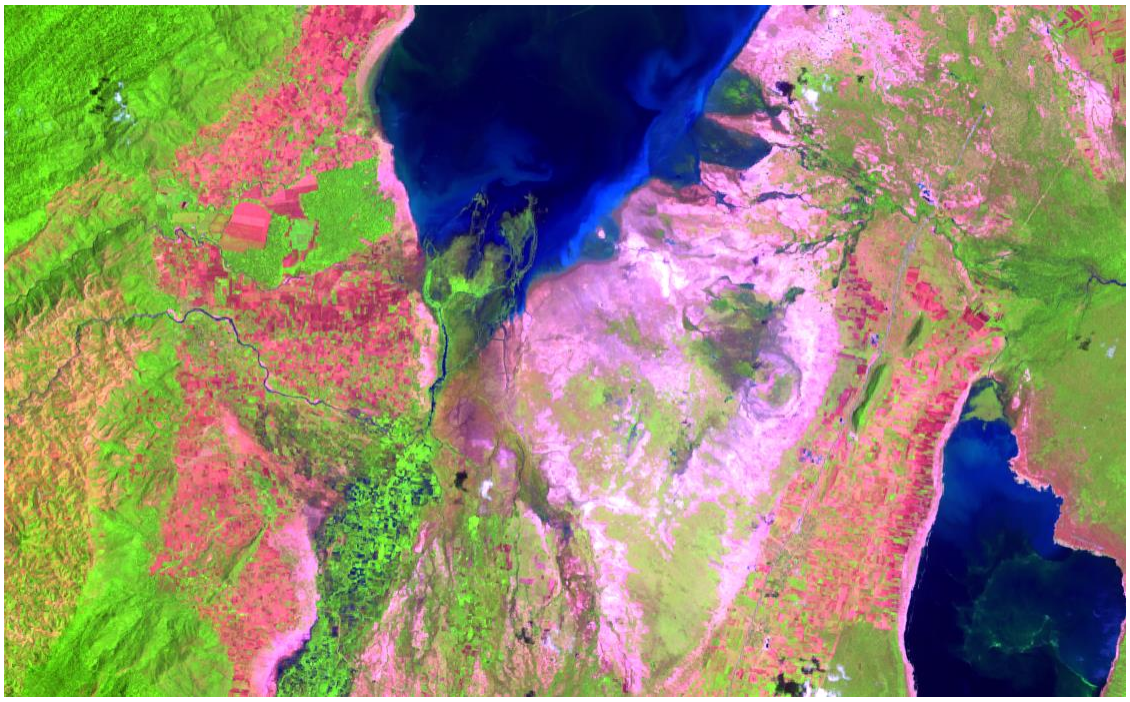

Appendix C.1: Landsat image (February 2017) showing the overflow from the Tarangire-Burunge system to Lake Manyara.

D. Land cover change

Land cover type	*Bushland*	*Agriculture*	*Forest*	*Wetland/ Riparian*	*Permanent savanna*	*Seasonal grassland*	*Bare*	*Saline grassland*	*Water bodies*	*Mosaic*	*Irrigation*	*Total area 1988*	*Loss*
Bushland	**2052.6**	977.5	133.1	51.9	1,175.4	217.5	33.0	15.9	0.7	30.0	131.8	4822.5	2766.7
Agriculture	71.2	**1474.0**	27.6	21.8	98.5	67.6	39.9	7.2	1.2	34.3	116.3	1960.8	485.6
Forest	56.5	54.7	**1040.8**	10.2	8.9	6.1	0.2	0.8	0.0	30.2	43.1	1252.9	210.8
Wetland/Riparian	50.3	41.9	18.1	**81.5**	105.8	32.7	1.3	17.4	7.5	2.1	80.8	439.5	357.9
Permanent savanna	849.9	1,001.5	45.2	116.6	**3573.9**	358.7	144.4	64.8	0.5	25.2	40.4	6223.0	2647.3
Seasonal grassland	134.7	945.5	0.9	26.7	556.6	**742.2**	99.4	42.9	1.4	10.4	4.1	2566.0	1822.8
Bare/Degraded	5.9	14.8	0.0	0.9	5.4	10.0	**35.1**	0.2	0.0	0.0	0.0	72.3	37.1
Saline grassland	4.4	6.4	0.6	61.1	43.1	15.9	10.2	**121.8**	49.4	0.0	0.2	313.2	191.3
Water bodies	0.1	0.6	0.1	6.1	0.1	0.0	0.0	0.2	**429.0**	0.0	0.0	436.3	7.2
Mosaic	1.8	16.7	20.7	0.4	1.6	0.2	0.0	0.1	0.0	**181.5**	0.1	223.3	41.7
Irrigation	3.2	11.0	5.9	2.4	0.1	2.3	0.1	0.9	0.0	0.2	**36.2**	62.2	26.0
Total area 2016	3232.7	4547.2	1293.9	379.8	5571.5	1454.1	363.6	272.2	489.8	314.1	453.1	18372.0	
Gain	1178.1	3070.6	252.3	298.1	1995.5	711.1	328.4	150.3	60.8	132.4	416.8		

Appendix D.1: Cross-tabulation table with the absolute values (in km^2) per land cover type of persistence (bold), transitions to other types, total area, losses and gains.

Tributary	*Agriculture*	*Bare*	*Bushland*	*Forest*	*Irrigation*	*Mosaic*	*Permanent grassland*	*Saline grassland*	*Seasonal grassland*	*Water bodies*	*Wetland / riparian*
DUD	26.3	0	10	18.3	17.9	13.3	1.7	3	5.7	0.5	3.3
END	38	0	3.6	45.8	0.2	8.2	1.3	0.6	1.5	0.1	0.6
KIR	47.7	1	5.6	37.6	0	0	3.3	0.8	0.1	0.5	3.5
MAK	19.2	10.9	15.9	3.6	0	0	24.2	0.8	22.4	0.3	2.7
MWM	24.3	1.5	5.2	25.1	3.2	0	1.4	3.3	34.6	0.1	1.2
SIM	11	0	1.3	56.6	3.2	0	25.5	1	0.3	0.2	0.9
TAR	25.8	0.2	22.3	0.9	0.4	0	43.3	1.1	4.1	0.4	1.5

Appendix D.2: Tributary catchment (Dudumera, Endabash, Kirurumo, Makuyuni, Mto Wa Mbu, Simba, Tarangire) land cover percentages.

Land cover type	*Bushland*	*Agriculture*	*Forest*	*Wetland/ Riparian*	*Permanent savanna*	*Seasonal grassland*	*Bare*	*Saline grassland*	*Water bodies*	*Mosaic*	*Irrigation*	*Grey (%)*	*False (%)*
Bushland	**26**	0	0	0	1	0	0	0	0	0	0	3.7	0
Agriculture	1	**22**	0	0	2	2	0	0	0	0	0	14.8	3.7
Forest	0	0	**27**	0	0	0	0	0	0	0	0	0	0
Wetland/Riparian	0	1	1	**21**	1	0	0	0	1	0	3	17.3	10.3
Permanent savanna	0	1	0	0	**26**	0	0	0	0	0	0	3.7	0
Seasonal grassland	1	1	0	0	1	**24**	0	0	0	0	0	7.4	3.7
Bare/Degraded	3	2	0	1	0	2	**20**	0	0	0	0	7.1	21.4
Saline grassland	0	0	0	0	0	1	0	**26**	0	0	0	3.7	0
Water bodies	0	0	0	0	0	0	0	0	**27**	0	0	0	0
Mosaic	1	1	0	0	0	0	0	0	0	**25**	0	7.4	0
Irrigation	0	2	0	2	0	0	0	0	0	0	**23**	14.8	0

Appendix D.3: Confusion matrix with numbers and percentages of correct (diagonal), unsure and false classification per land cover type.

E. Erosion risk mapping

Study	*Cover type*	*Country/Region*	*C-factor*
Angima et al., 2003	Maize-bean	Kenya	0.343
Angima et al., 2003	Coffee	Kenya	0.394
Angima et al., 2003	Banana	Kenya	0.089
Ligonja & Shrestha, 2015	Forest	Tanzania	0.012
Ligonja & Shrestha, 2015	Bushland	Tanzania	0.085
Ligonja & Shrestha, 2015	Savanna grasslands	Tanzania	0.13
Ligonja & Shrestha, 2015	Croplands	Tanzania	0.09
Ligonja & Shrestha, 2015	Water	Tanzania	0.002
Ligonja & Shrestha, 2015	Bare soil	Tanzania	0.45
Ligonja & Shrestha, 2015	Built up	Tanzania	0.042
Mati, 1999	Barley	Kenya	0.25
Mati, 1999	Rangeland	Kenya	0.40-1.00
Mati, 1999	Grass	Kenya	0.003-0.30
Mati, 1999	Potatoes	Kenya	0.10-0.90
Gelagay & Minale, 2016	Water bodies	Ethiopia	0
Gelagay & Minale, 2016	Cultivated	Ethiopia	0.1
Gelagay & Minale, 2016	Forest	Ethiopia	0.01
Gelagay & Minale, 2016	Bushland	Ethiopia	0.014
Gelagay & Minale, 2016	Rangeland	Ethiopia	0.05
Panagos et al., 2015	Wheat and spelt	Europe	0.20
Panagos et al., 2015	Durum wheat	Europe	0.20
Panagos et al., 2015	Rye	Europe	0.20
Panagos et al., 2015	Barley	Europe	0.21
Panagos et al., 2015	Maize	Europe	0.38
Panagos et al., 2015	Rice	Europe	0.15
Panagos et al., 2015	Dried pulses	Europe	0.32
Panagos et al., 2015	Potatoes	Europe	0.34
Panagos et al., 2015	Sugar beet	Europe	0.34
Panagos et al., 2015	Oilseeds	Europe	0.28
Panagos et al., 2015	Rape and turnip	Europe	0.30
Panagos et al., 2015	Sunflower	Europe	0.32
Panagos et al., 2015	Linseed	Europe	0.25
Panagos et al., 2015	Soya	Europe	0.28
Panagos et al., 2015	Cotton seed	Europe	0.50
Panagos et al., 2015	Tobacco	Europe	0.49
Panagos et al., 2015	Fallow	Europe	0.50

Appendix E.1: C-factor values from other RUSLE studies.

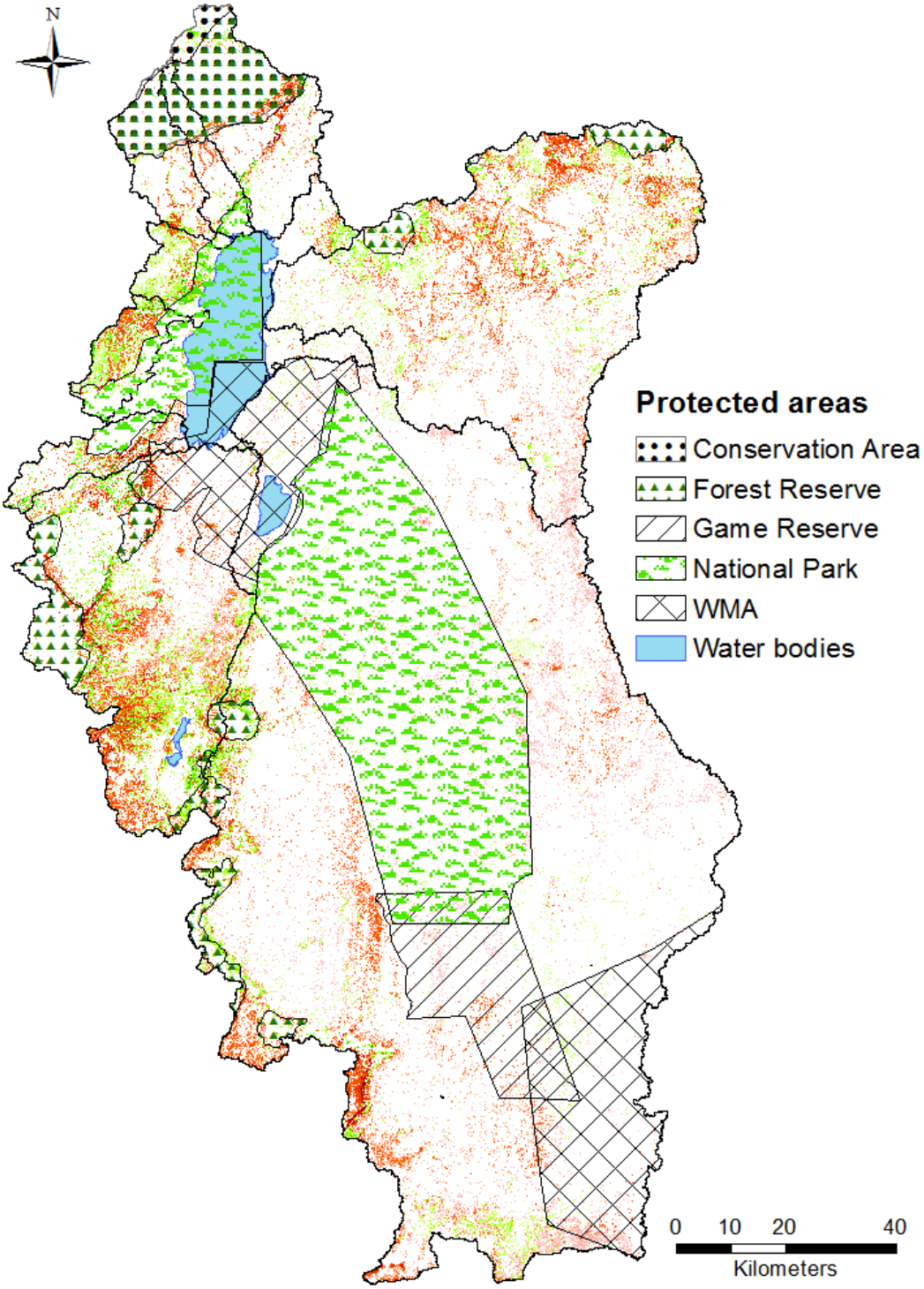

Appendix E.2: Erosion risk change map (red is increase, green decrease) overlaid with protected areas and delineation of the different sub-catchments to highlight the effect of land management and the spatial variability of the risk change.

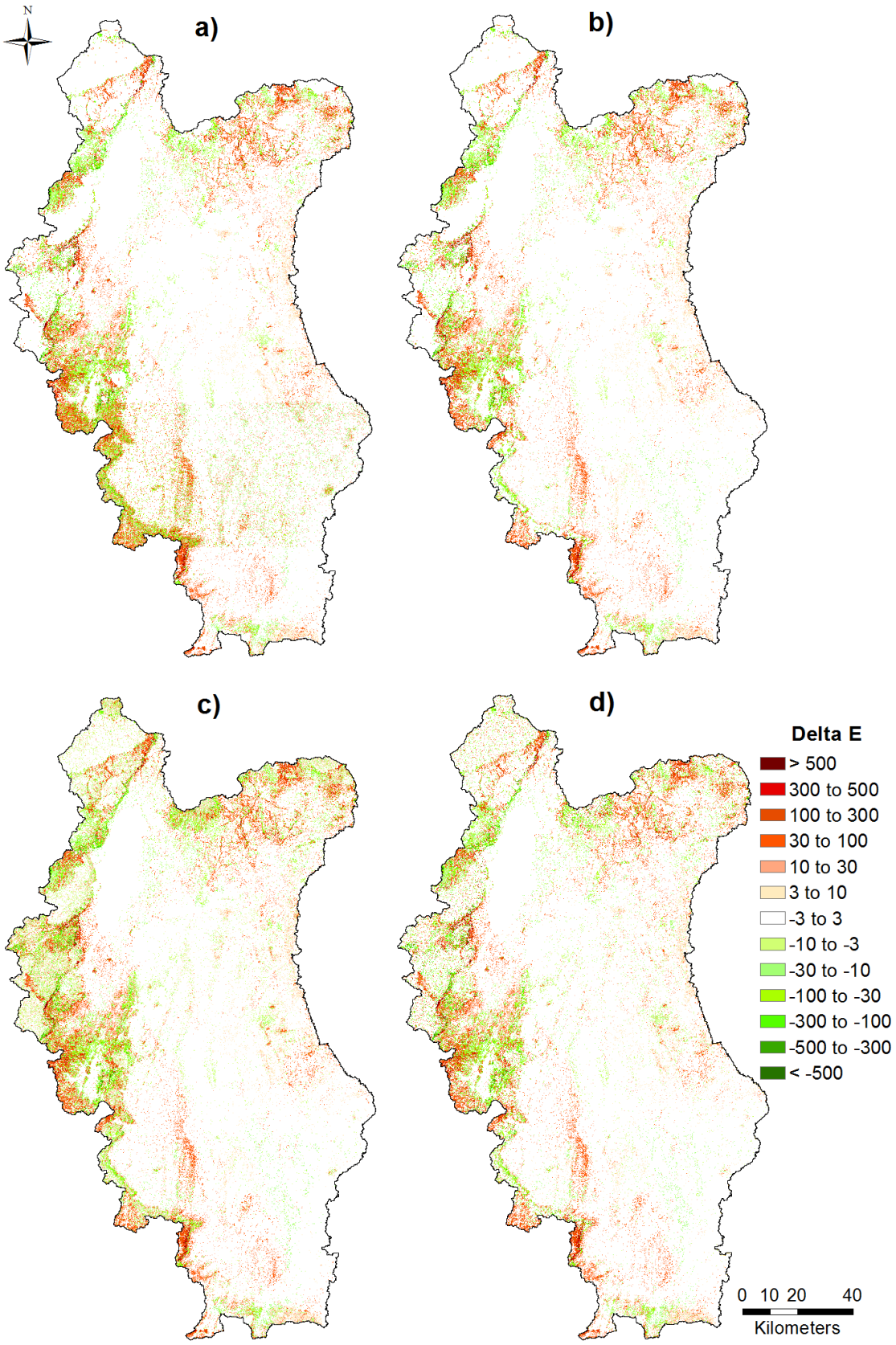

Appendix E.3: Sensitivity analysis of the model output (Delta E= changes in surface erosion risk) with 10% random errors in the model inputs of a) the LS factor, b) R-factor and c) K-factor, while keeping the other factors stable, and d) the land cover error introduced in the C-factor. Note the high similarity in spatial risk distribution.

F. CRS-standard approach

With s_n as the experimentally derived dry bulk density in section n, the cumulative dry mass m_n above sediments at depth x_n can be calculated as:

$$m_n = m_{n-1} + s_n(x_n - x_{n-1}) \quad \text{(F.1)}$$

Where C_n is the experimentally derived $^{210}Pb_{ex}$ activity at layer n, the cumulative $^{210}Pb_{ex}$ inventory can be calculated using the trapezium rule:

$$\hat{A}_n = \hat{A}_{n-1} + \frac{C_{n-1} - C_n}{\ln\left(\frac{C_{n-1}}{C_n}\right)}(m_n - m_{n-1}) \quad \text{(F.2)}$$

The total $^{210}Pb_{ex}$ (in Bq m^{-2}) inventory $A(0)$ of the sediment core is then equal to the $\hat{A}_n$ value in the deepest layer. The residual $^{210}Pb_{ex}$ (in Bq m^{-2}) inventory in the sediment core below depth n can subsequently be easily calculated by subtracting $\hat{A}_n$ from $A(0)$. Following the CRS model and with λ_{Pb} as the ^{210}Pb radioactive decay constant of 0.03114 y^{-1}, the age t of the sediment layer at depth n can be estimated by:

$$t = \frac{1}{\lambda_{Pb}} \ln\left(\frac{A(0)}{A(n)}\right) \quad \text{(F.3)}$$

The sedimentation rate r at depth z can subsequently be calculated as follows:

$$r = \frac{\lambda_{Pb} A(n)}{C(n)} \quad \text{(F.4)}$$

G. CRS-fitted approach

If $\hat{A}_{ref}$ denotes the entire $^{210}Pb_{ex}$ inventory above the reference level t_{ref}, the inventory below that level can be obtained by the following formula:

$$A_{ref} = \frac{\hat{A}_{ref}}{e^{\lambda t_{ref}} - 1} \quad \text{(G.1)}$$

The total inventory is then:

$$A(0) = \hat{A}_{ref} + A_{ref} \qquad \text{(G.2)}$$

Sediment dates and accumulation rates can subsequently be calculated using equations F.3 and F.4 respectively.

H. Lake $^{210}Pb_{ex}$ profiles and tributary $^{210}Pb_{ex}$ activities

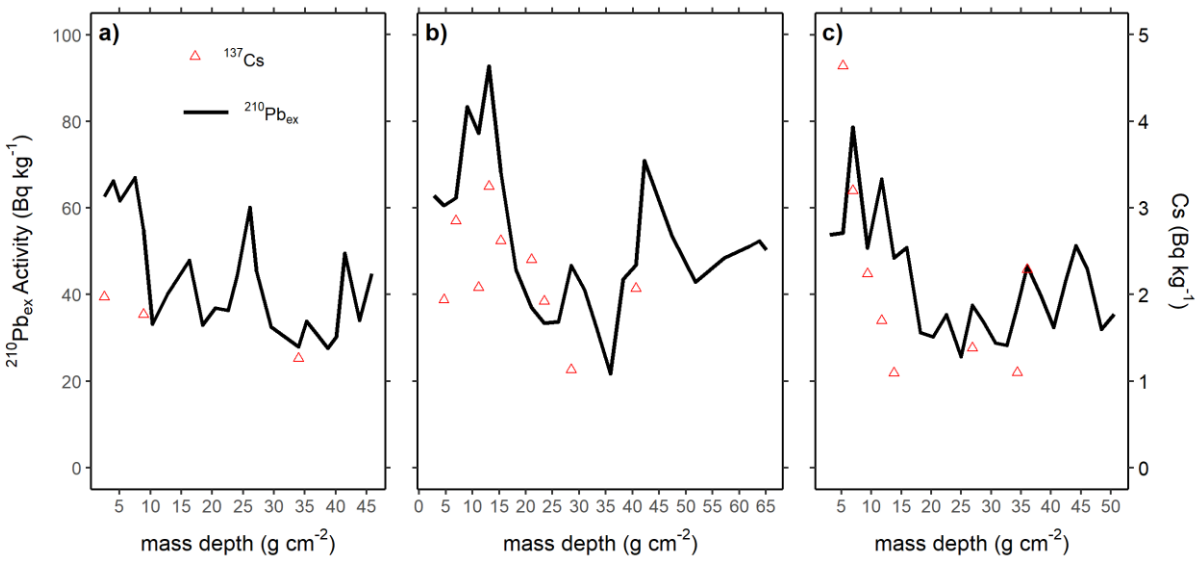

Appendix H.1: $^{210}Pb_{ex}$ and ^{137}Cs profiles of a) core1, b) core 4, and c) core 5

$^{210}Pb_{ex}$ (Bq kg^{-1})	*Dudumera*	*Endabash*	*Makuyuni*	*MtoWaMbu*	*Ngorongoro*	*Tarangire*
Mean	**38.8**	**19.7**	**11.7**	**15.8**	**10.2**	**13.7**
SD	6.1	5.3	5.8	6.3	1.7	3.3

Appendix H.2: Mean and standard deviation (SD) of tributary sediment $^{210}Pb_{ex}$ activities.

I. Lake and tributary geochemical characteristics

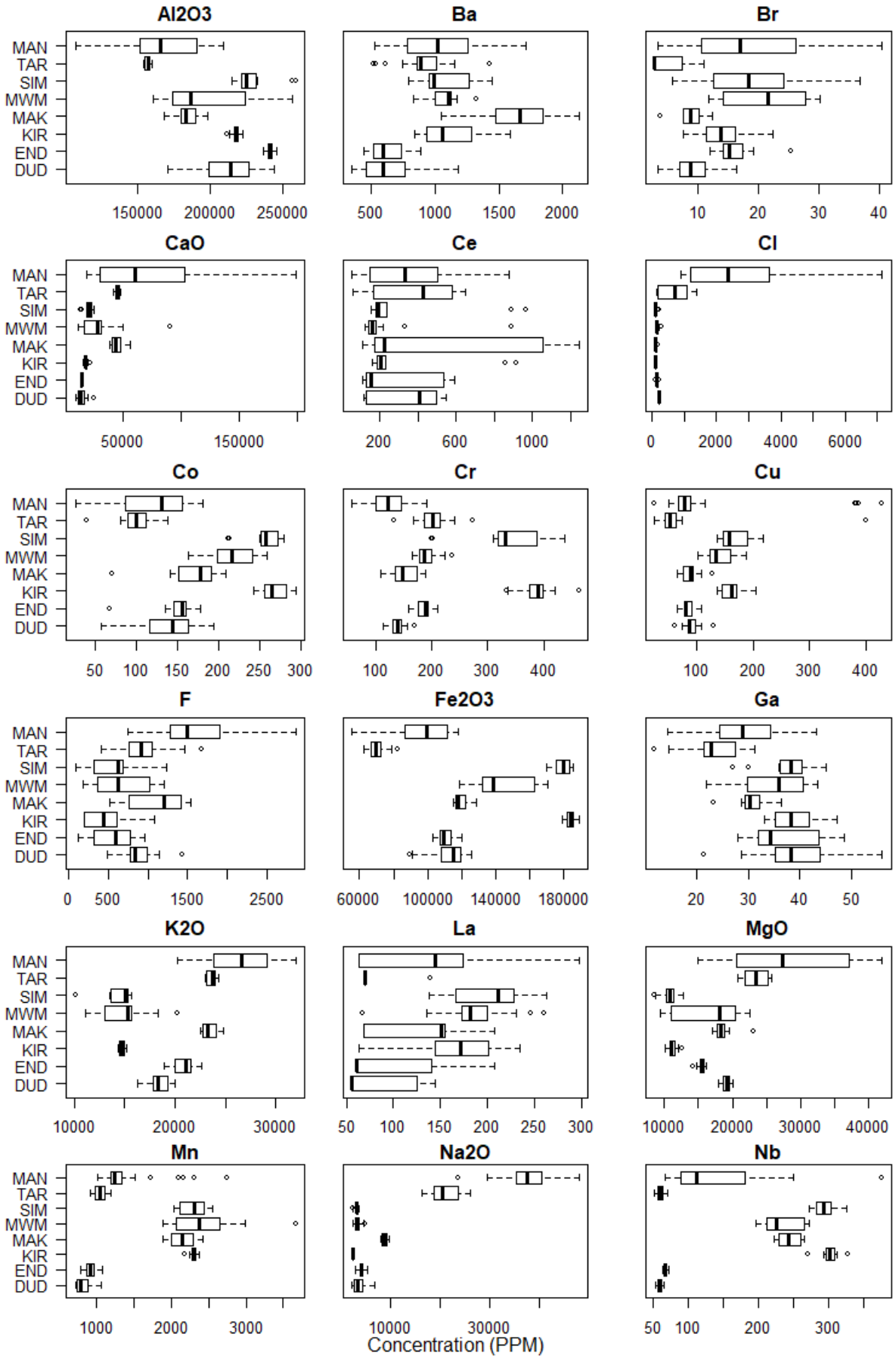

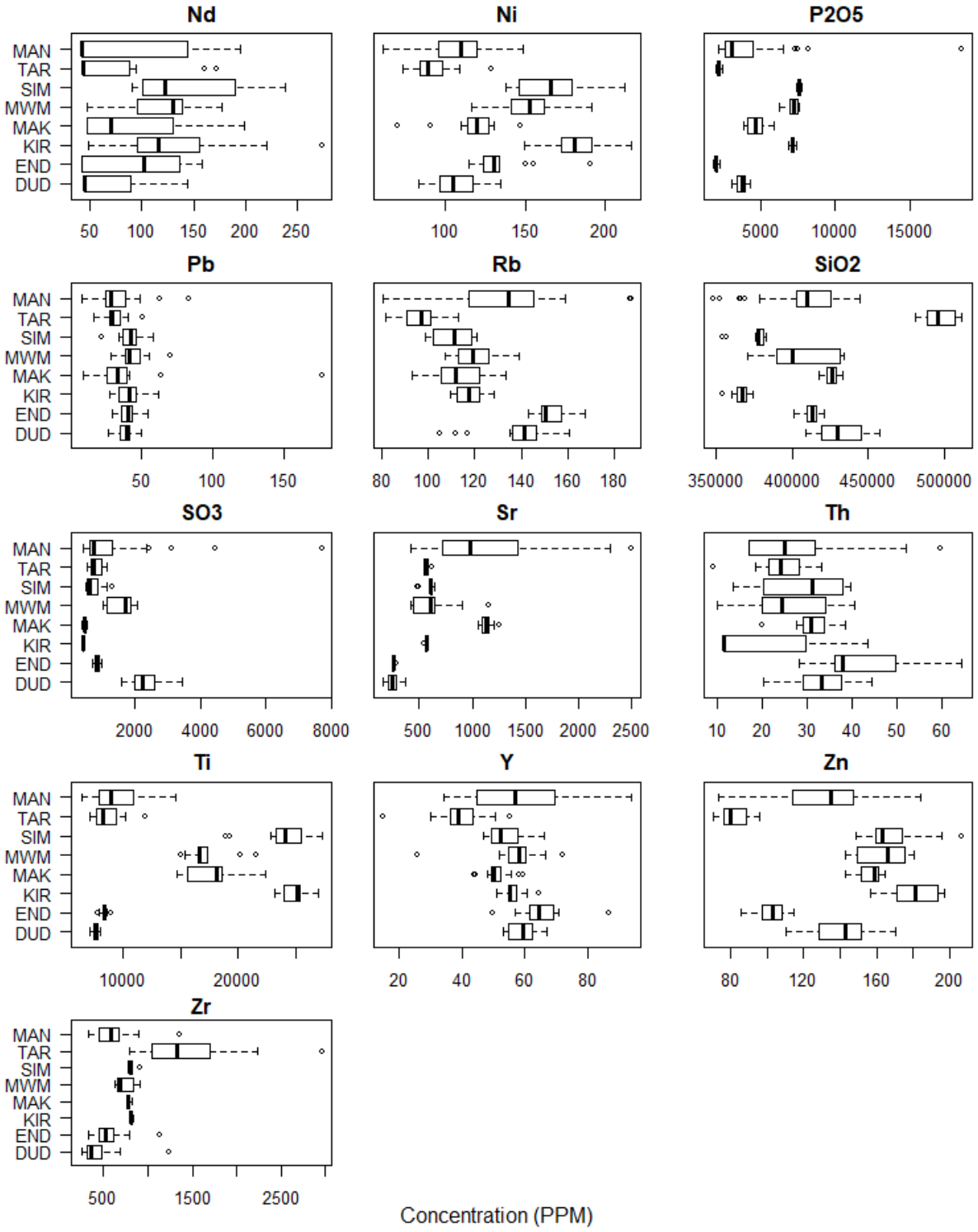

Appendix I.1: Tracer element range tests between tributary sources (DUD, END, KIR, MAK, MWM, SIM, TAR) and the lake (MAN). In the box plots, median is shown by central line, interquartile range by box, range by whiskers with circles indicating outliers

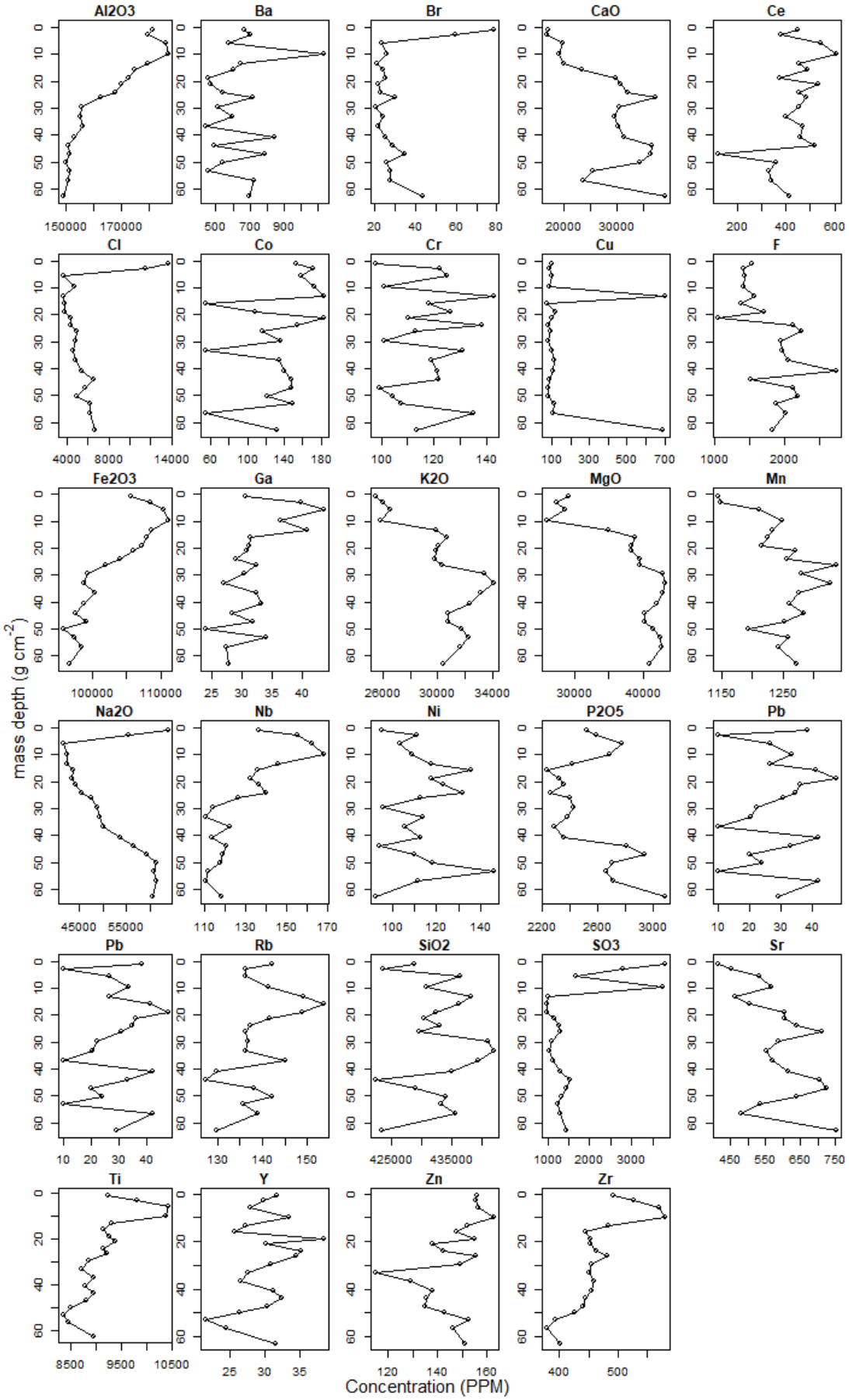

Appendix I.2: Geochemical depth profiles of core 2

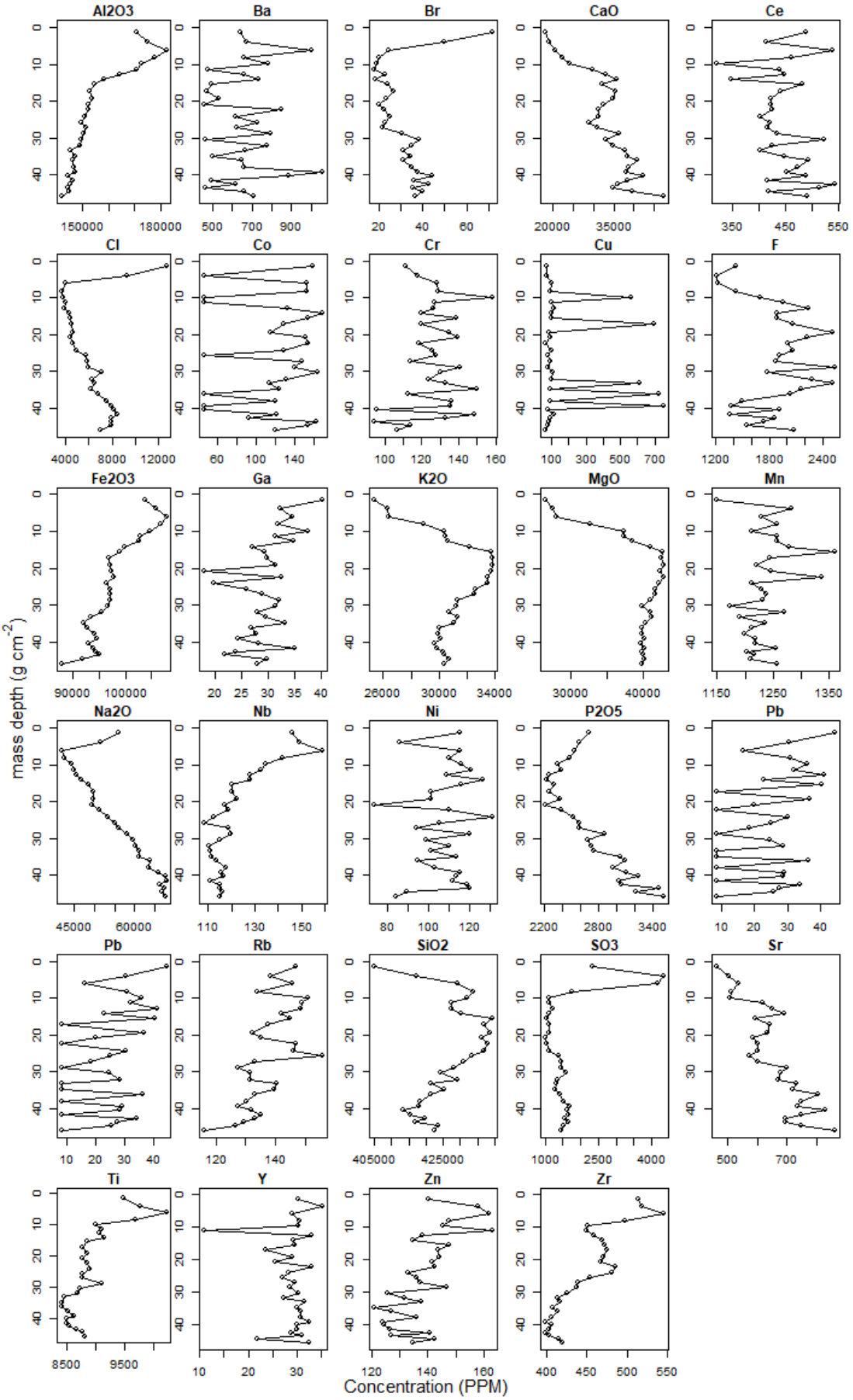

Appendix I.3: Geochemical depth profiles of core 3

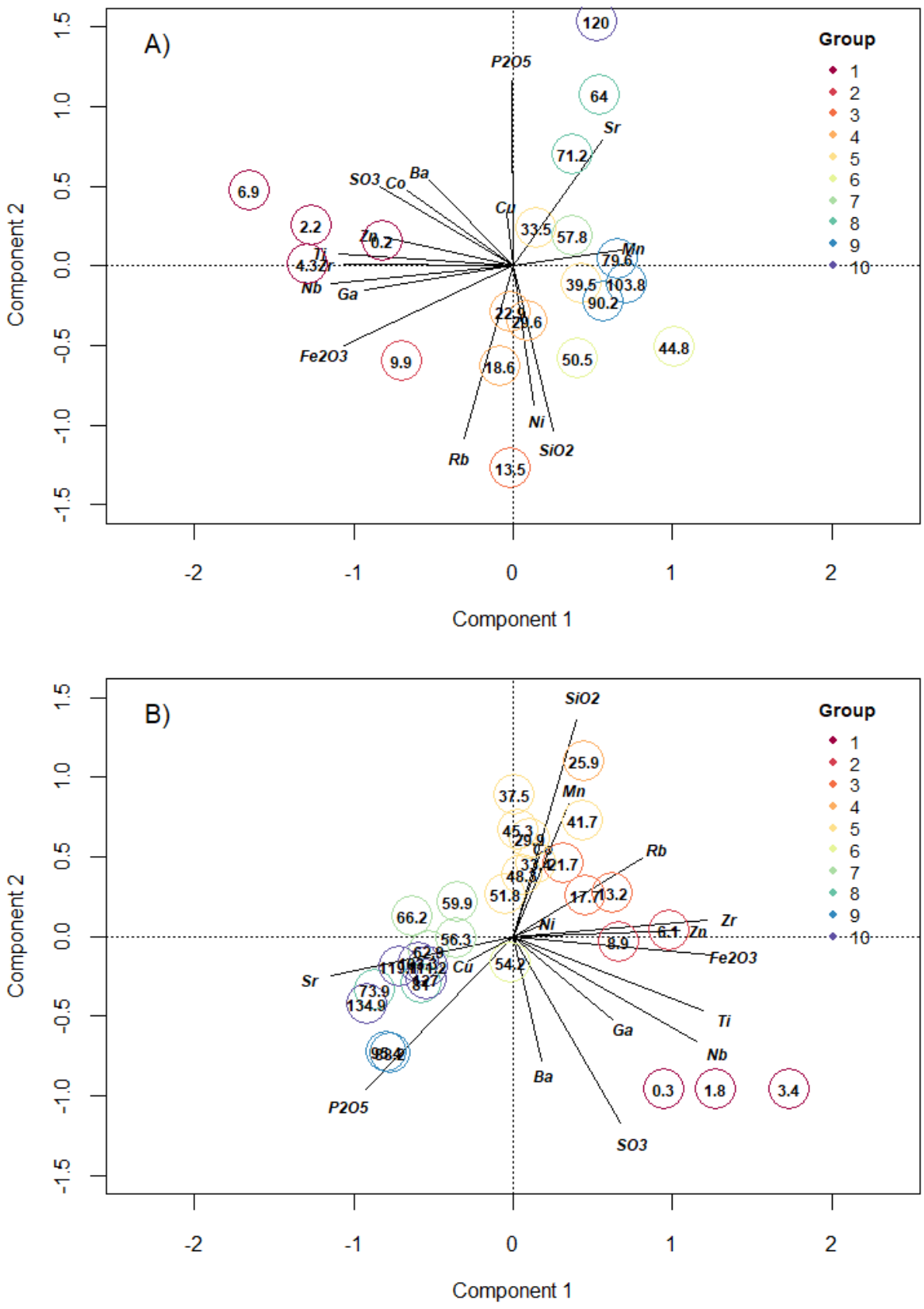

Appendix I.4: Ordination plot of the two major principal components visualising the geochemical drivers of variance in A) Core 2 (explaining 37.5% and 19.2% of variance) and B) core 3 (explaining 39.6% and 15.9% of variance). Groups are as used for fixed categorical effect in the BMM.

J. Bayesian Mixing model output

Tributary	Global		Northeast		Northwest		Southeast		Southwest	
	Mean	Diag.	Mean	Diag.	Mean	Diag.	Mean	Diag.	Mean	Diag.
Dudumera	0.582	1.006	0.149	1.014	0.226	1.016	0.064	1.014	0.161	1.017
Endabash	0.011	1.006	0.074	1.010	0.471	1.014	0.027	1.001	0.069	1.002
Makuyuni	0.359	1.008	0.618	1.015	0.209	1.027	0.148	1.009	0.184	1.017
Mto Wa Mbu	0.011	1.002	0.060	1.002	0.035	1.006	0.025	1.020	0.540	1.001
Ngorongoro	0.017	1.000	0.023	1.022	0.017	1.032	0.008	1.017	0.013	1.015
Tarangire	0.020	1.004	0.076	1.002	0.043	1.001	0.729	1.013	0.034	1.000

Appendix J.1: The mean values and Gelman diagnostics (Diag.) of the Bayesian Mixing model runs for both 'global' and 'spatial' model builds.

Core groups	Dudumera		Endabash		Makuyuni		Mto Wa Mbu		Ngorongoro		Tarangire	
	Mean	Diag.	Mean	Diag.	Mean	Diag.	Mean	Diag.	Mean	Diag.	Mean	Diag.
1	0.499	1.003	0.038	1.003	0.208	1.006	0.018	1.016	0.223	1.005	0.014	1.000
2	0.537	1.001	0.042	1.004	0.148	1.002	0.017	1.002	0.243	1.001	0.012	1.011
3	0.592	1.001	0.031	1.002	0.168	1.003	0.025	1.018	0.174	1.001	0.012	1.002
4	0.542	1.003	0.073	1.002	0.154	1.006	0.016	1.012	0.199	1.004	0.016	1.002
5	0.626	1.001	0.037	1.000	0.181	1.005	0.021	1.007	0.118	1.005	0.017	1.000
6	0.607	1.002	0.083	1.002	0.159	1.003	0.018	1.005	0.103	1.002	0.029	1.002
7	0.603	1.000	0.07	1.000	0.153	1.005	0.026	1.007	0.118	1.003	0.03	1.005
8	0.574	1.002	0.074	1.001	0.192	1.001	0.018	1.008	0.106	1.000	0.037	1.003
9	0.669	1.001	0.043	1.001	0.125	1.002	0.02	1.008	0.129	1.003	0.014	1.000
10	0.633	1.001	0.034	1.001	0.175	1.001	0.023	1.014	0.117	1.002	0.019	1.003

Appendix J.2: The mean values and Gelman diagnostics (Diag.) of the Bayesian Mixing model output of core 2, specified for grouped core sections.

Core groups	Dudumera		Endabash		Makuyuni		Mto Wa Mbu		Ngorongoro		Tarangire	
	Mean	Diag.	Mean	Diag.	Mean	Diag.	Mean	Diag.	Mean	Diag.	Mean	Diag.
1	0.462	1.009	0.035	1.010	0.411	1.018	0.009	1.000	0.051	1.024	0.032	1.002
2	0.523	1.003	0.038	1.003	0.351	1.006	0.011	1.012	0.055	1.008	0.023	1.002
3	0.581	1.004	0.037	1.009	0.285	1.001	0.009	1.008	0.069	1.001	0.02	1.004
4	0.596	1.002	0.049	1.002	0.259	1.002	0.012	1.014	0.054	1.003	0.03	1.003
5	0.626	1.003	0.036	1.007	0.276	1.003	0.007	1.001	0.025	1.005	0.03	1.000
6	0.574	1.002	0.05	1.004	0.264	1.006	0.016	1.011	0.054	1.009	0.042	1.005
7	0.487	1.005	0.145	1.006	0.23	1.002	0.009	1.006	0.037	1.004	0.093	1.004
8	0.56	1.002	0.048	1.000	0.262	1.002	0.011	1.010	0.03	1.007	0.09	1.002
9	0.543	1.002	0.05	1.002	0.262	1.004	0.011	1.012	0.03	1.005	0.104	1.002
10	0.564	1.002	0.042	1.005	0.248	1.002	0.008	1.003	0.036	1.002	0.102	1.001

Appendix J.3: The mean values and Gelman diagnostics (Diag.) of the Bayesian Mixing model output of core 3, specified for grouped core sections.

K. Makuyuni sub-tributary characteristics

Subtributary	Size (km^2)	Min elevation (m)	Max elevation (m)	Dominant land use
Ardai	390	1193	2658	Rangeland/Agriculture
Lesimingore A	78	1027	2159	Rangeland
Lesimingore B	62	1043	2167	Rangeland
Lolkisale	474	1160	2132	Rangeland
Meserani Chini	11	1187	1354	Rangeland
Meserani Juu	123	1212	1601	Rangeland
Musa	182	1211	2642	Agriculture
Nanja	240	1159	2124	Rangeland/Agriculture

Appendix K.1: Sub-catchment characteristics of the selected sub-tributaries.

L. Makuyuni sub-tributary range tests

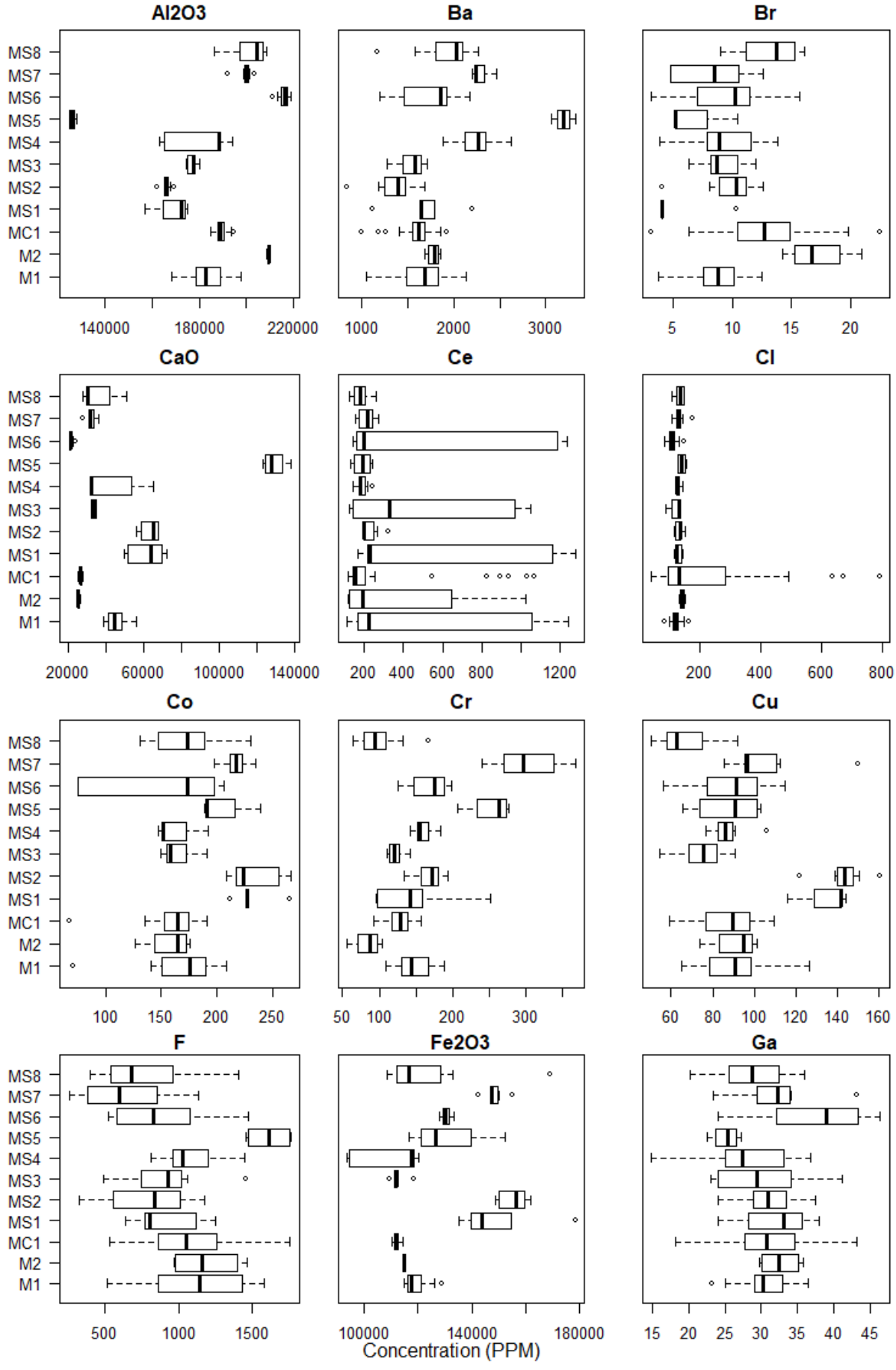

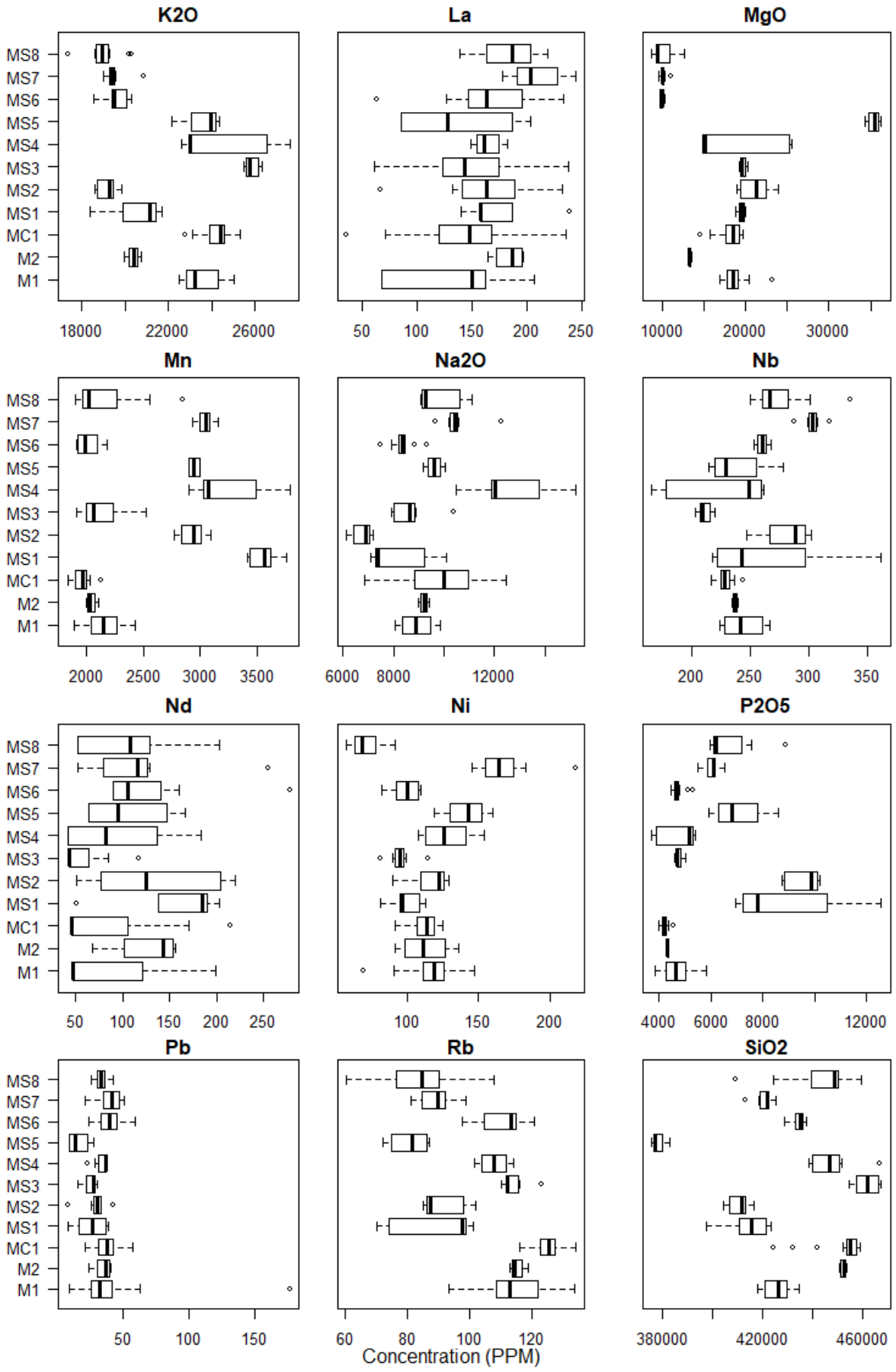
K2O
La
MgO
Mn
Na2O
Nb
Nd
Ni
P2O5
Pb
Rb
SiO2
MS8
MS7
MS6
MS5
MS4
MS3
MS2
MS1
MC1
M2
M1
18000
22000
26000
50
100
150
200
250
10000
20000
30000
2000
2500
3000
3500
6000
8000
12000
200
250
300
350
4000
6000
8000
12000
60
80
100
120
380000
420000
460000
Concentration (PPM)

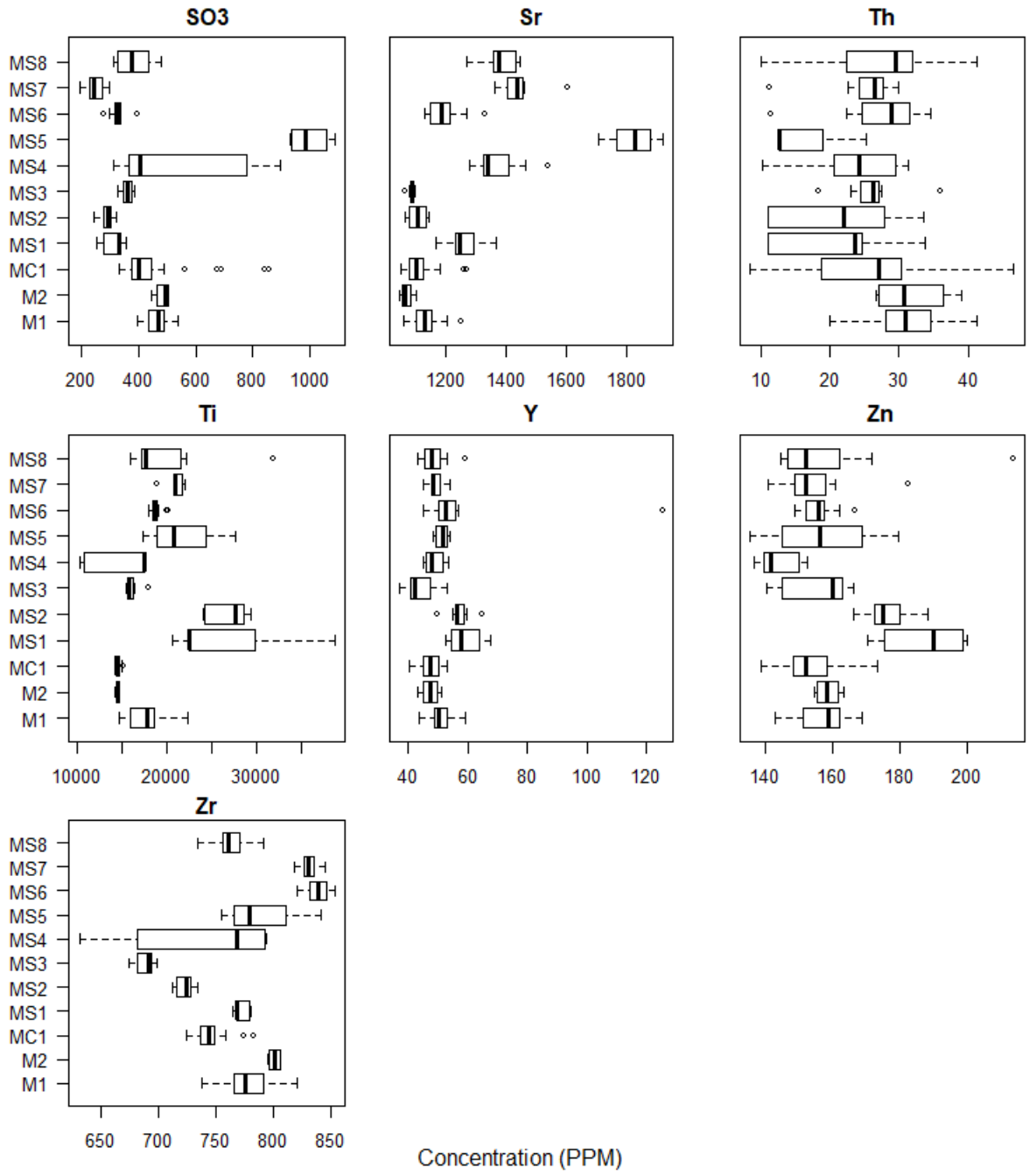

Appendix L.1: Tracer element range tests between sub-tributaries (MS 1-8: Lesimingore A, Lesimingore B, Nanja, Lolkisale, Meserani Chini, Ardai, Meserani Juu, and Musa respectively), nested Makuyuni reaches (M1 and M2), and Meserani core (MC1). See Figure 1 for upstream connectivity. The median is shown by central line, interquartile range by box, range by whiskers with circles indicating outliers.

M. Meserani core Bayesian Mixing Model output

Core groups	***Ardai***		***Lolkisale***		***Musa***		***Meserani Juu***		***Meserani Chini***	
	Mean	*Diag.*	*Mean*	*Diag.*	*Mean*	*Diag.*	*Mean*	*Diag.*	*Mean*	*Diag.*
1	0.746	1.002	0.207	1.002	0.021	1.000	0.014	1.003	0.012	1.007
2	0.755	1.003	0.202	1.003	0.020	1.001	0.013	1.001	0.010	1.002
3	0.746	1.001	0.217	1.001	0.014	1.000	0.011	1.001	0.013	1.003
4	0.778	1.002	0.169	1.002	0.032	1.001	0.012	1.000	0.009	1.004
5	0.591	1.004	0.352	1.004	0.025	1.000	0.018	1.001	0.014	1.007
6	0.753	1.001	0.182	1.001	0.027	1.000	0.021	1.001	0.016	1.010
7	0.706	1.002	0.209	1.002	0.043	1.013	0.024	1.000	0.018	1.002
8	0.751	1.002	0.213	1.002	0.015	1.002	0.012	1.001	0.009	1.005
9	0.789	1.001	0.162	1.001	0.023	1.000	0.015	1.000	0.010	1.005

Appendix M.1: The mean values and Gelman diagnostics (Diag.) of the Bayesian Mixing model output, specified for grouped core sections.

N. Tracer selection for northern Makuyuni sub-tributaries

Ardai		**Nanja**		**Musa**	
Riverine	*Core*	*Riverine*	*Core*	*Riverine*	*Core*
δ^{13} (C22, C23, C24, C26, C28, C30, C32), Ba, CaO, Co, Cu, Fe_2O_3, K_2O, MgO, Nb, P_2O_5, Rb, SiO_2, SO_3, Sr, Ti, Zn	Al_2O_3, Ba, Br, CaO, Cl, Cr, Fe_2O_3, K2O, MgO, Mn, Na_2O, Nb, P_2O_5, Rb, SiO_2, SO_3, Sr, Ti, Y, Zn, Zr	Ba, CaO, Co, Cr, Cu, F, Fe_2O_3, K_2O, Mn, Na_2O, Ni, P_2O_5, Rb, SiO_2, SO_3, Th, Ti, Y, Zn	δ^{13} (C22, C23, C24, C25, C26, C27, C28, C29, C30, C31, C32), Al_2O_3, Ba, CaO, Co, F, Fe_2O_3, K_2O, MgO, Mn, Na_2O, Nb, Ni, P_2O_5, Rb, SiO_2, SO_3, Sr, Ti, Y, Zr	Al_2O_3, Ba, Br, CaO, Cr, Fe_2O_3, MgO, Mn, Nb, Ni, P_2O_5, Rb, SiO_2, SO_3, Sr, Ti, Y, Zr	Al_2O_3, Ba, Br, CaO, Cl, Co, Cr, Fe_2O_3, K_2O, MgO, Mn, Na_2O, Nb, P_2O_5, Pb, Rb, SiO_2, SO_3, Sr, Ti, Zn, Zr

Appendix N.1: an overview of selected tracers for soil-to-sediment BMM and core PCA.

O. Soil-to-sediment tracer range tests and PCA plots

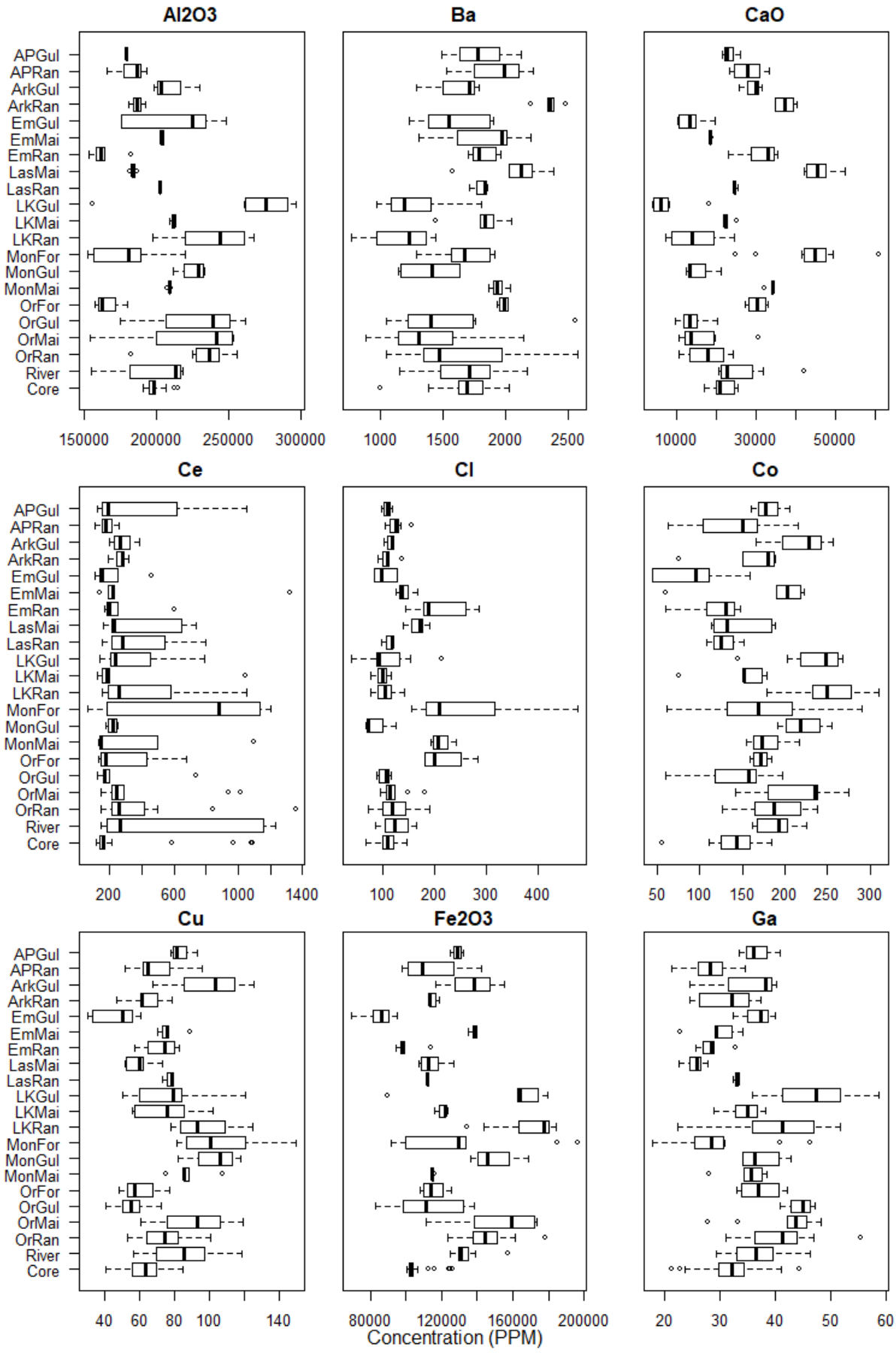
Al2O3
Ba
CaO
Ce
Cl
Co
Cu
Fe2O3
Ga
APGul
APRan
ArkGul
ArkRan
EmGul
EmMai
EmRan
LasMai
LasRan
LKGul
LKMai
LKRan
MonFor
MonGul
MonMai
OrFor
OrGul
OrMai
OrRan
River
Core
150000 200000 250000 300000
1000 1500 2000 2500
10000 30000 50000
200 600 1000 1400
100 200 300 400
50 100 150 200 250 300
40 60 80 100 140
80000 120000 160000 200000
20 30 40 50 60
Concentration (PPM)

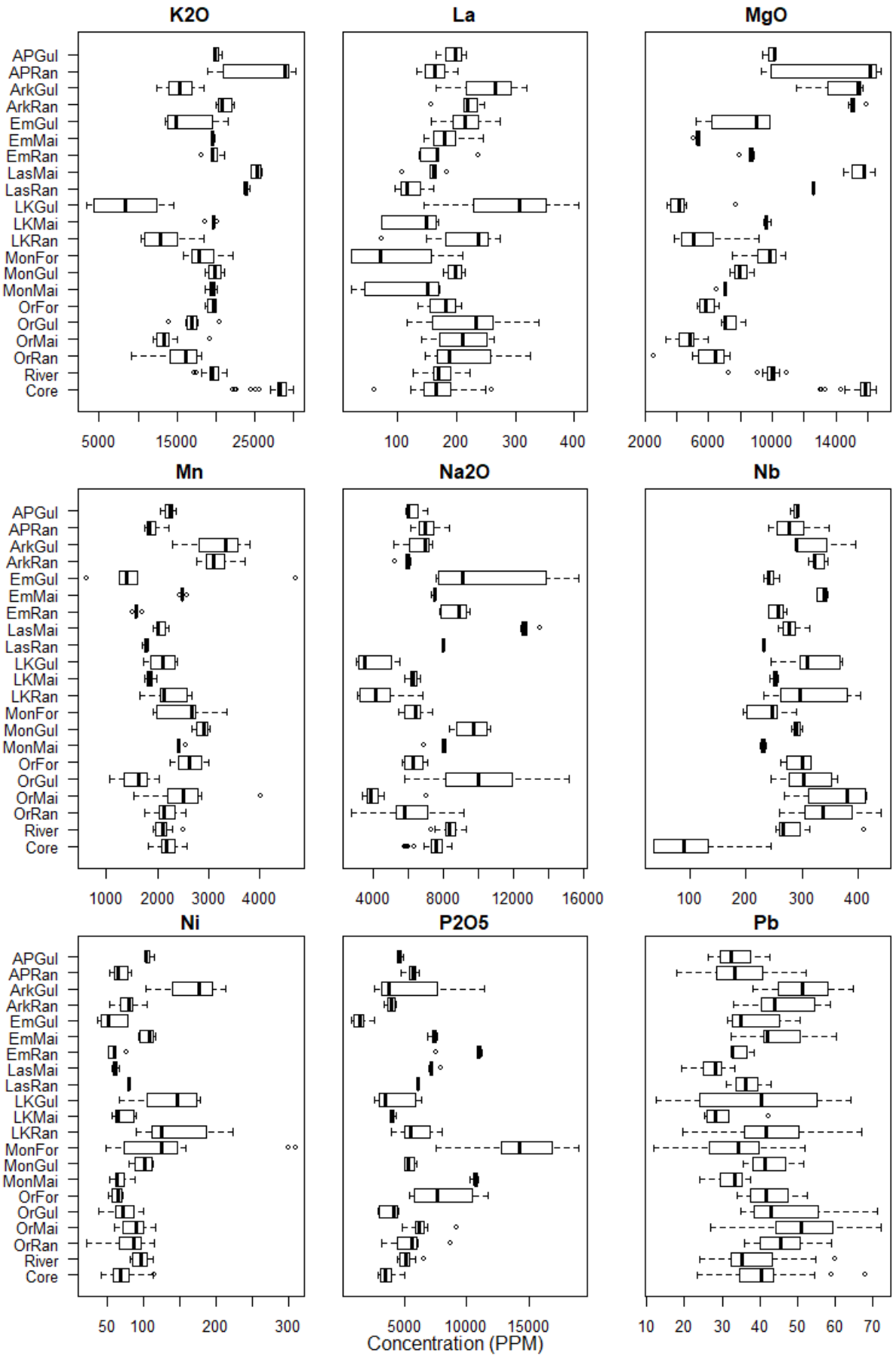
K2O
La
MgO
Mn
Na2O
Nb
Ni
P2O5
Pb
APGul
APRan
ArkGul
ArkRan
EmGul
EmMai
EmRan
LasMai
LasRan
LKGul
LKMai
LKRan
MonFor
MonGul
MonMai
OrFor
OrGul
OrMai
OrRan
River
Core
5000 15000 25000
100 200 300 400
2000 6000 10000 14000
1000 2000 3000 4000
4000 8000 12000 16000
100 200 300 400
50 100 200 300
5000 10000 15000
10 20 30 40 50 60 70
Concentration (PPM)

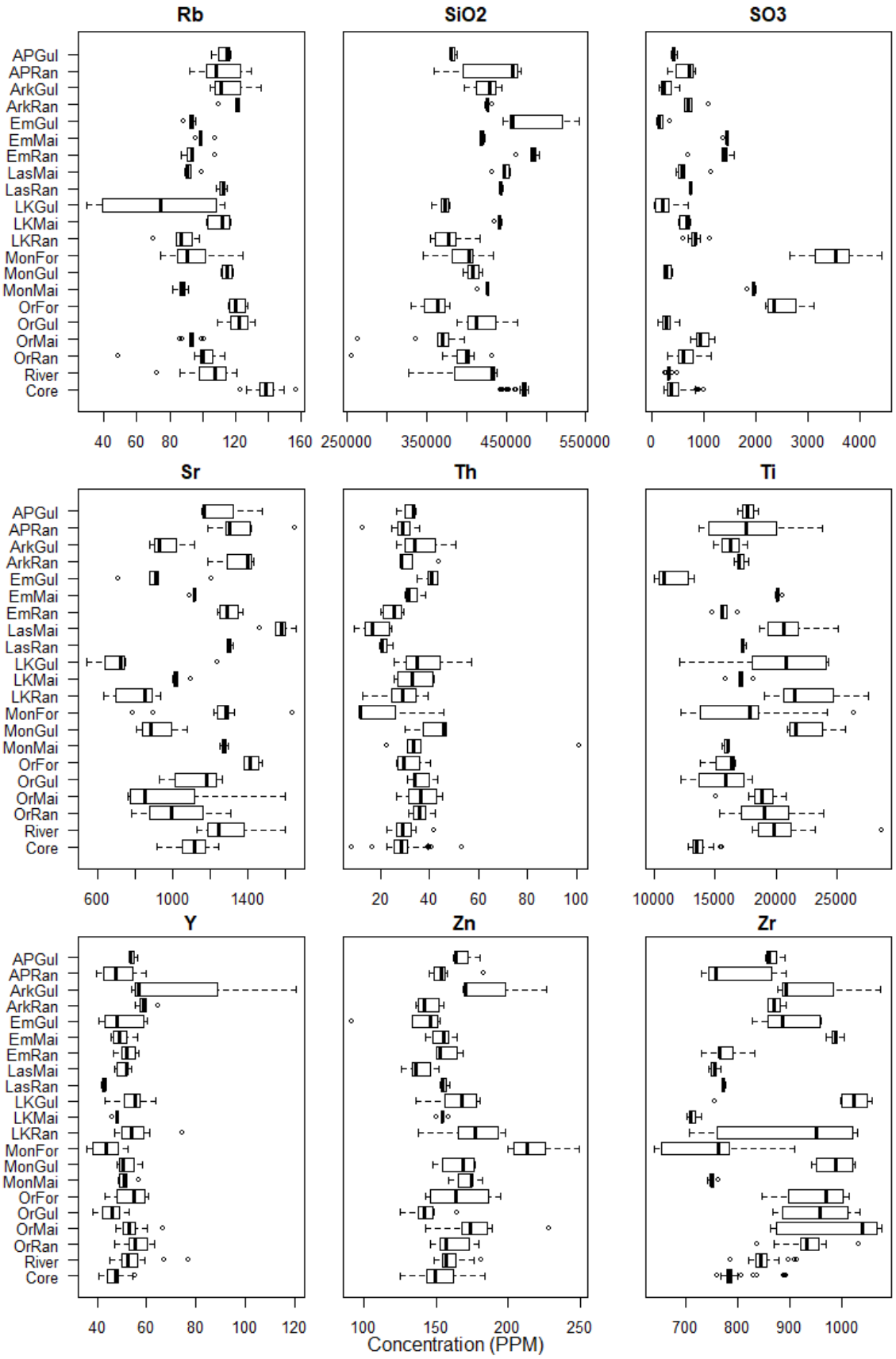

Appendix O.1: Geochemical tracer range tests between soil sampling locations (APGul-OrRan), riverine sediment (River) and sediment core (Core) within the Ardai sub-catchment. Median is shown by central line, interquartile range by box, range by whiskers with circles indicating outliers.

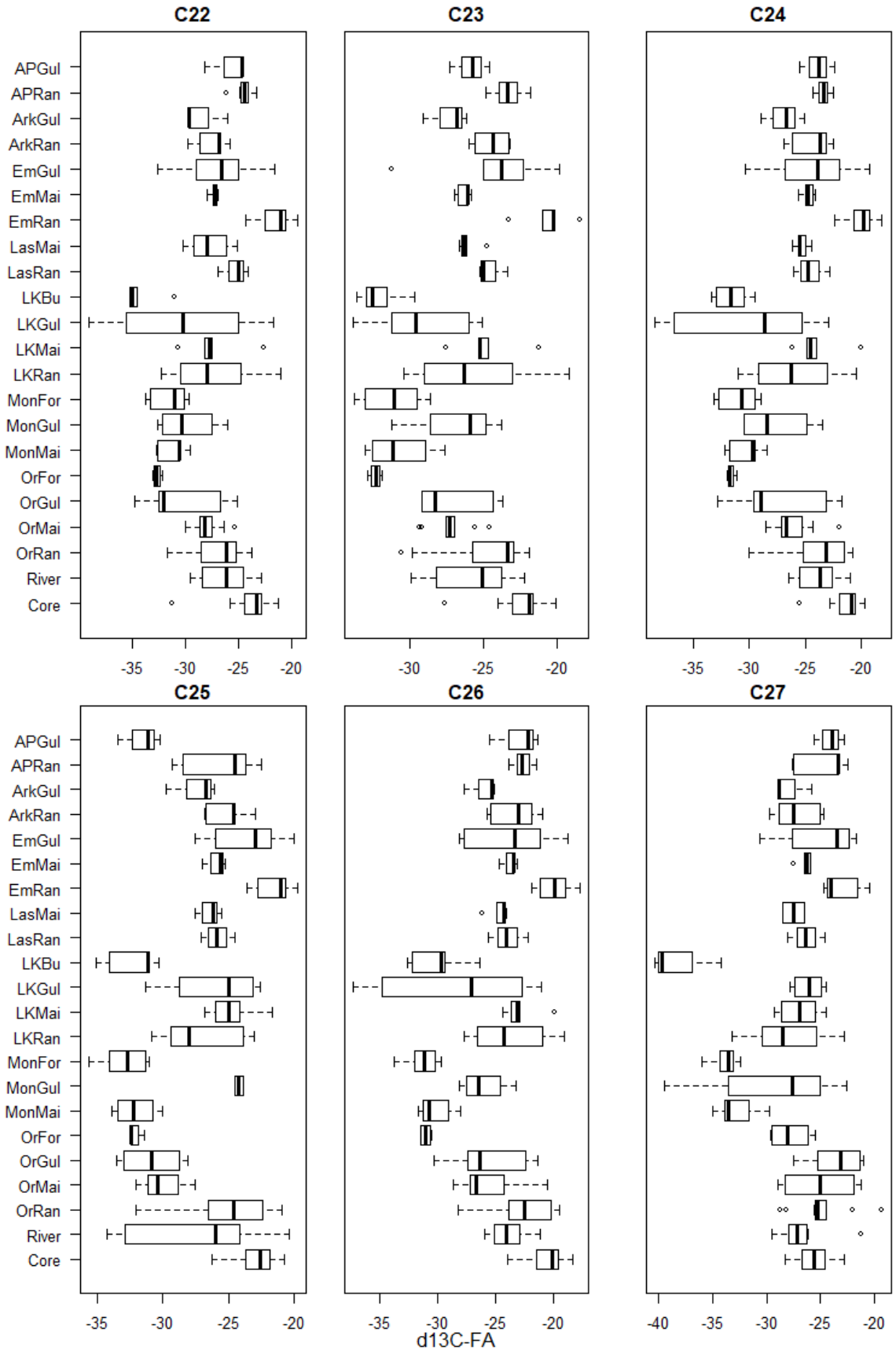
C22
C23
C24
C25
C26
C27
APGul
APRan
ArkGul
ArkRan
EmGul
EmMai
EmRan
LasMai
LasRan
LKBu
LKGul
LKMai
LKRan
MonFor
MonGul
MonMai
OrFor
OrGul
OrMai
OrRan
River
Core
-35
-30
-25
-20
-40
d13C-FA

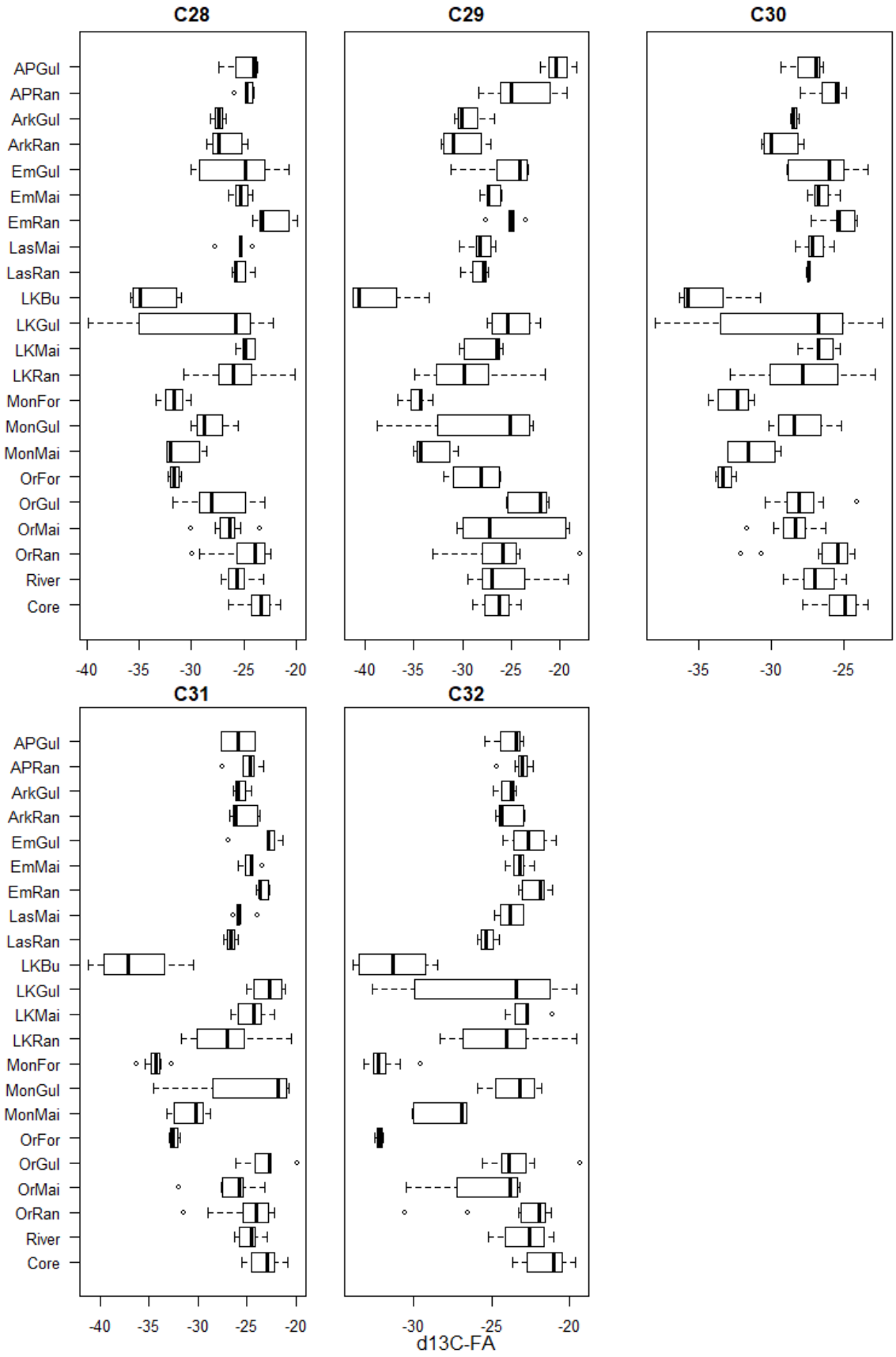

Appendix O.2: δ^{13} FA tracer range tests between soil sampling locations (APGul-OrRan), riverine sediment (River) and sediment core (Core) within the Ardai sub-catchment. Median is shown by central line, interquartile range by box, range by whiskers with circles indicating outliers.

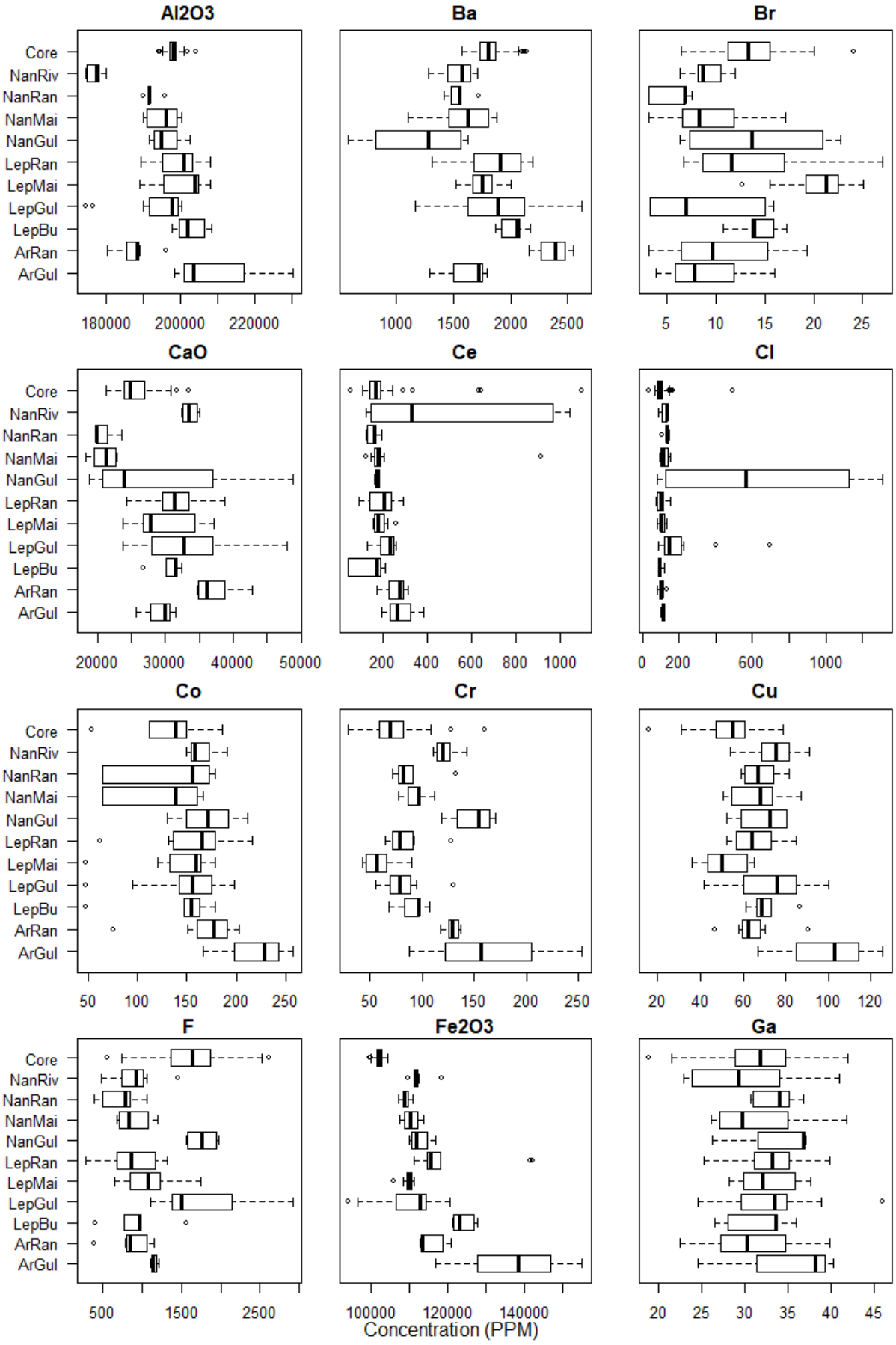
Al2O3
Ba
Br
CaO
Ce
Cl
Co
Cr
Cu
F
Fe2O3
Ga
Core
NanRiv
NanRan
NanMai
NanGul
LepRan
LepMai
LepGul
LepBu
ArRan
ArGul
180000 200000 220000
1000 1500 2000 2500
5 10 15 20 25
20000 30000 40000 50000
200 400 600 800 1000
0 200 600 1000
50 100 150 200 250
50 100 150 200 250
20 40 60 80 100 120
500 1500 2500
100000 120000 140000
20 25 30 35 40 45
Concentration (PPM)

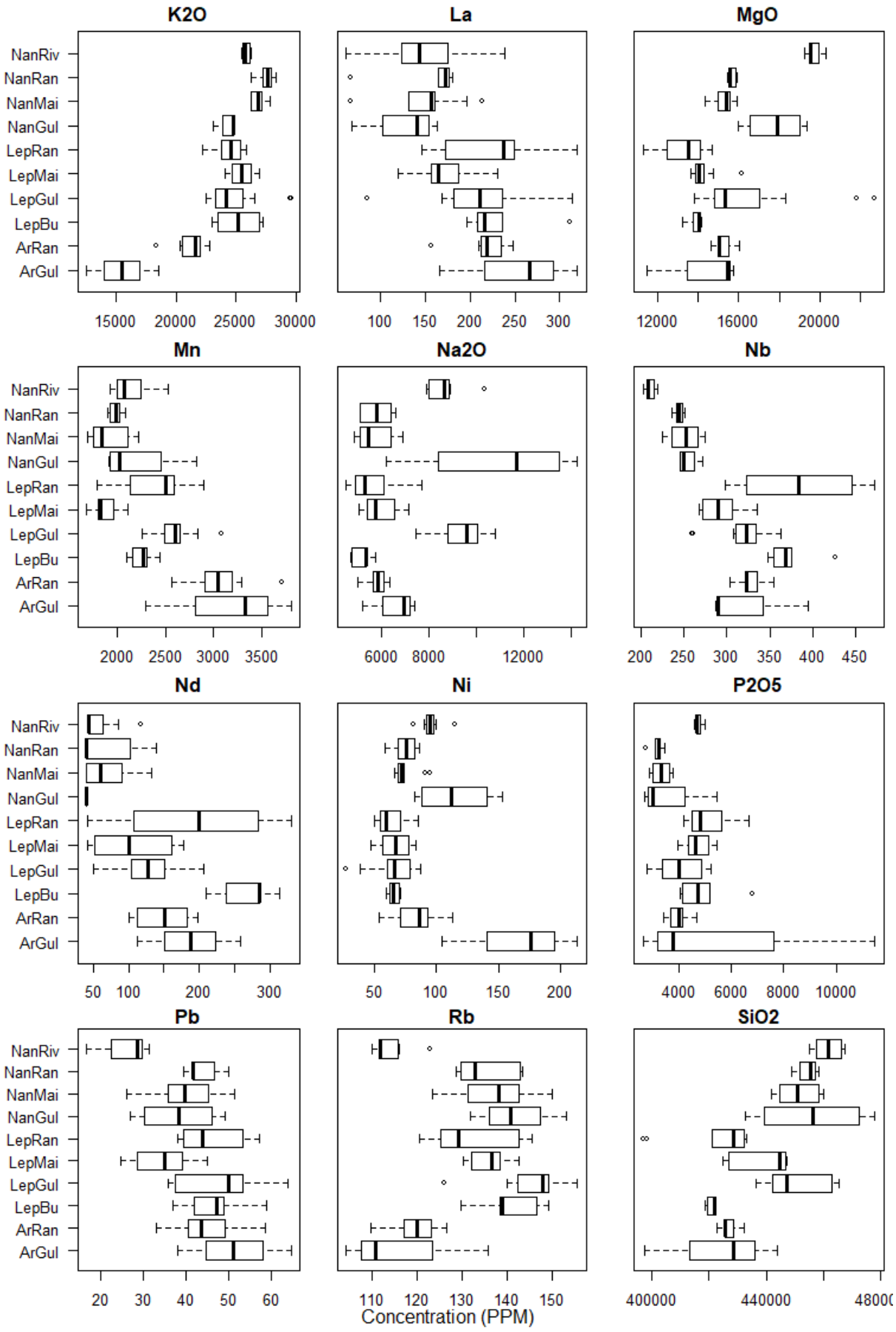
K2O
La
MgO
Mn
Na2O
Nb
Nd
Ni
P2O5
Pb
Rb
SiO2
NanRiv
NanRan
NanMai
NanGul
LepRan
LepMai
LepGul
LepBu
ArRan
ArGul
15000 20000 25000 30000
100 150 200 250 300
12000 16000 20000
2000 2500 3000 3500
6000 8000 12000
200 250 300 350 400 450
50 100 200 300
50 100 150 200
4000 6000 8000 10000
20 30 40 50 60
110 120 130 140 150
400000 440000
Concentration (PPM)

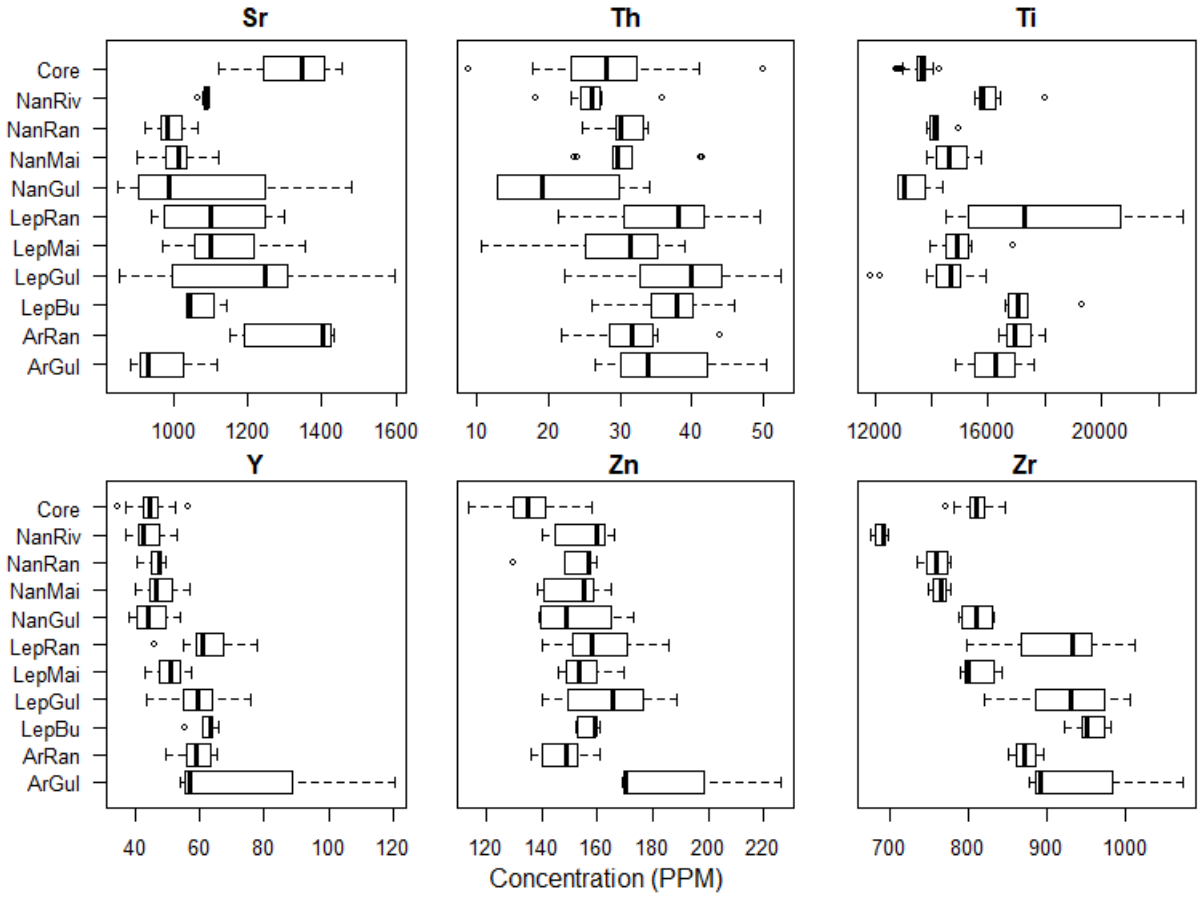

Appendix O.3: Geochemical tracer range tests between soil sampling locations, riverine sediment and sediment core within the Nanja sub-catchment. Median is shown by central line, interquartile range by box, range by whiskers with circles indicating outliers.

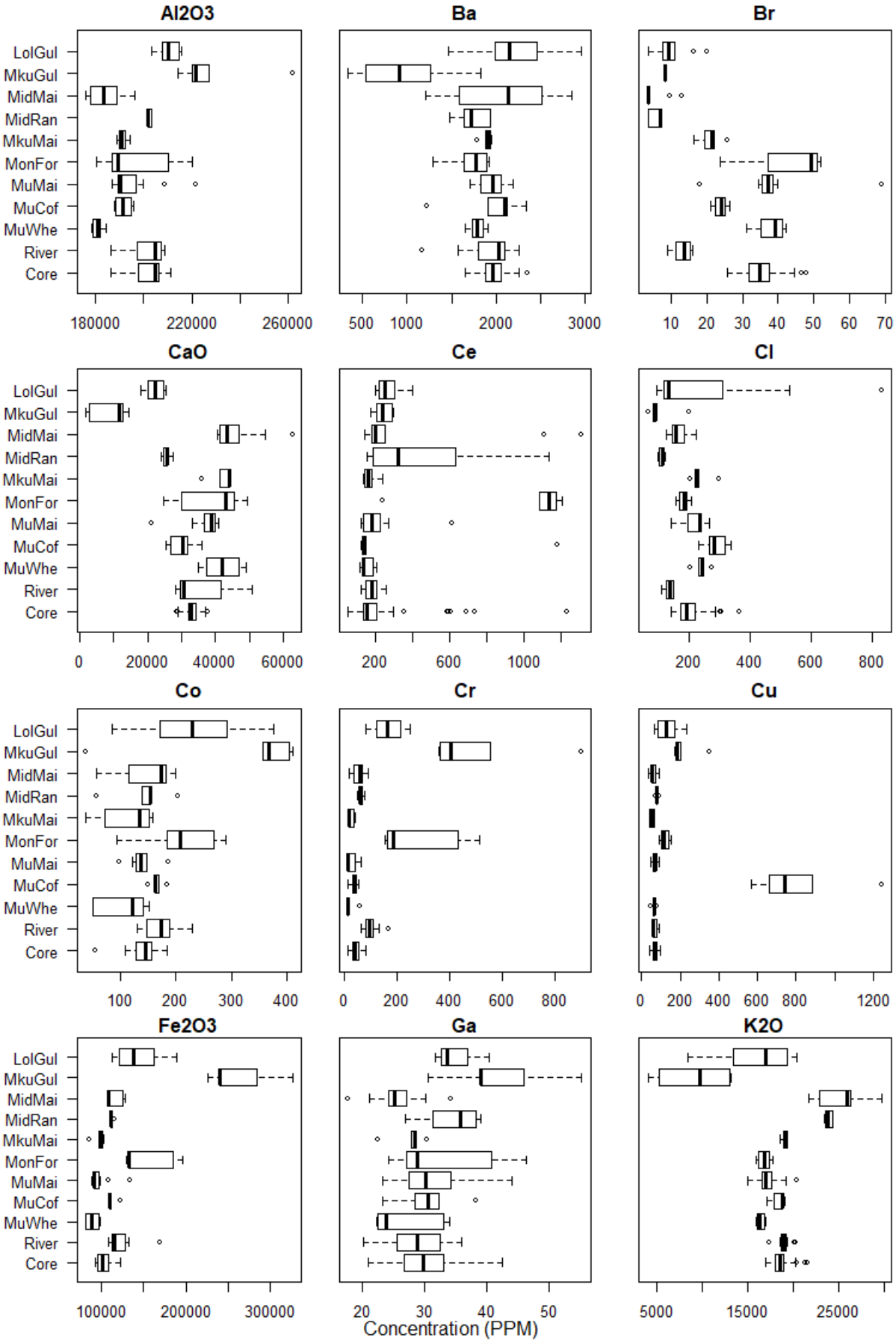
Al2O3
Ba
Br
CaO
Ce
Cl
Co
Cr
Cu
Fe2O3
Ga
K2O
LolGul
MkuGul
MidMai
MidRan
MkuMai
MonFor
MuMai
MuCof
MuWhe
River
Core
180000 220000 260000
500 1000 2000 3000
10 20 30 40 50 60 70
0 20000 40000 60000
200 600 1000
200 400 600 800
100 200 300 400
0 200 400 600 800
0 200 400 600 800 1200
100000 200000 300000
20 30 40 50
5000 15000 25000
Concentration (PPM)

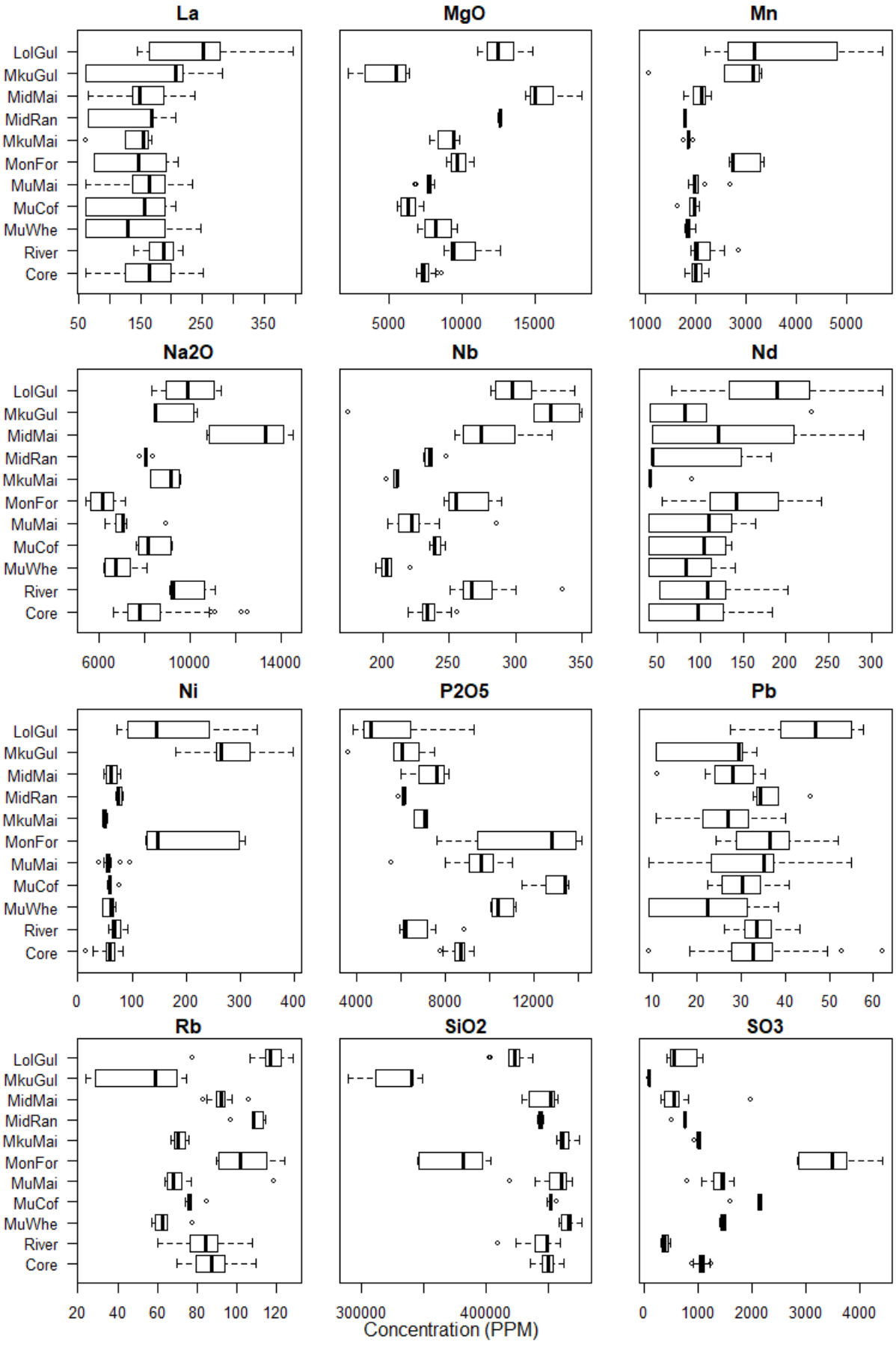
La
MgO
Mn
Na2O
Nb
Nd
Ni
P2O5
Pb
Rb
SiO2
SO3
LolGul
MkuGul
MidMai
MidRan
MkuMai
MonFor
MuMai
MuCof
MuWhe
River
Core
50 150 250 350
5000 10000 15000
1000 2000 3000 4000 5000
6000 10000 14000
200 250 300 350
50 100 150 200 250 300
0 100 200 300 400
4000 8000 12000
10 20 30 40 50 60
20 40 60 80 100 120
300000 400000
0 1000 2000 3000 4000
Concentration (PPM)

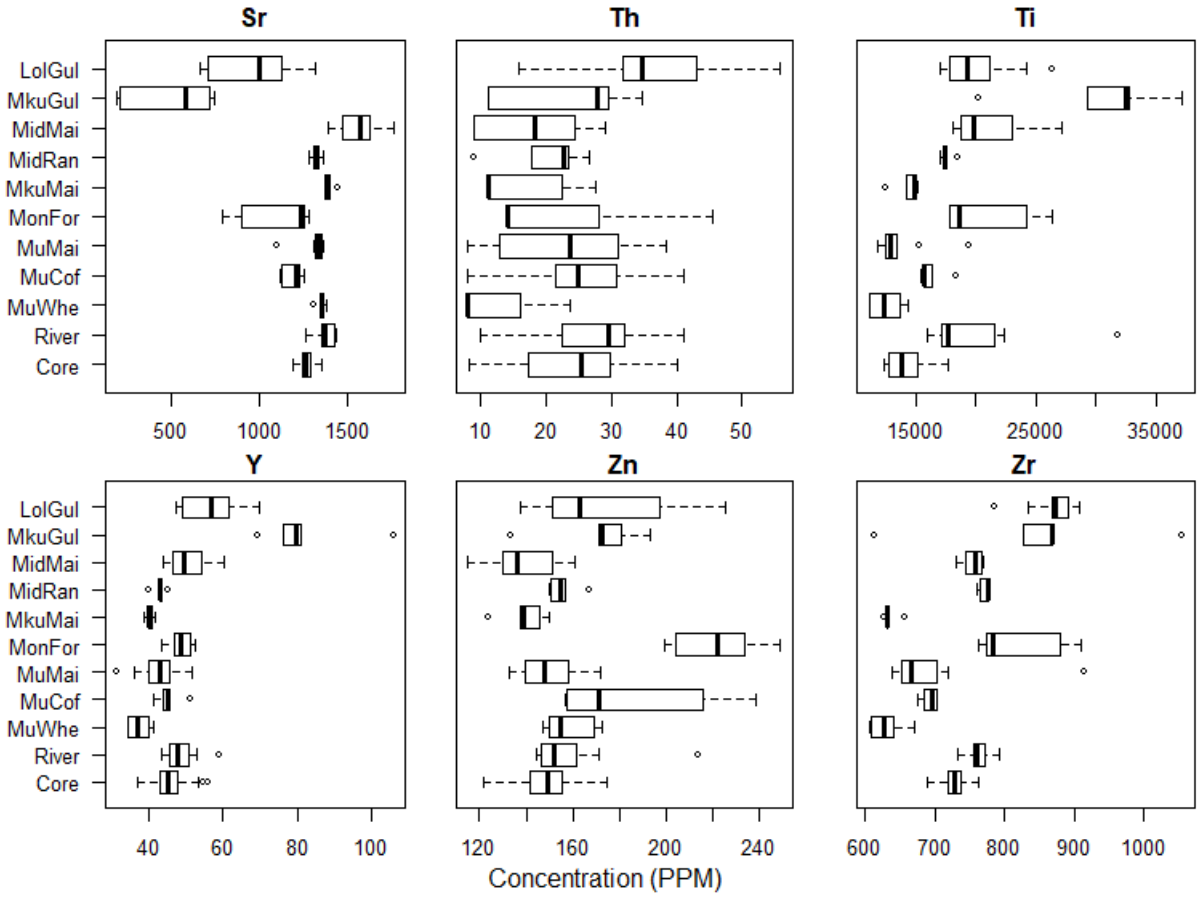

Appendix O.4: Geochemical tracer range tests between soil sampling locations, riverine sediment and sediment core within the Musa sub-catchment. Median is shown by central line, interquartile range by box, range by whiskers with circles indicating outliers.

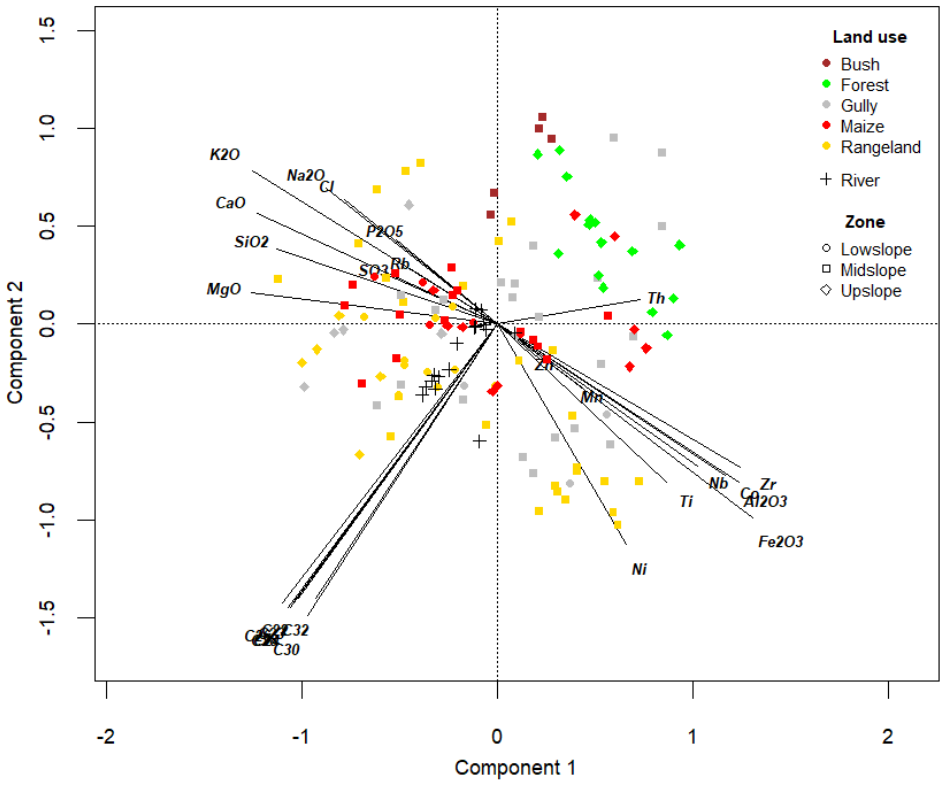

Appendix O.5: Composite PCA plot (explaining 29.4% and 23.7%) of soil samples and riverine sediment in the Ardai sub-catchment

P. Northern Makuyuni Bayesian Mixing Model outputs

A) Geochemical

Bedrock Incision		**Lower zone hillslopes**		**Middle zone hillslopes**		**Upper zone hillslopes**		**Saprolite**	
Mean	*Diag.*	*Mean*	*Diag.*	*Mean*	*Diag.*	*Mean*	*Diag.*	*Mean*	*Diag.*
0.060	1.001	0.111	1.000	0.725	1.003	0.055	1.004	0.050	1.000

B) δ^{13}-FA

Maize cropland		**Bushland**		**Open Rangeland**		**Upland Agriculture**		**Upland Forest**	
Mean	*Diag.*	*Mean*	*Diag.*	*Mean*	*Diag.*	*Mean*	*Diag.*	*Mean*	*Diag.*
0.256	1.001	0.043	1.001	0.630	1.000	0.048	1.001	0.024	1.000

Appendix P.1: Mean values and Gelman-Rubin diagnostics (diag.) from the separate A) geochemical BMM, and B) δ^{13}-FA BMM, in the Ardai sub-catchment.

A) Nanja source groups

Bedrock incision		**Hillslope gully**		**Lowzone surface**		**Midzone maize**		**East Mid-rangeland**		**West Mid-rangeland**	
Mean	*Diag.*	*Mean*	*Diag.*	*Mean*	*Diag.*	*Mean*	*Diag.*	*Mean*	*Diag.*	*Mean*	*Diag.*
0.039	1.000	0.037	1.002	0.041	1.000	0.029	1.000	0.826	1.000	0.028	1.008

B) Musa source groups

Midslope Gully		**Midslope Surface**		**Upland Mixed Agriculture**		**Upland Forest**		**Upland Gully**	
Mean	*Diag.*	*Mean*	*Diag.*	*Mean*	*Diag.*	*Mean*	*Diag.*	*Mean*	*Diag.*
0.013	1.003	0.798	1.006	0.158	1.001	0.016	1.001	0.014	1.005

Appendix P.2: Mean values and Gelman-Rubin diagnostics (diag.) from the soil-to-sediment BMM in the A) Nanja sub-catchment, and B) Musa sub-catchment.

Q. Geochemical profiles of northern Makuyuni sediment cores

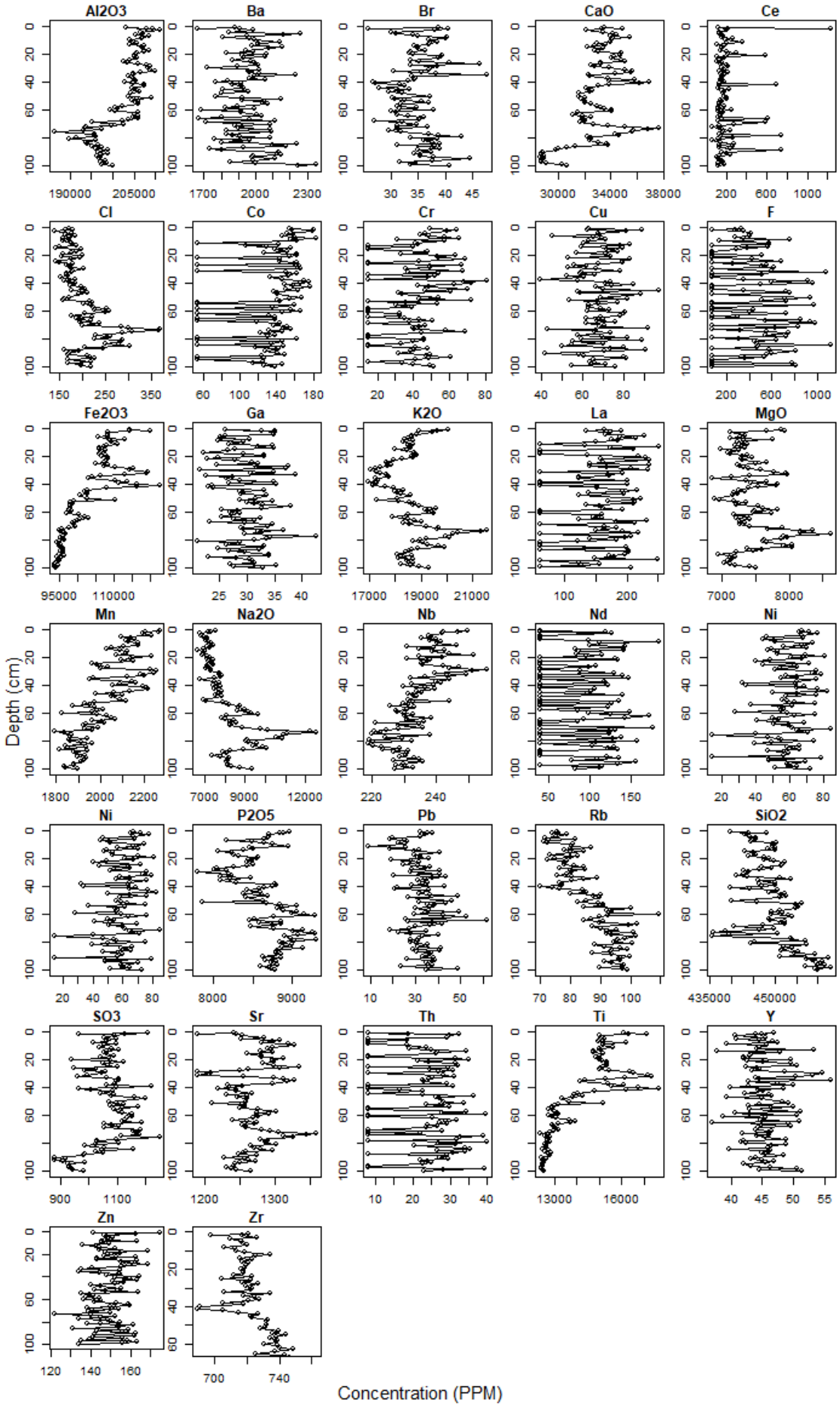

Appendix Q.1: Geochemical tracer profiles of the Naidosoito core.

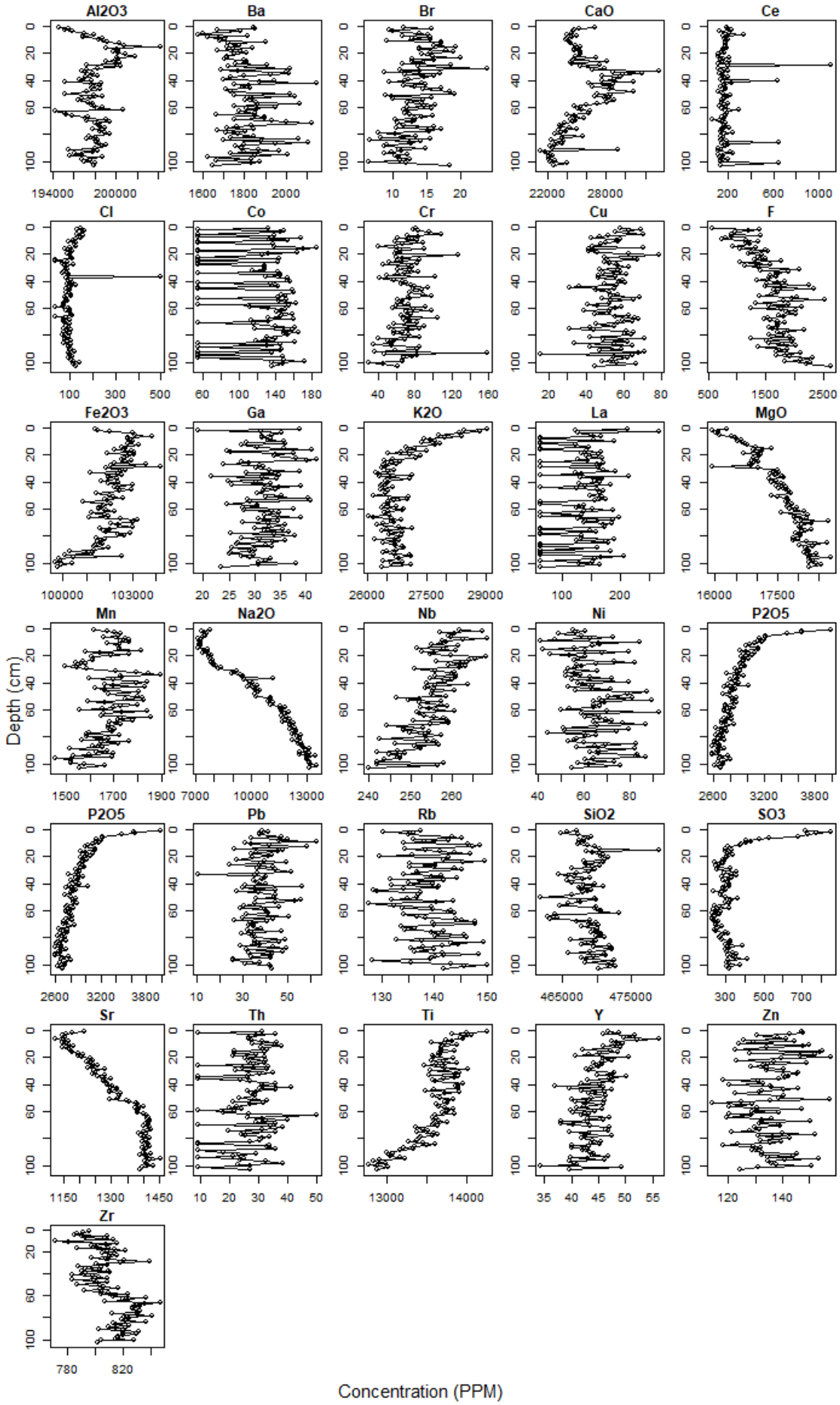

Appendix Q.2: Geochemical tracer profiles of the Nanja core

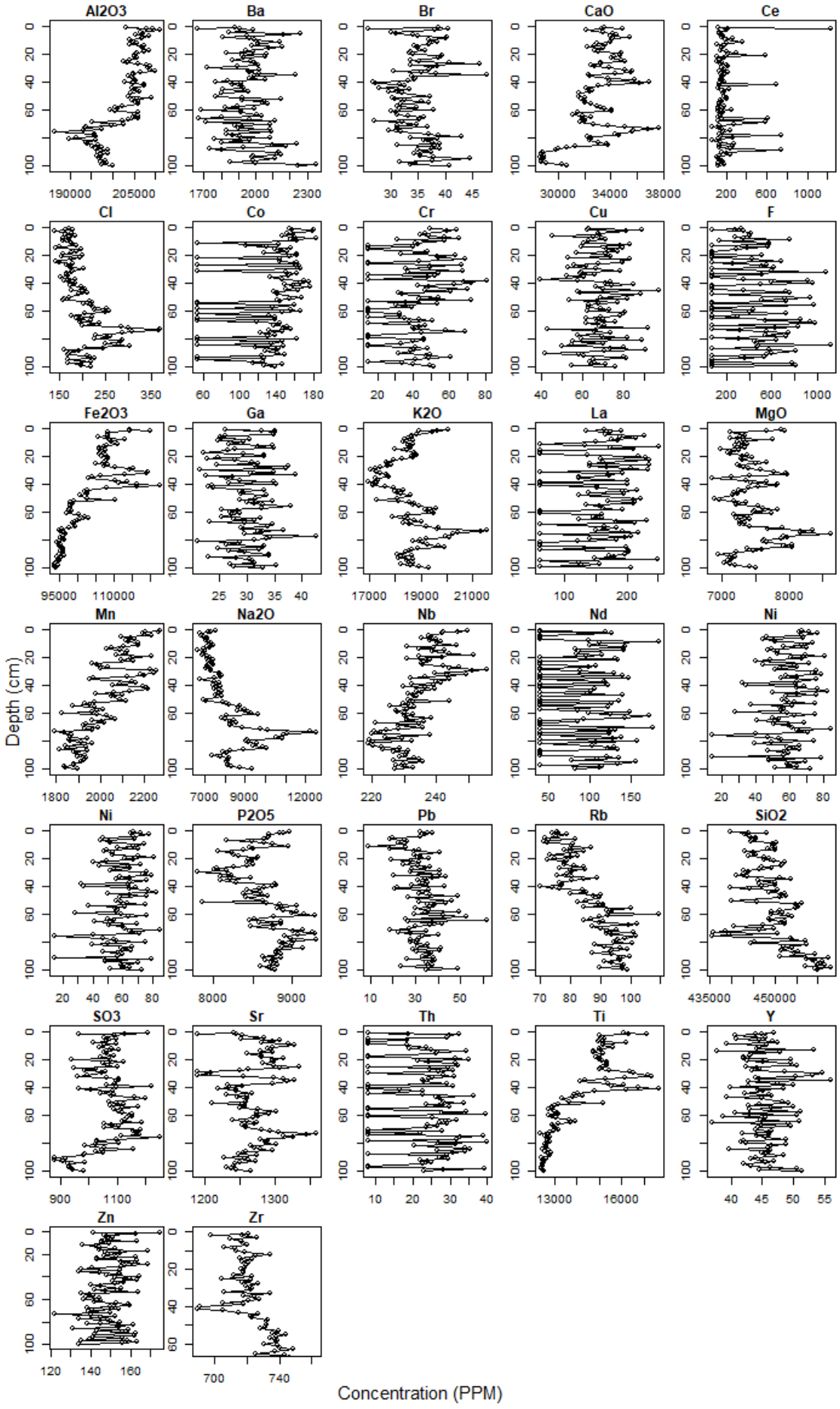

Appendix Q.3: Geochemical tracer profiles of the Musa core.

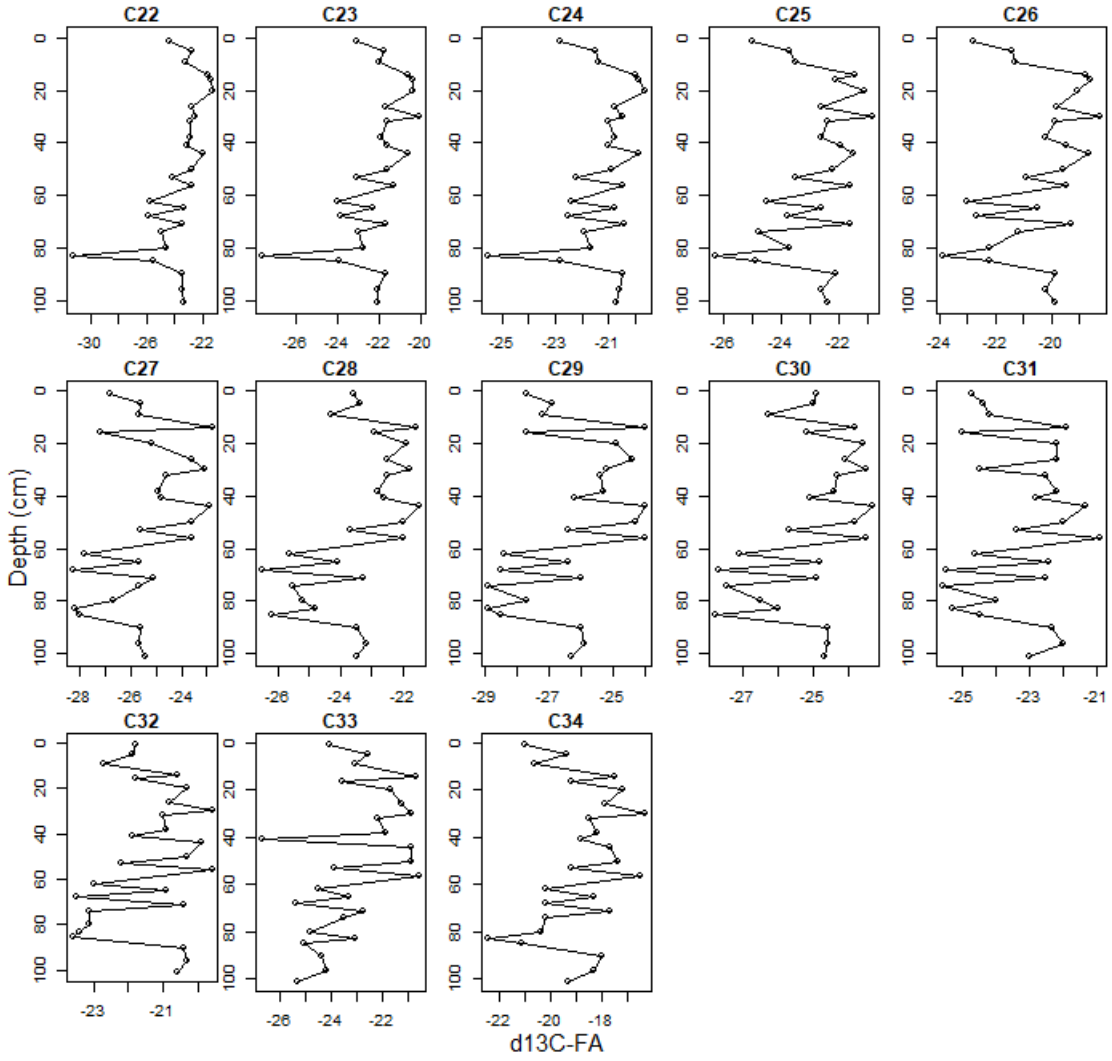

Appendix Q.4: δ^{13}C-FA profiles of the Nanja core.

R. Soil organic matter and aggregate stability

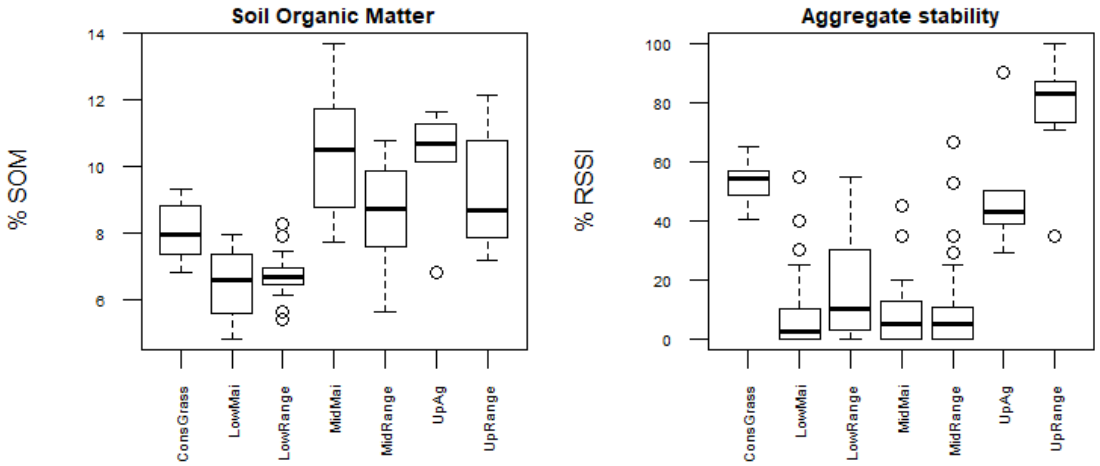

Appendix R.1: Boxplot of SOM content (% of total) and Aggregate stability (% aggregates remaining after 60 runs of 30 seconds on 30 mm/hr intensity rainfall) in different land use types / catchment zones combinations.

S. Photographic evidence of soil degradation and erosion

Appendix S.1: Exposed plant root evidence of >2cm topsoil removal on rangelands by sheet erosion (Lat: -3.333751°, Lon: 36.360225°), and evidence of surface crusting and rill erosion (Lat: -3.410499°, Lon: 36.407072°). Photos by William Blake.

Appendix S.2: Gully incision on deeply weathered hillslope soils (saprolites, Lat: -3.334067°, Lon: 36.360801°). The gully was >7m deep at some places and still did not hit the bedrock. Photo by Carey Marks.

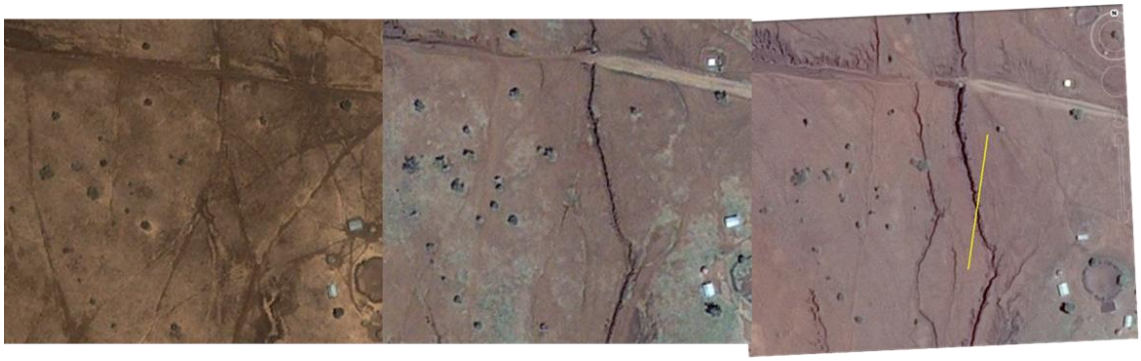

Appendix S.3: Repeated aerial photography showing recent rapid gully formation, deepening and hillslope progression (Lat: -3.334067°, Lon: 36.360801°). The yellow line corresponds with 100m (Source: Google Earth).

Appendix S.4: Interlinking of sheet erosion with lateral and upslope progression of gullies leading to badland formation. Exposed roots indicate over 50cm of soil removal (Lat: -3.316011°, Lon: 36.423080°). Photo by Maarten Wynants.

Appendix S.5: Degraded hillslope that has turned into badland (Lat: -3.339357°, Lon: 36.354331°). Photo by Carey Marks.

Appendix S.6: Hillslope terrace collapse after abandonment of agricultural soil conservation practices (Lat: -3.344074°, 36.521724°). Photo by Carey Marks.

Appendix S.7: Soil conservation practices with contour terraces that are buffered by permanent vegetation strips (Lat: -3.301534°, Lon: 36.519732°). Photo by Carey Marks.

References

Aalto, R. & Nittrouer, C. A. (2012) '210 Pb geochronology of flood events in large tropical river systems'. *Philosophical Transactions of the Royal Society A: Mathematical, Physical and Engineering Sciences*, 370 (1966), pp. 2040-2074.

Abrahams, A. D., Parsons, A. J. & Hirsch, P. J. (1992) 'Field and laboratory studies of resistance to interrill overland flow on semi-arid hillslopes, southern Arizona'. *Overland flow: Hydraulics and erosion mechanics*, pp. 1-23.

African Wildlife Foundation (2003) *Lake Manyara Watershed Assessment: progress report.* African Wildlife foundation 27 pp. Available.

Aksoy, H. & Kavvas, M. L. (2005) 'A review of hillslope and watershed scale erosion and sediment transport models'. *Catena*, 64 (2), pp. 247-271.

Alabaster, J. S. & Lloyd, R. S. (2013) *Water quality criteria for freshwater fish.* Elsevier.

Alewell, C., Birkholz, A., Meusburger, K., Schindler Wildhaber, Y. & Mabit, L. (2016) 'Quantitative sediment source attribution with compound-specific isotope analysis in a C3 plant-dominated catchment (central Switzerland)'. *Biogeosciences*, 13 (5), pp. 1587-1596.

Allison, F. E. (1973) *Soil organic matter and its role in crop production.* vol. 3. Elsevier.

Ambroise, B. (2004) 'Variable ‘active’versus ‘contributing’areas or periods: a necessary distinction'. *Hydrological processes*, 18 (6), pp. 1149-1155.

Ananda, J. & Herath, G. (2003) 'Soil erosion in developing countries: a socio-economic appraisal'. *Journal of environmental management*, 68 (4), pp. 343-353.

Anderson, D. (1984) 'Depression, dust bowl, demography, and drought: the colonial state and soil conservation in East Africa during the 1930s'. *African Affairs*, 83 (332), pp. 321-343.

Angima, S., Stott, D., O’neill, M., Ong, C. & Weesies, G. (2002) 'Use of calliandra–Napier grass contour hedges to control erosion in central Kenya'. *Agriculture, ecosystems & environment*, 91 (1-3), pp. 15-23.

Angima, S. D., Stott, D. E., O'Neill, M. K., Ong, C. K. & Weesies, G. A. (2003) 'Soil erosion prediction using RUSLE for central Kenyan highland conditions'. *Agriculture Ecosystems & Environment*, 97 (1-3), pp. 295-308.

Appleby, P. (2002) 'Chronostratigraphic techniques in recent sediments', *Tracking environmental change using lake sediments.* Springer, pp. 171-203.

Appleby, P., Semertzidou, P., Piliposian, G., Chiverrell, R., Schillereff, D. & Warburton, J. (2019) 'The transport and mass balance of fallout radionuclides in Brotherswater, Cumbria (UK)'. *Journal of Paleolimnology*, 62 (4), pp. 389-407.

Appleby, P. G. (2008) 'Three decades of dating recent sediments by fallout radionuclides: a review'. *The Holocene*, 18 (1), pp. 83-93.

Appleby, P. G. & Oldfield, F. (1978) 'The calculation of lead-210 dates assuming a constant rate of supply of unsupported 210Pb to the sediment'. *Catena*, 5 (1), pp. 1-8.

Arnaud, F., Magand, O., Chapron, E., Bertrand, S., Boës, X., Charlet, F. & Mélières, M. A. (2006) 'Radionuclide dating (210Pb, 137Cs, 241Am) of recent lake sediments in a highly active geodynamic setting (Lakes Puyehue and Icalma—Chilean Lake District)'. *Science of the total environment*, 366 (2), pp. 837-850.

Ashbridge, D. (1995) 'Processes of river bank erosion and their contribution to the suspended sediment load of the River Culm, Devon'. *Sediment and water quality in river catchments*, pp. 229-245.

Atwood, D. A. (1990) 'Land registration in Africa: The impact on agricultural production'. *World development*, 18 (5), pp. 659-671.

Auzet, A. V., Boiffin, J., Papy, F., Ludwig, B. & Maucorps, J. (1993) 'Rill erosion as a function of the characteristics of cultivated catchments in the north of France'. *Catena*, 20 (1-2), pp. 41-62.

Barber, R., Thomas, D. & Moore, T. (1981) 'Studies on soil erosion and runoff and proposed design procedures for terraces in the cultivated, semi-arid areas of Machakos District, Kenya', *Proceedings of Conservation 80, the International Conference on Soil Conservation*. National College of Agricultural Engineering, Silsoe, Beford, UK Chichester [England], Wiley.

Barbier, B. (1998) 'Induced innovation and land degradation: Results from a bioeconomic model of a village in West Africa'. *Agricultural Economics*, 19 (1), pp. 15-25.

Barron, J., Rockström, J., Gichuki, F. & Hatibu, N. (2003) 'Dry spell analysis and maize yields for two semi-arid locations in east Africa'. *Agricultural and forest meteorology*, 117 (1), pp. 23-37.

Barrow, C. J. (1991) *Land degradation: development and breakdown of terrestrial environments.* Cambridge University Press.

Baskaran, M., Nix, J., Kuyper, C. & Karunakara, N. (2014) 'Problems with the dating of sediment core using excess 210 Pb in a freshwater system impacted by large scale watershed changes'. *Journal of environmental radioactivity*, 138 pp. 355-363.

Bates, R. (1986) 'Some contemporary orthodoxies in the study of agrarian change', in Kohli, A. (ed.) *The State and Development in the Third World.* Princeton University Press, pp. 67-87.

Belmont, P., Willenbring, J. K., Schottler, S. P., Marquard, J., Kumarasamy, K. & Hemmis, J. M. (2014) 'Toward generalizable sediment fingerprinting with tracers that are conservative and nonconservative over sediment routing timescales'. *Journal of soils and sediments*, 14 (8), pp. 1479-1492.

Ben Slimane, A., Raclot, D., Evrard, O., Sanaa, M., Lefevre, I. & Le Bissonnais, Y. (2016) 'Relative contribution of rill/interrill and gully/channel erosion to small reservoir siltation in Mediterranean environments'. *Land Degradation & Development*, 27 (3), pp. 785-797.

Benedict, J. B. (1976) 'Frost creep and gelifluction features: a review'. *Quaternary Research*, 6 (1), pp. 55-76.

Berkes, F., Colding, J. & Folke, C. (2000) 'Rediscovery of traditional ecological knowledge as adaptive management'. *Ecological applications*, 10 (5), pp. 1251-1262.

Berkes, F., Folke, C. & Colding, J. (2000) *Linking social and ecological systems: management practices and social mechanisms for building resilience.* vol. 1. Cambridge University Press.

Bernard, B. & Lux, A. (2017) 'How to feed the world sustainably: an overview of the discourse on agroecology and sustainable intensification'. *Regional Environmental Change*, 17 (5), pp. 1279-1290.

Bhola, N., Ogutu, J. O., Piepho, H.-P., Said, M. Y., Reid, R. S., Hobbs, N. T. & Olff, H. (2012) 'Comparative changes in density and demography of large herbivores in the Masai Mara Reserve and its surrounding human-dominated

pastoral ranches in Kenya'. *Biodiversity and Conservation*, 21 (6), pp. 1509-1530.

Bilotta, G. & Brazier, R. (2008) 'Understanding the influence of suspended solids on water quality and aquatic biota'. *Water research*, 42 (12), pp. 2849-2861.

Bissonnais, Y. l. (1990) 'Experimental study and modelling of soil surface crusting processes'. *Catena, Supplement*, (17), pp. 13-28.

Bissonnais, Y. l. (1996) 'Aggregate stability and assessment of soil crustability and erodibility: I. Theory and methodology'. *European Journal of soil science*, 47 (4), pp. 425-437.

Blaikie, P. (2016) *The political economy of soil erosion in developing countries.* London: Routledge.

Blaikie, P. & Brookfield, H. (2015) *Land degradation and society.* London: Routledge.

Blake, W. H., Boeckx, P., Stock, B. C., Smith, H. G., Bodé, S., Upadhayay, H. R., Gaspar, L., Goddard, R., Lennard, A. T., Lizaga, I., Lobb, D. A., Owens, P. N., Petticrew, E. L., Kuzyk, Z. Z. A., Gari, B. D., Munishi, L., Mtei, K., Nebiyu, A., Mabit, L., Navas, A. & Semmens, B. X. (2018a) 'A deconvolutional Bayesian mixing model approach for river basin sediment source apportionment'. *Scientific Reports*, 8 (1), pp. 13073.

Blake, W. H., Ficken, K. J., Taylor, P., Russell, M. A. & Walling, D. E. (2012) 'Tracing crop-specific sediment sources in agricultural catchments'. *Geomorphology*, 139 pp. 322-329.

Blake, W. H., Rabinovich, A., Wynants, M., Kelly, C., Nasseri, M., Ngondya, I., Patrick, A., Mtei, K., Munishi, L., Boeckx, P., Navas, A., Smith, H., Gilvear, D., Wilson, G., Roberts, N. & Ndakidemi, P. (2018b) 'Soil erosion in East Africa: an interdisciplinary approach to realising pastoral land management change'. *Environmental Research Letters*,

Blessing, M., Jochmann, M. A. & Schmidt, T. C. (2008) 'Pitfalls in compound-specific isotope analysis of environmental samples'. *Analytical and bioanalytical chemistry*, 390 (2), pp. 591-603.

Bluwstein, J., Lund, J. F., Askew, K., Stein, H., Noe, C., Odgaard, R., Maganga, F. & Engström, L. (2018) 'Between dependence and deprivation: the interlocking nature of land alienation in Tanzania'. *Journal of agrarian change*, 18 (4), pp. 806-830.

Boardman, J., Poesen, J. & Evans, R. (2003) 'Socio-economic factors in soil erosion and conservation'. *Environmental Science & Policy*, 6 (1), pp. 1-6.

Bonython, C. W. & Mason, B. (1953) 'The filling and drying of Lake Eyre'. *The Geographical Journal*, 119 (3), pp. 321-330.

Borrelli, P., Robinson, D. A., Fleischer, L. R., Lugato, E., Ballabio, C., Alewell, C., Meusburger, K., Modugno, S., Schütt, B., Ferro, V., Bagarello, V., Oost, K. V., Montanarella, L. & Panagos, P. (2017) 'An assessment of the global impact of 21st century land use change on soil erosion'. *Nature Communications*, 8 (1), pp. 2013.

Borselli, L., Cassi, P. & Torri, D. (2008) 'Prolegomena to sediment and flow connectivity in the landscape: a GIS and field numerical assessment'. *Catena*, 75 (3), pp. 268-277.

Boserup, E. (2017) *The conditions of agricultural growth: The economics of agrarian change under population pressure.* New York: Routledge.

Botte, R. (1985a) 'Rwanda and Burundi, 1889-1930: chronology of a slow assassination, part 1'. *The International Journal of African Historical Studies*, 18 (1), pp. 53-91.

Botte, R. (1985b) 'Rwanda and Burundi, 1889-1930: chronology of a slow assassination, part 2'. *The International Journal of African Historical Studies*, 18 (2), pp. 289-314.

Bracken, L., Wainwright, J., Ali, G., Tetzlaff, D., Smith, M., Reaney, S. & Roy, A. (2013) 'Concepts of hydrological connectivity: research approaches, pathways and future agendas'. *Earth-Science Reviews*, 119 pp. 17-34.

Bracken, L. J. & Croke, J. (2007) 'The concept of hydrological connectivity and its contribution to understanding runoff‐dominated geomorphic systems'. *Hydrological processes*, 21 (13), pp. 1749-1763.

Bruce, J. W. (1988) 'A perspective on indigenous land tenure systems and land concentration'. *Land and society in contemporary Africa*, pp. 23-52.

Brundtland, G. (1987) 'Our common future: Report of the 1987 World Commission on Environment and Development'. *United Nations, Oslo*, 1 pp. 59.

Bryan, R. & Yair, A. (1982) 'Perspectives of studies of badland geomorphology'. *Badland Geomorphology and Piping. Geobooks, Norwich, CT*, pp. 1-12.

Bryceson, D. F. (2002) 'The scramble in Africa: reorienting rural livelihoods'. *World development*, 30 (5), pp. 725-739.

Bull, L. J. (2002) *Dryland rivers: hydrology and geomorphology of semi-arid channels.* John Wiley & Sons.

Cadwalader, G. O., Renshaw, C. E., Jackson, B. P., Magilligan, F. J., Landis, J. D. & Bostick, B. C. (2011) 'Erosion and physical transport via overland flow of arsenic and lead bound to silt-sized particles'. *Geomorphology*, 128 (1), pp. 85-91.

Cambray, R., Playford, K., Lewis, G. & Carpenter, R. (1989) 'Radioactive fallout in air and rain: results to the end of 1988. AERE-R 13575'. *Atomic Energy Authority, London, UK*,

Campbell, B. M., Gordon, I. J., Luckert, M. K., Petheram, L. & Vetter, S. (2006) 'In search of optimal stocking regimes in semi-arid grazing lands: one size does not fit all'. *Ecological Economics*, 60 (1), pp. 75-85.

Casenave, A. & Valentin, C. (1992) 'A runoff capability classification system based on surface features criteria in semi-arid areas of West Africa'. *Journal of Hydrology*, 130 (1-4), pp. 231-249.

Castillo, C. & Gómez, J. (2016) 'A century of gully erosion research: Urgency, complexity and study approaches'. *Earth-Science Reviews*, 160 pp. 300-319.

Cerdà, A. & Garcıa-Fayos, P. (2002) 'The influence of seed size and shape on their removal by water erosion'. *Catena*, 48 (4), pp. 293-301.

Chabal, P. (2013) *Africa: the politics of suffering and smiling.* London: Zed Books Ltd.

Chazdon, R. L. (2008) 'Beyond deforestation: restoring forests and ecosystem services on degraded lands'. *science*, 320 (5882), pp. 1458-1460.

Chepil, W. (1946) 'Dynamics of wind erosion: Vi. Sorting of soil material by the wind'. *Soil Science*, 61 (4), pp. 331.

Christensen, B. T., Olesen, J. E., Hansen, E. M. & Thomsen, I. K. (2011) 'Annual variation in δ13C values of maize and wheat: Effect on estimates of

decadal scale soil carbon turnover'. *Soil Biology and Biochemistry*, 43 (9), pp. 1961-1967.

Christie, I., Christie, I. T., Fernandes, E., Messerli, H. & Twining-Ward, L. (2014) *Tourism in Africa: Harnessing tourism for growth and improved livelihoods.* World Bank Publications.

Cihlar, J. (2000) 'Land cover mapping of large areas from satellites: status and research priorities'. *International Journal of Remote Sensing*, 21 (6-7), pp. 1093-1114.

Claessens, L., Van Breugel, P., Notenbaert, A., Herrero, M. & Van De Steeg, J. (2008) 'Mapping potential soil erosion in East Africa using the Universal Soil Loss Equation and secondary data'. *IAHS publication*, 325 pp. 398.

Clark, E. (1987) 'Soil erosion: off-site environmental effects'.

Cliffe, L. R. (1970) 'Nationalism and the reaction to enforced agricultural change in Tanzania during the Colonial period'. *Taamuli*, 1 (1), pp. 3-15.

Cobo, J. G., Dercon, G. & Cadisch, G. (2010) 'Nutrient balances in African land use systems across different spatial scales: a review of approaches, challenges and progress'. *Agriculture, ecosystems & environment*, 136 (1-2), pp. 1-15.

Cochet, H. (2003) 'A half century of Agrarian crisis in Burundi (1890-1945): The incapacity of the colonial administration in managing the Agrarian crisis of the late eighteen-hundreds'. *African economic history*, (31), pp. 19-42.

Codd, G. A. (2000) 'Cyanobacterial toxins, the perception of water quality, and the prioritisation of eutrophication control'. *Ecological engineering*, 16 (1), pp. 51-60.

Cohen, J. M. (1980) *Land tenure and rural development in Africa.* Holt Saunders Ltd.

Congalton, R. G., Gu, J., Yadav, K., Thenkabail, P. & Ozdogan, M. (2014) 'Global land cover mapping: a review and uncertainty analysis'. *Remote Sensing*, 6 (12), pp. 12070-12093.

Conte, C. A. (1999) 'The forest becomes desert: Forest use and environmental change in Tanzania's West Usambara mountains'. *Land Degradation & Development*, 10 (4), pp. 291-309.

Correa, S. W., Mello, C. R., Chou, S. C., Curi, N. & Norton, L. D. (2016) 'Soil erosion risk associated with climate change at Mantaro River basin, Peruvian Andes'. *Catena*, 147 pp. 110-124.

Costanza, R., d'Arge, R., De Groot, R., Farber, S., Grasso, M., Hannon, B., Limburg, K., Naeem, S., O'neill, R. V. & Paruelo, J. (1997) 'The value of the world's ecosystem services and natural capital'. *Nature*, 387 (6630), pp. 253.

Coulson, A. (1981) 'Agricultural policies in mainland Tanzania, 1946–76', *Rural development in tropical Africa.* Springer, pp. 52-89.

Croke, J., Fryirs, K. & Thompson, C. (2013) 'Channel–floodplain connectivity during an extreme flood event: implications for sediment erosion, deposition, and delivery'. *Earth surface processes and landforms*, 38 (12), pp. 1444-1456.

Croke, J. & Mockler, S. (2001) 'Gully initiation and road‐to‐stream linkage in a forested catchment, southeastern Australia'. *Earth surface processes and landforms*, 26 (2), pp. 205-217.

D'Haen, K., Verstraeten, G. & Degryse, P. (2012) 'Fingerprinting historical fluvial sediment fluxes'. *Progress in Physical Geography*, 36 (2), pp. 154-186.

Dabney, S., Yoder, D. & Vieira, D. (2012) 'The application of the Revised Universal Soil Loss Equation, Version 2, to evaluate the impacts of alternative climate change scenarios on runoff and sediment yield'. *Journal of soil and water conservation*, 67 (5), pp. 343-353.

Dagnew, D. C., Guzman, C. D., Zegeye, A. D., Tibebu, T. Y., Getaneh, M., Abate, S., Zemale, F. A., Ayana, E. K., Tilahun, S. A. & Steenhuis, T. S. (2015) 'Impact of conservation practices on runoff and soil loss in the sub-humid Ethiopian Highlands: The Debre Mawi watershed'. *Journal of Hydrology and Hydromechanics*, 63 (3), pp. 210-219.

Darkoh, M. K. (1989) 'Desertification in Africa'. *Journal of Eastern African Research & Development*, pp. 1-50.

Davies, S. J., Lamb, H. F. & Roberts, S. J. (2015) 'Micro-XRF core scanning in palaeolimnology: recent developments', *Micro-XRF studies of sediment cores.* Springer, pp. 189-226.

De Vente, J., Poesen, J., Verstraeten, G., Govers, G., Vanmaercke, M., Van Rompaey, A., Arabkhedri, M. & Boix-Fayos, C. (2013) 'Predicting soil erosion and sediment yield at regional scales: Where do we stand?'. *Earth-Science Reviews*, 127 pp. 16-29.

Desmet, P. & Govers, G. (1996) 'A GIS procedure for automatically calculating the USLE LS factor on topographically complex landscape units'. *Journal of soil and water conservation*, 51 (5), pp. 427-433.

Desta, S. & Coppock, D. L. (2004) 'Pastoralism under pressure: tracking system change in southern Ethiopia'. *Human Ecology*, 32 (4), pp. 465-486.

Deus, D., Gloaguen, R. & Krause, P. (2013) 'Water balance modeling in a semi-arid environment with limited in situ data using remote sensing in Lake Manyara, East African Rift, Tanzania'. *Remote Sensing*, 5 (4), pp. 1651-1680.

Devarajan, S. & Kasekende, L. A. (2011) 'Africa and the global economic crisis: Impacts, policy responses and political economy'. *African Development Review*, 23 (4), pp. 421-438.

Dewitte, O., Daoudi, M., Bosco, C. & Van Den Eeckhaut, M. (2015) 'Predicting the susceptibility to gully initiation in data-poor regions'. *Geomorphology*, 228 pp. 101-115.

Donkor, N., Gedir, J., Hudson, R., Bork, E., Chanasyk, D. & Naeth, M. (2002) 'Impacts of grazing systems on soil compaction and pasture production in Alberta'. *Canadian Journal of soil science*, 82 (1), pp. 1-8.

Droppo, I. & Ongley, E. (1989) 'Flocculation of suspended solids in southern Ontario rivers'. *Sediment and the Environment (Proceeding of the Baltimore Symposium, May 1989)*, 184 pp. 95-103.

Du, P. & Walling, D. (2012) 'Using 210 Pb measurements to estimate sedimentation rates on river floodplains'. *Journal of environmental radioactivity*, 103 (1), pp. 59-75.

Du, P. & Walling, D. E. (2017) 'Fingerprinting surficial sediment sources: Exploring some potential problems associated with the spatial variability of source material properties'. *Journal of environmental management*, 194 pp. 4-15.

Du Toit, G. v. N., Snyman, H. & Malan, P. (2009) 'Physical impact of grazing by sheep on soil parameters in the Nama Karoo subshrub/grass rangeland of South Africa'. *Journal of Arid Environments*, 73 (9), pp. 804-810.

Dunne, T., Zhang, W. & Aubry, B. F. (1991) 'Effects of rainfall, vegetation, and microtopography on infiltration and runoff'. *Water Resources Research*, 27 (9), pp. 2271-2285.

Ellis, J. E. & Swift, D. M. (1988) 'Stability of African pastoral ecosystems: alternate paradigms and implications for development'. *Rangeland Ecology & Management/Journal of Range Management Archives*, 41 (6), pp. 450-459.

Ellman, A. (1975) 'Development of Ujamaa Policy in Tanzania in Rural Cooperation in Tanzania (edited by Cliffe and Lawrence)'.[in Tanzania Publishing House. Dar es Salaam. (Accessed:Ellman, A.

Enfors, E. & Gordon, L. (2007) 'Analysing resilience in dryland agro-ecosystems: A case study of the Makanya catchment in Tanzania over the past 50 years'. *Land Degradation & Development*, 18 (6), pp. 680-696.

Erskine, W. D. & Warner, R. F. (1999) 'Significance of river bank erosion as a sediment source in the alternating flood regimes of south-eastern Australia'. *Fluvial processes and environmental change*, pp. 139-163.

Evans, R. (1980) 'Mechanics of water erosion and their spatial and temporal controls: an empirical viewpoint'. *Soil erosion*, pp. 109-128.

Evans, R. O., Cassel, D. & Sneed, R. (1991) 'Soil, water, and crop characteristics important to irrigation scheduling'. *AG-North Carolina Agricultural Extension Service, North Carolina State University*,

FAO (2019) 'FAOSTAT statistical database', Food and Agriculture Organization of the United Nations.

Farr, T. G., Rosen, P. A., Caro, E., Crippen, R., Duren, R., Hensley, S., Kobrick, M., Paller, M., Rodriguez, E. & Roth, L. (2007) 'The shuttle radar topography mission'. *Reviews of geophysics*, 45 (2),

Farres, P. (1987) 'The dynamics of rainsplash erosion and the role of soil aggregate stability'. *Catena*, 14 (1-3), pp. 119-130.

Feakins, S. J., Bentley, L. P., Salinas, N., Shenkin, A., Blonder, B., Goldsmith, G. R., Ponton, C., Arvin, L. J., Wu, M. S. & Peters, T. (2016) 'Plant leaf wax biomarkers capture gradients in hydrogen isotopes of precipitation from the Andes and Amazon'. *Geochimica et Cosmochimica Acta*, 182 pp. 155-172.

Feeny, D., Berkes, F., McCay, B. J. & Acheson, J. M. (1990) 'The tragedy of the commons: twenty-two years later'. *Human Ecology*, 18 (1), pp. 1-19.

Fernandez-Gimenez, M. E. & Allen-Diaz, B. (1999) 'Testing a non‐equilibrium model of rangeland vegetation dynamics in Mongolia'. *Journal of Applied Ecology*, 36 (6), pp. 871-885.

Fiedler, F. R., Frasier, G. W., Ramirez, J. A. & Ahuja, L. R. (2002) 'Hydrologic response of grasslands: Effects of grazing, interactive infiltration, and scale'. *Journal of Hydrologic Engineering*, 7 (4), pp. 293-301.

Fitzjohn, C., Ternan, J. & Williams, A. (1998) 'Soil moisture variability in a semi-arid gully catchment: implications for runoff and erosion control'. *Catena*, 32 (1), pp. 55-70.

Fleitmann, D., Dunbar, R. B., McCulloch, M., Mudelsee, M., Vuille, M., McClanahan, T. R., Cole, J. E. & Eggins, S. (2007) 'East African soil erosion recorded in a 300 year old coral colony from Kenya'. *Geophysical Research Letters*, 34 (4),

Foley, J. A., DeFries, R., Asner, G. P., Barford, C., Bonan, G., Carpenter, S. R., Chapin, F. S., Coe, M. T., Daily, G. C. & Gibbs, H. K. (2005) 'Global consequences of land use'. *Science*, 309 (5734), pp. 570-574.

Foody, G. M. (2002) 'Status of land cover classification accuracy assessment'. *Remote Sensing of Environment*, 80 (1), pp. 185-201.

Foster, I. D. (1995) 'Lake and reservoir bottom sediments as a source of soil erosion and sediment transport data in the UK'. *Sediment and water quality in river catchments*, pp. 265-283.

Foster, I. D. (2010) 'Lakes and reservoirs in the sediment cascade'. *Sediment cascades: an integrated approach. Wiley, Chichester*, pp. 345-376.

Foster, I. D., Boardman, J. & Keay-Bright, J. (2007) 'Sediment tracing and environmental history for two small catchments, Karoo Uplands, South Africa'. *Geomorphology*, 90 (1), pp. 126-143.

Foster, I. D. L., Dearing, J. A. & Appleby, P. G. (1986) 'Historical Trends in Catchment Sediment Yields - a Case-Study in Reconstruction from Lake-Sediment Records in Warwickshire, Uk'. *Hydrological Sciences Journal-Journal Des Sciences Hydrologiques*, 31 (3), pp. 427-443.

Fox, D. M. & Bryan, R. B. (2000) 'The relationship of soil loss by interrill erosion to slope gradient'. *Catena*, 38 (3), pp. 211-222.

Franklin, S. E., Ahmed, O. S., Wulder, M. A., White, J. C., Hermosilla, T. & Coops, N. C. (2015) 'Large area mapping of annual land cover dynamics using multitemporal change detection and classification of Landsat time series data'. *Canadian Journal of Remote Sensing*, 41 (4), pp. 293-314.

Fratkin, E. (1986) 'Stability and resilience in East African pastoralism: the Rendille and the Ariaal of northern Kenya'. *Human Ecology*, 14 (3), pp. 269-286.

Fratkin, E. & Roth, E. A. (2006) *As pastoralists settle: social, health, and economic consequences of the pastoral sedentarization in Marsabit District, Kenya.* vol. 1. New York and London: Kluwer Academic Publishers.

Fryirs, K. (2013) '(Dis) Connectivity in catchment sediment cascades: a fresh look at the sediment delivery problem'. *Earth surface processes and landforms*, 38 (1), pp. 30-46.

Fynn, R. & O'connor, T. (2000) 'Effect of stocking rate and rainfall on rangeland dynamics and cattle performance in a semi‐arid savanna, South Africa'. *Journal of Applied Ecology*, 37 (3), pp. 491-507.

Gabet, E. J. & Dunne, T. (2003) 'Sediment detachment by rain power'. *Water Resources Research*, 39 (1),

Gale, S. & Haworth, R. (2005) 'Catchment-wide soil loss from pre-agricultural times to the present: transport-and supply-limitation of erosion'. *Geomorphology*, 68 (3), pp. 314-333.

Gelagay, H. S. & Minale, A. S. (2016) 'Soil loss estimation using GIS and Remote sensing techniques: A case of Koga watershed, Northwestern Ethiopia'. *International Soil and Water Conservation Research*, 4 (2), pp. 126-136.

Gellis, A. C. & Noe, G. B. (2013) 'Sediment source analysis in the Linganore Creek watershed, Maryland, USA, using the sediment fingerprinting approach: 2008 to 2010'. *Journal of soils and sediments*, 13 (10), pp. 1735-1753.

Gelman, A., Carlin, J. B., Stern, H. S., Dunson, D. B., Vehtari, A. & Rubin, D. B. (2013) *Bayesian data analysis.* Chapman and Hall/CRC.

Gerden, C., Khawange, G., Mallya, J., Mbuya, J. & Sanga, R. (1992) *The Wild Lake: The 1990 floods in Babati, Tanzania—rehabilitation and prevention.* RCU Report. Available.

Gibbs, M. (2008) 'Identifying source soils in contemporary estuarine sediments: a new compound-specific isotope method'. *Estuaries and Coasts*, 31 (2), pp. 344-359.

Gilvear, D., Winterbottom, S. & Sichingabula, H. (2000) 'Character of channel planform change and meander development: Luangwa River, Zambia'. *Earth Surface Processes and Landforms: The Journal of the British Geomorphological Research Group*, 25 (4), pp. 421-436.

Giri, C., Pengra, B., Long, J. & Loveland, T. R. (2013) 'Next generation of global land cover characterization, mapping, and monitoring'. *International Journal of Applied Earth Observation and Geoinformation*, 25 pp. 30-37.

Glazier, J. (1985) *Land and the Uses of Tradition among the Mbeere of Kenya.* Lanham, USA: University Press of America.

Goldberg, E. (1963) 'Geochronology with 210Pb Radioactive dating'. *International Atomic Energy Agency, Vienna*, 121 pp. 130.

Gómez, C., White, J. C. & Wulder, M. A. (2016) 'Optical remotely sensed time series data for land cover classification: A review'. *ISPRS Journal of Photogrammetry and Remote Sensing*, 116 pp. 55-72.

Goudie, A. (1989) 'Wind erosion in deserts'. *Proceedings of the Geologists' Association*, 100 (1), pp. 83-92.

Govers, G. (1992) 'Relationship between discharge, velocity and flow area for rills eroding loose, non-layered materials'. *Earth surface processes and landforms*, 17 (5), pp. 515-528.

Govers, G. & Poesen, J. (1988) 'Assessment of the interrill and rill contributions to total soil loss from an upland field plot'. *Geomorphology*, 1 (4), pp. 343-354.

Govers, G. & Rauws, G. (1986) 'Transporting capacity of overland flow on plane and on irregular beds'. *Earth surface processes and landforms*, 11 (5), pp. 515-524.

Greenland, D. J. & Lal, R. (1978) 'Soil conservation and management in the humid tropics'. *Soil Science*, 126 (1), pp. 61.

Greenway, D. (1987) 'Vegetation and slope stability'. *Slope stability: geotechnical engineering and geomorphology/edited by MG Anderson and KS Richards*,

Griffiths, P., van der Linden, S., Kuemmerle, T. & Hostert, P. (2013) 'A pixel-based Landsat compositing algorithm for large area land cover mapping'. *IEEE Journal of Selected Topics in Applied Earth Observations and Remote Sensing*, 6 (5), pp. 2088-2101.

Griggs, D., Stafford-Smith, M., Gaffney, O., Rockström, J., Öhman, M. C., Shyamsundar, P., Steffen, W., Glaser, G., Kanie, N. & Noble, I. (2013) 'Policy: Sustainable development goals for people and planet'. *Nature*, 495 (7441), pp. 305.

Grove, J., Croke, J. & Thompson, C. (2013) 'Quantifying different riverbank erosion processes during an extreme flood event'. *Earth surface processes and landforms*, 38 (12), pp. 1393-1406.

Gual, M. A. & Norgaard, R. B. (2010) 'Bridging ecological and social systems coevolution: A review and proposal'. *Ecological Economics*, 69 (4), pp. 707-717.

Guzha, A., Rufino, M., Okoth, S., Jacobs, S. & Nóbrega, R. (2018) 'Impacts of land use and land cover change on surface runoff, discharge and low flows: Evidence from East Africa'. *Journal of Hydrology: Regional Studies*, 15 pp. 49-67.

Guzmán, G., Quinton, J. N., Nearing, M. A., Mabit, L. & Gómez, J. A. (2013) 'Sediment tracers in water erosion studies: current approaches and challenges'. *Journal of soils and sediments*, 13 (4), pp. 816-833.

Gyssels, G., Poesen, J., Bochet, E. & Li, Y. (2005) 'Impact of plant roots on the resistance of soils to erosion by water: a review'. *Progress in Physical Geography*, 29 (2), pp. 189-217.

Haddadchi, A., Hicks, M., Olley, J. M., Singh, S. & Srinivasan, M. S. (2019) 'Grid-based sediment tracing approach to determine sediment sources'. *Land Degradation & Development*, pp. 1-19.

Haddadchi, A., Ryder, D. S., Evrard, O. & Olley, J. (2013) 'Sediment fingerprinting in fluvial systems: review of tracers, sediment sources and mixing models'. *International Journal of Sediment Research*, 28 (4), pp. 560-578.

Hamel, P., Falinski, K., Sharp, R., Auerbach, D. A., Sánchez-Canales, M. & Dennedy-Frank, P. J. (2017) 'Sediment delivery modeling in practice: Comparing the effects of watershed characteristics and data resolution across hydroclimatic regions'. *Science of the total environment*, 580 pp. 1381-1388.

Hamza, M. & Anderson, W. (2005) 'Soil compaction in cropping systems: a review of the nature, causes and possible solutions'. *Soil and Tillage Research*, 82 (2), pp. 121-145.

Hansen, M. C. & Loveland, T. R. (2012) 'A review of large area monitoring of land cover change using Landsat data'. *Remote Sensing of Environment*, 122 pp. 66-74.

Hardin, G. (1968) 'The Tragedy of the Commons'. *Science*, 162 (3859), pp. 1243-1248.

Harrod, T. (1994) 'Runoff, soil erosion and pesticide pollution in Cornwall'.

Harvey, A. (1996) 'Holocene hillslope gully systems in the Howgill Fells, Cumbria'. *Advances in hillslope processes*, 2 pp. 731-752.

Harvey, A. M. (2012) 'The coupling status of alluvial fans and debris cones: a review and synthesis'. *Earth surface processes and landforms*, 37 (1), pp. 64-76.

Haugerud, A. (1989) 'Land tenure and agrarian change in Kenya'. *Africa*, 59 (1), pp. 61-90.

Hautier, Y., Niklaus, P. A. & Hector, A. (2009) 'Competition for light causes plant biodiversity loss after eutrophication'. *Science*, 324 (5927), pp. 636-638.

He, Q. & Walling, D. (1997) 'The distribution of fallout 137Cs and 210Pb in undisturbed and cultivated soils'. *Applied radiation and isotopes*, 48 (5), pp. 677-690.

Heckmann, T. & Schwanghart, W. (2013) 'Geomorphic coupling and sediment connectivity in an alpine catchment—Exploring sediment cascades using graph theory'. *Geomorphology*, 182 pp. 89-103.

Heckmann, T. & Vericat, D. (2018) 'Computing spatially distributed sediment delivery ratios: inferring functional sediment connectivity from repeat high-resolution digital elevation models'. *Earth surface processes and landforms*, 43 (7), pp. 1547-1554.

Heede, B. H. (1975) 'Stages of development of gullies in the west'. *Present and prospective technology for predicting sediment yields and sources*, pp. 155-161.

Hein, L. (2006) 'The impacts of grazing and rainfall variability on the dynamics of a Sahelian rangeland'. *Journal of Arid Environments*, 64 (3), pp. 488-504.

Heritage, G., Large, A., Moon, B. & Jewitt, G. (2004) 'Channel hydraulics and geomorphic effects of an extreme flood event on the Sabie River, South Africa'. *Catena*, 58 (2), pp. 151-181.

Heywood, V. H. & Watson, R. T. (1995) *Global biodiversity assessment.* vol. 1140. Cambridge University Press Cambridge.

Hiemstra-van der Horst, G. & Hovorka, A. J. (2009) 'Fuelwood: The “other” renewable energy source for Africa?'. *Biomass and bioenergy*, 33 (11), pp. 1605-1616.

Hiernaux, P., Bielders, C. L., Valentin, C., Bationo, A. & Fernández-Rivera, S. (1999) 'Effects of livestock grazing on physical and chemical properties of sandy soils in Sahelian rangelands'. *Journal of Arid Environments*, 41 (3), pp. 231-245.

Hodgson, D. L. (2011) *Being Maasai, becoming indigenous: Postcolonial politics in a neoliberal world.* Indiana University Press.

Hoffmann, T. (2015) 'Sediment residence time and connectivity in non-equilibrium and transient geomorphic systems'. *Earth-Science Reviews*, 150 pp. 609-627.

Hofstad, O. (1997) 'Woodland deforestation by charcoal supply to Dar es Salaam'. *Journal of Environmental Economics and Management*, 33 (1), pp. 17-32.

Homer-Dixon, T. F. (1991) 'On the threshold: environmental changes as causes of acute conflict'. *International security*, 16 (2), pp. 76-116.

Homer-Dixon, T. F. (1994) 'Environmental scarcities and violent conflict: evidence from cases'. *International security*, 19 (1), pp. 5-40.

Homewood, K. (1995) 'Development, demarcation and ecological outcomes in Maasailand'. *Africa*, 65 (3), pp. 331-350.

Homewood, K., Coast, E. & Thompson, M. (2004) 'In-migrants and exclusion in East African rangelands: access, tenure and conflict'. *Africa*, 74 (4), pp. 567-610.

Hooke, J. (2003) 'Coarse sediment connectivity in river channel systems: a conceptual framework and methodology'. *Geomorphology*, 56 (1), pp. 79-94.

Hooke, J. M. (1979) 'An analysis of the processes of river bank erosion'. *Journal of Hydrology*, 42 (1-2), pp. 39-62.

Horton, R. E. (1941) 'An approach toward a physical interpretation of infiltration-capacity'. *Soil Science Society of America Journal*, 5 (C), pp. 399-417.

Hovius, N., Meunier, P., Lin, C.-W., Chen, H., Chen, Y.-G., Dadson, S., Horng, M.-J. & Lines, M. (2011) 'Prolonged seismically induced erosion and the mass balance of a large earthquake'. *Earth and Planetary Science Letters*, 304 (3), pp. 347-355.

Hudson, N. (1981) 'Soil Conservation. London: Batsford'. *RCP Morgan (1995). Soil Erosion and Conservation. Second Edition. Longman Group Limited*,

Hudson, N. & Jackson, D. (1959) 'Results achieved in the measurement of erosion and runoff in Southern Rhodesia', *Inter-African Soils Conference. Dalaba, Central African Republic*.

Hydén, G. (1980) *Beyond Ujamaa in Tanzania: underdevelopment and an uncaptured peasantry.* Univ of California Press.

Ijjasz-Vasquez, E. J. & Bras, R. L. (1995) 'Scaling regimes of local slope versus contributing area in digital elevation models'. *Geomorphology*, 12 (4), pp. 299-311.

Iliffe, J. (1979) *A modern history of Tanganyika.* Cambridge University Press.

Illius, A. W. & O'Connor, T. G. (1999) 'On the relevance of nonequilibrium concepts to arid and semiarid grazing systems'. *Ecological applications*, 9 (3), pp. 798-813.

Istomina, M., Kocharyan, A. & Lebedeva, I. (2005) 'Floods: genesis, socioeconomic and environmental impacts'. *Water resources*, 32 (4), pp. 349-358.

Iverson, R. M. (1997) 'The physics of debris flows'. *Reviews of geophysics*, 35 (3), pp. 245-296.

Jacobs, S. R., Timbe, E., Weeser, B., Rufino, M. C., Butterbach-Bahl, K. & Breuer, L. (2018) 'Assessment of hydrological pathways in East African

montane catchments under different land use'. *Hydrology and Earth System Sciences*, 22 pp. 4981-5000.

Jayne, T. S., Chapoto, A., Sitko, N., Nkonde, C., Muyanga, M. & Chamberlin, J. (2014) 'Is the scramble for land in Africa foreclosing a smallholder agricultural expansion strategy?'. *Journal of International Affairs*, 67 (2), pp. 35.

Jia, G. & Torri, G. (2007) 'Determination of 210Pb and 210Po in soil or rock samples containing refractory matrices'. *Applied radiation and isotopes*, 65 (1), pp. 1-8.

Jones, W. O. (1980) 'Agricultural trade within tropical Africa: historical background', in Bates, R.H. and Lofchie, M.F. (eds.) *Agricultural development in Africa: issues of public policy.* pp. 10-45.

Kaaya, L. T. (2015) 'Towards a classification of Tanzanian rivers: a bioassessment and ecological management tool. A case study of the Pangani, Rufiji and Wami–Ruvu river basins'. *African Journal of Aquatic Science*, 40 (1), pp. 37-45.

Kahyarara, G. & Mchallo, I. (2008) 'The strategic environmental assessment (SEA) of tourism development in the northern tourist circuit of Tanzania. International Association for Impact Assessment, Centre for Environmental Economics and Development Research. Retrieved March 2, 2009'.[in. (Accessed:Kahyarara, G. & Mchallo, I.

Karger, D. N., Conrad, O., Böhner, J., Kawohl, T., Kreft, H., Soria-Auza, R. W., Zimmermann, N. E., Linder, H. P. & Kessler, M. (2017) 'Climatologies at high resolution for the earth's land surface areas'. *Scientific Data*, 4 pp. sdata2017122.

Kelly, C., Ferrara, A., Wilson, G. A., Ripullone, F., Nolè, A., Harmer, N. & Salvati, L. (2015) 'Community resilience and land degradation in forest and shrubland socio-ecological systems: Evidence from Gorgoglione, Basilicata, Italy'. *Land use policy*, 46 pp. 11-20.

Kennedy, R. E., Yang, Z. & Cohen, W. B. (2010) 'Detecting trends in forest disturbance and recovery using yearly Landsat time series: 1. LandTrendr—Temporal segmentation algorithms'. *Remote Sensing of Environment*, 114 (12), pp. 2897-2910.

Kiage, L. M. (2013) 'Perspectives on the assumed causes of land degradation in the rangelands of Sub-Saharan Africa'. *Progress in Physical Geography*, 37 (5), pp. 664-684.

Kikula, I. S. (1997) *Policy implications on environment: the case of villagisation in Tanzania.* Nordic Africa Institute.

Kimaro, D., Poesen, J., Msanya, B. & Deckers, J. A. (2008) 'Magnitude of soil erosion on the northern slope of the Uluguru Mountains, Tanzania: Interrill and rill erosion'. *Catena*, 75 (1), pp. 38-44.

Kirkby, M. J. (1980) 'The problem', in Kirkby, M.J.a.M., R.P.C. (ed.) *Soil erosion.* Chichester: Wiley, pp. 1-16.

Kirkby, M. J. (2008) 'Erosion, weathering and landform evolution', in Holden, J. (ed.) *An introduction to Physical Geography and the Environment.* Harlow: Pearson Education Limited, pp. 295-324.

Kiunsi, R. & Meadows, M. (2006) 'Assessing land degradation in the Monduli District, northern Tanzania'. *Land Degradation & Development*, 17 (5), pp. 509-525.

Kiwango, Y. A. (2010) *Report On Lake Manyara Bathymetry.* Arusha: Lake Manyara National Park, TANAPA. 16 pp. Available.

Kiwango, Y. A. (2012) *Status report: Lake Manyara Frequent Dry-ups and Siltation.* Arusha: Ecological Monitoring Department, Lake Manyara National Park, TANAPA. 15 pp. Available.

Kjekshus, H. (1977) 'The Tanzanian villagization policy: implementational lessons and ecological dimensions'. *Canadian Journal of African Studies/La Revue canadienne des études africaines*, 11 (2), pp. 269-282.

Kjekshus, H. (1996) *Ecology control & economic development in East African history: the case of Tanganyika 1850-1950.* Ohio University Press.

Klopp, J. M. (2001) '"Ethnic clashes" and winning elections: The case of Kenya's electoral despotism'. *Canadian Journal of African Studies/La Revue canadienne des études africaines*, 35 (3), pp. 473-517.

Koenig, R. (2006a) 'The pink death: die-offs of the Lesser Flamingo raise concern'. *Science*, 313 (5794), pp. 1724-1725.

Koenig, R. (2006b) 'The pink death: die-offs of the Lesser Flamingo raise concern'.[in American Association for the Advancement of Science. (Accessed:Koenig, R.

Koiter, A., Owens, P., Petticrew, E. & Lobb, D. (2013) 'The behavioural characteristics of sediment properties and their implications for sediment fingerprinting as an approach for identifying sediment sources in river basins'. *Earth-Science Reviews*, 125 pp. 24-42.

Koning, N. & Smaling, E. (2005) 'Environmental crisis or 'lie of the land'? The debate on soil degradation in Africa'. *Land use policy*, 22 (1), pp. 3-11.

Koons, P. O., Upton, P. & Barker, A. D. (2012) 'The influence of mechanical properties on the link between tectonic and topographic evolution'. *Geomorphology*, 137 (1), pp. 168-180.

Korotayev, A. & Zinkina, J. (2015) 'East Africa in the Malthusian Trap?'. *Journal of Developing Societies*, 31 (3), pp. 385-420.

Krishnaswamy, S., Lal, D., Martin, J. & Meybeck, M. (1971) 'Geochronology of lake sediments'. *Earth and Planetary Science Letters*, 11 (1-5), pp. 407-414.

Kurukulasuriya, P. & Mendelsohn, R. O. (2008) *How will climate change shift agro-ecological zones and impact African agriculture?* The World Bank.

Laceby, J. P., Evrard, O., Smith, H. G., Blake, W. H., Olley, J. M., Minella, J. P. & Owens, P. N. (2017) 'The challenges and opportunities of addressing particle size effects in sediment source fingerprinting: A review'. *Earth-Science Reviews*,

Laceby, J. P., Olley, J., Pietsch, T. J., Sheldon, F. & Bunn, S. E. (2015) 'Identifying subsoil sediment sources with carbon and nitrogen stable isotope ratios'. *Hydrological processes*, 29 (8), pp. 1956-1971.

Lal, R. (1976) 'Soil erosion problems on an Alfisol in Western Nigeria and their control'.

Lal, R. (1990a) *Soil erosion in the tropics: principles and management.* McGraw-Hill Inc.

Lal, R. (1990b) 'Soil erosion and land degradation: the global risks', *Advances in soil science.* Springer, pp. 129-172.

Lal, R. (1996) 'Deforestation and land‐use effects on soil degradation and rehabilitation in western Nigeria. III. Runoff, soil erosion and nutrient loss'. *Land Degradation & Development*, 7 (2), pp. 99-119.

Lal, R. (2001) 'Soil degradation by erosion'. *Land Degradation & Development*, 12 (6), pp. 519-539.

Lambert, C. & Walling, D. (1987) 'Floodplain sedimentation: a preliminary investigation of contemporary deposition within the lower reaches of the River Culm, Devon, UK'. *Geografiska Annaler. Series A. Physical Geography*, pp. 393-404.

Lambin, E. F. & Geist, H. J. (2008) *Land-use and land-cover change: local processes and global impacts.* Springer Science & Business Media.

Lambin, E. F., Turner, B. L., Geist, H. J., Agbola, S. B., Angelsen, A., Bruce, J. W., Coomes, O. T., Dirzo, R., Fischer, G. & Folke, C. (2001) 'The causes of land-use and land-cover change: moving beyond the myths'. *Global environmental change*, 11 (4), pp. 261-269.

Lane, C. R. & Pretty, J. N. (1990) *Displaced pastoralists and transferred wheat technology in Tanzania.* IIED, International Institute for Environment and Development.

Lane, S., Reaney, S. & Heathwaite, A. L. (2009) 'Representation of landscape hydrological connectivity using a topographically driven surface flow index'. *Water Resources Research*, 45 (8),

Lang, C. & Stump, D. (2017) 'Geoarchaeological evidence for the construction, irrigation, cultivation, and resilience of 15 th--18 th century AD terraced landscape at Engaruka, Tanzania'. *Quaternary Research*, 88 (3), pp. 382-399.

Langbein, W. B. & Schumm, S. A. (1958) 'Yield of sediment in relation to mean annual precipitation'. *Eos, Transactions American Geophysical Union*, 39 (6), pp. 1076-1084.

Langdale, G., West, L., Bruce, R., Miller, W. & Thomas, A. (1992) 'Restoration of eroded soil with conservation tillage'. *Soil Technology*, 5 (1), pp. 81-90.

Last, W. & Schweyen, T. (1983) 'Sedimentology and geochemistry of saline lakes of the Great Plains'. *Hydrobiologia*, 105 (1), pp. 245-263.

Lavee, H., Imeson, A. C. & Sarah, P. (1998) 'The impact of climate change on geomorphology and desertification along a mediterranean‐arid transect'. *Land Degradation & Development*, 9 (5), pp. 407-422.

Lawi, Y. Q. (2002) *May the spider web blind witches and wild animals: Local knowledge and the political ecology of natural resource use in the Iraqwland, Tanzania, 1900-1985*. Leiden University.

Lawi, Y. Q. (2007) 'Tanzania's Operation Vijiji and Local Ecological Consciousness: The Case of Eastern Iraqwland, 1974–1976'. *The Journal of African History*, 48 (1), pp. 69-93.

Lazaroff, C. (2001) 'Biodiversity gives carbon sinks a boost'. *Environment News Service*, 13

Le Houerou, H. N. (1984) 'Rain use efficiency: a unifying concept in arid-land ecology'. *Journal of Arid Environments*, 7 (3), pp. 213-247.

Leach, M. & Mearns, R. (1996) 'Environmental Change and Policy', in Leach, M. and Mearns, R. (eds.) *The lie of the land: Challenging received wisdom on the African environment.* International African Institute, pp. 1-33.

Leh, M., Bajwa, S. & Chaubey, I. (2013) 'Impact of land use change on erosion risk: an integrated remote sensing, geographic information system and modeling methodology'. *Land Degradation & Development*, 24 (5), pp. 409-421.

Lele, V., Stone, S. W., Larios, J. F., Robinson, A. S., Ezekiel, H., Cunningham, E. P., Crosnier, J., Mulhern, F. J., Gimeno, E. J., Gorondim, P. E. & Felton Junior, E. (1989) *Population pressure the environment and agricultural intensification. Variations on the Boserup hypothesis.* vol. GTZ-884. Washington, D.C.: The World Bank.

Lema, A. (1993) *Africa Divided: The Creation of" ethnic Groups".* vol. 6. Lund University Press.

Lemmens, P., Teffera, F. E., Wynants, M., Govaert, L., Deckers, J., Bauer, H., Woldeyes, F., Brendonck, L., Bouillon, S. & De Meester, L. (2017) 'Intra‐and interspecific niche variation as reconstructed from stable isotopes in two ecologically different Ethiopian Rift Valley lakes'. *Functional Ecology*,

Leopold, L. B., Wolman, M. G. & Miller, J. P. (2012) *Fluvial processes in geomorphology.* Courier Corporation.

Lewis, H. & Brown, M. (2001) 'A generalized confusion matrix for assessing area estimates from remotely sensed data'. *International Journal of Remote Sensing*, 22 (16), pp. 3223-3235.

Ligonja, P. & Shrestha, R. (2015) 'Soil erosion assessment in kondoa eroded area in Tanzania using universal soil loss equation, geographic information systems and socioeconomic approach'. *Land Degradation & Development*, 26 (4), pp. 367-379.

Little, P. D. (1996) 'Pastoralism, biodiversity, and the shaping of savanna landscapes in East Africa'. *Africa*, 66 (1), pp. 37-51.

Little, P. D., McPeak, J., Barrett, C. B. & Kristjanson, P. (2008) 'Challenging orthodoxies: understanding poverty in pastoral areas of East Africa'. *Development and Change*, 39 (4), pp. 587-611.

Liu, J., Dietz, T., Carpenter, S. R., Alberti, M., Folke, C., Moran, E., Pell, A. N., Deadman, P., Kratz, T. & Lubchenco, J. (2007) 'Complexity of coupled human and natural systems'. *Science*, 317 (5844), pp. 1513-1516.

Lizaga, I., Gaspar, L., Blake, W. H., Latorre, B. & Navas, A. (2019) 'Fingerprinting changes of source apportionments from mixed land uses in stream sediments before and after an exceptional rainstorm event'. *Geomorphology*, 341 pp. 216-229.

Lizaga, I., Quijano, L., Palazón, L., Gaspar, L. & Navas, A. (2018) 'Enhancing connectivity index to assess the effects of land use changes in a Mediterranean catchment'. *Land Degradation & Development*, 29 (3), pp. 663-675.

Łokas, E., Wachniew, P., Ciszewski, D., Owczarek, P. & Chau, N. D. (2010) 'Simultaneous use of trace metals, 210Pb and 137Cs in floodplain sediments of a lowland river as indicators of anthropogenic impacts'. *Water, Air, and Soil Pollution*, 207 (1-4), pp. 57-71.

López-Bermúdez, F. & Romero-Diaz, M. A. (1989) 'PIPING, EROSION AND RADILAND DEVELOPMENT IN SOUTH-EAST SPAIN'. *Arid and Semi-arid Environments: Geomorphological and Pedological Aspects: Selected Papers*, 14 pp. 59.

López, R. (1997) *Where development can or cannot go: the role of poverty-environment linkages.* The World Bank.

Lopez, R. & Mitra, S. (2000) 'Corruption, pollution, and the Kuznets environment curve'. *Journal of Environmental Economics and Management*, 40 (2), pp. 137-150.

Lowdermilk, W. C. (1953) *Conquest of the land through 7,000 years.* US Department Of Agriculture; Washington.

Lu, H., Moran, C. J. & Prosser, I. P. (2006) 'Modelling sediment delivery ratio over the Murray Darling Basin'. *Environmental Modelling & Software*, 21 (9), pp. 1297-1308.

Lugomela, C., Pratap, H. B. & Mgaya, Y. D. (2006) 'Cyanobacteria blooms—a possible cause of mass mortality of Lesser Flamingos in Lake Manyara and Lake Big Momela, Tanzania'. *Harmful Algae*, 5 (5), pp. 534-541.

Luk, S. & Cai, Q. (1990) 'Laboratory experiments on crust development and rainsplash erosion of loess soils, China'. *Catena*, 17 (3), pp. 261-276.

Lundgren, B. (1978) *Soil conditions and nutrient cycling under natural and plantation forests in Tanzanian highlands.* Swedish University of Agricultural Sciences.

Lundgren, L. & Lundgren, B. (1979) 'Rainfall, interception and evaporation in the Mazumbai forest reserve, West Usambara Mts., Tanzania and their importance in the assessment of land potential'. *Geografiska Annaler: Series A, Physical Geography*, 61 (3-4), pp. 157-178.

Mabit, L., Benmansour, M. & Walling, D. (2008) 'Comparative advantages and limitations of the fallout radionuclides 137 Cs, 210 Pb ex and 7 Be for assessing soil erosion and sedimentation'. *Journal of environmental radioactivity*, 99 (12), pp. 1799-1807.

Mackenzie, F. (1989) 'Land and territory: the interface between two systems of land tenure, Murang'a District, Kenya'. *Africa*, 59 (1), pp. 91-109.

Maerker, M., Quénéhervé, G., Bachofer, F. & Mori, S. (2015) 'A simple DEM assessment procedure for gully system analysis in the Lake Manyara area, northern Tanzania'. *Natural Hazards*, 79 (1), pp. 235-253.

Maingi, J. K. & Marsh, S. E. (2002) 'Quantifying hydrologic impacts following dam construction along the Tana River, Kenya'. *Journal of Arid Environments*, 50 (1), pp. 53-79.

Maitima, J. M., Mugatha, S. M., Reid, R. S., Gachimbi, L. N., Majule, A., Lyaruu, H., Pomery, D., Mathai, S. & Mugisha, S. (2009) 'The linkages between land use change, land degradation and biodiversity across East Africa'. *African Journal of Environmental Science and Technology*, 3 (10),

Mamdani, M. (2018) *Citizen and subject: Contemporary Africa and the legacy of late colonialism.* Princeton University Press.

Mango, L. M., Melesse, A. M., McClain, M. E., Gann, D. & Setegn, S. (2011) 'Land use and climate change impacts on the hydrology of the upper Mara River Basin, Kenya: results of a modeling study to support better resource management'. *Hydrology and Earth System Sciences*, 15 (7), pp. 2245-2258.

Manjoro, M., Rowntree, K., Kakembo, V., Foster, I. & Collins, A. L. (2017) 'Use of sediment source fingerprinting to assess the role of subsurface erosion in the supply of fine sediment in a degraded catchment in the Eastern Cape, South Africa'. *Journal of environmental management*, 194 (Supplement C), pp. 27-41.

Marchant, R., Richer, S., Capitani, C., Courtney-Mustaphi, C., Prendergast, M., Stump, D., Boles, O., Lane, P., Wynne-Jones, S. & Vázquez, C. F. (2018) 'Drivers and trajectories of land cover change in East Africa: Human and environmental interactions from 6000years ago to present'. *Earth-Science Reviews*,

Mati, B. M. (1999) *Erosion hazard assessment in the Upper Ewaso Ng'iro basin of Kenya: Application of GIS, USLE and EUROSEM.*

Mati, B. M., Mutie, S., Gadain, H., Home, P. & Mtalo, F. (2008) 'Impacts of land-use/cover changes on the hydrology of the transboundary Mara River, Kenya/Tanzania'. *Lakes & Reservoirs: Research & Management*, 13 (2), pp. 169-177.

Mati, B. M. & Veihe, A. (2001) 'Application of the USLE in a Savannah environment: Comparative experiences from East and West Africa'. *Singapore Journal of Tropical Geography*, 22 (2), pp. 138-155.

Matlon, P. J. & Spencer, D. S. (1984) 'Increasing food production in Sub-Saharan Africa: Environmental problems and inadequate technological solutions'. *American Journal of Agricultural Economics*, 66 (5), pp. 671-676.

McClanahan, T. R. & Young, T. P. (1996) *East African ecosystems and their conservation.* Oxford University Press on Demand.

McCool, D. K., Foster, G. R., Mutchler, C. & Meyer, L. (1989) 'Revised slope length factor for the Universal Soil Loss Equation'. *Transactions of the ASAE*, 32 (5), pp. 1571-1576.

McDonald, M., Healey, J. & Stevens, P. (2002) 'The effects of secondary forest clearance and subsequent land-use on erosion losses and soil properties in the Blue Mountains of Jamaica'. *Agriculture, ecosystems & environment*, 92 (1), pp. 1-19.

Meade, R. H. (1972) 'Transport and deposition of sediments in estuaries'. *Geological Society of America Memoirs*, 133 pp. 91-120.

Meade, R. H., Dunne, T., Richey, J. E., Santos, U. D. M. & Salati, E. (1985) 'Storage and remobilization of suspended sediment in the lower Amazon River of Brazil'. *Science*, 228 (4698), pp. 488-490.

Medina-Roldan, E., Huber-Sannwald, E. & Arredondo, J. T. (2013) 'Plant phenotypic functional composition effects on soil processes in a semiarid grassland'. *Soil Biology & Biochemistry*, 66 pp. 1-9.

Meindertsma, J. & Kessler, J. J. (1997) 'Planning for a better environment in Monduli District'. *Monduli District Council, Arusha*,

Merritt, E. (1984) 'The identification of four stages during micro‐rill development'. *Earth surface processes and landforms*, 9 (5), pp. 493-496.

Meyer, L. & Wischmeier, W. (1969) 'Mathematical simulation of the process of soil erosion by water'. *Transactions of the ASAE*, 12 (6), pp. 754-0758.

Michaelides, K. & Wainwright, J. (2002) 'Modelling the effects of hillslope–channel coupling on catchment hydrological response'. *Earth surface processes and landforms*, 27 (13), pp. 1441-1457.

Migot-Adholla, S., Hazell, P., Blarel, B. & Place, F. (1991) 'Indigenous land rights systems in sub-Saharan Africa: a constraint on productivity?'. *The World Bank Economic Review*, 5 (1), pp. 155-175.

Moeyersons, J. (1983) 'Measurements of splash saltation fluxes under oblique rain'. *Catena*, pp. 19-31.

Montgomery, D. R. (1994) 'Road surface drainage, channel initiation, and slope instability'. *Water Resources Research*, 30 (6), pp. 1925-1932.

Montgomery, D. R. (2007) 'Soil erosion and agricultural sustainability'. *Proceedings of the National Academy of Sciences*, 104 (33), pp. 13268-13272.

Montgomery, D. R. (2012) *Dirt: the erosion of civilizations.* vol. 3. Berkeley and Los Angeles, California: University of California Press.

Montgomery, D. R. & Buffington, J. M. (1998) 'Channel processes, classification, and response'.

Montgomery, D. R. & Dietrich, W. E. (1992) 'Channel initiation and the problem of landscape scale'. *Science*, 255 (5046), pp. 826-830.

Moore, T. R. (1979) 'Rainfall Erosivity in East-Africa'. *Geografiska Annaler Series a-Physical Geography*, 61 (3-4), pp. 147-156.

Morgan, R. P. C. (2005) *Soil Erosion and Conservation* ed. Morgan, R.P.C., vol. 3. Oxford: Blackwell Science Ltd.

Morgan, R. P. C., Martin, L. & Noble, C. (1987) *Soil erosion in the United Kingdom: a case study from mid-Bedfordshire.* Silsoe College, Cranfield Institute of Technology.

Morgan, W. B. (1969) 'Peasant agriculture in tropical Africa'. *Environment and land use in Africa*, pp. 241-272.

Motha, J., Wallbrink, P., Hairsine, P. & Grayson, R. (2002) 'Tracer properties of eroded sediment and source material'. *Hydrological processes*, 16 (10), pp. 1983-2000.

Mottram, H. R. & Evershed, R. P. (2003) 'Practical considerations in the gas chromatography/combustion/isotope ratio monitoring mass spectrometry of 13C-enriched compounds: detection limits and carryover effects'. *Rapid communications in mass spectrometry*, 17 (23), pp. 2669-2674.

Mukundan, R., Walling, D. E., Gellis, A. C., Slattery, M. C. & Radcliffe, D. E. (2012) 'Sediment source fingerprinting: transforming from a research tool to a management tool'. *JAWRA Journal of the American Water Resources Association*, 48 (6), pp. 1241-1257.

Mung'ong'o, C. G., Loiske, V. M., Simon, D., Spengen, W. V., Dixon, C. & Närman, A. (1995) 'Structural adjustment programmes and peasant responses in Tanzania', in Simon, D., Van Spengen, W., Dixon, C. and Narman, A. (eds.) *Structurally adjusted Africa. Poverty, debt and basic needs.* London: Pluto Press, pp. 159-183.

Murphree, C. & McGregor, K. (1991) 'Runoff and sediment yield from a flatland watershed in soybeans'. *Transactions of the ASAE*, 34 (2), pp. 407-0411.

Mutchler, C. K. & Young, R. A. (1975) 'Soil detachment by raindrops'. *Present Prospective Technology for Predicting Sediment Yields and Sources*, pp. 114-117.

Muyungi, R. (2007) 'Managing land use, protecting land and mitigating land degradation: Tanzania case study', *Climate and Land Degradation.* Springer, pp. 437-445.

Myers, N. (1990) 'The biodiversity challenge: expanded hot-spots analysis'. *The environmentalist*, 10 (4), pp. 243-256.

Myers, N. (1993) 'Gaia: An atlas of planet management. Anchor and Doubleday'. *Garden City, NY*,

Myers, N. & Kent, J. (2001) *Perverse subsidies: how tax dollars can undercut the environment and the economy.* Washington, D.C.: Island press.

Nachtergaele, F., van Velthuizen, H., Verelst, L., Batjes, N., Dijkshoorn, J., van Engelen, V., Fischer, G., Jones, A., Montanarella, L. & Petri, M. (2008) *Harmonized world soil database (version 1.0).* Food and Agric Organization of the UN (FAO); International Inst. for Applied Systems Analysis (IIASA); ISRIC-World Soil Information; Inst of Soil Science-Chinese Acad of Sciences (ISS-CAS); EC-Joint Research Centre (JRC). Available.

Ndomba, P. (2007) 'Modelling of erosion processes and reservoir sedimentation upstream of Nyumba ya Mungu reservoir in the Pangani river basin'. *A PhD Thesis (Water Resources Engineering) of University of Dar es Salaam*,

Nearing, M., Pruski, F. & O'neal, M. (2004) 'Expected climate change impacts on soil erosion rates: a review'. *Journal of soil and water conservation*, 59 (1), pp. 43-50.

Newcombe, C. P. & MacDonald, D. D. (1991) 'Effects of suspended sediments on aquatic ecosystems'. *North American journal of fisheries management*, 11 (1), pp. 72-82.

Ngecu, W. & Mathu, E. (1999) 'The El-Nino-triggered landslides and their socioeconomic impact on Kenya'. *Environmental Geology*, 38 (4), pp. 277-284.

Ngwira, A., Thierfelder, C., Eash, N. & Lambert, D. M. (2013) 'Risk and maize-based cropping systems for smallholder Malawi farmers using conservation agriculture technologies'. *Experimental Agriculture*, 49 (4), pp. 483-503.

Niamir-Fuller, M. (2000) 'The resilience of pastoral herding in Sahelian Africa', in Berkes, F., Folke, C. and Colding, J. (eds.) *Linking social and ecological systems: Management practices and social mechanisms for building resilience.* Cambridge, UK: Cambridge University Press, pp. 250-284.

Nicholson, S. E. (1996) 'A review of climate dynamics and climate variability in Eastern Africa', in Johnson, T.C.a.O., E.O. (ed.) *The limnology, climatology and paleoclimatology of the East African lakes.* Amsterdam, the Netherlands Gordon and Breach Publishers, pp. 25-56.

Nonga, H., Mdegela, R., Lie, E., Sandvik, M. & Skaare, J. (2010) 'Socio-economic values of wetland resources around lake Manyara, Tanzania: assessment of environmental threats and local community awareness on environmental degradation and their effects'.

Nonga, H., Mdegela, R., Lie, E., Sandvik, M. & Skaare, J. (2011a) 'Assessment of farming practices and uses of agrochemicals in Lake Manyara basin, Tanzania'. *African Journal of Agricultural Research*, 6 pp. 2216-2230.

Nonga, H., Sandvik, M., Miles, C., Lie, E., Mdegela, R., Mwamengele, G., Semuguruka, W. & Skaare, J. (2011b) 'Possible involvement of microcystins in the unexplained mass mortalities of Lesser Flamingo (Phoeniconaias minor Geoffroy) at Lake Manyara in Tanzania'. *Hydrobiologia*, 678 (1), pp. 167-178.

O'Driscoll, M., Clinton, S., Jefferson, A., Manda, A. & McMillan, S. (2010) 'Urbanization effects on watershed hydrology and in-stream processes in the southern United States'. *Water*, 2 (3), pp. 605-648.

Odada, E. O., Olago, D. O., Bugenyi, F., Kulindwa, K., Karimumuryango, J., West, K., Ntiba, M., Wandiga, S., Aloo-Obudho, P. & Achola, P. (2003) 'Environmental assessment of the East African rift valley lakes'. *Aquatic sciences*, 65 (3), pp. 254-271.

Odgaard, R. (2002) 'Scrambling for land in Tanzania: Processes of formalisation and legitimisation of land rights'. *The European Journal of Development Research*, 14 (2), pp. 71-88.

Ogutu, J., Piepho, H. P., Dublin, H., Bhola, N. & Reid, R. (2009) 'Dynamics of Mara–Serengeti ungulates in relation to land use changes'. *Journal of Zoology*, 278 (1), pp. 1-14.

Olaya, V. (2014) 'Hydrological Analysis', in Thiede, R., Sutton, T., Duster, H. and Sutton, M. (ed.) *QGIS Training Manual, Release 2.2. .* pp. 485-495.

Oldeman, L. R. (1992) 'Global extent of soil degradation', *Bi-Annual Report 1991-1992/ISRIC.* ISRIC, pp. 19-36.

Oliveira, J. D. A., Dominguez, J. M. L., Nearing, M. A. & Oliveira, P. T. (2015) 'A GIS-based procedure for automatically calculating soil loss from the

universalsoil loss equation: Gisus-m'. *Applied Engineering in Agriculture*, 31 (6), pp. 907.

Olofsson, P., Foody, G. M., Herold, M., Stehman, S. V., Woodcock, C. E. & Wulder, M. A. (2014) 'Good practices for estimating area and assessing accuracy of land change'. *Remote Sensing of Environment*, 148 pp. 42-57.

Olson, K. & Nizeyimana, E. (1988) 'Effects of soil erosion on corn yields of seven Illinois soils'. *Journal of Production Agriculture*, 1 (1), pp. 13-19.

Osborne, C. P. (2008) 'Atmosphere, ecology and evolution: what drove the Miocene expansion of C4 grasslands?'. *Journal of Ecology*, 96 (1), pp. 35-45.

Ostrom, E. (2000) 'Collective action and the evolution of social norms'. *Journal of economic perspectives*, 14 (3), pp. 137-158.

Ostrom, E. (2009) 'A general framework for analyzing sustainability of social-ecological systems'. *Science*, 325 (5939), pp. 419-422.

Owens, P., Blake, W., Gaspar, L., Gateuille, D., Koiter, A., Lobb, D., Petticrew, E., Reiffarth, D., Smith, H. & Woodward, J. (2016) 'Fingerprinting and tracing the sources of soils and sediments: Earth and ocean science, geoarchaeological, forensic, and human health applications'. *Earth-Science Reviews*, 162 pp. 1-23.

Palmer, R. S. (1963) 'The influence of a thin water layer on waterdrop impact forces'. *International Association of Science and Hydrology Publication*, 65 pp. 141-148.

Panagos, P., Borrelli, P., Meusburger, K., Alewell, C., Lugato, E. & Montanarella, L. (2015a) 'Estimating the soil erosion cover-management factor at the European scale'. *Land use policy*, 48 pp. 38-50.

Panagos, P., Borrelli, P., Poesen, J., Ballabio, C., Lugato, E., Meusburger, K., Montanarella, L. & Alewell, C. (2015b) 'The new assessment of soil loss by water erosion in Europe'. *Environmental Science & Policy*, 54 pp. 438-447.

Parsons, A. J., Abrahams, A. D. & Luk, S.-H. (1990) 'Hydraulics of interrill overland flow on a semi-arid hillslope, southern Arizona'. *Journal of Hydrology*, 117 (1-4), pp. 255-273.

Parsons, A. J., Wainwright, J., Brazier, R. E. & Powell, D. M. (2006) 'Is sediment delivery a fallacy?'. *Earth Surface Processes and Landforms: The Journal of the British Geomorphological Research Group*, 31 (10), pp. 1325-1328.

Pedersen, H. S. & Hasholt, B. (1995) 'Influence of wind speed on rainsplash erosion'. *Catena*, 24 (1), pp. 39-54.

Pfeifer, M., Disney, M., Quaife, T. & Marchant, R. (2012) 'Terrestrial ecosystems from space: a review of earth observation products for macroecology applications'. *Global Ecology and Biogeography*, 21 (6), pp. 603-624.

Phillips, J., Russell, M. & Walling, D. (2000) 'Time‐integrated sampling of fluvial suspended sediment: a simple methodology for small catchments'. *Hydrological processes*, 14 (14), pp. 2589-2602.

Pimentel, D. (1997) 'Soil erosion'. *Environment*, 39 (10), pp. 4-5.

Pimentel, D. (2006) 'Soil erosion: a food and environmental threat'. *Environment, development and sustainability*, 8 (1), pp. 119-137.

Pimentel, D., Harvey, C., Resosudarmo, P., Sinclair, K., Kurz, D., McNair, M., Crist, S., Shpritz, L., Fitton, L. & Saffouri, R. (1995) 'Environmental and economic costs of soil erosion and conservation benefits'. *Science-AAAS-Weekly Paper Edition*, 267 (5201), pp. 1117-1122.

Pimentel, D. & Kounang, N. (1998) 'Ecology of soil erosion in ecosystems'. *Ecosystems*, 1 (5), pp. 416-426.

Pinckney, T. C. & Kimuyu, P. K. (1994) 'Land tenure reform in East Africa: Good, bad or unimportant?'. *Journal of African Economies*, 3 (1), pp. 1-28.

Poesen, J. (1985) 'An improved splash transport model'. *Zeitschrift für Geomorphologie*, 29 pp. 193-211.

Poesen, J. (1989) 'Conditions for gully formation in the Belgian loam belt and some ways to control them'.

Poesen, J. (1992) 'Mechanisms of overland-flow generation and sediment production on loamy and sandy soils with and without rock fragments.', in Parsons, A.J., Abrahams, A.D. (ed.) *Overland Flow Hydraulics and Erosion Mechanics.* Routledge, London, pp. 275–305.

Poesen, J. (1993) 'Gully typology and gully control measures in the European loess belt', *Farm Land Erosion.* Elsevier, pp. 221-239.

Poesen, J. (2011) 'Challenges in gully erosion research'. *Landform analysis*, 17 pp. 5-9.

Poesen, J. & Govers, G. (1986) 'A field-scale study on surface sealing and compaction on loam and sandy loam soils. Part II. Impact of soil surface sealing and compaction on water erosion processes', *Assessment of Soil Surface Sealing and Crusting*. State University of Ghent, Ghent, pp. 183-193.

Poesen, J., Nachtergaele, J., Verstraeten, G. & Valentin, C. (2003) 'Gully erosion and environmental change: importance and research needs'. *Catena*, 50 (2), pp. 91-133.

Pontius Jr, R. G., Shusas, E. & McEachern, M. (2004) 'Detecting important categorical land changes while accounting for persistence'. *Agriculture, Ecosystems & Environment*, 101 (2-3), pp. 251-268.

Powell, D. M., Laronne, J. B., Reid, I. & Barzilai, R. (2012) 'The bed morphology of upland single‐thread channels in semi‐arid environments: evidence of repeating bedforms and their wider implications for gravel‐bed rivers'. *Earth surface processes and landforms*, 37 (7), pp. 741-753.

Pretty, J. (2003) 'Social capital and the collective management of resources'. *Science*, 302 (5652), pp. 1912-1914.

Pretty, J. N., Noble, A. D., Bossio, D., Dixon, J., Hine, R. E., Penning de Vries, F. W. & Morison, J. I. (2006) 'Resource-conserving agriculture increases yields in developing countries'. *Environmental Science and Technology*, 40 (4), pp. 1114-1119.

Pricope, N. G., Husak, G., Lopez-Carr, D., Funk, C. & Michaelsen, J. (2013) 'The climate-population nexus in the East African Horn: Emerging degradation trends in rangeland and pastoral livelihood zones'. *Global environmental change*, 23 (6), pp. 1525-1541.

Prins, H. & Loth, P. (1988) 'Rainfall patterns as background to plant phenology in northern Tanzania'. *Journal of Biogeography*, pp. 451-463.

Prosser, I. P. & Winchester, S. J. (1996) 'History and processes of gully initiation and development in eastern Australia'. *Zeitschrift fur Geomorphologie Supplementband*, pp. 91-109.

Puttock, A., Macleod, C. J., Bol, R., Sessford, P., Dungait, J. & Brazier, R. E. (2013) 'Changes in ecosystem structure, function and hydrological connectivity

control water, soil and carbon losses in semi‐arid grass to woody vegetation transitions'. *Earth surface processes and landforms*, 38 (13), pp. 1602-1611.

QGIS Development Team (2009) *Quantum GIS 2.14.8.* [Computer Program]. Open Source Geospatial Foundation,. Available

Quinn, N., Morgan, R. & Smith, A. (1980) 'Simulation of soil erosion induced by human trampling'. *Journal of environmental management*, 10 pp. 155-165.

Quinton, J. N. & Catt, J. A. (2007) 'Enrichment of heavy metals in sediment resulting from soil erosion on agricultural fields'. *Environmental science & technology*, 41 (10), pp. 3495-3500.

Quinton, J. N., Catt, J. A. & Hess, T. M. (2001) 'The selective removal of phosphorus from soil'. *Journal of Environmental Quality*, 30 (2), pp. 538-545.

Rammel, C., Stagl, S. & Wilfing, H. (2007) 'Managing complex adaptive systems—a co-evolutionary perspective on natural resource management'. *Ecological Economics*, 63 (1), pp. 9-21.

Rapp, A., Murray-Rust, D. H., Christiansson, C. & Berry, L. (1972) 'Soil erosion and sedimentation in four catchments near Dodoma, Tanzania'. *Geografiska Annaler. Series A. Physical Geography*, pp. 255-318.

Reid, S. C., Lane, S. N., Berney, J. M. & Holden, J. (2007a) 'The timing and magnitude of coarse sediment transport events within an upland, temperate gravel-bed river'. *Geomorphology*, 83 (1), pp. 152-182.

Reid, S. C., Lane, S. N., Montgomery, D. R. & Brookes, C. J. (2007b) 'Does hydrological connectivity improve modelling of coarse sediment delivery in upland environments?'. *Geomorphology*, 90 (3), pp. 263-282.

Reiffarth, D., Petticrew, E., Owens, P. & Lobb, D. (2016) 'Sources of variability in fatty acid (FA) biomarkers in the application of compound-specific stable isotopes (CSSIs) to soil and sediment fingerprinting and tracing: A review'. *Science of the total environment*, 565 pp. 8-27.

Reij, C., Scoones, I. & Toulmin, C. (2013) *Sustaining the soil: indigenous soil and water conservation in Africa.* London: Routledge.

Renard, K., Meyer, L. & Foster, G. (1997) *Predicting soil erosion by water: a guide to conservation planning with the revised universal soil loss equation (RUSLE).* Agricultural handbook. U.S. Department of Agriculture.

Reubens, B., Poesen, J., Danjon, F., Geudens, G. & Muys, B. (2007) 'The role of fine and coarse roots in shallow slope stability and soil erosion control with a focus on root system architecture: a review'. *Trees*, 21 (4), pp. 385-402.

Reynolds, J. F., Smith, D. M. S., Lambin, E. F., Turner, B., Mortimore, M., Batterbury, S. P., Downing, T. E., Dowlatabadi, H., Fernández, R. J. & Herrick, J. E. (2007) 'Global desertification: building a science for dryland development'. *Science*, 316 (5826), pp. 847-851.

Rhoton, F. E., Shipitalo, M. J. & Lindbo, D. L. (2002) 'Runoff and Soil Loss from Midwestern and Southeastern US Silt Loam Soils as Affected by Tillage Practice and Soil Organic Matter Content'. *Soil and Tillage Research*, 66 pp. 1-11.

Robbins, J. A. (1978) 'Geochemical and geophysical applications of radioactive lead'. *Biogeochemistry of Lead in the Environment*, pp. 285-393.

Rodney, W. (1972) *How europe underdeveloped africa.* London: Bogle-L'Ouverture Publications.

Roehl, J. (1962) 'Sediment source areas, and delivery ratios influencing morphological factors'. *Int. Assoc. Hydro. Sci.*, 59 pp. 202-213.

Roering, J. J., Almond, P., Tonkin, P. & McKean, J. (2002) 'Soil transport driven by biological processes over millennial time scales'. *Geology*, 30 (12), pp. 1115-1118.

Rohde, R. & Hilhorst, T. (2001) *A profile of environmental change in the Lake Manyara Basin, Tanzania.* International Institute for Environment and Development, Drylands Programme.

Roose, E. (1986) 'Runoff and erosion before and after clearing depending on the type of crop in western Africa'. *Land clearing and development in the tropics"(R. Lal, ed.)*, pp. 317-330.

Ropelewski, C. F. & Halpert, M. S. (1987) 'Global and regional scale precipitation patterns associated with the El Niño/Southern Oscillation'. *Monthly weather review*, 115 (8), pp. 1606-1626.

Rosgen, D. L. (1994) 'A classification of natural rivers'. *Catena*, 22 (3), pp. 169-199.

Roth, E. A. (1996) 'Traditional pastoral strategies in a modern world: An example from northern Kenya'. *Human Organization*, pp. 219-224.

Roy, D. P., Ju, J., Mbow, C., Frost, P. & Loveland, T. (2010) 'Accessing free Landsat data via the Internet: Africa's challenge'. *Remote Sensing Letters*, 1 (2), pp. 111-117.

Rudel, T. K., Defries, R., Asner, G. P. & Laurance, W. F. (2009) 'Changing drivers of deforestation and new opportunities for conservation'. *Conservation Biology*, 23 (6), pp. 1396-1405.

Rufino, M. C., Thornton, P. K., Mutie, I., Jones, P., Van Wijk, M. & Herrero, M. (2013) 'Transitions in agro-pastoralist systems of East Africa: impacts on food security and poverty'. *Agriculture, ecosystems & environment*, 179 pp. 215-230.

Ruthenberg, H. (1968) *Smallholder farming and smallholder development in Tanzania.* München: Weltforum Verlag.

Ruthenberg, H. & Jahnke, H. E. (1985) *Innovation policy for small farmers in the tropics: The economics of technical innovations for agricultural development.* Clarendon Press.

Ruttan, L. M., Borgerhoff Mulder, M., Berkes, F., Colding, J., Folke, C., Fratkin, E., Galaty, J. G., Homewood, K., Little, P. D. & Ostrom, E. (1999) 'Are East African pastoralists truly conservationists?'. *Current anthropology*, 40 (5), pp. 621-652.

Rutten, M. M. E. M. (1992) *Selling wealth to buy poverty: the process of the individualization of landownership among the Maasai pastoralists of Kajiado district, Kenya, 1890-1990*. Universiteit Leiden.

Saiz, G., Wandera, F. M., Pelster, D. E., Ngetich, W., Okalebo, J. R., Rufino, M. C. & Butterbach-Bahl, K. (2016) 'Long-term assessment of soil and water conservation measures (Fanya-juu terraces) on soil organic matter in South Eastern Kenya'. *Geoderma*, 274 pp. 1-9.

Salami, A., Kamara, A. B. & Brixiova, Z. (2010) *Smallholder agriculture in East Africa: Trends, constraints and opportunities.* African Development Bank Tunis.

Sanchez-Cabeza, J. & Ruiz-Fernández, A. (2012) '210Pb sediment radiochronology: an integrated formulation and classification of dating models'. *Geochimica et Cosmochimica Acta*, 82 pp. 183-200.

Sanchez, P. A. (2002) 'Soil fertility and hunger in Africa'. *Science*, 295 (5562), pp. 2019-2020.

Sandford, G. (1919) *An administrative and political history of the Masai Reserve.*

Savat, J. (1982) 'Common and uncommon selectivity in the process of fluid transportation: field observations and laboratory experiments on bare surfaces'. *Catena Supplement*, 1 pp. 139-160.

Scheffer, M., Carpenter, S., Foley, J. A., Folke, C. & Walker, B. (2001) 'Catastrophic shifts in ecosystems'. *Nature*, 413 (6856), pp. 591.

Scherr, S. J. (1999) *Soil degradation: a threat to developing-country food security by 2020?* vol. 27. Intl Food Policy Res Inst.

Schertz, D., Moldenhauer, W., Livingston, S., Weesies, G. & Hintz, E. (1989) 'Effect of past soil erosion on crop productivity in Indiana'. *Journal of soil and water conservation*, 44 (6), pp. 604-608.

Schlesinger, W. H., Reynolds, J. F., Cunningham, G. L., Huenneke, L. F., Jarrell, W. M., Virginia, R. A. & Whitford, W. G. (1990) 'Biological feedbacks in global desertification'. *Science(Washington)*, 247 (4946), pp. 1043-1048.

Schumm, S. A. (1979) 'Geomorphic thresholds: the concept and its applications'. *Transactions of the Institute of British Geographers*, pp. 485-515.

Selby, M. J. (1982) 'Hillslope materials and processes'. *Hillslope materials and processes.*,

Sendalo, D. (2009) *A review of land tenure policy implications on pastoralism in Tanzania.* Dar es Salaam: Ministry of Livestock Development and Fisheries. Available.

Sepuru, T. K. & Dube, T. (2018) 'An appraisal on the progress of remote sensing applications in soil erosion mapping and monitoring'. *Remote Sensing Applications: Society and Environment*, 9 pp. 1-9.

Shechambo, F. (1998) 'Land Use by people living around protected areas: The case of Lake Manyara National Park'. *Utafiti Journal*, 4 (1),

Sherriff, S. C., Franks, S. W., Rowan, J. S., Fenton, O. & Ó'hUallacháin, D. (2015) 'Uncertainty-based assessment of tracer selection, tracer non-

conservativeness and multiple solutions in sediment fingerprinting using synthetic and field data'. *Journal of soils and sediments*, 15 (10), pp. 2101-2116.

Shields, A. (1936) 'Anwendung der Aehnlichkeitsmechanik und der Turbulenzforschung auf die Geschiebebewegung'. *PhD Thesis Technical University Berlin*,

Shongwe, M. E., van Oldenborgh, G. J., van den Hurk, B. & van Aalst, M. (2011) 'Projected changes in mean and extreme precipitation in Africa under global warming. Part II: East Africa'. *Journal of Climate*, 24 (14), pp. 3718-3733.

Simon, A. & Rinaldi, M. (2006) 'Disturbance, stream incision, and channel evolution: The roles of excess transport capacity and boundary materials in controlling channel response'. *Geomorphology*, 79 (3-4), pp. 361-383.

Sinclair, A. & Fryxell, J. (1985) 'The Sahel of Africa: ecology of a disaster'. *Canadian Journal of Zoology*, 63 (5), pp. 987-994.

Singer, M. J. & Le Bissonnais, Y. (1998) 'Importance of surface sealing in the erosion of some soils from a Mediterranean climate'. *Geomorphology*, 24 (1), pp. 79-85.

Smith, C. D. (1989) *Did colonialism capture the peasantry?: a case study of the Kagera District, Tanzania.* Nordic Africa Institute.

Smith, H. G. & Blake, W. H. (2014) 'Sediment fingerprinting in agricultural catchments: a critical re-examination of source discrimination and data corrections'. *Geomorphology*, 204 pp. 177-191.

Smith, H. G. & Dragovich, D. (2008) 'Sediment budget analysis of slope–channel coupling and in-channel sediment storage in an upland catchment, southeastern Australia'. *Geomorphology*, 101 (4), pp. 643-654.

Smith, H. G., Evrard, O., Blake, W. H. & Owens, P. N. (2015) 'Preface—Addressing challenges to advance sediment fingerprinting research'. *Journal of soils and sediments*, 15 (10), pp. 2033-2037.

Smith, V. H., Tilman, G. D. & Nekola, J. C. (1999) 'Eutrophication: impacts of excess nutrient inputs on freshwater, marine, and terrestrial ecosystems'. *Environmental pollution*, 100 (1), pp. 179-196.

Snyder, K. A. (1996) 'Agrarian change and land-use strategies among Iraqw farmers in northern Tanzania'. *Human Ecology*, 24 (3), pp. 315-340.

Sombroek, W. (1993) 'Amounts, dynamics and sequestering of carbon in tropical and subtropical soils'. *Ambio*, 22 pp. 417-426.

Sorrenson, M. P. K. (1968) *Origins of European settlement in Kenya.* Oxford, UK: Oxford University Press.

Souverijns, N., Thiery, W., Demuzere, M. & Van Lipzig, N. P. (2016) 'Drivers of future changes in East African precipitation'. *Environmental Research Letters*, 11 (11), pp. 114011.

Spear, T. & Waller, R. (1993) *Being Maasai: ethnicity and identity in East Africa.* Ohio University Press.

Stanley, H. M. (1889) *Through the Dark Continent: Or, The Sources of the Nile, Around the Great Lakes of Equatorial Africa, and Down the Livingstone River to the Atlantic Ocean.* Sampson, Low.

Stewart, B., Wischmeier, W. & Woolhiser, D. (1975) 'Control of water pollution from cropland: vol. 1, a manual for guideline development, vol. 2, an overview'. *USA: United States Department of Agriculture*,

Stock, B. C., Jackson, A. L., Ward, E. J., Parnell, A. C., Phillips, D. L. & Semmens, B. X. (2018) 'Analyzing mixing systems using a new generation of Bayesian tracer mixing models'. *PeerJ*, 6 pp. e5096.

Stock, B. C. & Semmens, B. X. (2016) 'Unifying error structures in commonly used biotracer mixing models'. *Ecology*, 97 (10), pp. 2562-2569.

Stock, B. C. & Semmens, B. X. (2017) *MixSIAR GUI User Manual v3.1.* [Computer Program]. http://dx.doi.org/10.5281/zenodo.47719: Available

Stoner, C., Caro, T., Mduma, S., Mlingwa, C., Sabuni, G., Borner, M. & Schelten, C. (2007) 'Changes in large herbivore populations across large areas of Tanzania'. *African Journal of Ecology*, 45 (2), pp. 202-215.

Stump, D. (2010) '"Ancient and backward or long-lived and sustainable?" The role of the past in debates concerning rural livelihoods and resource conservation in Eastern Africa'. *World development*, 38 (9), pp. 1251-1262.

Suding, K. N., Gross, K. L. & Houseman, G. R. (2004) 'Alternative states and positive feedbacks in restoration ecology'. *Trends in ecology & evolution*, 19 (1), pp. 46-53.

Sullivan, S. & Rohde, R. (2002) 'On non‐equilibrium in arid and semi‐arid grazing systems'. *Journal of Biogeography*, 29 (12), pp. 1595-1618.

Sundquist, B. (2000) 'Topsoil loss–Causes, effects and implications: A global perspective'. *The Earth's Carrying Capacity–some literature reviews*,

Suriya, S. & Mudgal, B. (2012) 'Impact of urbanization on flooding: The Thirusoolam sub watershed–A case study'. *Journal of Hydrology*, 412 pp. 210-219.

Swan, A. (2010) 'How increased urbanisation has induced flooding problems in the UK: A lesson for African cities?'. *Physics and Chemistry of the Earth, Parts A/B/C*, 35 (13), pp. 643-647.

Tabacchi, E., Lambs, L., Guilloy, H., Planty‐Tabacchi, A. M., Muller, E. & Decamps, H. (2000) 'Impacts of riparian vegetation on hydrological processes'. *Hydrological processes*, 14 (16‐17), pp. 2959-2976.

Tarboton, D. G., Bras, R. L. & Rodriguez‐Iturbe, I. (1991) 'On the extraction of channel networks from digital elevation data'. *Hydrological processes*, 5 (1), pp. 81-100.

Tarchitzky, J., Banin, A., Morin, J. & Chen, Y. (1984) 'Nature, formation and effects of soil crusts formed by water drop impact'. *Geoderma*, 33 (2), pp. 135-155.

Teffera, F. E., Lemmens, P., Deriemaecker, A., Brendonck, L., Dondeyne, S., Deckers, J., Bauer, H., Gamo, F. W. & De Meester, L. (2017) 'A call to action: strong long-term limnological changes in the two largest Ethiopian Rift Valley lakes, Abaya and Chamo'. *Inland Waters*, pp. 1-9.

Temple, D. M. (1982) 'Flow retardance of submerged grass channel linings'. *Transactions of the ASAE*, 25 (5), pp. 1300-1303.

Temple, P. H. & Rapp, A. (1972) 'Landslides in the Mgeta area, western Uluguru mountains, Tanzania'. *Geografiska Annaler. Series A. Physical Geography*, pp. 157-193.

Tengberg, A. & Stocking, M. (1997) 'Erosion-induced loss in soil productivity and its impacts on agricultural production and food security'. *FAO/AGRITEX Expert Consultation on Integrated Soil Management for Sustainable Agriculture*

and Food Security in Southern and Eastern Africa, Harare, Zimbabwe, pp. 8-12.

Tengö, M. & Hammer, M. (2003) 'Management practices for building adaptive capacity: a case from northern Tanzania', in Berkes, F., Colding, J. and Folke, C. (eds.) *Navigating social-ecological systems: Building resilience for complexity and change.* Cambridge, UK: Cambridge University Press, pp. 116-132.

The World Bank (2017) 'PovcalNet: an online analysis tool for global poverty monitoring'.

Thenkabail, P. S. & Lyon, J. G. (2016) *Hyperspectral remote sensing of vegetation.* CRC Press.

Thevenon, F., Graham, N. D., Chiaradia, M., Arpagaus, P., Wildi, W. & Poté, J. (2011) 'Local to regional scale industrial heavy metal pollution recorded in sediments of large freshwater lakes in central Europe (lakes Geneva and Lucerne) over the last centuries'. *Science of the total environment*, 412-413 (Supplement C), pp. 239-247.

Thompson, J. (1887) *Through Masai Land: A journey of exploration among the snowclad volcanic mountains and strange tribes of eastern equatorial Africa.* London: Low, Marston, Searle, & Rivington.

Thornes, J. B. (1990) *Vegetation and erosion: processes and environments.* Available.

Thornton, R. J. (1980) *Space, time, and culture among the Iraqw of Tanzania.* Cambridge, USA: Academic Press.

Throup, D. (1987) *Economic & social origins of Mau Mau 1945-53.* James Currey.

Tiffen, M., Mortimore, M. & Gichuki, F. (1994) *More people, less erosion: environmental recovery in Kenya.* John Wiley & Sons Ltd.

Tittonell, P. & Giller, K. E. (2013) 'When yield gaps are poverty traps: The paradigm of ecological intensification in African smallholder agriculture'. *Field Crops Research*, 143 pp. 76-90.

Tosh, J. (1973) 'Colonial chiefs in a stateless society: a case-study from northern Uganda'. *The Journal of African History*, 14 (3), pp. 473-490.

Trærup, S. L. & Mertz, O. (2011) 'Rainfall variability and household coping strategies in northern Tanzania: a motivation for district-level strategies'. *Regional Environmental Change*, 11 (3), pp. 471-481.

Trapnell, C. & Griffiths, J. (1960) 'The rainfall-altitude relation and its ecological significance in Kenya'. *The East African Agricultural Journal*, 25 (4), pp. 207-213.

Trewartha, G. T. & Zelinsky, W. (1954) 'The population geography of Belgian Africa'. *Annals of the Association of American Geographers*, 44 (2), pp. 163-193.

Trimble, S. W. (1983) 'A Sediment Budget for Coon Creek Basin in the Driftless Area, Wisconsin, 1853-1977'. *American Journal of Science*, 283 (5), pp. 454-474.

Trimble, S. W. (1999) 'Decreased rates of alluvial sediment storage in the Coon Creek Basin, Wisconsin, 1975-93'. *Science*, 285 (5431), pp. 1244-1246.

Troeh, F., Hobbs, J. & Donahue, R. (1991) *Soil and Water Conservation* Englewood Cliffs: Prentice Hall

Turner, B. L., Hydén, G. & Kates, R. W. (1993) *Population growth and agricultural change in Africa.* Gainesville, FL (USA): University Press of Florida.

UNDESA (2017) 'Population Division – World Population Prospects'.[in Division, U.N.P. *The 2017 review*. (Accessed:UNDESA

Unesco (1969) *Discharge of selected rivers of the world.* Unesco.

UNESCO (2015) *Man and the Biosphere (MAB) Programme - Biosphere reserve periodic review.* 68 pp. Available.

Upadhayay, H. R., Bodé, S., Griepentrog, M., Huygens, D., Bajracharya, R. M., Blake, W. H., Dercon, G., Mabit, L., Gibbs, M. & Semmens, B. X. (2017) 'Methodological perspectives on the application of compound-specific stable isotope fingerprinting for sediment source apportionment'. *Journal of soils and sediments*, 17 (6), pp. 1537-1553.

Valentin, C., Poesen, J. & Li, Y. (2005) 'Gully erosion: impacts, factors and control'. *Catena*, 63 (2), pp. 132-153.

Vallet-Coulomb, C., Legesse, D., Gasse, F., Travi, Y. & Chernet, T. (2001) 'Lake evaporation estimates in tropical Africa (Lake Ziway, Ethiopia)'. *Journal of Hydrology*, 245 (1), pp. 1-18.

Vanacker, V., Bellin, N., Molina, A. & Kubik, P. W. (2014) 'Erosion regulation as a function of human disturbances to vegetation cover: a conceptual model'. *Landscape ecology*, 29 (2), pp. 293-309.

Vanmaercke, M., Poesen, J., Broeckx, J. & Nyssen, J. (2014) 'Sediment yield in Africa'. *Earth-Science Reviews*, 136 pp. 350-368.

Veihe, A. (2002) 'The spatial variability of erodibility and its relation to soil types: a study from northern Ghana'. *Geoderma*, 106 (1), pp. 101-120.

Verhoeven, H. (2013) 'The politics of African energy development: Ethiopia's hydro-agricultural state-building strategy and clashing paradigms of water security'. *Philosophical Transactions of the Royal Society A: Mathematical, Physical and Engineering Sciences*, 371 (2002), pp. 20120411.

von Höhnel, L. R. (1894) *Discovery of Lakes Rudolf and Stefanie: A Narrative of Count Samuel Teleki's Exploring & Hunting Expedition in Eastern Equatorial Africa in 1887 & 1888.* vol. 2. Longmans, Green.

Vrieling, A. (2006) 'Satellite remote sensing for water erosion assessment: A review'. *Catena*, 65 (1), pp. 2-18.

Vrieling, A., Hoedjes, J. C. & van der Velde, M. (2014) 'Towards large-scale monitoring of soil erosion in Africa: Accounting for the dynamics of rainfall erosivity'. *Global and Planetary Change*, 115 pp. 33-43.

Walling, D., Bradley, S. & Lambert, C. (1986) 'Conveyance losses of suspended sediment within a flood plain system'. *IAHS-AISH publication*, (159), pp. 119-131.

Walling, D. & Collins, A. (2008) 'The catchment sediment budget as a management tool'. *Environmental Science & Policy*, 11 (2), pp. 136-143.

Walling, D., Collins, A., Sichingabula, H. & Leeks, G. (2001) 'Integrated assessment of catchment suspended sediment budgets: a Zambian example'. *Land Degradation & Development*, 12 (5), pp. 387-415.

Walling, D. & He, Q. (2000) 'The global distribution of bomb-derived 137Cs reference inventories'. *Final report on IAEA technical contract*, 10361 pp. 1-11.

Walling, D. & Kleo, A. (1979) 'Sediment yields of rivers in areas of low precipitation: a global view'. *Proceedings... The Hydrology of areas of low precipitation*,

Walling, D. E. (1983) 'The sediment delivery problem'. *Journal of Hydrology*, 65 (1-3), pp. 209-237.

Walling, D. E. (1999) 'Linking land use, erosion and sediment yields in river basins', *Man and River Systems.* Springer, pp. 223-240.

Walling, D. E. (2013) 'The evolution of sediment source fingerprinting investigations in fluvial systems'. *Journal of soils and sediments*, 13 (10), pp. 1658-1675.

Walling, D. E. & Webb, B. (1983) 'Patterns of sediment yield', *BACKGROUND TO PALAEOHYDROLOGY. A PERSPECTIVE., 1983.* pp. 69-100.

Walsh, K. & Rowe, M. (2001) 'Biodiversity Increases Ecosystems' Ability to Absorb CO2 and Nitrogen'. *Brookhaven National Laboratory*,

Wardle, D. A., Bardgett, R. D., Klironomos, J. N., Setälä, H., Van Der Putten, W. H. & Wall, D. H. (2004) 'Ecological linkages between aboveground and belowground biota'. *Science*, 304 (5677), pp. 1629-1633.

Warren, A. (1995) 'Changing understandings of African pastoralism and the nature of environmental paradigms'. *Transactions of the Institute of British Geographers*, pp. 193-203.

Wendt, R., Alberts, E. & Hjelmfelt, A. (1986) 'Variability of runoff and soil loss from fallow experimental plots'. *Soil Science Society of America Journal*, 50 (3), pp. 730-736.

Western, D., Groom, R. & Worden, J. (2009) 'The impact of subdivision and sedentarization of pastoral lands on wildlife in an African savanna ecosystem'. *Biological Conservation*, 142 (11), pp. 2538-2546.

White, J., Wulder, M., Hobart, G., Luther, J., Hermosilla, T., Griffiths, P., Coops, N., Hall, R., Hostert, P. & Dyk, A. (2014) 'Pixel-based image compositing for large-area dense time series applications and science'. *Canadian Journal of Remote Sensing*, 40 (3), pp. 192-212.

Whittaker, A. C., Attal, M. & Allen, P. A. (2010) 'Characterising the origin, nature and fate of sediment exported from catchments perturbed by active tectonics'. *Basin Research*, 22 (6), pp. 809-828.

Widgren, M. & Sutton, J. E. (1999) *'Islands' of intensive agriculture in the East African Rift and highlands: a 500-year perspective.* Stockholm: Departments of Human and Physical Geography, University of Stockholm.

Wilkinson, S. N., Hancock, G. J., Bartley, R., Hawdon, A. A. & Keen, R. J. (2013) 'Using sediment tracing to assess processes and spatial patterns of erosion in grazed rangelands, Burdekin River basin, Australia'. *Agriculture, ecosystems & environment*, 180 pp. 90-102.

Willis, J. P., Turner, K. & Pritchard, G. (2011) *XRF in the workplace: a guide to practical XRF spectrometry.* PANalytical Australia.

Wischmeier, W. H. & Smith, D. D. (1978) 'Predicting rainfall erosion losses-a guide to conservation planning'. *Predicting rainfall erosion losses-a guide to conservation planning.*,

Wolff, C., Haug, G. H., Timmermann, A., Damsté, J. S. S., Brauer, A., Sigman, D. M., Cane, M. A. & Verschuren, D. (2011) 'Reduced interannual rainfall variability in East Africa during the last ice age'. *Science*, 333 (6043), pp. 743-747.

Wulder, M. A., White, J. C., Loveland, T. R., Woodcock, C. E., Belward, A. S., Cohen, W. B., Fosnight, E. A., Shaw, J., Masek, J. G. & Roy, D. P. (2016) 'The global Landsat archive: Status, consolidation, and direction'. *Remote Sensing of Environment*, 185 pp. 271-283.

Yanda, P. Z. & Madulu, N. (2005) 'Water resource management and biodiversity conservation in the Eastern Rift Valley Lakes, Northern Tanzania'. *Physics and Chemistry of the Earth, Parts A/B/C*, 30 (11-16), pp. 717-725.

Young, A. (1989) *Agroforestry for soil conservation.* CAB international Wallingford, UK.

Yu, G. A., Li, Z., Disse, M. & Huang, H. Q. (2017) 'Sediment dynamics of an allogenic river channel in a very arid environment'. *Hydrological processes*, 31 (11), pp. 2050-2061.

Zhang, H., Yang, Q., Li, R., Liu, Q., Moore, D., He, P., Ritsema, C. J. & Geissen, V. (2013) 'Extension of a GIS procedure for calculating the RUSLE equation LS factor'. *Computers & Geosciences*, 52 pp. 177-188.

Zhang, X. C. & Liu, B. L. (2016) 'Using multiple composite fingerprints to quantify fine sediment source contributions: A new direction'. *Geoderma*, 268 (Supplement C), pp. 108-118.

Zhang, Y., Hernandez, M., Anson, E., Nearing, M., Wei, H., Stone, J. & Heilman, P. (2012) 'Modeling climate change effects on runoff and soil erosion in southeastern Arizona rangelands and implications for mitigation with conservation practices'. *Journal of soil and water conservation*, 67 (5), pp. 390-405.

Zhu, Z. & Woodcock, C. E. (2014) 'Continuous change detection and classification of land cover using all available Landsat data'. *Remote Sensing of Environment*, 144 pp. 152-171.